

# Development and Applications of Frother Analysis in Flotation Circuits

Azin Zangooi

Department of Mining and Materials Engineering

McGill University

Montreal, Quebec

A thesis submitted to the Faculty of Graduate Studies and research in partial  
fulfillment of the requirements for the degree of Doctor of Philosophy

© Azin Zangooi

January, 2014

“It is the time you have wasted for your rose  
that makes your rose so important.”<sup>1</sup>

To my immortal beloved ones: my parents and my sister

---

<sup>1</sup> Excerpt from “The Little Prince” by Antoine de Saint-Exupéry (1900-1944). Copyright 1943 by Harcourt  
Brace & Company; Copyright renewed 1971 by Harcourt Brace & Company.

## ABSTRACT

Flotation machines disperse air into bubbles using a variety of devices. Since the characteristics of the bubble population are controlled by frother, measurement of frother concentration it is vital to understand and control performance. A previously developed colorimetric technique, based on a reaction between a dehydrated frother molecule and an aldehyde proposed by Komarowsky, was refined to increase analysis rate and reproducibility, particularly for low-solubility frothers.

The refinements included replacing volumetric preparation of frother solutions by weighing of components. This permitted a reduction in the concentration of the solutions which facilitated analysis of low-solubility frothers. Extraction of frother into chloroform demonstrated that the choice of chloroform was critical. A significant change was in the construction of the calibration curve, where the wavelength selected (in the range 300-700 nm) was which given the minimum sum of squares of residuals. Use of a blank and a sample with no frother, resulted in linear calibrations through the origin. Developing a way to process samples in batches increased the daily analysis rate to 20 samples making it suited to plant surveys.

The reproducibility of the refined technique showed a relative error at the 95% confidence interval of about 2.5% which included solution preparation. The detection limit was approximately 0.2 ppm, although the technique is still able to detect frother at concentrations below 0.1 ppm.

A database was created to document experiences in selecting standards for commercial frothers, which will help users of the technique.

The method was exploited in a basic study to determine frother coverage on bubbles, which required novel equipment and procedures. The results, expressed as area of adsorbed frother molecule, were comparable to the estimation from the Gibbs adsorption isotherm. In an industrial application, frother partitioning (ratio of overflow to underflow

concentration) was shown to be significant, in some cases helping to explain downstream problems. The technique was integrated into the gas dispersion technology used to troubleshoot flotation cell hydrodynamics.

Transfer of the technology was undertaken. It was shown how frother concentration varies with location and time in a circuit. Such information was not available previously. This was referred to as 'frother mapping' and proved useful in diagnosing stability of frother delivery, adequacy of number and location of addition points, and in detecting units operating with potentially too low a frother concentration. Experience at several concentrators is discussed along with possible implications and remedies.

## RÉSUMÉ

Les appareils assurant la flottation dispersent l'air en formant des bulles par divers moyens. Les caractéristiques de la population de bulles dépendent de la concentration du moussant. Il est donc essentiel de comprendre et de pouvoir contrôler le fonctionnement de ces appareils. Une méthode colorimétrique déjà développée par Komarowsky, fondée sur une réaction entre une molécule déshydratée du moussant et un aldéhyde, a été affinée afin d'augmenter le taux d'analyses et leur reproductibilité, en particulier pour les moussants faiblement solubles.

Parmi les affinements, la préparation volumétrique des solutions de moussant a été remplacée par une préparation pondérale, ce qui a permis de réduire la concentration des solutions, et a mené à une analyse plus facile des moussants faiblement solubles. L'extraction du moussant dans le chloroforme s'est avérée d'importance critique. Une amélioration importante a eu lieu dans la construction de la courbe de calibrage, où la longueur d'onde choisie, entre 300 et 700 nm, est celle qui produit la somme résiduelle minimale. L'utilisation d'un blanc et d'un échantillon dépourvu de moussant a mené à un calibrage linéaire passant par l'origine. Le développement d'une façon de procéder avec échantillons groupés a augmenté le taux d'analyses quotidien jusqu'à 20, ce qui est pratique pour évaluations dans une usine.

La reproductibilité de la technique affinée, y compris l'étape de la préparation des solutions, a démontré une erreur relative d'environ 2.5% à un intervalle de confiance de 95%. Le seuil de détection était d'environ 0.2 ppm, quoique la méthode permet de déceler le moussant à un seuil inférieur à 0.1 ppm.

La méthode a été exploitée dans une étude fondamentale visant à évaluer le taux de recouvrement d'une molécule moussant sur les bulles, ce qui a exigé un nouvel équipement et des procédures modifiées. L'aire du moussant adsorbé qui en a résultée est comparable à la valeur estimée selon l'isotherme d'adsorption de Gibbs. Dans une application industrielle, la répartition du moussant (rapport des concentrations au

surverse et sousverse) est importante dans certains cas afin d'expliquer les problèmes éventuels. La technique modifiée a pu être intégrée à la technologie de dispersion des gaz pour dépannage en ce qui touche les aspects hydrodynamiques des cellules de flottation.

On a entrepris un transfert de la nouvelle technologie. La concentration du moussant dans un circuit peut varier selon l'endroit et le temps, information non disponible antérieurement. Une telle "cartographie du moussant" s'avère d'une grande utilité pour évaluer la stabilité de livraison du moussant, l'adéquation du nombre et d'endroits de points d'ajout, et la détection d'unités ayant des concentrations potentiellement trop faibles. L'analyse comprend une évaluation de plusieurs concentrateurs, ainsi que des implications possibles et des procédures d'amélioration.

## ACKNOWLEDGMENTS

I would like to express my appreciation to all whose cooperation and support allowed the completion of this study.

As always, first and foremost, I wish to offer my immense gratitude to my tireless supervisor Professor James A. Finch for expert guide during the different stages of this undertaking and for his patience with the writing process.

Special thanks are likewise expressed to Dr. César O. Gómez (Pato), my technical advisor, for providing perspective that contributed significant to this work, and also for doing it with good humor. I am grateful for his diligent efforts to mentor me in many directions throughout my years as a PhD student. Thanks for teaching me to live my learning.

I am eternally thankful to one of my best teachers ever; my late uncle, S. Mehdi Shivaiei, for his great impact on my early education.

I would like to extend my heartfelt gratitude to the late Dr. Azimi, Tehran University, for providing support during the rough ride of my undergraduate education.

I am also indebted to Professor Olivia Jenson, Earth and Planetary Sciences at McGill, for encouraging me to continue pursuing my education.

Professor Robert F. Martin, Earth and Planetary Sciences at McGill, kindly provided the French translation of the abstract.

Thanks are extended to Ms. Barbara Hanley, for her effective assistance with administrative matters, to Ms. Monique Riendeau, for sharing her experience in operating analytical instrumentation, and to Mr. Armando Navarrete, for his help in drawing some of the figures included in Chapter 2 of this dissertation.

My profound thanks to Mr. Steven Malinovsky for his highly professional contribution to collect the gas dispersion data used in parts of this dissertation.

I wish to acknowledge, most gratefully to all the staff and operators who helped me at plant sites: Troilus (Canada), Salvador (Chile), Chuquicamata (Chile), CMDI Collahuasi (Chile), Telfer (Australia) and Voisey's Bay (Canada). And to many others whom I have failed to mention in this abbreviated list, my sincere thanks.

Throughout my study at McGill, I appreciate the financial support received from NSERC (Natural Sciences and Engineering Research Council of Canada) Industry Chair in Mineral Processing, and from the AMIRA P9 project.

My family deserves a very special mention not only for their support but also for giving me the luxury to design my life: my father, Nasrollah Zangoi, who instilled the principles of learning to my very core and was the first person who showed me the joy of intellectual pursuit; my extraordinary mother, Heshi Shivaie, for her keen eyes, for giving me strength when I am struggling, for boundless love every single day, and for being my best friend; Negin Zangoi, my supporting and caring sister who always reminds me: "If you want to be successful, you cannot be too good"; my late grandmothers, Fatemeh Iranmanesh and Fatemeh Sami, for being such great iconic figures in my life by directing me "to take full advantage of the miracle of being born and never to give in to cowardice"<sup>2</sup>; Behdad Bayat, my nephew, and Bahar Bayat, my niece, for making me laugh when I have been down for as long as I remember.

And last but certainly not least, words fail me to express my appreciation to my Godot<sup>3</sup> because in the act of waiting for him I found the strength to complete this work.

---

<sup>2</sup> Excerpt from "Letter to a Child Never Born" by Oriana Fallaci (1929-2006). Translated to English by John Shepley. Published by Simon and Schuster (1976).

<sup>3</sup> "Waiting for Godot" by Samuel Beckett (1906-1989).



## TABLE OF CONTENTS

ABSTRACT .....	i
RÉSUMÉ .....	iii
ACKNOWLEDGMENTS .....	v
TABLE OF CONTENTS .....	vii
LIST OF FIGURES .....	x
LIST OF TABLES .....	xiv
CHAPTER 1. INTRODUCTION .....	1
1.1 THESIS OBJECTIVES .....	5
1.2 THESIS SCOPE .....	5
1.3 THESIS STRUCTURE .....	6
CHAPTER 2. LITERATURE REVIEW.....	8
2.1 FLOTATION .....	8
2.2 FLOTATION FROTHERS.....	10
2.2.1 Alcohol-type .....	12
2.2.2 Alkoxy-type .....	13
2.2.3 Polyglycol-type .....	13
2.3 FROTHER ROLES .....	15
2.3.1 Preserving bubble size .....	15
2.3.2 Stabilizing the froth phase .....	19
2.4 FROTHER CHARACTERIZATION TECHNIQUES .....	22
2.4.1 Hydrophile-lypophile balance (HLB) .....	22
2.4.2 Dynamic frothability index (DFI) .....	23
2.4.3 Critical coalescence concentration (CCC) .....	23
2.4.4 Hydrodynamic characteristics of frother chemistry .....	25
2.5 INTERFACIAL PROPERTIES .....	25
2.5.1 Surface tension .....	25
2.5.2 Fractional surface coverage .....	26
2.5.3 Surface elasticity .....	27

2.6	FROTHER ANALYSIS TECHNIQUES .....	28
2.7	FROTHER COVERAGE .....	30
CHAPTER 3. FROTHER ANALYSIS TECHNIQUE .....		34
3.1	INTRODUCTION .....	34
3.2	LITERATURE REVIEW .....	36
3.2.1	Application of gas chromatography .....	36
3.2.2	Colorimetric technique .....	37
3.2.3	Other Methods .....	37
3.3	COLORIMETRIC TECHNIQUE FOR THE ANALYSIS OF FROTHERS .....	37
3.4	REFINEMENTS TO THE FROTHER ANALYSIS TECHNIQUE.....	40
3.4.1	Preparation of reagents and calibration standards .....	40
3.4.2	Frother extraction .....	40
3.4.3	Formation of a colored solution .....	43
3.4.4	Collection of UV-VIS spectrum .....	48
3.5	CALCULATION OF FROTHER CONCENTRATION .....	50
3.6	REPRODUCIBILITY .....	55
3.7	DETECTION LIMIT .....	59
3.8	CONCLUDING REMARKS .....	60
CHAPTER 4. FROTHER ANALYSIS DATABASE .....		63
CHAPTER 5. FROTHER ANALYSIS: APPLICATIONS IN FUNDAMENTAL RESEARCH .....		73
5.1	INTRODUCTION .....	73
5.2	FROTHER PARTITIONING .....	73
5.2.1	Establishing technique .....	73
5.3	FROTHER COVERAGE .....	81
5.3.1	Introduction .....	81
5.3.2	Theoretical Consideration .....	81
5.3.3	Experimental Aspects .....	84
5.3.4	Results .....	85

CHAPTER 6. INDUSTRIAL APPLICATIONS OF FROTHER ANALYSIS .....	94
6.1 INTRODUCTION .....	94
6.2 REQUIREMENTS FOR PLANT FROTHER ANALYSES .....	95
6.3 FROTHER CONTENT IN PROCESS AND RECYCLE WATERS .....	99
6.4 INTERFERING SPECIES .....	101
6.5 STABILITY OF FROTHER DELIVERY .....	104
6.6 DETERMINATION OF FROTHER PARTITIONING .....	106
6.7 CONSTRUCTION OF FROTHER DISTRIBUTION MAPS .....	110
6.7.1 Sampling Program and Analysis .....	112
6.7.2 Results and discussion .....	112
6.7.3 Conclusions .....	118
CHAPTER 7. CONCLUSIONS AND CONTRIBUTIONS TO ORIGINAL .....	121
RESEARCH AND KNOWLEDGE	
7.1 CONCLUSIONS .....	121
7.2 CLAIMS TO ORIGINAL RESEARCH .....	123
7.3 CONTRIBUTIONS TO KNOWLEDGE .....	124
7.4 RECOMMENDATIONS .....	125
REFERENCES .....	126
APPENDIX 1 .....	137

## LIST OF FIGURES

Figure 2.1 -	Structure of TEB .....	13
Figure 2.2 -	Schematic representation of adsorbed molecules of polypropyleneglycol (PPG). (Tan 2005)	14
Figure 2.3 -	Effect of frother concentration on bubble size in a flotation cell (Cho and Laskowski 2002a)	17
Figure 2.4 -	Change in Sauter mean diameter as a function of impeller speed above CCC. Grau and Heiskanen (2005)	18
Figure 2.5 -	Experimental results signifying changes in Sauter mean diameter with impeller speed above CCC ( Finch et al., 2008)	19
Figure 2.6 -	Effect of frother concentration on bubble velocity (Krazan et al., 2007)	20
Figure 2.7 -	Effect of frother concentration on bubble size and gas holdup (Azgomi et al., 2007)	21
Figure 2.8 -	Water carrying rate as a function of gas holdup (Moyo et al., 2007)	22
Figure 2.9 -	DFI as a function of CCC for tested frothers Laskowski et al. (2003b)	24
Figure 2.10 -	Bubble size as a function of fractional surface coverage for the series of n-alcohol (Comley, 2001)	27
Figure 3.1 -	Frother analysis: frother extraction stage .....	38
Figure 3.2 -	Frother analysis: reaction to form colored solution .....	39
Figure 3.3 -	Effect of chloroform type on color obtained in the analysis of samples with no frother: a) with ethanol- and amylene-stabilized chloroform; and b), with ethanol-stabilized chloroform samples apparently having different shelf lives	41
Figure 3.4 -	Spectra for colored solutions depicted in Figure 3.3 .....	42
Figure 3.5 -	Frother extractions and partition ratios obtained for increasing chloroform extraction stages	43
Figure 3.6 -	Effect of indicator addition volume (0- and 10-ppm F150 standards)	44
Figure 3.7 -	Spectrum evolution with increasing boiling time (15-ppm F150 solution)	45
Figure 3.8 -	Absorbance as a function of boiling time: a) same frother at different wavelengths; b) different frothers at same wavelength	46

Figure 3.9 - Calibration spectra for frother DSF004 prepared with: .....	47
a) tap water; and b), process water	
Figure 3.10 - Calibration spectra for frother Matfroth533 prepared with:.....	47
a) tap water; b) process water; and c), sea water	
Figure 3.11 - Spectra obtained in the analysis of concentrated solutions .....	48
of mineral species prepared in: a) water; and b) a 3-ppm MIBC solution	
Figure 3.12 - Spectra collected for the same sample using different .....	49
reference solutions (F140)	
Figure 3.13 - Collected spectra for MIBC standards .....	50
Figure 3.14 - SSR as a function of wavelength for MIBC .....	51
Figure 3.15 - Spectra (a), comparison of calibration curves (b), and estimated ...	53
vs. measured concentrations (c) for MIBC analysis	
Figure 3.16 - Calibration spectra (a), and comparison of calibration .....	54
Curves (b) and estimated vs. measured concentrations (c) for PPG425 analysis	
Figure 3.17 - Repeat 1-pentanol spectra collected to estimate error analysis at ...	56
a) low (2 ppm), and b), high (7 ppm) concentrations	
Figure 3.18 - Relative error in absorbance in the analysis of .....	58
samples and standards of different frothers	
Figure 3.19 - Relative errors in absorbance in the analysis of low- and .....	58
high-concentration solutions of different frothers	
Figure 3.20 - Calibration curve constructed for 1-octanol at .....	59
486 nm (minimum SSR)	
Figure 3.21 - Calibration curve predictions for low-concentration .....	60
solutions of 1-octanol	
Figure 4.1 - Calibration spectra: (a) covering a too narrow absorbance .....	64
range, and (b) with one standard out of range (absorbance > 3 over wavelength~ 420-550nm)	
Figure 4.2 - Calibration curve obtained with standards covering .....	64
narrow and wide concentration ranges (wavelength 552 nm)	
Figure 4.3 - Database entry for pentanol .....	68
Figure 4.4 - Database entry for PPG425 .....	69
Figure 4.5 - Database entry for a MIBC .....	70
Figure 4.6 - Database entry for F150 .....	71
Figure 4.7 - Database entry for a eucalyptus oil sample .....	72
Figure 5.1 - Details of laboratory bubble column installation .....	74

Figure 5.2 -	Stream concentrations as a function of frother (DF250) concentration .....	75
Figure 5.3 -	Partitioning as a function of underflow concentration (DF250) in bubble column tests .....	76
Figure 5.4 -	Stream concentrations measured in tests run at several gas velocities in bubble column .....	77
Figure 5.5 -	Partitioning as a function of gas velocity for two frother/concentration conditions in bubble column .....	77
Figure 5.6 -	Details of downcomer installation .....	78
Figure 5.7-	Stream concentrations measured in tests run at several frother (DF250) concentrations in Jameson cell .....	80
Figure 5.8 -	Partitioning as a function of underflow frother (DF250) concentration in Jameson cell tests .....	80
Figure 5.9 -	Details of laboratory bubble column setup .....	84
Figure 5.10 -	Total mass balances obtained from a) measured, and b), reconciled data .....	88
Figure 5.11 -	Stream mass balances obtained from a) measured, and b), reconciled data .....	88
Figure 5.12 -	Frother coverage results as a function of feed frother concentration .....	89
Figure 5.13 -	Determination of surface excess from surface tension data for frothers MIBC, F150 and 1-octanol .....	91
Figure 5.14 -	Measured and predicted average areas of adsorbed molecules on the surface of bubbles: a) MIBC, b) PPG425, and c), 1-octanol .....	92
Figure 5.15 -	Measured and predicted areas of adsorbed molecules on the surface of bubbles for 1-octanol .....	93
Figure 6.1 -	UV-VIS spectra obtained at the three speeds .....	96
Figure 6.2 -	Concentrations (at 500 nm) with spectrum collection rates .....	96
Figure 6.3 -	Measurement of analysis standard deviation in plant sites .....	97
Figure 6.4 -	Determination of effect of storage time on analysis results .....	98
Figure 6.5 -	Determination of remnant frother concentration .....	100
Figure 6.6 -	Remnant frother in samples of process waters .....	101
Figure 6.7 -	Calibration curves in tap water for the combination frother/collector in use at Chuquicamata .....	103
Figure 6.8 -	Calibration curves in tap water for the combination frothers/collector in use at Codelco-Salvador Division (Chile) .....	103

Figure 6.9 - Calibration curves in tap water for the combination of frothers/collector in use at Telfer .....	104
Figure 6.10 - Frother concentration measured in a cell over time at Chuquicamata .....	105
Figure 6.11 - Frother concentration profile measured in a nine-cell bank at Codelco-Salvador Division (Chile) .....	106
Figure 6.12 - Frother partitioning measured in rougher cells at Telfer .....	107
Figure 6.13 - Frother partitioning measured in rougher cells at Voisey's Bay.....	108
Figure 6.14 - Frother partitioning measured in rougher circuits at Chuquicamata .....	109
Figure 6.15 - Chuquicamata flotation circuit .....	111
Figure 6.16 - Concentration of frother in line feeds to different circuits .....	115
Figure 6.17 - Measured concentration in feed and tailings streams (Roughers A1 and A2) .....	116
Figure 6.18 - Measured concentrations in tailings and concentrate streams (Rougher A2) .....	117
Figure 6.19 - Measured concentrations in tailings and concentrate streams (Rougher A2) .....	117
Figure 6.20 - Measured concentrations in Rougher A0 streams .....	119
Figure 6.21 - Measured concentrations in streams of Rougher circuits A1 and A2 .....	120
Figure 6.22 - Frother concentrations in streams water samples .....	120

## LIST OF TABLES

Table 2.1 -	Classification of flotation frothers ..... (after Laskowski and Woodburn, 1998)	11
Table 2.2 -	List of frothers, their chemical formulae, molecular weight, ..... CCC and DFI values (after, Laskowski 2003)	24
Table 3.1 -	Absorbance and relative errors obtained in the analysis of ..... 5-ppm standards of the frother TX13072	55
Table 3.2 -	Relative absorbance errors for the analysis of samples and ..... standards of various frothers at a low and a high concentration (5 replicates)	57
Table 4.1 -	Frothers analyzed .....	66
Table 4.2 -	Calibration results and maximum standard concentration .....	67
Table 5.1 -	Stream flow rates and measured and reconciled concentrations ....	86
Table 5.2 -	Gas dispersion measurements and coverage results .....	90
Table 6.2 -	Samples collected for construction of frother distribution map .....	113



## CHAPTER 1 - INTRODUCTION

Metal production from ore bodies is achieved by combining a number of unit operations. Mineral processing comprises the methods by which gangue (non-valuable minerals) and valuable minerals are separated. The initial step is size reduction (comminution), which is followed by a separation process such as gravity concentration, dense medium separation, magnetic separation and flotation. Size reduction comprises crushing and grinding, where ore is broken down into small particles. Once particles are fine enough to have liberation of minerals, the mill product is delivered to the separation stage. In mineral processing case, the separation process of interest is flotation, which is based on the surface properties of minerals.

The basic property is wettability. A surface that is hydrophobic or non-polar does not form hydrogen bonds with water; a surface that is hydrophilic or polar, forms hydrogen bonds with water. This property is the basis of selectively separate particles by flotation. Most minerals associated with metallic elements are naturally hydrophilic, but hydrophobicity can also be induced by the selective adsorption of chemicals called collectors. By injecting and dispersing air to form a swarm of rising bubbles, hydrophobic particles collide with and stick to the bubble to reduce contact with water; the bubble-particle aggregates formed rise to the top (float) where they accumulate in a froth. Therefore, flotation proceeds in two zones: the pulp or collection zone where conditions are selected for particles and bubbles to collide and form bubble-particle aggregates, and the froth or cleaning zone where these aggregates are concentrated and separated into a concentrate stream.

Second only to the collector, flotation is driven by bubbles and controlling their size is essential to the process. There is a wide variety of gas dispersion techniques used in industrial flotation machines (or cells) including: forcing or aspirating air through holes in the blades of a rotating impeller in mechanical cells, injecting air through one or multiple holes in spargers in flotation columns; contacting aspirated air with a high-speed pulp jet hitting a pulp surface, in Jameson cells (Wills and Napier-Munn, 2006). In

combination with a second reagent, the frother, gas dispersion techniques generate bubbles with a distribution of sizes; the nature of the bubble population is arguably the most important contribution of the flotation machine. The bubble population produced is described by three gas dispersion parameters: superficial gas velocity, gas holdup and bubble size.

Superficial gas (air) velocity is the volumetric gas rate per unit of cell cross sectional area, and gas holdup is the volumetric fraction of gas in a gas-slurry (in this case) mixture. In the case of bubble size, the measurement provides a distribution of sizes which is used to calculate an average value. Sensors and techniques to measure these parameters in plant installations have been developed over the last 15 years by different groups (Gorain et al., 1999, Gomez and Finch, 2002; 2007, Amelunxen and Rothman, 2009, Yianatos et al., 2010). These measurements have become a tool to characterize industrial flotation cells, for example to define operating ranges, to diagnose instrumentation and operation practices, and to provide a relationship with metallurgical performance for process control.

Performance of a flotation machine depends on how effectively gas is dispersed and distributed throughout its volume. In general, effective gas dispersion means the formation of a narrow bubble size distribution, typically between 0.5 to 3 mm (reference) which may vary depending on the particle size to be processed. Bubble size in flotation defines the interfacial surface area over which particles and bubbles interact: the smaller the bubbles, the larger is the interaction area, and the process becomes more efficient. Bubble surface area flux ( $S_b$ ), a variable that quantifies the area generated by gas dispersion, is calculated from two of the gas dispersion parameters (gas velocity and bubble size) (Finch and Dobby, 1990). It is considered a measurement of the impact that the machine has on the process and it has been correlated with the flotation rate constant (Gorain et al., 1997; Gorain et al., 1998; Hernandez et al., 2003). The importance of bubble size in controlling flotation efficiency has been repeatedly demonstrated (Ahmed and Jameson, 1985; Dobby and Finch, 1986; Yoon and Luttrell, 1986; Fuerstenau, 1999). Bubble size not only affects the value of  $S_b$ , but also two of the most important

phenomena associated with the flotation of minerals: number of bubble-particle collisions and formation of bubble-particle aggregates by attachment after a successful collision (Dai et al., 2000; Tao, 2000).

The effect of frothers on bubble size and to a lesser extent rise velocity have significant consequences in flotation, recognized in the increasing volume of research in recent years to understand and characterize frother roles and their impact on mineral recovery (Malysa et al., 1987; Laskowski, 2003; Laskowski et al., 2003 a, b; Azgomi et al., 2007; 2009; Moyo et al., 2007; Comley et al., 2007; Tsatouhas et al., 2006; Gomez et al., 2011). Frothers are active at the air/water interface (bubble surface) because the molecule comprises a hydrophilic (commonly OH) group combined with a hydrophobic hydrocarbon chain (the simplest representative being an alcohol). The frother molecule adsorbs on the bubble surface with the hydrophilic group to the water-side and the hydrophobic hydrocarbon chain to the air-side of the air/water interface, thus providing a thermodynamically stable orientation. The hydrophilic group forms hydrogen bonds with water molecules resulting in a water film around the bubble with properties differing from bulk water.

Frothers have three major effects relevant to flotation. The prime one is bubble size control by preservation of the generated bubble size, which is attributed to coalescence inhibition by the frother's presence on the bubble surface (Harris, 1976). Another factor is the stabilization of the froth layer by increasing the amount of water that is carried into the froth (Moyo et al., 2007). This water carrying function appears related to the adsorbed frother increasing the viscosity of the water layer on the bubble surface through H bonding (Godbole et al., 1984; Yasunishi et al., 1986; Neme et al., 1997; Crabtree and Bridgwater, 1971; Li and Prakash, 1997) which also decreases drainage rate from the froth. The third effect is that frother adsorption retards bubble rise velocity, increasing bubble retention time in the pulp which influences collision rates (Rafiei and Finch, 2009; Azgomi et al., 2007).

Measurements in laboratory equipment as well as in plant units have demonstrated that the magnitude of these effects is a strong function of the frother type and concentration (Gomez et al., 2011). The improvement of cell operation to optimize metallurgical performance (grade and recovery) makes it necessary to know the concentration and distribution of frother in flotation circuits. Frother is commonly added (dosed) based on the solids feed rate (e.g. g frother/tonne solids) but calculation of the concentration from dosage is difficult because of several factors such as incomplete frother dissolution, adsorption on bubble surface, presence of frother in recycle water, frother portioning and frother-like contaminants added with other reagents. There have been efforts to develop a frother analysis technique (Gelinas and Finch, 2005; Tsatouhas, 2006; Zhang et al., 2013), but none of them seems entirely appropriate for on-site plant work. Major objections are the low analysis rate and the error associated with the analysis of low solubility frothers.

## **1.1 THESIS OBJECTIVES**

### Hypothesis

The proposition guiding this work is the development of a reliable analytical technique for the determination of frother concentration in water samples collected in laboratory and industrial flotation units, with a minimum analysis rate, and applicable to low solubility frothers.

### Objectives

1. Complete a literature review to identify frother analysis techniques for laboratory and industrial water samples;
2. Select an analysis technique with requirements compatible with conditions existing in industrial sites;
3. Refine the selected technique by developing procedures to provide the required analysis rate (20 samples per day) and the ability to process samples of low solubility frothers;
4. Test the refined technique by analysing pure (products from chemical catalogs) and commercial frothers in laboratory and plant installations. Organize and build up a frother analysis database;
5. Apply the analytical technique in fundamental studies involving frother distribution and mass balancing in flotation machines; and
6. Use the analytical technique to diagnose frother delivery and distribution in industrial cells and circuits.

## **1.2 THESIS SCOPE**

The selection of an analytical technique greatly considered factors such as equipment portability, as mineral processing plants tend to be isolated, and operation simplicity, to make possible on-site implementation and facilitate technology transfer. The colorimetric technique selected, proposed initially by Gelinis and Finch (2005), was

considered to meet these requirements. This technique is based on the formation of a colored solution, through the Komarowsky reaction, which is specific to frothers among the normal range of flotation reagents. This was the case for the more than 40 frother compounds tested in this work.

The development of an analytical procedure required the characterization of the phenomena associated in the several steps involved in the analysis.

Testing of the technique considered pure compounds, natural oils and extracts, and commercial frothers. These products included highly insoluble compounds, and in many cases, blends, which was the case of many commercial frothers. In this case, the frothers were analyzed as one compound and no attempt was made to separate contributions of individual components.

### **1.3 THESIS STRUCTURE**

The thesis is organized in seven (7) chapters and one (1) appendix, which organize the work done and achievements as follows:

**Chapter 1- Introduction** presents a general overview of mineral processing and flotation to provide a background for justifying the needs and importance of developing a reliable frother analysis technique. The objectives and scope of the work accomplished were established.

**Chapter 2- Literature Review** focuses on aspects related to frother effects on flotation such as: frother types and roles, frother characterization techniques and classification approaches, and frother analysis techniques.

**Chapter 3- Frother Analysis Technique** describes the development of the analytical procedure, including characterization of the several stages involved in the analysis, and the selection of conditions resulting in a reliable technique. Also included are the determination of technique accuracy and reproducibility.

**Chapter 4- Frother Analysis Database** compiles the calibration data collected for pure substances, natural oils and commercial frothers in the course of this work. The information provided, for each compound, includes UV-VIS spectra for the selected calibration standards and the calibration curve determined following the analysis procedure. Current number of entries is 38.

**Chapter 5- Frother Analysis: Applications in Fundamental Research** includes the application of the analytical technique to study frother partitioning in flotation units, and to determine frother coverage on air-water interfaces in a bubble column. In the latter case, the approach was based on frother mass balancing around a bubble column, especially designed and operated.

**Chapter 6- Industrial Applications of Frother Analysis** includes special requirements and corresponding procedures for plant sample analyses, and summarizes frother analysis results obtained in flotation plants. Case studies included are: the determination of remnant frother in recycle waters; the detection and determination of diluting frother in collectors; the stability of frother delivery; the measurement of frother partitioning in cells and circuits; and the construction of frother distribution (maps) in banks, lines and circuits.

**Chapter 7- Conclusions and Contributions to Original Research and Knowledge** presents conclusions, claims of original research, and suggestions for future research directions.

## CHAPTER 2. LITERATURE REVIEW

### 2.1 FLOTATION

Flotation is a separation process based on the collection of particles by bubbles. Flotation depends on making small bubbles (ca. 1 mm) and on making selected mineral particles hydrophobic and others hydrophilic. These properties are controlled by reagents. The three common reagent classes are: frothers to help to control bubble size and froth formation; collectors to convert hydrophilic particles to hydrophobic; and modifying agents which assist collectors. The process involves two sequential stages occurring in zones with different roles: formation of bubble-particle aggregates by collision and capture of particles on the surface of air bubbles in the pulp or collection zone; and concentration and removal of these aggregates into a concentrate stream in the froth zone. The phenomena occurring in these zones, which have significantly different air concentrations and hydrodynamic conditions, are highly interactive and depend on machine characteristics and on physico-chemical factors such as frother type, particle size and composition. The metallurgical performance (recovery/grade) depends on the individual zone recoveries, which in the case of the collection zone is associated with the bubble surface area flux (BSAF) generated, while in the froth zone it appears to be related to the water recovery.

It is well established that frothers have two important functions (roles) in flotation: bubble size reduction by preserving bubble formation size (Laskowski, 2003; Ata, 2008; Cappuccitti and Finch, 2008), and froth stabilization by defining the water carrying rate into and drainage rate from the froth (Moyo et al., 2007). Understanding these roles for a particular frother as a function of concentration is crucial to select conditions leading to stable operation and maximum metallurgical performance.

Bubble size preservation occurs by the adsorption of frother on the bubble surface, which retards coalescence (Harris, 1976). Frother adsorption also affects the bubble rise velocity that correlates with gas hold up (Azgomi et al., 2007), and the amount of water



that is carried into the froth (Moyo et al., 2007). Frother adsorption, measured as adsorption density (concentration per unit surface area), is a function of frother concentration in the bulk solution, which is rarely known with certainty in an operating plant. Frother is commonly dosed on the basis of solids tonnage, for example, g frother/tonne ore, and it is difficult to calculate concentration in solution from this due to factors such as incomplete dissolution, and unknown distribution between pulp and froth. Additionally, several commercial products are blends of frothers (e.g. alcohols and glycols) and it is the relative proportion of each in solution that needs to be estimated. Other complications are alcohol contaminants in some other reagents (e.g. xanthates) and residual frother in recycle waters.

Flotation machines disperse air into bubbles using a variety of mechanisms such as passing air through a rotor/stator in mechanical machines, through various porous and jet-type spargers in flotation columns and by self-aspiration through an orifice in Jameson cells (Wills, 2006). Measurement of properties of the bubble population, so-called gas dispersion parameters (superficial gas velocity, gas holdup and bubble size), has become a valuable tool to characterize industrial flotation cells, for example to define the operating range and relationship to metallurgical performance (Gomez and Finch, 2002; 2007). These cell characterization measurements have provided evidence that gas dispersion properties are strongly affected by frother type and concentration.

Superficial gas (air) velocity is the volumetric gas rate per unit cell cross sectional area. Typically, superficial gas velocity (gas rate) in flotation systems is 0.5-2.5 cm/s depending on factors such as bubble size and slurry rheology (Finch and Dobby, 1990). Increasing gas rate increases the number of bubbles, which results in the recovery of more particles, up to a limiting condition where recovery passes through a maximum (Finch and Dobby, 1990; Smith et al., 2009).

Gas holdup is the volumetric fraction of gas in a gas-liquid mixture, or in the case of flotation a gas-slurry mixture. It reflects the combination of gas velocity and bubble size or, more precisely, bubble rise velocity. Gas holdup is a function of a number of factors:

chemical (frother type and concentration), operational (gas rate) and machine (bubble generation system). Gas holdup generally increases with increasing gas rate to a limiting condition (Shah et al., 1982; Finch and Dobby, 1990; Dahlke et al., 2005) and with decreasing bubble size (e.g., resulting from an increase in frother addition) as smaller bubbles ( $\leq 2$  mm) rise more slowly (Finch and Dobby, 1990).

The dependence of gas holdup on bubble size is dampened if the frother does not significantly reduce bubble rise velocity (Azgomi et al., 2007; Rafiei et al., 2011). Other factors that influence bubble rise velocity are bubble particle loading (Garibay et al., 2002) and rheological (viscosity) effects (Crabtree and Bridgwater, 1971; Godbole et al., 1984; Yasunishi et al., 1986; Neme et al., 1997; Li and Prakash, 1997).

## **2.2 FLOTATION FROTHERS**

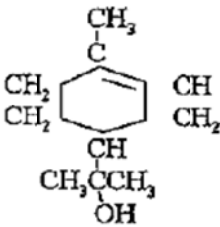
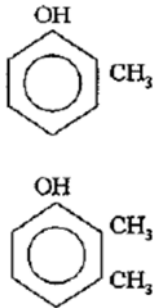
Frothers are surfactants, reagents that impact the air-water interfacial properties at low concentration by adsorption at the interface. Frother molecules comprise hydrophobic (non-polar) and hydrophilic (polar) groups. The number, type and distributions of these polar groups, as well as length of the non-polar chain, and any branching dictate frother solubility and surface activity (Ross and van Deventer, 1988; Rosen, 1989; Jachminska et al., 1995). The non-polar chain is almost universally a hydrocarbon chain (Jachminska et al., 1995) and the polar groups are typically OH and O. The balance between the groups partly defines the properties, i.e., the hydrophilic-lipophilic balance (HLB), as does their spatial configuration which controls orientation at the air-water interface (Kitchener, 1992).

Flotation frothers are classed into three main families, (Booth, 1973; Lovell, 1982; Crozier and Klimpel, 1989; Laskowski and Woodburn, 1998; Laskowski, 2003) namely;

- 1) Alcohol-type;
- 2) Alkoxy-type; and
- 3) Polyglycol-type.

Table 2.1 presents some common frother types in these three families (Laskowski and Woodburn, 1998). The following sections contain generalized information relating to the frothers within these groups, their properties and solubilities.

Table 2.1 - Classification of flotation frothers (after Laskowski and Woodburn, 1998)

Name	Formula	Solubility in H <sub>2</sub> O
<b>(1) Aliphatic Alcohols</b>	R-OH	
Methyl isobutyl Carbinol MIBC	$\text{CH}_3\text{CH}(\text{CH}_3)\text{CH}_2\text{CH}_2\text{OH}$	Low
2-ethyl hexanol	$\text{CH}_3\text{CH}_2\text{CH}_2\text{CH}_2\text{CH}(\text{CH}_2\text{CH}_3)\text{CH}_2\text{OH}$	Low
Diacetone alcohol	$\text{CH}_3\text{C}(\text{OH})(\text{CH}_3)\text{CH}_2\text{C}(\text{O})(\text{CH}_3)\text{CH}_3$	Very Good
2,2,4-trimethylpentanediol 1,3-monoisobutyrate TEXANOL	$\text{CH}_3\text{C}(\text{OH})(\text{CH}_3)\text{CH}_2\text{C}(\text{O})(\text{CH}_3)\text{CH}_2\text{C}(\text{O})(\text{CH}_3)\text{CH}_3$	Insoluble
<b>(2) Cyclic Alcohols</b>		
$\alpha$ -terpineol (active constituent of pine oil)		Low
Cyclohexanol	$\text{C}_6\text{H}_{11}\text{OH}$	Low
<b>(3) Aromatic Alcohols</b>		
Cresylic acid (mixture of cresols and xylenols)		Low
<b>(4) Alkoxy-type frothers</b>		
1,1,3-triethoxybutane TEB	$\text{CH}_3\text{C}(\text{OC}_2\text{H}_5)_2\text{CH}_2\text{C}(\text{OC}_2\text{H}_5)_2$	Low
<b>(5) Polyglycol-type frothers</b>		
	$\text{R}(\text{X})_n\text{OH}$ $\text{R}=\text{H}$ or $\text{C}_n\text{H}_{2n+1}$ $\text{X}=\text{EO}$ , $\text{PO}$ or $\text{BO}$	<b>Very good or completely miscible</b>
DF-250	$\text{CH}_3(\text{PO})_4\text{OH}$	Total
DF-1012	$\text{CH}_3(\text{PO})_{6.3}\text{OH}$	32%
Aerofroth 65	$\text{H}(\text{PO})_{6.5}\text{OH}$	Total
DF-400		
DF-1263	$\text{CH}_3(\text{PO})_4\text{OHBO}$	Very good

### 2.2.1 Alcohol-type

In the alcohol frother family ( $C_nH_{2n+1}OH$ ) the polar group is the hydroxyl ( $-OH$ ) and the non-polar group is an alkyl chain ( $C_nH_{2n+1}$ ), linear or branched. The alcohol frothers tend to produce relatively shallow froths that carry little water (froth is said to be 'dry') (Klimpel and Hansen, 1988; Cytex Handbook, 2002).

The less powerful frothing nature of these frothers assists in making them more selective than their more powerful counterparts, the polyglycols, as they do not recover as much water with its associated entrained hydrophilic particles. This characteristic is a disadvantage in collecting coarse particles, which is favored by more stable froths. Explicitly, alcohol frothers are more suited to recover fine to medium particle sizes.

On the basis of the structure of the hydrocarbon group, alcohol-type frothers can be divided into three subgroups namely aliphatic, cyclic and aromatic alcohols.

Aliphatic Alcohols. These include both linear and branched forms with chain length 5 to 8 carbon atoms. The most common member of this group is Methyl-Isobutyl Carbinol (MIBC). Regarding branched vs. linear, each one has its advantages and disadvantages. There is some evidence of collector-frother interaction (Leja and Schulman, 1952) and in that regard molecular branching is reported to be more favorable to collector interactions (Klimpel and Hansen, 1988; Cytex Handbook, 2002) while linear counterparts result in close packing at the interface and thus are less able to accommodate collector molecules. Addison (1945) noted that molecular branching makes the molecule metastable, which appears to correlate with more effective frothing.

Cyclic Alcohols. Cyclic alcohols are typically represented by pine and eucalyptus oils which were the conventional frothers before the polyglycol family was developed. These frothers have become less common in flotation due to cost, inconsistency and availability. As late as the 80s pine oil was still widely used in copper concentrators (Lovell, 1982). Pine oil's main active ingredient is the cyclic alcohol  $\alpha$ -terpineol.

Aromatic Alcohols. Aromatic alcohols are available in a wide variety of grades usually selected by the boiling range. Those of the lower boiling range produce lighter, less persistent froths (Lovell, 1982). They have lost popularity in flotation as they are not water soluble. One of the most common aromatic alcohols is cresylic acid.

### 2.2.2 Alkoxy-type

These are alcohol derivatives with a more powerful frothing action; one of the most common alkoxy-type frothers is tri-ethoxybutane (TEB). They adsorb at much slower rates than alcohols; therefore the equilibrium is too slow to prevent coalescence and preserve bubble formation (Wrobel, 1951; Subrahmanyam and Forsberg, 1988). This slower adsorption is useful when a stable froth is required without a large reduction in bubble size, which may confer a practical advantage at the rougher stage.

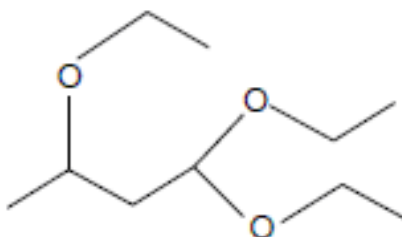


Figure 2.1 - Structure of TEB

### 2.2.3 Polyglycol-type

Polyglycols are polymeric derivatives of ethylene and propylene oxide and with alcohols comprise the two major families of commercial frothers (Klimpel and Isherwood, 1991; Laskowski and Woodburn, 1998).

Major members are the methyl esters of polyethylene glycol, polypropylene glycol, and the glycols themselves. They are available with varying molecular weight based on molecular structure described by the general formula  $[C_nH_{2n+1}(OC_2H_4)_mOH]$  or  $[C_nH_{2n+1}(OC_3H_6)_mOH]$  (Klimpel and Hansen, 1988; Cytec Handbook, 2002), where both  $n$  and  $m$  are integers,  $n$  representing the number of  $-CH_2-$  groups in the alkyl chain and  $m$  representing the number of propylene oxide or ethylene oxide groups. Polyglycols

generally provide reduction in bubble size at lower concentrations than alcohols and yield deeper froth that carries more water (froth is ‘wet’). Several commercial frothers are blends of alcohols and glycols and it is the relative proportion of each that controls the system properties.

The properties of polyglycol-type frothers are dependent on their molar mass, which determines both their solubility and frothing ability. Increasing the chain length (i.e. higher molecular weight) leads eventually to a loss in surface activity due to molecular coiling (Figure 2.2) at the interface as a consequence of the stronger van der Waals forces acting between components in the molecule itself (Tan, 2005; Chang and Franses, 1995; Comley et al., 2002). The loss in surface activity decreases the capability of froth formation. Johansson and Pugh (1992) assumed that molecule coiling is due to branching: polyoxy chains contained within polyglycol molecules typically indicate branching, which can result in coiling of these molecules.

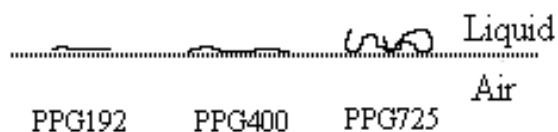


Figure 2.2 - Schematic representation of adsorbed molecules of polypropylene glycol (PPG). (Tan 2005)

Tan et al. (2006) attribute the loss of froth formation as a function of the lower spreading rate of these molecules as opposed to the linear ones. Linear molecules stabilize the interface through the Marangoni effect (Harris, 1982); the force also promotes flow in the water adjoining the surface of the bubble towards the higher surface tension (i.e., lower frother concentration) region that further opposes the flow out of water. The spreading rate is a function of the molecular interaction of neighboring molecules as a consequence of van der Waals forces, which are stronger in the case of the coiled molecules. This interaction effectively decreases the rate at which these molecules are able to migrate across the surface and so weakens the Marangoni effect.

## 2.3 FROTHER ROLES

In many flotation systems, the key factor controlling bubble size is the presence of frother. Frothers appear to function by controlling (retarding) bubble coalescence in balance with breakup of the air mass. This stabilizes fine size bubble dispersion in the slurry (pulp) phase, which both increases collision rate with particles and helps enable a stable froth to form, which permits collected particles to overflow from the cell.

Bubble size distribution is a factor determining metallurgical response. Bubbles must not be too large or too small. When bubbles are too small, particles may have insufficient contact time to attach, or if attachment does occur, the bubble buoyancy may be too low for practical recovery. On the other hand, as bubble size increases the strength of the water streamline around the bubble increases, making collision between particles and bubbles more difficult.

### 2.3.1 Preserving bubble size

Bubble size in flotation defines the surface area over which particles and bubbles interact and affects the system hydrodynamics (Dobby and Finch, 1986). The Sauter mean diameter ( $D_{32}$ ) is commonly considered the mean size relevant to flotation, typically ca. 0.5 - 2.0 mm (Gorain et al., 1995). The importance of bubble size in controlling bubble-particle collection efficiency has been repeatedly argued (Ahmed and Jameson, 1985; Dobby and Finch, 1986; Yoon and Luttrell, 1986; Fuerstenau, 1999). To be efficient, it is essential to generate a high population of small bubbles. Consequently, any factor with a major effect on bubble size will affect particle collection kinetics. Frother type and concentration have the most influence in controlling bubble size (Harris, 1976; Finch et al., 2006). The significance of this is revealed in a number of studies on bubble size, swarm behavior and rise velocity (Zhou et al., 1993; Sweet et al., 1997; Azgomi et al., 2007; Raffei and Finch, 2009). Other factors that influence bubble size are gas rate and the bubble generation device (Klimpel, 1984).

The mechanism controlling bubble size is related to the frother molecule adsorbing at the air-water interface oriented with the hydrophilic group to the water-side and the hydrophobic hydrocarbon chain to the air-side which provides a thermodynamically stable arrangement. The hydrophilic group forms hydrogen bonds with water molecules resulting in a water film around the bubble with properties differing from bulk water (Aston et al., 1989, Finch et al., 2006). The resilience of the film resists coalescence preserving the bubble size produced by the machine. The surface film can be considered to have a surface viscosity, i.e. a viscosity different from the bulk viscosity, which will differ in magnitude with frother type and concentration.

It can be readily demonstrated that frothers inhibit coalescence. Ata (2008) in the classical experiment where two bubbles are brought into contact showed that time for coalescence increased in the presence of frothers. In tests simulating the instant of bubble generation, Kracht and Finch (2009 a, b) showed again that frothers retarded coalescence. This gives rise to the notion that the machine produces small bubbles and the frother preserves the size. A decrease in the rate of coalescence is a compelling explanation of the decrease in bubble size with increasing frother concentration (Harris, 1976; Cho and Laskowski, 2002 a, b). Finch et al. (2008) noted some difficulties with the concept; for example observing that a typical bubble size in the absence of frother is ca 4 mm and with frother it is ca 1 mm, meaning the simultaneous suppression of coalescence of 64 bubbles has been achieved.

A role of the bubble surface water film properties was raised by Finch et al. (2006) to account for bubble size reduction in the presence of salts, noting that salt ions in solution may increase the rigidity of the surface film (Zieminski et al., 1967; Mackay, 1987). Although coalescence inhibition is the generally accepted explanation, fine bubbles in the presence of frother could result from an effect on breakup of the air stream entering a flotation cell (Finch et al., 2008).

Many studies have demonstrated the effect of frother on bubble size in the pulp zone (Klassen and Mokrousov, 1963; Finch and Dobby, 1990; Zhou et al., 1993; Sweet et al.,



1997). Bubble size in flotation machines decreases with increasing frother dosage to a certain concentration, now referred to as the critical coalescence concentration (CCC) (Cho and Laskowski, 2002 a, b), above which bubble size (at least the Sauter mean,  $D_{32}$ ) remains approximately constant. The use of the CCC term implies that coalescence is the governing mechanism and at the CCC bubble coalescence is completely prevented. Cho and Laskowski (2002 a) introduced CCC as a measure to characterize frothers on the basis that each frother possesses a “characteristic” CCC (Figure 2.3). Using CCC to characterize frothers has been evaluated subsequently by several authors. Grau and Heiskanen (2005) implied that CCC is independent of the machine type and mechanism used for dispersing the air and the operating conditions (air flow rate and impeller speed). Nasset et al. (2012) showed CCC is independent of impeller speed but does increase, albeit slowly, with increasing air rate. There are simply not enough data to comment on whether there is a machine type effect on CCC. Nasset et al. (2007) and Finch et al. (2008) used a model fit to define the end point (CCC) of an exponential curve and estimated CCC95, i.e. concentration achieving 95% of bubble size reduction compared to water alone.

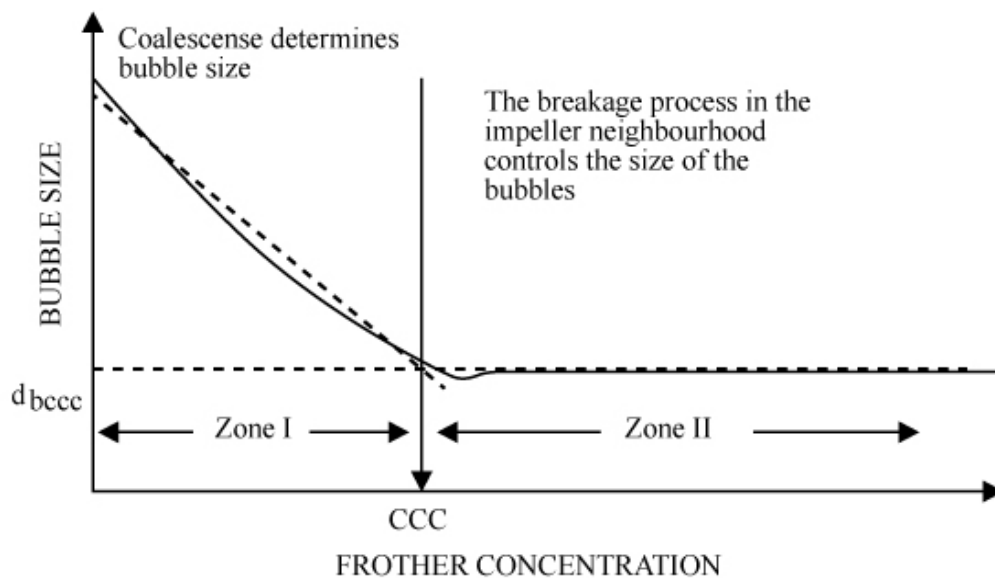


Figure 2.3 - Effect of frother concentration on bubble size in a flotation cell (Cho and Laskowski 2002a)

Grau and Heiskanen (2005) used solutions of three commercial frothers (Dow Frothers DF-200, DF-250 and DF-1012) in two Outokumpu cylindrical flotation cells, a stainless steel 50 dm<sup>3</sup> and a plexiglass 70 dm<sup>3</sup> referred to as OK-50 and OK-70, respectively. They demonstrated that preserving bubble size above the CCC is a function of operating parameters such as gas flowrate and impeller speed. Figure 2.4 indicates that the Sauter mean diameter is a function of impeller tip speed. In a similar exercise using a 0.8 m<sup>3</sup> Metso cell and DF 250 (Figure 2.5), Finch et al. (2008) reported no change in bubble size with increasing impeller tip speed. The authors believed that dominant factors in controlling bubble size are frother concentration and gas flowrate over the normal range of impeller speeds. Although data from both studies differ with regards to the impeller speed effect, both clearly show that controlling bubble size remains a function of cell operating variables.

Azgomi et al. (2007) determined that Sauter mean diameter remained constant above the CCC, but that gas holdup continued to increase. They showed that there was an increase in population of small bubbles at a concentration above the CCC, but the D<sub>32</sub> calculation is not sufficiently sensitive to track this change. That is, the constancy on bubble size above the CCC is partly due to the use of D<sub>32</sub>.

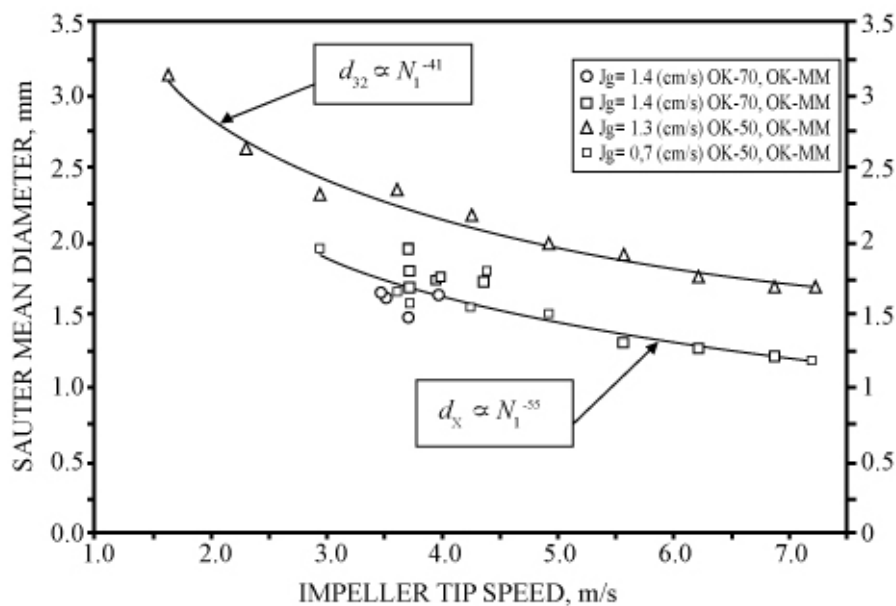


Figure 2.4 - Change in Sauter mean diameter as a function of impeller speed above CCC (Grau and Heiskanen, 2005)

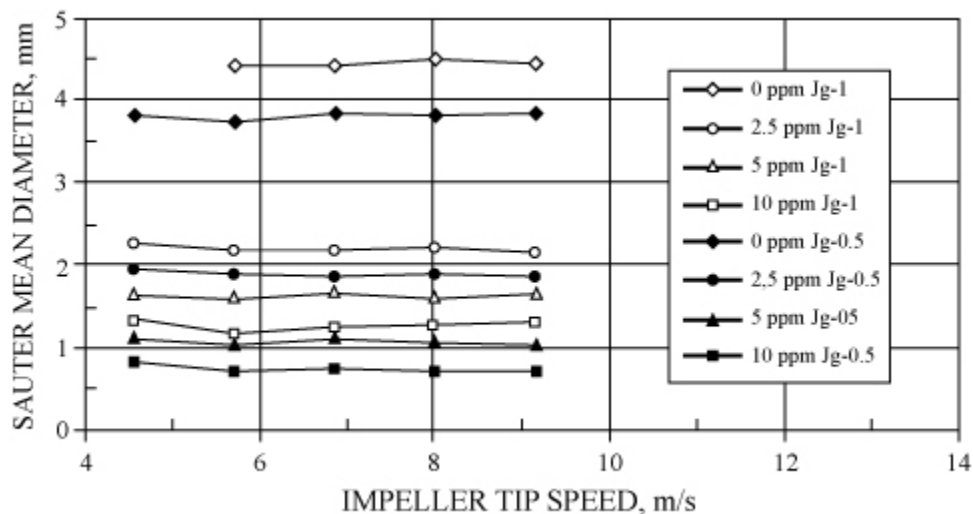


Figure 2.5 - Experimental results signifying the change in Sauter mean diameter with impeller speed above CCC (Finch et al., 2008)

Typically, and in the case of all examples presented in this section, CCC values are determined in water-frother solutions, i.e., in the absence of particles. Nasset et al. (2007) noted that prediction from two-phase results fitted plant data well suggesting a limited impact of solids. Grau and Heiskanen (2005) demonstrated an increase in bubble size at a high percent of solids. It was proposed that the increase in bubble size was a function of suppressing the turbulence with increasing solids concentration and an increase in the apparent density and viscosity of the pulp phase which can be expected to affect bubble size.

Thus in summary, while CCC or CCC95 is not totally a material constant it does help to quantify the role of frother type in bubble size reduction.

### 2.3.2 Stabilizing the froth phase

The second most important role of frothers in flotation is their effect on froth stabilization. The importance of the froth is reflected in the common reference to ‘froth flotation’. In an operating plant the froth is all that is seen so it was natural that the impact of frother on the froth attracted attention. Froth formation depends on the bubbles carrying water from the pulp into the froth at a rate sufficient to counter the natural drainage from the froth. In the absence of particles, this depends on two factors: the

bubble surface area flux, that is the rate of bubble surface area delivered into the froth (Xu et al., 1991); and the second is the frother type, which may influence how much water is carried per bubble, for example through an effect on the water film. This transport of water is important as it governs unselective recovery of particles by entrainment and consequently controls metallurgical (grade/recovery) performance.

Moyo et al. (2007) claimed that the amount of water transported per bubble was related to frother type but this work did not properly de-couple the water carried into the froth from that draining out of the froth; in other words the effect of frother type may have been on controlling drainage from the froth rather than on the amount of water carried into the froth. Nevertheless work continues to suggest a frother type effect on water transport into the froth (Zhang et al., 2010).

An effect of frother concentration on adsorption density can be expected. For example, Krzan et al. (2007) showed that single bubble velocity is a function of frother concentration (Figure 2.6). However, it is recognized that reaching steady state depends on how far the bubble has moved, i.e., how long it has been exposed to the solution as it rises (Sam et al., 1996).

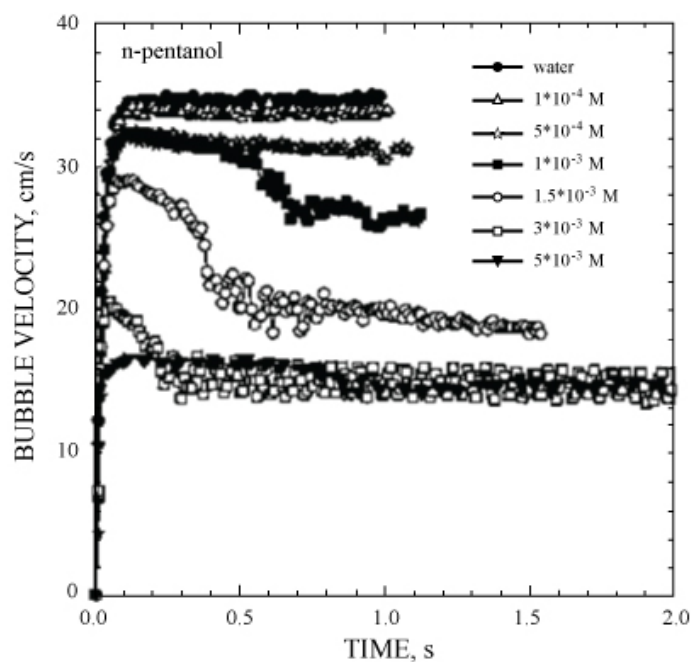


Figure 2.6 - Effect of frother concentration on bubble velocity (Krazan et al., 2007)

Correlation of properties with adsorption density, for instance calculated from the Gibbs adsorption isotherm using surface tension data, is problematic for moving bubbles. Azgomi et al. (2007) demonstrated that gas holdup increased with frother concentration (Figure 2.7) and Moyo et al. (2007) found that the amount of water overflowing a column operated with a constant froth layer increased with gas holdup (Figure 2.8). A possible explanation is that coverage is a function of frother concentration, which affects the amount of water associated with the bubble. The question remains how to estimate frother adsorption density for moving bubble swarms. This is one topic addressed in this thesis.

Before coverage can be estimated in flotation systems, frother concentration in solution is required. Frother addition (dosage) is commonly based on solids feed rate (i.e., g/ton) rather than concentration in solution. The solution concentration is the control variable but cannot easily be calculated from dosage due to effects such as water recycle (often carrying residual frother), incomplete dissolution, and contaminants in other reagents (for example xanthate collectors which have alcohol diluents). Measurement of frother concentration is the second topic addressed in this thesis.

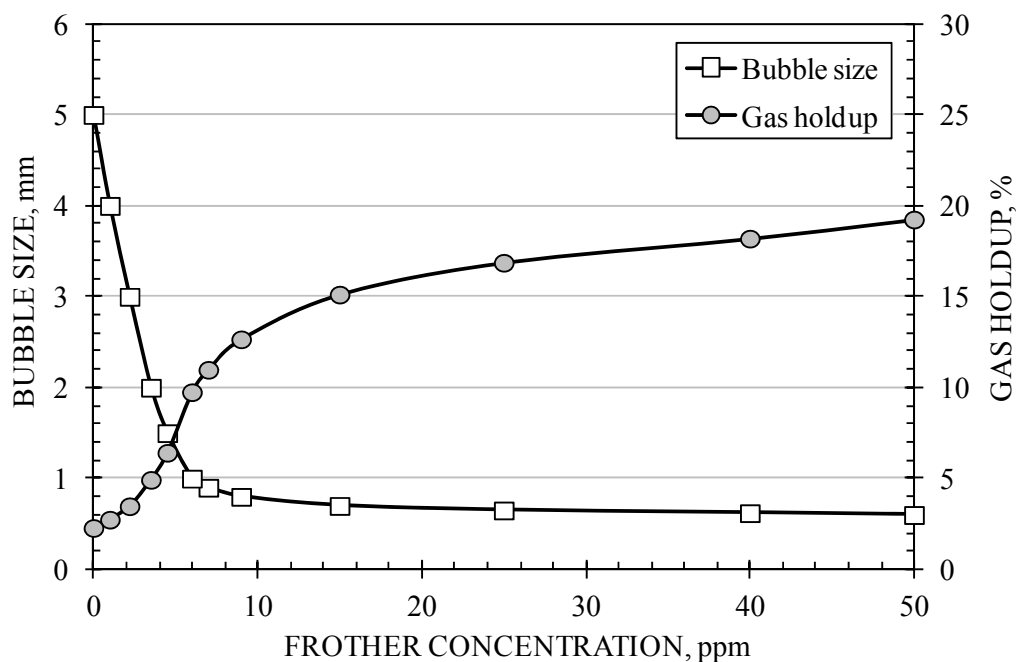


Figure 2.7 - Effect of frother concentration on bubble size and gas holdup (Azgomi et al., 2007)

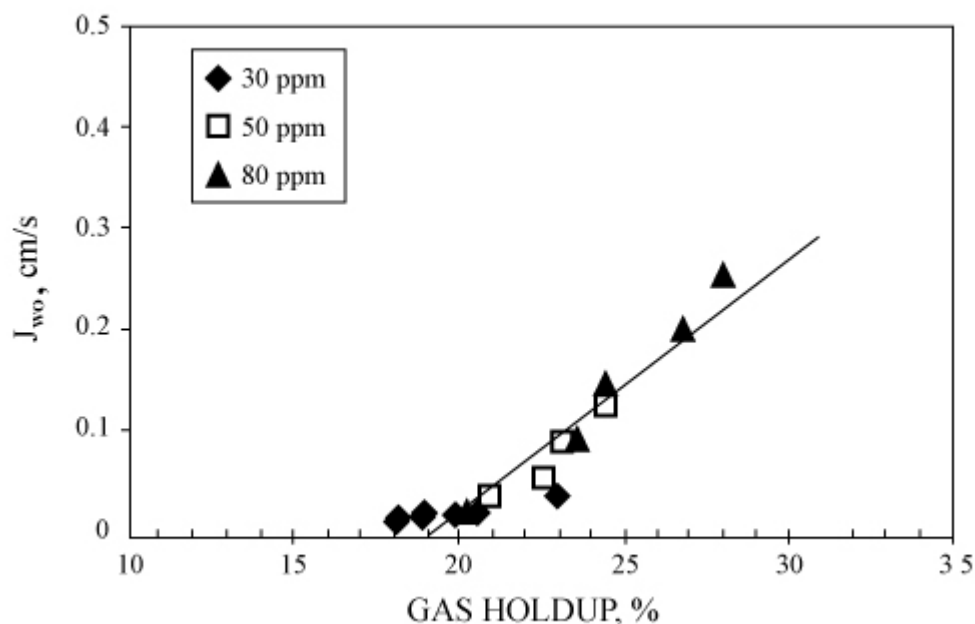


Figure 2.8 - Water carrying rate as a function of gas holdup (Moyo et al., 2007)

## 2.4 FROTHER CHARACTERIZATION TECHNIQUES

### 2.4.1 Hydrophile-lipophile balance (HLB)

The hydrophile-lipophile balance (HLB) was first proposed by Griffin (1949, 1954) for determining the hydrophilic characteristic of non-ionic surfactants and their tendency to form water/oil or oil/water emulsions. Laskowski and Woodburn (1998) used HLB as an empirical measurement for characterizing frother structure. A simplified commonly used method of HLB determination is that proposed by Davies (1957; Davies and Rideal, 1961). Davies assumed that HLB was an additive and constitutive indicator with hydrophilic and lipophilic (hydrophobic) group numbers assigned to various structural components. In the Davies approach the HLB is calculated by:

1.  $HLB = 7 + \Sigma (\text{hydrophilic group members}) - \Sigma (\text{lipophilic group numbers})$   
Knowing the chemical structural components (e.g.  $-\text{CH}-$  and  $-\text{O}-$  groups) the HLB number can be calculated (Laskowski and Woodburn, 1998).
2. HLB values vary between 1 and 20, with high numbers representing high water solubility whereas low numbers indicate low water solubility (Tanaka and

Igarashi, 2005). The HLB relates to the application: for example 4-10 HLB values are applied to frothers and 10-20 to collectors.

Laskowski (2003) and Pugh (2007) noted that frothers with low HLB numbers had low CCC values. Consequently, knowing HLB may facilitate selection of a frother to obtain the desired bubble size. However, the idea is not easily generalized. Zhang et al. (2012) proposed empirical relationships combining HLB and molecular weight based on a range of pure surfactants of the alcohol and polyglycol families to correlate with CCC.

#### 2.4.2 Dynamic frothability index (DFI)

Frothability is the focus of most frother characterization studies. As most frothability measurements are done in two-phase systems, foamability is perhaps the more appropriate term. These measurements depend on the physico-chemical conditions of testing, the test method and the application. The most well-known and widely used measurement, the dynamic frothability index (DFI) was introduced by Malysa (1981). The DFI builds on the foaminess unit,  $\Sigma$ , originally proposed by Bikerman (1973). Like the foaminess unit, the DFI is independent of the volumetric gas flowrate, cylinder geometry and sintered disc pore size. The main difference between Bikerman's foaminess unit and the DFI is the definition of residence time. In the DFI technique the lifetime is from bubble generation to bursting at the top of the froth and thus is the residence time of the whole system. (Note that in this definition the residence time also reflects the magnitude of gas holdup; it is quite possible in that case to have a DFI with no froth formation). In Bikerman's case, residence time is associated only with the froth, i.e. is equivalent to the average bubble lifetime in the foam.

#### 2.4.3 Critical coalescence concentration (CCC)

The combined use of CCC, HLB and DFI aims to provide a complete frother characterization test in the sense that it captures both the bubble size and froth stabilization functions (Laskowski, 2003) (Table 2.2). A relationship between CCC and DFI is shown in Figure 2.9.

Table 2.2 - List of frothers, their chemical formulae, molecular weight, CCC and DFI values (after, Laskowski 2003)

Frother	Chemical formula	Molecular Mass (g/mol)	HLB	CCC (mmol/L)	DFI (s.L/mol)
MIBC	$\text{CH}_3\text{CHCH}_2\text{CH}(\text{OH})\text{CH}$	102.20	6.1	0.110	34 000
HEX	$\text{C}_6\text{H}_{13}\text{OH}$	102.20	6.0	0.079	33 000
DEMPH	$\text{C}_6\text{H}_{13}\text{OH}(\text{EO})_2(\text{PO})$	248.40	6.6	0.013	290 000
DEH	$\text{C}_6\text{H}_{13}\text{OH}(\text{EO})_2$	190.30	6.7	0.031	94 000
MPDEH	$\text{C}_6\text{H}_{13}\text{OH}(\text{PO})(\text{EO})_2$	248.40	6.6	0.016	170 000
(PO)1	$\text{CH}_3(\text{PO})\text{OH}$	90.12	8.3	0.520	5 700
(PO)2	$\text{CH}_3(\text{PO})_2\text{OH}$	148.12	8.15	0.170	35 000
DF200	$\text{CH}_3(\text{PO})_3\text{OH}$	206.29	8.0	0.089	196 000
DF250	$\text{CH}_3(\text{PO})_4\text{OH}$	264.37	7.8	0.033	208 000
DF1012	$\text{CH}_3(\text{PO})_{6.3}\text{OH}$	397.95	7.5	0.015	267 000

(EO) and (PO) are abbreviations for  $(-\text{OC}_2\text{H}_4-)$  and  $(-\text{OC}_3\text{H}_6-)$ , respectively

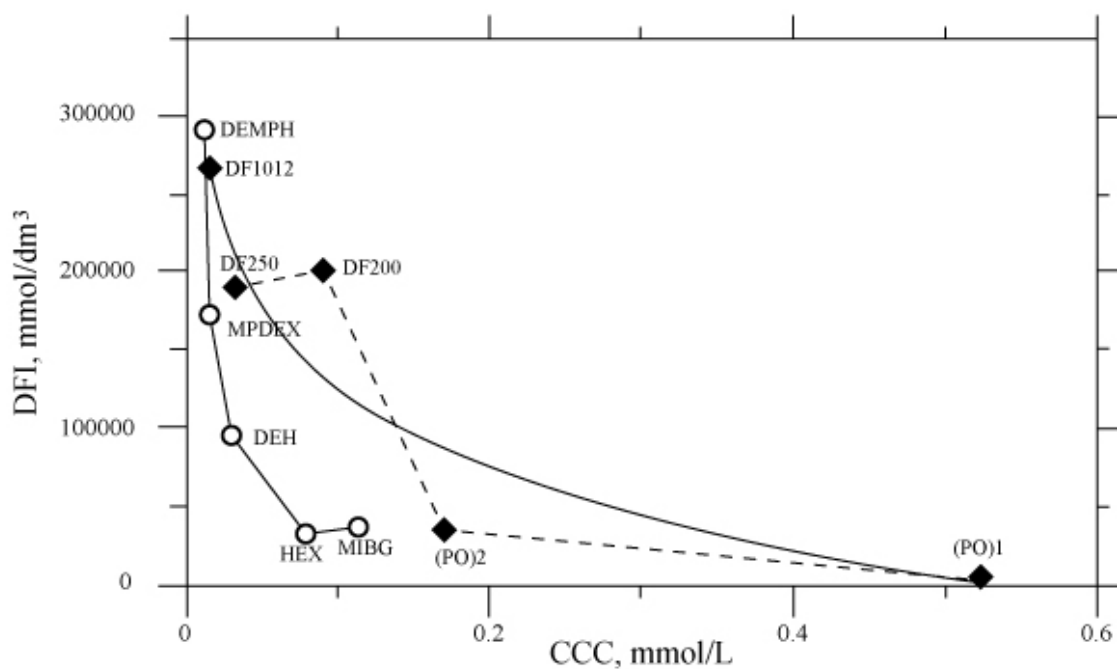


Figure 2.9 - DFI as a function of CCC for tested frothers Laskowski et al. (2003b)



#### 2.4.4 Hydrodynamic characteristics of frother chemistry

Based on the work of Azgomi et al. (2007) and Moyo et al. (2007), Cappuccitti and Nasset (2009), proposed a method to classify frothers using gas hold up (Eg) vs. froth height in a column test to capture the two frother functions. This, for example, readily identifies frothers giving more control over froth stability, namely the polyglycols, from those giving more control over gas holdup (i.e., bubble size), namely the alcohols.

### 2.5 INTERFACIAL PROPERTIES

The frother adsorption at the gas-liquid interface, controls bubble size reduction and froth stabilization. The properties of the adsorption layer, formed at the liquid interface, are in direct correlation with the frother structure as demonstrated by Fainerman (1992). These properties include the surface activity of the surfactant, the character of the surface tension isotherm and details of adsorption layer composition. There are three potential parameters to characterize frothers based on their interfacial properties, namely:

1. Surface tension;
2. Fractional surface coverage; and
3. Surface elasticity.

#### 2.5.1 Surface tension

Surface tension measurement is the principal method for determination of frother adsorption at the interface through its relation to the surface excess concentration using an appropriate adsorption isotherm. Time to reach equilibrium and adsorption density depends on frother type and concentration. In a dynamic process such as bubble formation in a flotation machine where there might not be adequate time for frother adsorption to reach equilibrium, dynamic surface tension may be of use. Assuming bubbles have enough time to attain equilibrium by the time they reach the pulp-froth interface, then equilibrium surface tension could be considered applicable in that situation (Addison, 1945; Aston et al., 1989 and Comley et al., 2002).

A shortcoming of using surface tension is the limited response in the concentration range in flotation (Sweet et al., 1997; Laskowski and Woodburn, 1998). Sweet et al. (1997) demonstrated a decrease in bubble size for n-hexanol and MIBC whereas over a similar concentration range there was no significant lowering in surface tension.

Although surface tension is considered a parameter related to the interfacial impact of frother adsorption, which connects with the state of the interface (Malysa et al., 1987 and Jachminska et al., 1995), at least the equilibrium value has limited applicability in flotation studies. Regardless, surface tension-related phenomena continue to attract attention in characterizing frothers, as discussed next.

### 2.5.2 Fractional surface coverage

Fractional surface coverage ( $\theta$ ) is derived from surface tension data. It is a measure of frother coverage at the interface relative to monolayer frother coverage:

$$\theta = \Gamma / \Gamma_{\text{inf}} \quad (2.1)$$

Where  $\Gamma$  represents the surface excess concentration for a given bulk concentration at a given time and  $\Gamma_{\text{inf}}$  represents the maximum surface excess concentration at monolayer coverage.

Comley (2001) suggested the use of this adsorption parameter to demonstrate that bubble size was a function of fractional surface coverage thus eliminating the influence of frother type at least for the family of frothers (Figure 2.10).

As a function of the fractional surface coverage Comley (2001) also performed similar experiments for the comparison of the water recovery rate affected by frother type and concentration using n-alcohol and Dowfroth 200. Although for the n- alcohols similar water recovery results were obtained, Dowfroth 200 showed significantly higher values rates for the same fractional surface coverage range. The assumption was that the difference may well be due to differences in the polar groups of these frothers and their connection (H-bonding) with surrounding water molecules: Dowfroth 200 contains three ( $-\text{O}-$ ) groups and one group ( $-\text{OH}-$ ) group, therefore it can interact with seven water

molecules (two per  $-O-$  group and one per  $-OH-$  group) in comparison to the n-alcohols with a single  $-OH-$  group.

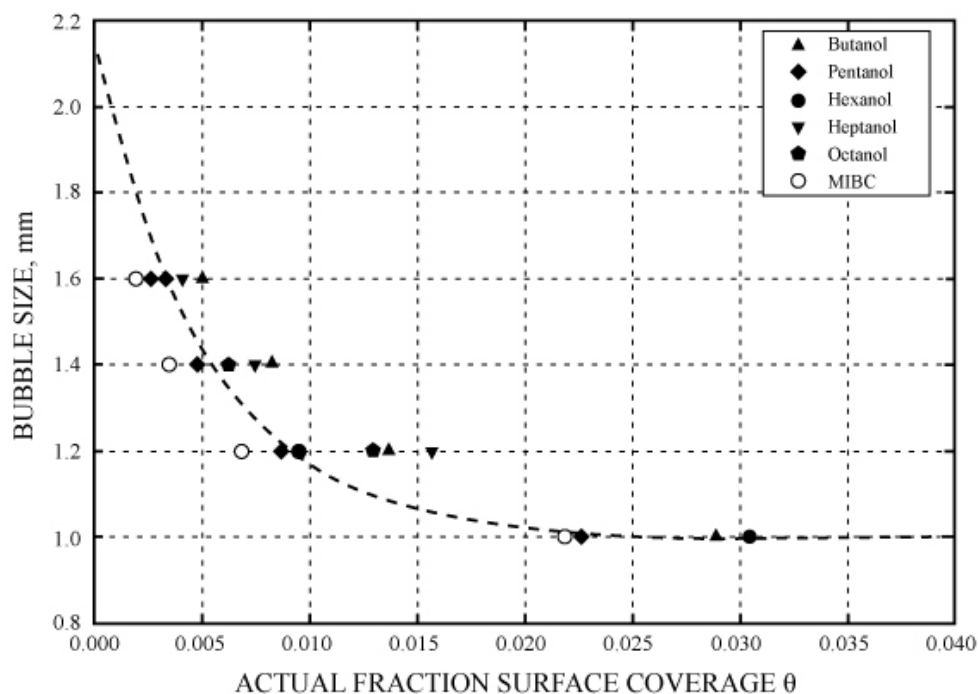


Figure 2.10 - Bubble size as a function of fractional surface coverage for the series of n-alcohol (Comley, 2001)

Water recovery rates vary as a function of frother type. In comparison with n-hexanol, in n-heptanol, owing to the additional  $-CH-$  group in the hydrocarbon chain, there is a stronger hydrogen bond with water molecules. Therefore, the amount of water held up within the froth will be more than that of n-hexanol (Comley, 2001).

### 2.5.3 Surface elasticity

Surface elasticity is a derivative of surface tension. It is a consequence of change in bubble size and the resulting re-distribution of surfactant on the bubble surface. It depends on the bulk frother concentration and the local differences of the accumulated frother adsorbed on one part of the surface compared to another. There are two surface elasticities:

Gibbs elasticity or equilibrium elasticity refers to the lateral movement of adsorbed molecules along an interface as a consequence of a disturbance causing a change in

surface area which exceeds the adsorption rate of molecules from the bulk solution to re-establish equilibrium. In such situations, the adsorbed layer behaves as an insoluble monolayer with no transfer of molecules from the bulk solution. It is believed that Gibbs elasticity can explain the correlation between surface elasticity and froth stability (Wang and Yoon, 2007).

Marangoni elasticity is measured some time before equilibrium (ultimate value of surface concentration) is reached; hence it is temporary and it is quantified through surface dilational elasticity and viscosity, and surface shear elasticity and viscosity (Tan et al., 2005). Marangoni elasticity is larger than Gibbs elasticity (Ross and Morrison, 1987).

The water-air interface in the dynamic condition of flotation systems is probably never at equilibrium. In consequence, it may well be more appropriate to use Marangoni elasticity rather than Gibbs elasticity. Findings of Malysa et al. (1985) support the relevance of surface dilational elasticity in the foaming process. However Gibbs elasticity is usually easier to measure due to the complexity of surface dilational measurements (Tan, 2005; Tan et al., 2005; Wang and Yoon, 2007).

## **2.6 FROTHER ANALYSIS TECHNIQUES**

To make use of our understanding of frother roles in flotation, it is necessary to know frother concentration. The techniques reported to measure frother concentrations include Gas Chromatography (GC) (Giachetti et al., 1996; Veulemans et al., 1987; Huang et al., 2002), total organic carbon (Hadler et al., 2005; Zhang et al., 2010) and a colorimetric technique (Gelinas and Finch, 2005), the latter developed for on-site i.e., at-plant analysis (Zangoi et al., 2010).

Chromatography, gas (GC) or high pressure liquid (HPLC), although versatile for laboratory experiments, for on-site applications is limited by equipment and standards availability as demonstrated in the extraction of polar glycol ethers from aqueous solutions (Bormett et al., 1995). Tsatouhas et al. (2006) used GC to determine the frother concentration in the filtrate samples from a plant. The samples, however, were

transported off-site and thus risked loss of frother by evaporation and decomposition. This unknown source of error limits the method's suitability for tracking frother concentration in a circuit. Acknowledging these limitations, Tsatouhas et al. (2006) demonstrated a preference for the frother at this particular plant to remain in the bulk solution in similar quantities as the initial dosage rather than being concentrated in the froth phase as generally thought. The authors concluded that the lack of froth stability in scavenger flotation cells was not the consequence of a lack of frother but the lack of particles. In situations where floatable solids are in low concentration, as in scavengers, regardless of frother concentration froth stability is compromised. Similar GC measurements were carried out by Zanin et al. (2009) and Gredelj et al. (2009) to understand frother behavior in a flotation circuit. They measured the concentration of a blend frother and MIBC in two different concentrators. In one case, MIBC was lost from solution as a consequence of adsorption due to hydrophobic interaction with carbonaceous material present. In this case addition of 400g/t MIBC was required to compensate for the large fraction adsorbed at the mineral surface (Gredelj et al., 2009). Otherwise results were similar to that of Tsatouhas et al. (2006) whereby the frother persists in the pulp phase.

Total Organic Carbon (TOC) is a fast and precise method for routine determination of organic carbon in waters. Hadler et al. (2005) employed TOC to take into account the contribution of carbon from the ore. However, the technique on its own is limited to cases where only one organic compound is involved (Zhang et al., 2010). Zhang (2012) combined TOC with NMR spectroscopy (Nuclear Magnetic Resonance) to extend analysis to blends.

The method suited to measure frother concentration in plant streams is the colorimetric technique adapted by Gelinis and Finch (2005). The technique is based on the Komarowsky reaction for the analysis of aliphatic alcohols (Coles and Tournay, 1942) and was first used for a frother, MIBC, by Parkhomovski et al. (1976). The Komarowsky reaction involves the reaction of dehydrated frother molecules and salicylaldehyde. As the reaction is slow at room temperature, the samples are maintained in a boiling water

bath. Reaction time plays a role in the color intensity of the product as the reaction approaches completion. The reaction is applicable to alcohols except ethanol and methanol (Ekkert, 1928, quoted by Gelinas and Finch, 2005), aromatic alcohols and phenols (Fellenberg, 1910, quoted by Gelinas and Finch, 2005) and polyglycol as demonstrated by Gelinas and Finch (2005). These chemistries describe most frothers used in mineral flotation today. The technique was applied to test whether frother partitioning between pulp and froth under plant conditions could be detected. In the case of MIBC partitioning was limited but in the case of the polyglycol F150 it was extensive and helped to explain excess frothing in downstream flotation banks.

The presence of frother in flotation is clearly important and knowing its concentration is crucial to understand and control cell operation. The first part of this thesis addresses measurement of frother concentration.

## **2.7 FROTHER COVERAGE**

When a bubble is formed its surface is accessible to adsorption of surfactant (Jachimska et al., 1998). Once in motion adsorption and desorption occurs. The movement of bubbles in a liquid is influenced by the kinetics of this adsorption-desorption process. In one interpretation, a steady state is reached after a certain time, with the amount of frother adsorbing on one part of the bubble surface (usually the leading part) being equal to the amount desorbing from another part (usually the rear). Here the motion of the surface appears as the driving force for adsorption-desorption. Theoretical work by Dukhin et al. (1995) considers that there is uneven coverage, caused by the viscous drag of the medium exerted on the air/water interface. Surface tension gradient-driven phenomena are connected with a non-uniform surfactant distribution.

In other studies (Jachimska et al., 2001) focus has been on bubble growth at the formation site to the moment of detachment (bubble formation time) which identifies if the diffusion rate and adsorption rate at the air/water interface are fast in comparison to the bubble expansion rate; if fast enough then the frother adsorption coverage reaches

equilibrium at every stage of bubble growth. They also consider different degrees of coverage depending on ratio of velocity of bubble growth and kinetics of frother adsorption.

Frumkin and Levich (1947, quoted by Zhang and Finch, 2001) developed a theory to explain the lowering of velocity of a bubble in frother solutions as a consequence of uneven frother distribution on the bubble surface. According to their theory, motion of a bubble induces adsorption–desorption exchange with the subsurface adjacent to the bubble surface. Frother molecules are transported to the bubble interface by convection and diffusion from the bulk solution and adsorb at the front of the bubble from where they are swept to the rear where they may desorb. In their view, there are unequal rates of frother uptake at the front of the bubble and loss from the rear, which induces surface tension gradients acting to increase drag and consequently retard bubble rise (see also Krzan et al., 2007).

In another interpretation, lower velocity of rising bubble is related to viscosity of the surface water film surrounding the bubble. By increasing frother concentration, more water molecules associate with the bubble, increasing surface viscosity and lowering the velocity (Nguyen and Schulze, 2004). Accompanying a slower bubble rise is an increase in gas holdup.

Several techniques have been proposed in the literature to measure surface coverage, for example the surface microtome method (McBain and Swain, 1936), the known-surface area foam collection and collapsing (Wilson et al., 1957) and the use of radio labelled surfactants (Nilsson, 1957). Although they represent a direct measurement, all these techniques have features that make them difficult to use, particularly in the case of rising bubbles, which is our case of interest.

A commonly used approach is to apply Gibbs' equation (2.2) to measurements of surface tension in frother solutions of varying concentrations. In this case, the concentration of frother molecules adsorbed at the interface  $\Gamma$  is calculated from the slope of the linear

part of the surface tension vs. frother concentration curve, which implies that  $\Gamma$  is a constant independent of the concentration.

$$\Gamma = \frac{C}{RT} \times \frac{d\sigma}{dC} \quad (2.2)$$

where,

- $\Gamma$  concentration of frother molecules adsorbed at the interface
- $C$  concentration of frother molecules in the bulk of the solution
- $\sigma$  surface tension
- $R$  ideal gas constant
- $T$  absolute temperature

Zhang et al. (2010) used this method to estimate equilibrium frother concentration on bubble surface (adsorption density) for four commercial frothers.

There are several problems with this approach. For example, surface tension is measured on a static surface which reaches equilibrium with the bulk solution, whereas in flotation, the rising bubble encounters frother molecules and equilibrium is more a case of reaching steady state between frother adsorbing and desorbing, which may result in a different surface coverage than that estimated via Gibbs. An additional shortcoming of using surface tension is the lack of response in the frother concentration range used in flotation (Sweet et al., 1997; Laskowski and Woodburn, 1998). Sweet et al. (1997) demonstrated a strong correlation between bubble size and frothability over a similar concentration range for n-hexanol and MIBC, whereas no significant difference was observed in measured surface tension.

The assumption that surface coverage is independent of frother concentration is not supported by published evidence. For example steady-state single bubble velocity, which is a consequence of bubble surface characteristics determined by adsorbed frother molecules, is a function of frother concentration (Sam et al., 1996; Krzan et al., 2007), as illustrated in Figure 2.6, with notable differences, as expected, for different frothers (Rafiei and Finch, 2009).



Changes in gas holdup and water carried by bubbles with frother concentration, both also a consequence of bubble surface characteristics, have also been reported. As previously indicated, Azgomi et al. (2007) demonstrated that gas holdup increased with frother concentration (Figure 2.7), and Moyo et al. (2007) found that the amount of water overflowing a column operated with a constant froth layer increased and correlated with gas holdup in the bubbly zone (Figure 2.8). In the case of Moyo et al. (2007), the results also suggested that the adsorption process is fast, as the column used was only 1 m high with some measurements made with a 0.35 m froth, which leaves a short distance for the bubbles to adsorb frother molecules. All these effects on bubble movement are a consequence of changes in the concentration of adsorbed molecules on the bubble surface, and demonstrate that coverage is affected by frother type and concentration. Therefore, the use of Gibbs' equation to estimate frother coverage seems suspect and an alternative approach is necessary for flotation related applications.

## CHAPTER 3 - FROTHER ANALYSIS TECHNIQUE

### 3.1 INTRODUCTION

Flotation is a separation process based on the selective collection of particles by bubbles. Measurement of properties of the bubble population, so-called gas dispersion parameters (gas velocity, gas holdup and bubble size), has become a tool to characterize industrial flotation cells (Gomez and Finch, 2002; 2007). The cell characterization measurements have shown the important role played by frothers in controlling bubble size and gas holdup. Frothers also play a role in stabilization of the froth layer (Rao and Leja, 2004). The stabilization is controlled by the water carried into and retained in the froth by the bubble swarm (Moyo et al., 2007). This transport of water is important as it governs unselective recovery of particles by entrainment. Recent efforts to understand frother functions suggest that knowing and manipulating frother type and concentration can be used effectively to improve cell operation and circuit performance (Gelinias and Finch, 2007; Cappuccitti and Nasset, 2009; Gomez et al., 2011).

The action of frother in reducing bubble size is commonly attributed to inhibiting coalescence (Harris, 1976). Basic studies bringing two bubbles into contact support this contention showing that the time to coalesce increases in the presence of frother (Cho and Laskowski, 2002 a; Ata, 2008). Measurements on bubble swarms also show that frothers retard coalescence (Kracht and Finch, 2009 a, b). These observations have introduced the hypothesis that machines produce small bubbles, and the frother preserves them. This hypothesis is illustrated in flotation machines where bubble size decreases with increasing frother dosage to a certain concentration above which bubble size is approximately constant (Finch and Dobby, 1990). This concentration has been termed the critical coalescence concentration (Cho and Laskowski, 2002 a, b) and the corresponding minimum bubble size identified with the size of bubble produced by the machine.

The action of frother in providing froth stability is connected to the transport of water by the bubble swarm. The notion that frothers influence how much water is carried per

bubble is still debated. Gelinas and Finch (2005) showed that the film thickness on a bubble blown in air depended on frother type. Laboratory experiments in flotation machines have demonstrated that water flow rate to the froth product does vary with frother type and concentration (Nguyen et al., 2003; Moyo et al., 2007; Zhang et al., 2010), however, the major impact on water recovery is the presence of hydrophobic particles that load the bubble and reduce coalescence in the froth by providing a mechanical (or steric) barrier (Hunter et al., 2008). There is also evidence indicating that frother influences bubble shape (Kracht and Finch, 2010), and a strong correlation between bubble shape and velocity has been demonstrated (Gomez et al., 2010; Quinn et al., 2013).

Although frothers are commonly added (dosed) on the basis of solids feed rate (e.g., g frother/ton ore), the frother concentration required is that in solution. Calculation of solution concentration (e.g. ppm) is straightforward if the pulp density (% solids) is known. However, possibilities such as incomplete frother dissolution, unknown frother content in recycled process water, and uptake (adsorption) of frother by solids (carbonaceous materials are particularly prone to do this) make reliable estimation of concentration difficult. Other difficulties in estimating concentration include the use of frother blends, and the contribution of reagents with frothing properties such as collectors like fatty acids and diluents such as alcohols in xanthate collectors. The calculation of the concentration in the froth inter-bubble water is even more complicated as the amount of frother adsorbed on bubbles and released to the water upon coalescence and bursting is not known.

Experience has demonstrated that frother concentration is crucial information to interpret gas dispersion properties (Gomez and Finch, 2007). A literature review indicated that a colorimetric technique (Gelinas and Finch, 2005) was appropriate for industrial settings. Using the analysis technique as originally described indicated that some refinements were necessary to increase the low analysis rate (4 to 6 samples per day) and to extend application to low solubility frothers (Zangooi et al., 2010). The use of the technique in many concentrators around the world further demonstrated that the procedure had to be

adaptable to reagents with different specifications and to waters containing diverse ions, sometimes at very high concentrations. The purpose of this chapter is to provide a detailed description of the frother analysis technique, the characterization of the steps in the procedure, and the refinements which made the technique acceptable to meet industrial requirements and standards.

## **3.2 LITERATURE REVIEW**

A search indicated that several techniques have been used to measure frother concentration in flotation systems: gas chromatography (Huang et al., 2002), color intensity (Gelinas and Finch, 2005), total organic carbon (Hadler et al., 2005), high performance liquid chromatography (HPLC) and nuclear magnetic resonance (NMR) (Zhang et al., 2013).

### **3.2.1 Application of gas chromatography**

One family of frothers is the glycol ethers which will serve to illustrate the application of gas chromatography GC). The common technique is GC with flame ionization detection (FID) (Giachetti et al., 1996; Veulemans et al., 1987). The technique can require extensive sample preparation, for example conversion of analytes to halogenated derivatives (pentafluorobenzyl) and extraction from aqueous solution into organic solvent (Bormett et al., 1995). Huang et al. (2002) employed GC-FID in conjunction with headspace solid-phase micro-extraction (HS-SPME) to determine glycol ethers. SPME is fast, inexpensive and solvent-free (Zhang et al., 1994) and the HS attachment means the sample does not come into contact with the polymer-coated silica fiber, thus minimizing matrix interferences (Zhang and Pawliszyn, 1993).

Tsahoutas et al. (2006) used gas chromatography to determine frother concentration in filtrates from plant samples. The samples had to be sent off-site, increasing analysis costs and raising concerns regarding sample integrity. The cost and sophistication of the technique make it unsuited to routine on-site plant applications.

### **3.2.2 Colorimetric technique**

The colorimetric technique for measuring frother concentration in samples of plant streams was introduced by Gelinas and Finch (2005). The technique is based on the Komarowsky reaction for the analysis of aliphatic alcohols (Coles and Tournay, 1942) and was first used for a frother, MIBC (methyl-iso-butylcarbinol), by Parkhomovski et al. (1976). The Komarowsky reaction involves the formation of a colored solution as a consequence of the dehydration of the frother molecule by concentrated sulfuric acid and its subsequent reaction with aldehyde. The reaction occurs in aliphatic alcohols except ethanol and methanol (Ekkert, 1928, quoted by Gelinas and Finch, 2005), and aromatic alcohols and phenols (Fellenberg, 1910, quoted by Gelinas and Finch, 2005), which are the three group chemistries that describe most frothers used in mineral flotation. The potential for process diagnosis and optimization was demonstrated (Gelinas and Finch, 2007), for example, the effect of frother dosage and location of addition points and the presence of remnant frother in recycle waters. The technique, however, had a fairly low analysis rate (4 to 6 samples per day) and limitations when applied to low solubility frothers.

### **3.2.3 Other methods**

Total organic carbon (TOC) offers a fast and precise method for routine analysis especially if there is only a single organic compound (Hadler et al., 2005; Zhang et al., 2010). Zhang et al. (2013) combined TOC with other analytical techniques to extend its application to frother blends. They used high performance liquid chromatography (HPLC) in one case and in a second a combination of proton nuclear magnetic resonance (H-NMR) and TOC analysis. While providing great flexibility in the analysis of frother blends, but on-site application is limited.

## **3.3 COLORIMETRIC TECHNIQUE FOR THE ANALYSIS OF FROTHERS**

The technique is based on the Komarowsky reaction which involves the interaction of a frother (specifically the OH group), concentrated sulfuric acid, and an appropriate

aldehyde. The color formation is due to the dehydration of the frother molecule by the sulfuric acid, and its subsequent reaction with the aldehyde. The color intensity is proportional to concentration over a certain range, which is used for constructing a calibration curve of UV-VIS spectrum (at a selected wavelength) vs. concentration.

The analysis involves several steps: a frother extraction stage, the formation of a colored solution, the collection of a UV-VIS spectrum, and the calculation of the frother concentration. The steps are described in detail to establish where refinements were necessary to improve analysis reliability.

1. Frother is extracted from the sample into chloroform. This is done by mixing the two phases in a 100 mL vial in the presence of 15 g of solid sodium chloride. The sodium chloride aids the transfer and reduces foaming at the interface. Although the partition coefficient favours transfer to the organic phase, two extractions were found to be necessary to extract all the frother. The loaded organic phase is separated and contacted with concentrated sulfuric acid (Figure 3.1). The frother dehydrates (loses a water molecule) at the chloroform-acid interface. The reaction rapidly goes to completion and the dehydrated frothers accumulate in the acid phase. The loaded acid is separated and passed to the next step, generation of the colored solution.

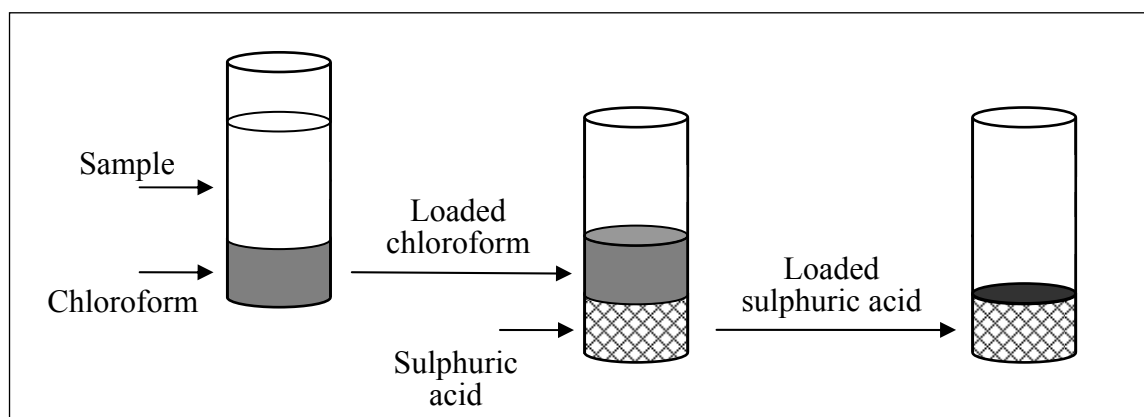


Figure 3.1 - Frother analysis: frother extraction stage

2. Formation of a colored solution via the Komarowsky reaction. This is accomplished by adding the color indicator (0.1 mL of 5% salicylaldehyde dissolved in a 1:1 solution of acetic acid in water) to the vial containing the loaded sulfuric acid, and maintaining the mixture at temperature in boiling water for a selected reaction time. The reaction is stopped by immersion of the vial in an ice bath (Figure 3.2).

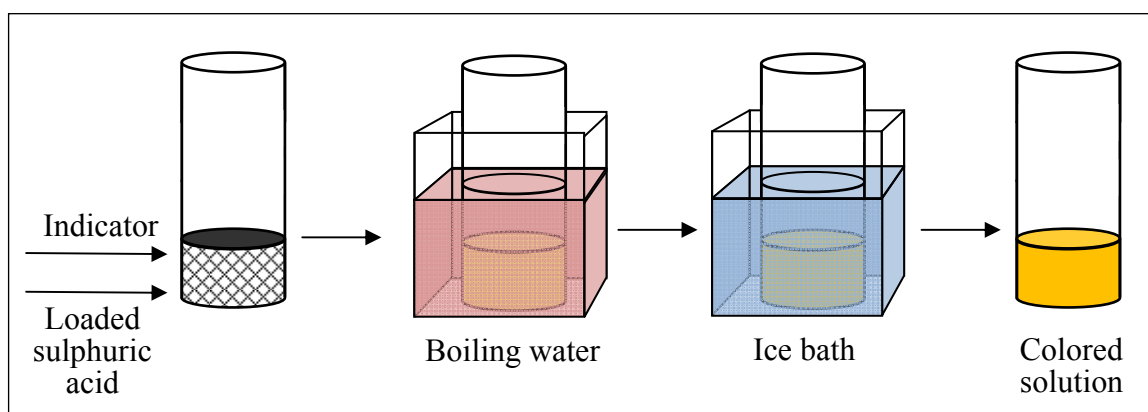


Figure 3.2 - Frother analysis: reaction to form colored solution

3. Collection of UV-VIS absorbance spectrum. The colored solution is transferred to a cuvette and loaded in the UV-VIS instrument. Some precautions are necessary as the maximum absorbance measurable in the UV-VIS spectrophotometer in use is 3 (i.e., the frother concentration in the sample must result in a solution with a color intensity giving an absorbance below 3). Absorbance spectra are collected for wavelength ranges between 490-560 nm.
4. Calculation of frother concentration. This requires comparison with a calibration curve, frother concentration vs. absorbance, constructed with absorbance values on standard solutions (known concentrations) at the selected wavelength in the 500-560 nm region. By ensuring that the concentration level is not too high, the calibration will be linear. Measuring the absorbance of the unknown sample at the same selected wavelength the unknown concentration can be 'read' from the calibration curve. The wavelength selection affects the accuracy of the analysis; the suggested selection criterion is the wavelength giving maximum (peak) absorbance.

### **3.4 REFINEMENTS TO THE ANALYTICAL PROCEDURE**

Refinements were initially driven to extend the technique to a wider range of frothers than tested by Gelinas and Finch (2005, 2007) and to speed up analysis while retaining reliability. As the work progressed, however, it became clear that scrutinizing every aspect of the procedure had the potential to increase accuracy (validity) and precision (reliability). The results of this examination are described.

#### **3.4.1 Preparation of reagents and calibration standards**

For this analysis the chloroform has to be stabilized with an additive. Securing reliable supplies proved difficult (see below). When the correct supply was available it could be used directly. The original 75% (by volume, v/v) concentrated sulfuric acid (84.6 % by weight) was replaced by 85% v/v to increase color intensity. The Komarowsky indicator was prepared as before, by diluting 5 mL of salicylaldehyde in 50 mL of glacial acetic acid and 45 mL of water.

The original procedure prepared a 500-ppm stock solution by dissolving 0.5 g of frother in 1 L of water and a second stock solution (50 ppm) prepared from the first by dilution, which was used to prepare the calibration standards. Weighing exactly 0.5 g of frother proved to be problematic. It was decided to prepare a single stock solution (25 ppm) by weighing close to 50 mg of frother and then adding to a 2 L flask the calculated weight of water. In the case of test samples, the 100 mL volumetric flask (with the sodium chloride) is filled to volume with water filtered from the pulp sample. Dilution may be necessary for samples with concentrations above the calibration range.

#### **3.4.2 Frother extraction**

##### Chloroform specifications

Poor reproducibility was apparent on occasions both at McGill and on site. The problem was tracked to the chloroform when products from different suppliers had different shelf lives, or when products from different suppliers did not have the same specifications. Chloroform requires a stabilizer to avoid decomposition and normally either of two



compounds is used: ethanol or amylene. The color developed by the same frother solution is different depending on the stabilizer used, with ethanol being a better choice as amylene gives too strong a color (Figure 3.3a) in the analysis of a sample with no frother (0 - ppm standard).

It was also found that ethanol-stabilized chloroform supplies may have different shelf lives resulting in different outcomes, as demonstrated when four different chloroform stocks were used in the analysis of samples with no frother (0-ppm solution). Although the chloroform shelf lives were unknown, the results suggest that the darkness of the final solution is affected by shelf life (Figure 3.3b).

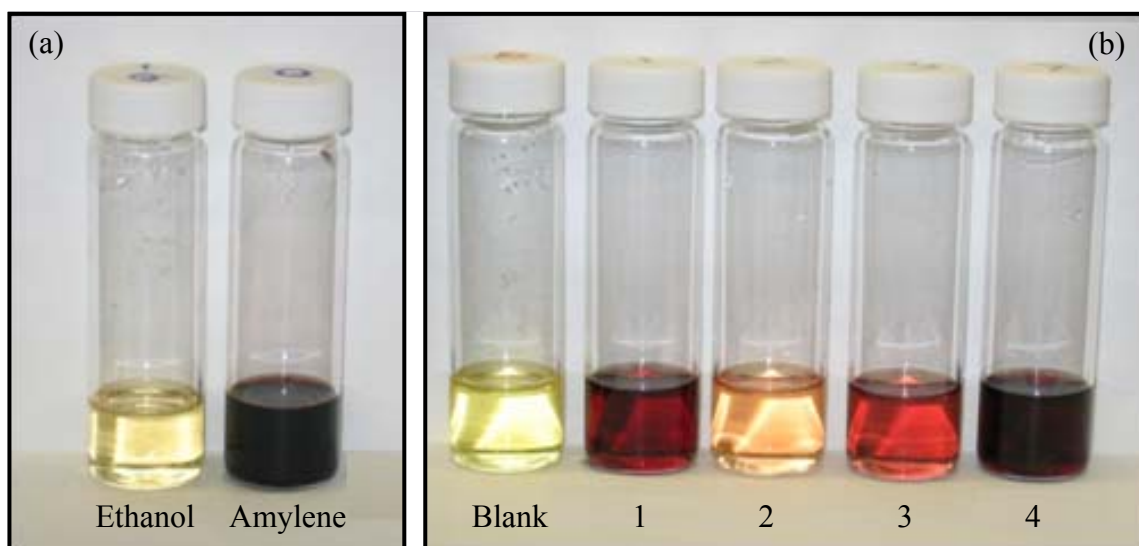


Figure 3.3 - Effect of chloroform type on color obtained in the analysis of samples with no frother: a) with ethanol- and amylene-stabilized chloroform; and b), with ethanol-stabilized chloroform samples apparently having different shelf lives

The UV-VIS spectra obtained from the solutions in Figure 3.3 are markedly different, as one would anticipate (Figure 3.4). These results demonstrated the importance of securing the correct chloroform, an unexpected difficulty. The use of amylene-stabilized chloroform should be avoided and calibration curves should be prepared close in time to the unknown sample analysis and the same chloroform must be used in both cases. From experience a three-week shelf life of ethanol-stabilized chloroform had no effect on

the analysis (in our case, longer intervals have not been necessary and their effects have not been evaluated).

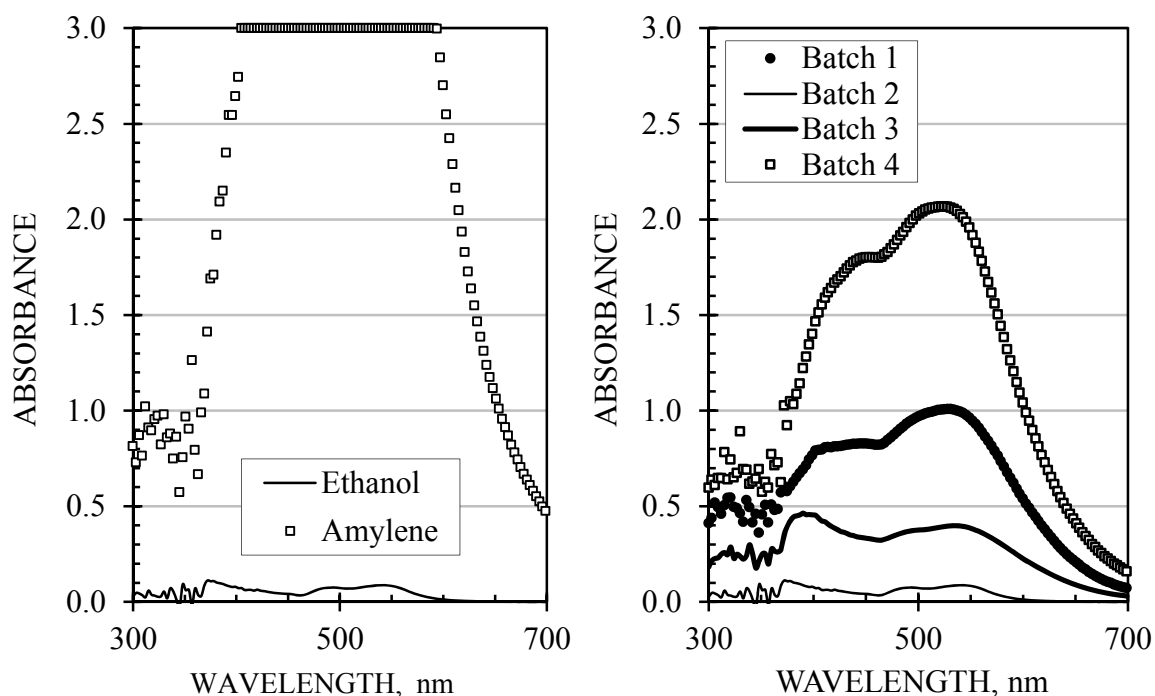


Figure 3.4 - Spectra for colored solutions depicted in Figure 3.3

#### Chloroform extraction stages

The original procedure used two chloroform extraction stages, which for a partition ratio of 40 (about average value for alcohols in chloroform-water mixtures at room temperature) and the liquid volumes selected (100 mL of frother solution and 10 mL of chloroform) should result in more than 95% frother extraction, if equilibrium is reached. A program to measure the partition ratio and the extent of frother extraction using MIBC was undertaken.

Two series of four extraction stages were run on 5-ppm solutions of MIBC: i) one on the same 100-mL frother sample extracted four times, with each of the 10-mL loaded chloroform fractions analyzed separately; and ii), the other on separate 100-mL frother samples which were extracted one, two, three and four times, respectively, but in this

case the corresponding 10-mL chloroform fractions were accumulated, which produced loaded chloroform samples of 10, 20, 30 and 40 mL, respectively.

The results showed that after two stages only 80% of the frother was extracted (Figure 3.5), and that the partition ratio was decreasing with an increasing number of stages, which indicates that equilibrium was not reached for the agitation procedure and separation times used. As the partition ratio should be constant for every stage, these results reflect that equilibrium takes longer to achieve as the concentration of the solution decreases.

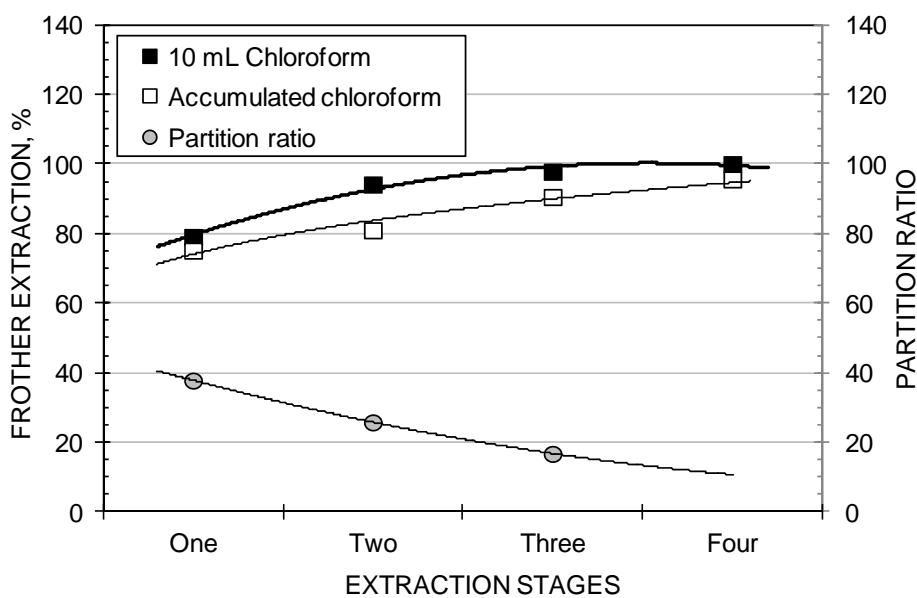


Figure 3.5 - Frother extractions and partition ratios obtained for increasing chloroform extraction stages

### 3.4.3 Formation of a colored solution

The procedure to form a colored solution via the Komarowsky reaction involves the addition of indicator to the loaded sulfuric acid and then boiling the mixture for a specified time. Experience revealed that conditions selected for these two steps, amount of indicator added and boiling time, affected the color intensity of the final solution:

### Indicator addition

The procedure calls for the addition of a small amount of indicator (0.1 mL), which was initially added using a mechanical pipette regulated to deliver 0.1-mL volumes. When darker than typical solutions were obtained, the color change was tracked to an excess volume delivered by the pipette (up to 0.3 mL). Figure 3.6 illustrates the effect of indicator addition volume on the spectra collected for 0- and 10-ppm F150 standards. This demonstrated that there is a significant effect of the amount of indicator added on the color intensity of the final solution and thus on the absorbance spectrum.

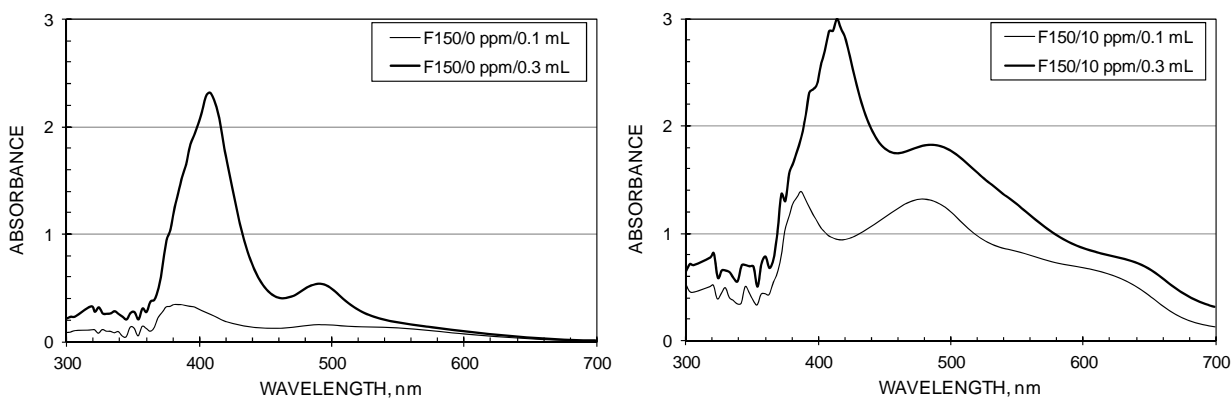


Figure 3.6 - Effect of indicator addition volume (0- and 10-ppm F150 standards)

Reproducibility was enhanced significantly when a syringe for injecting samples in chromatography was substituted to deliver the indicator dosage.

### Boiling time

The absorbance was affected by the boiling time, as illustrated in the spectra collected for 15-ppm F150 (Figure 3.7). The color evolved with boiling time from orange (peak ca. 420 nm) towards a dark red (peak ca. 470 nm).

The analysis requires the selection of a boiling time. The same time must be used for all samples (and calibration standards), but errors will be minimized if the selected value is in a range where little change occurs for a time variation of one to two minutes, as experience has taught that stopping the reaction cannot be done instantaneously. Plots of

absorbance vs. boiling time, for the same frother at different analysis wavelengths (Figure 3.8a), and for different frothers at the same wavelength (Figure 3.8b), illustrate the rationale for selecting a boiling time 40 min.

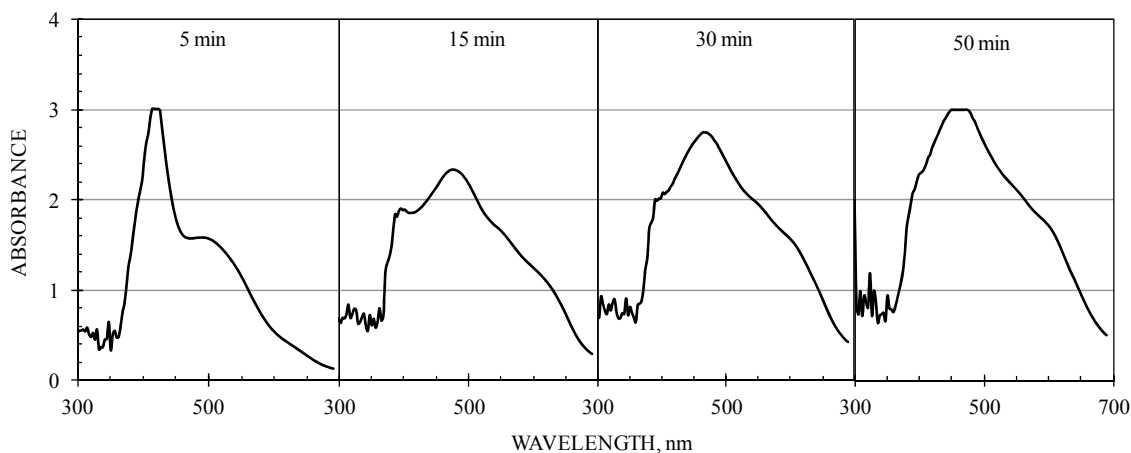


Figure 3.7 - Spectrum evolution with increasing boiling time (15-ppm F150 solution)

Selecting a boiling time involves a compromise between analysis time and absorbance stability. When the frother chemical structure is not known, or the quality of the water to prepare standards is suspect, or there is no ice available to stop the reaction quickly, then the boiling time of 40 min is recommended, but if the frother type is known and there is prior experience with it then a shorter time, with the benefit of increased sample analysis rate, is used, but never less than 15 minutes.

Another aspect to consider is that many concentrators are located at high altitude. Water will boil at lower temperatures and increasing the boiling time may be necessary to obtain the same stability as that obtained when the analysis is done at sea level.

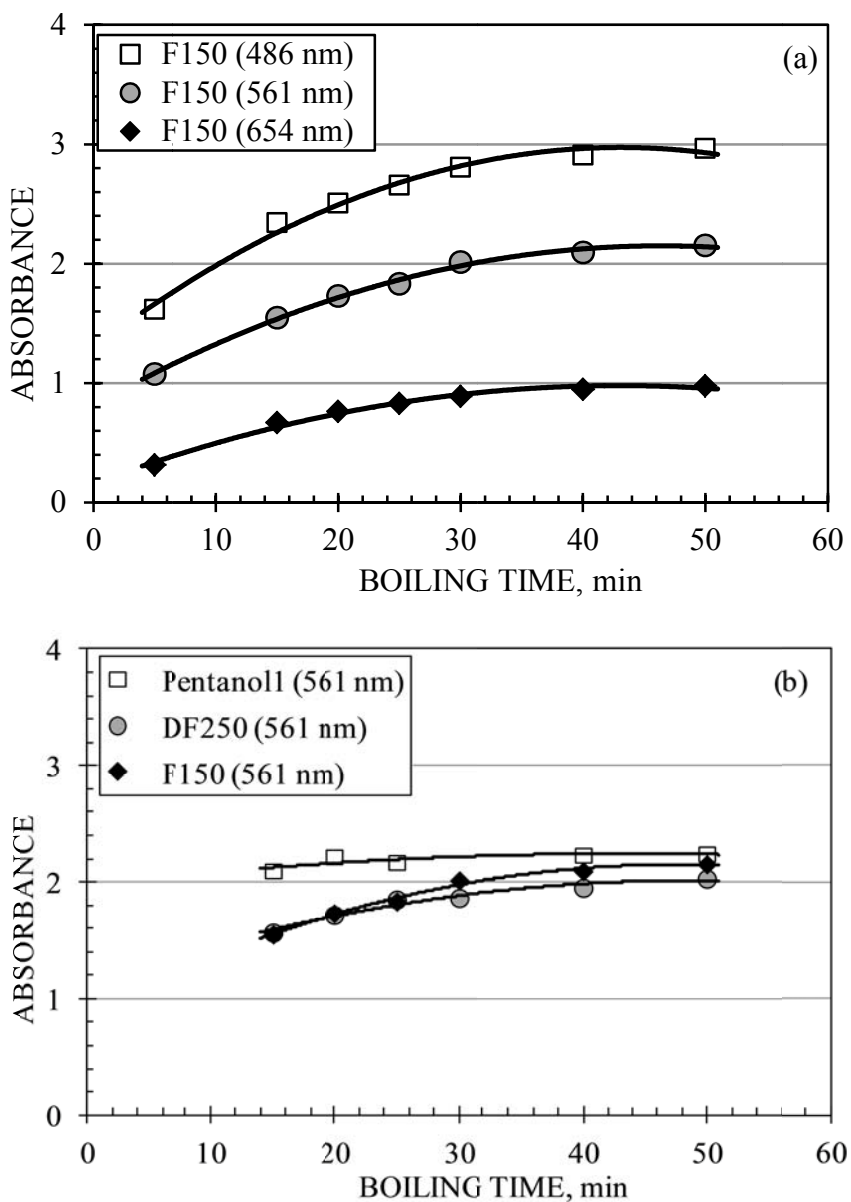


Figure 3.8 - Absorbance as a function of boiling time: a) same frother at different wavelengths; b) different frothers at same wavelength

#### Presence of inorganic salts

There are several cases where the calibration spectra differ for a frother in waters of different quality. This is illustrated for DSF004 in Figure 3.9, while for Matfroth533 no major effect of water quality was observed (Figure 3.10).

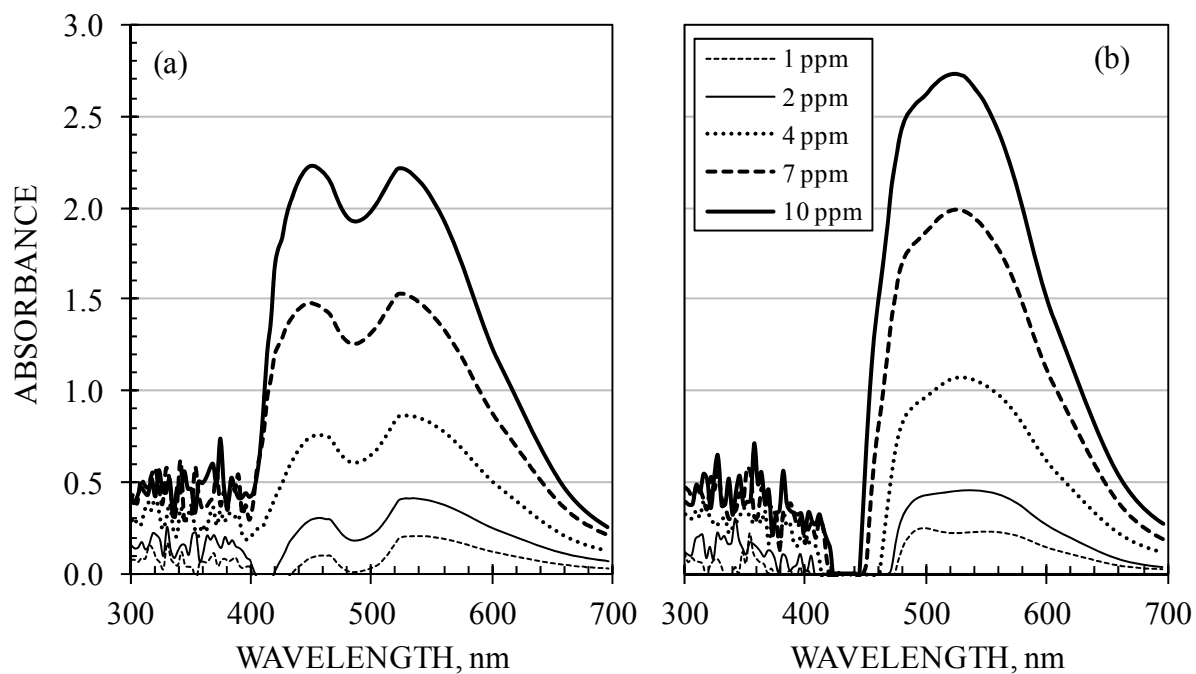


Figure 3.9 - Calibration spectra for frother DSF004 prepared with: a) tap water; and b), process water

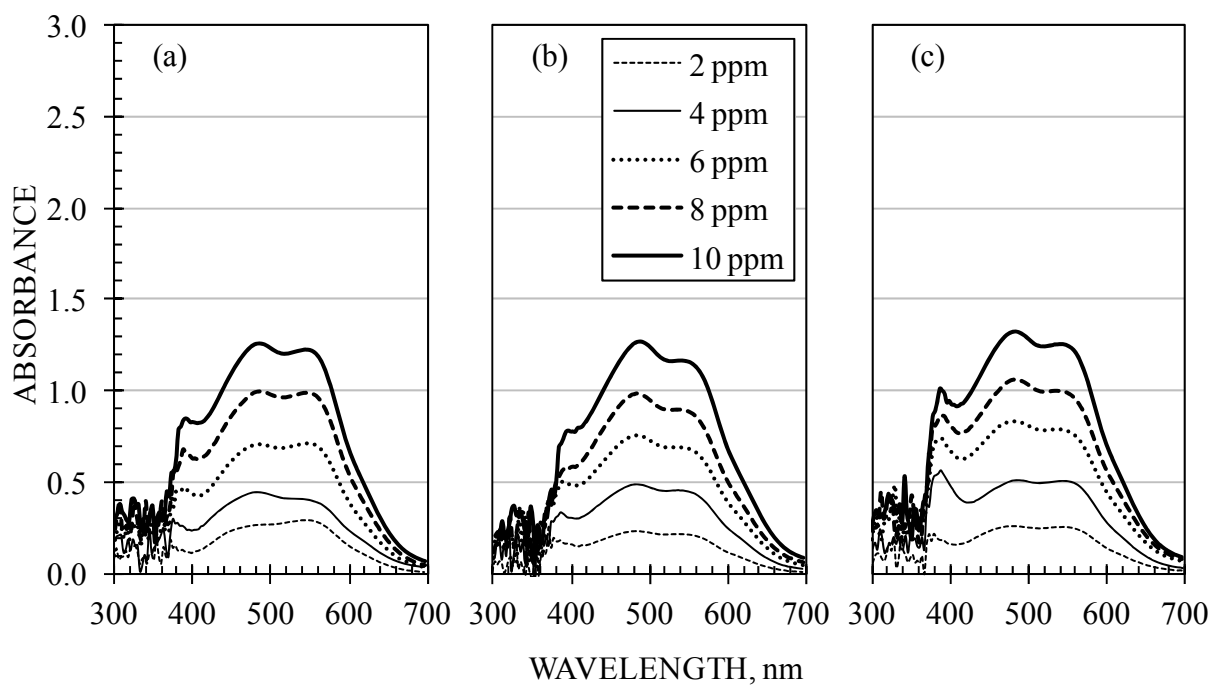


Figure 3.10 - Calibration spectra for frother Matfroth533 prepared with: a) tap water; b) process water; and c), sea water

To establish whether the presence of cations most commonly present in concentrator process waters (Na, K, Ca and Mg) have an effect on the color intensity, two series of tests were run on concentrated solutions of the four ions: one prepared with water only, and a second one with a 3-ppm solution of MIBC. The results (Figure 3.11) showed no effect when frother was not present and some minor effects for the MIBC solutions; the largest being that of the  $Mg^{++}$  ions.

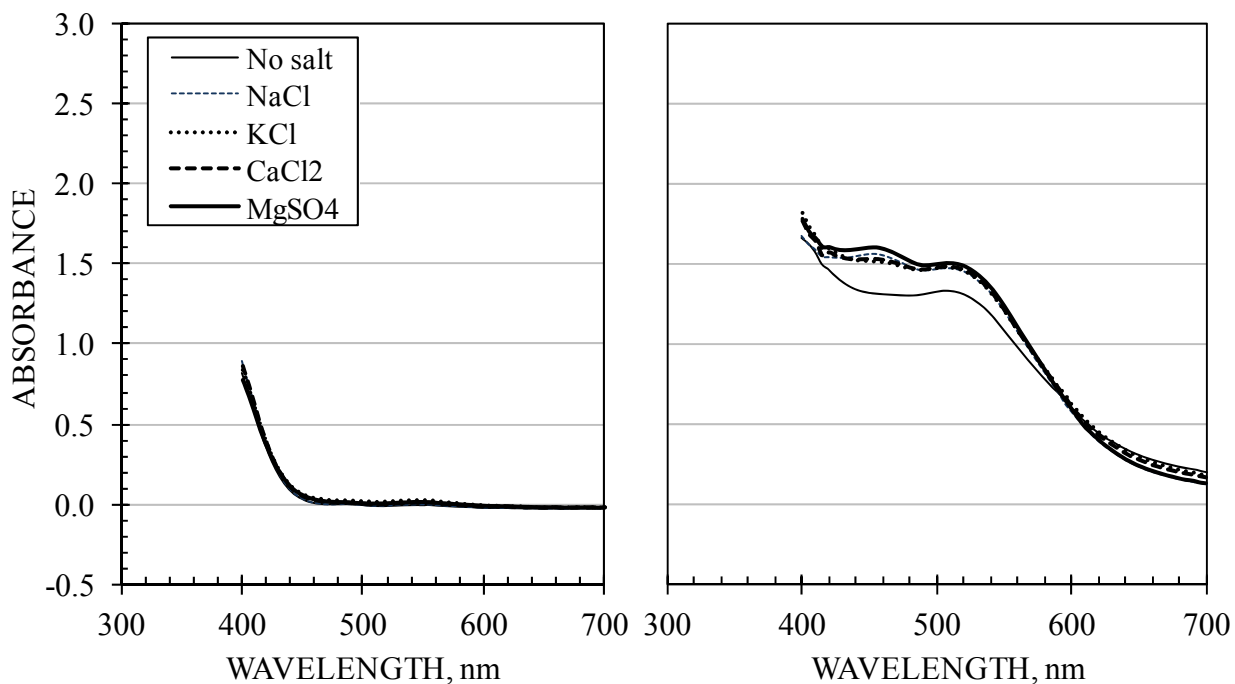


Figure 3.11 - Spectra obtained in the analysis of concentrated solutions of mineral species prepared in: a) water; and b) a 3-ppm MIBC solution

#### 3.4.4 Collection of UV-VIS spectrum

The original technique called for the collection of absorbance in wavelength ranges (490-560 nm) scanned with a UV-VIS spectrophotometer.

The absorbance spectrum for a frother solution, including standards for generation of the calibration curve, is relative to a reference solution. As a reference solution one of the following three options is used: water (tap, distilled or deionized); a blank (concentrated sulfuric acid with the Komarowsky indicator); and a 0-ppm standard (a sample with no frother going through the whole analytical procedure). The absorbance spectrum for a



sample depends on the choice of reference, as demonstrated for 10-ppm F140 (Figure 3.12).

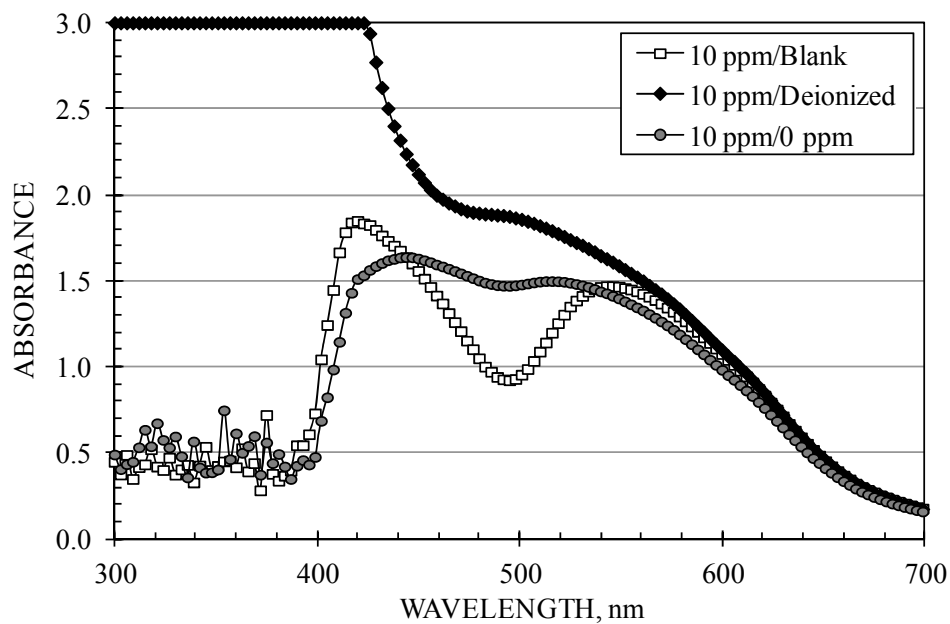


Figure 3.12 - Spectra collected for the same sample using different reference solutions (F140)

The original procedure used the 0-ppm standard as a reference solution for absorbance measurements (Gelinas and Finch, 2005), which resulted in calibration curves that did not go through the origin.

The analysis procedure was modified by using the blank (as defined above) as reference solution, and by including a 0-ppm standard for construction of the calibration curve. Also, the wavelength range for spectra collection was increased to be 300 to 700 nm. These changes made it possible to subtract contributions from factors not related to frother (by using the blank as reference), and to obtain calibration curves going through the origin by subtracting the 0-ppm spectrum from those of the other standards. Measured absorbances minus the absorbance of the 0-ppm standard, at the same wavelength, are designated as  $A_0$  in the following sections.

### 3.5 CALCULATION OF FROTHER CONCENTRATION

The construction of the calibration curve requires selection of a wavelength. The original procedure recommended the wavelength of maximum absorbance (peak) to obtain a calibration curve with minimum slope on the plot of concentration vs. absorbance (i.e., largest absorbance difference for a given concentration difference), which should result in the most precise measurements. This proved not always the case as there was sometimes greater scatter around the calibration line using the wavelength at maximum absorbance compared to selecting other wavelengths. A different criterion to select the wavelength was tested based on minimizing the sum of squared residuals (SSR), where the residual is the difference between measured and estimated frother concentration using the calibration curve. The differences between these two approaches will be illustrated through the construction of the calibration curve for MIBC.

The spectra collected for the series of standards selected in this case (0, 1, 2, 3, 4 and 5 ppm) are presented in Figure 3.13. After subtraction of the 0-ppm spectrum from those at the other concentrations, the wavelengths corresponding to peak absorbance and the minimum SSR are determined (Figure 3.14). The maximum absorbance occurred at a wavelength of 459 nm, while the minimum SSR was found at 432 nm, both indicated in Figure 3.15a.

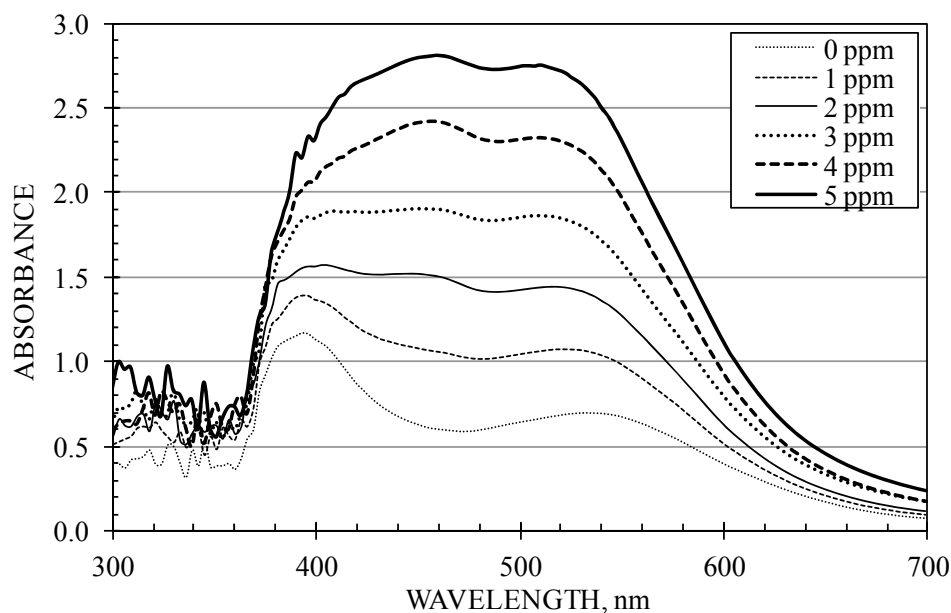


Figure 3.13 - Collected spectra for MIBC standards

The determination of the minimum SSR requires, for every wavelength, construction of a calibration curve, calculation of absorbance for each standard solution, and addition of the square of the differences between the calculated and measured absorbances. The result of this exercise for the MIBC included in Figure 3.13 is displayed in Figure 3.14 which shows how the minimum value of 432 nm was obtained.

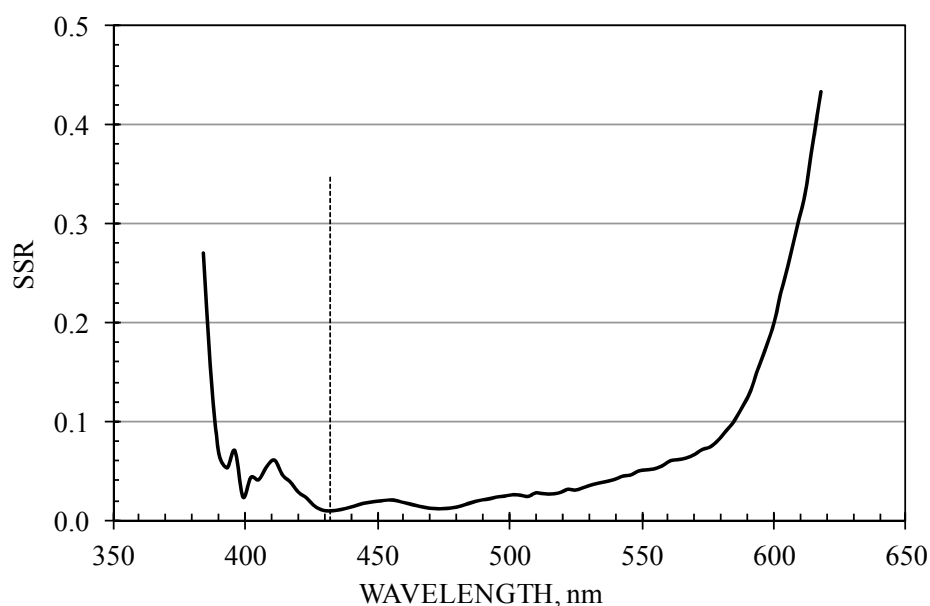


Figure 3.14 - SSR as a function of wavelength for MIBC

A comparison of the results obtained with these two approaches, use of wavelength at peak absorbance and at minimum SSR, is illustrated for the frothers MIBC (Figure 3.15) and PPG425 (Figure 3.16). The steps in the construction of the MIBC calibration curve are summarized in Figure 3.15: the “peak” and “SSR” wavelengths are indicated in Figure 3.15a, while the two calibration curves are displayed in Figure 3.15b. A comparison between measured and calculated concentrations is included in Figure 3.15c, which showed that although the differences are not large in this case, the estimated concentrations for the “SSR” case are closer to the reference line than those derived from the “peak” curve.

The wavelength selection was more important for PPG425; the maximum wavelength in the spectra was 480 nm, while that for the minimum SSR was 552 nm, both indicated in Figure 3.16a. The calibration curves at these two wavelengths are displayed in Figure

3.16b and the comparison between measured and calculated concentrations is shown in Figure 3.16c. The results clearly showed that the calibration curve at the wavelength for minimum SSR produced more precise estimates of the standard concentration than those of the calibration curve at the peak wavelength.

Another decision is to select the concentration range for the standards to give a linear calibration. When no information on concentrations appropriate for a given frother is available, the criterion is to cover the full absorbance range. Statistical considerations indicate that errors associated with the use of a calibration curve are larger at the extremes and minimum at the average concentration of the standards. Therefore, the selection of standard concentrations should be such that their average concentration corresponds with approximately the value expected in the plant samples. When dilution (with tap water) is necessary on plant samples the resultant concentrations should aim for the center of the calibration curve concentration range.

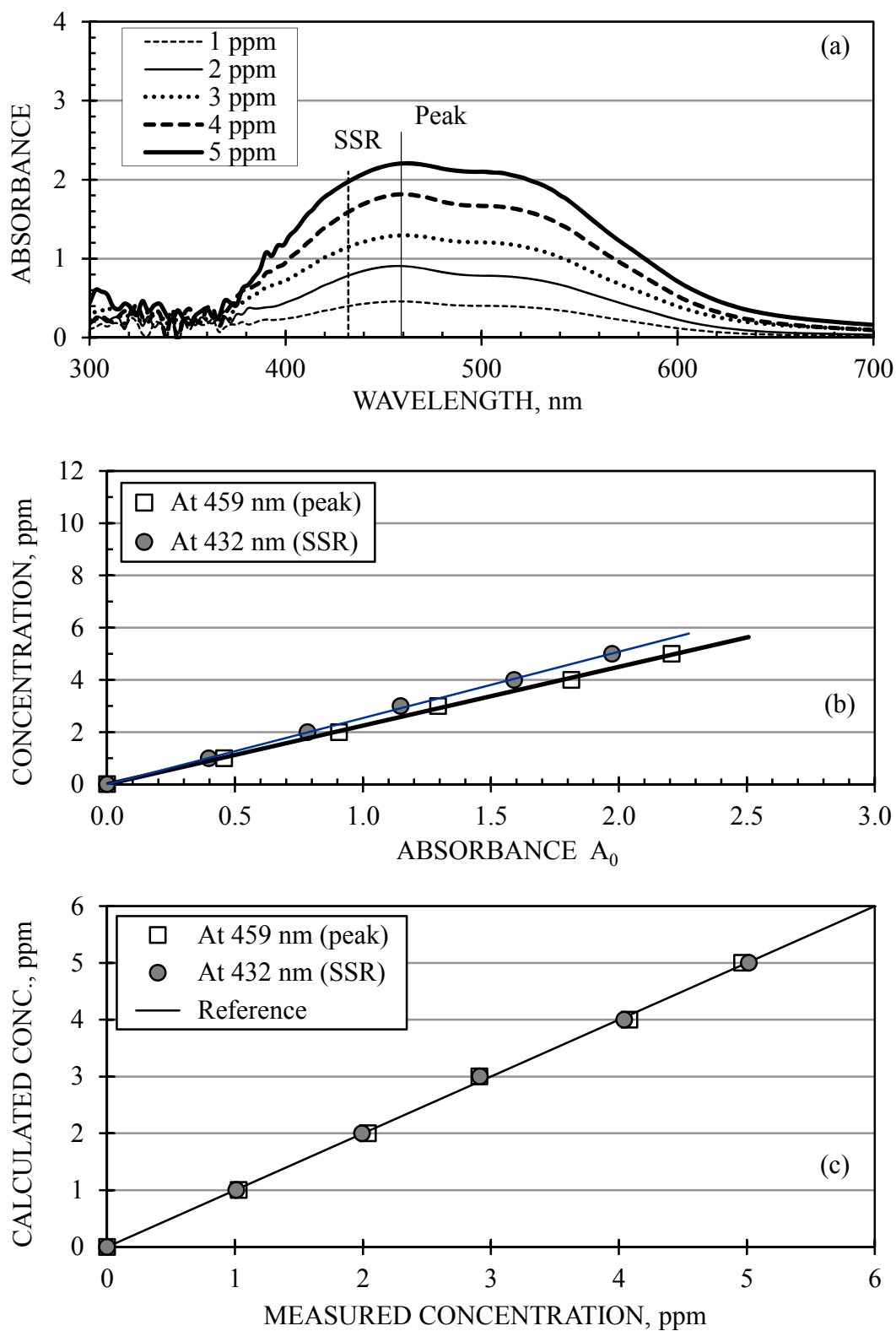


Figure 3.15 - Spectra (a), comparison of calibration curves (b), and estimated vs. measured concentrations (c) for MIBC analysis

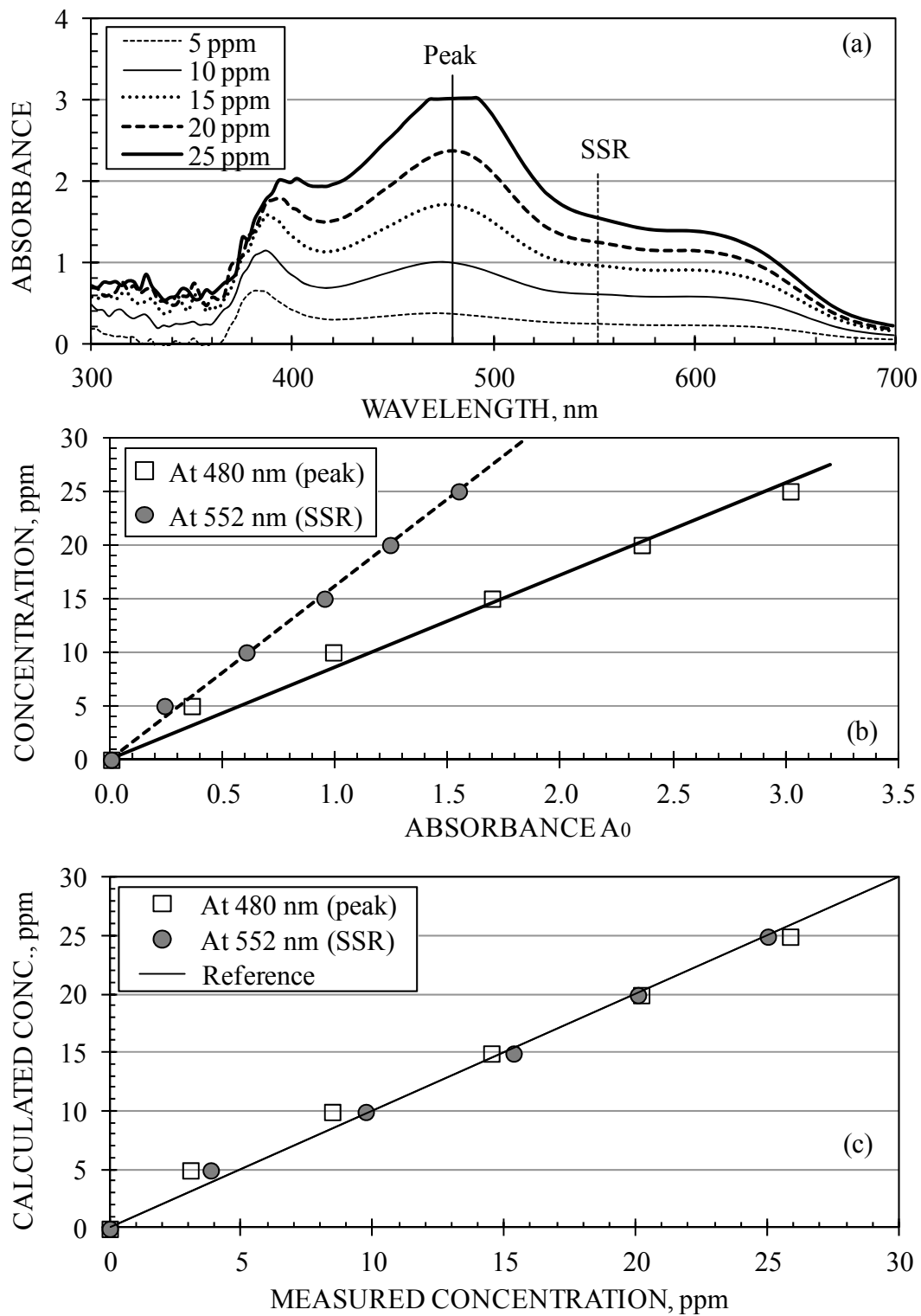


Figure 3.16 - Calibration spectra (a), and comparison of calibration curves (b) and estimated vs. measured concentrations (c) for PPG425 analysis

### 3.6 REPRODUCIBILITY

The refinements of the experimental procedure significantly improved reproducibility, as demonstrated with a 5-ppm standard of a commercial frother (Table 3.1). Absorbance was collected at 535 nm for five replicate samples prepared on five consecutive days (including a different stock solution every day). The results, summarized in Table 3.1, also include the calculated averages and standard deviations.

Table 3.1 - Absorbance and relative errors obtained in the analysis of 5-ppm standards of the frother TX13072

	Stock 1	Stock 2	Stock 3	Stock 4	Stock 5	Average	St. Dev	Error, % 95% C.I.
Sample 1	1.561	1.609	1.600	1.613	1.589	1.594	0.021	1.6
Sample 2	1.539	1.645	1.644	1.625	1.610	1.613	0.044	3.4
Sample 3	1.546	1.626	1.611	1.632	1.596	1.602	0.034	2.7
Sample 4	1.531	1.611	1.627	1.617	1.580	1.593	0.039	3.0
Sample 5	1.562	1.641	1.601	1.609	1.621	1.607	0.029	2.3
Average	1.548	1.626	1.617	1.619	1.599	1.602	0.033	2.6
St. Dev	0.014	0.017	0.019	0.009	0.016	0.015	-	-
Error, % 95% C.I.	1.1	1.3	1.4	0.7	1.3	1.2	-	-

The results show that the relative standard deviation among the sample analyses (columns in Table 3.1) is about 1% (last row), while the value for analysis including preparation of the stock solution (rows in Table 3.1) was about 2.5% (last column). These values demonstrate that the technique is reproducible, and that the associated errors are acceptable for the analysis of industrial streams.

As these tests were run on a commercial frother whose concentration was selected to have absorbance around the middle of the range (maximum absorbance is 3), it was decided to extend the test of reproducibility to other frothers (1-pentanol, 1-octanol and MIBC) at low and high concentrations in each case: 1-pentanol was run at 2 and 7 ppm, 1-octanol at 2 and 8 ppm, and MIBC at 1 and 4 ppm. A full spectrum was collected this

time; the results obtained are illustrated for the case of 1-pentanol at the low and high concentrations, in Figures 3.17a and 3.17b, respectively.

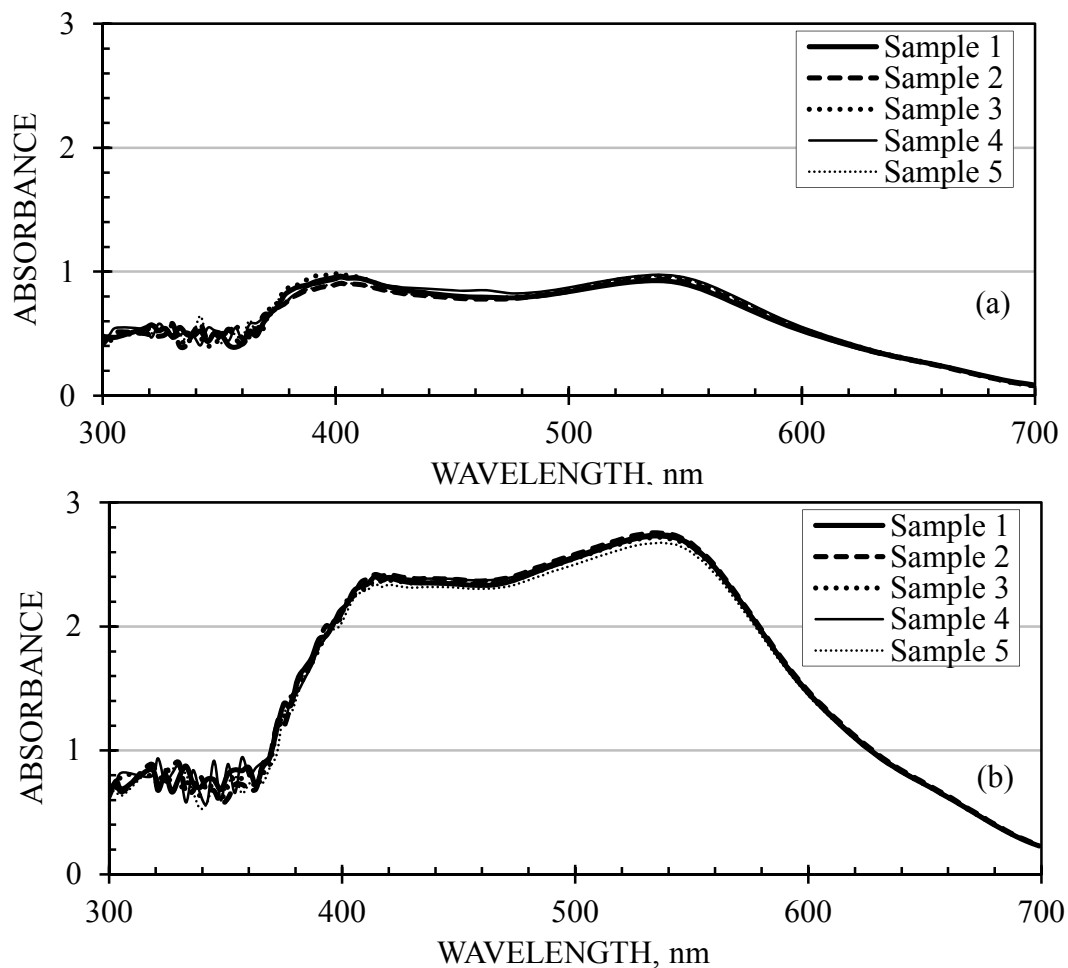


Figure 3.17 - Repeat 1-pentanol spectra collected to estimate error analysis at a) low (2 ppm), and b), high (7 ppm) concentrations

Errors were calculated at the wavelengths selected to construct the calibration curves (i.e., the wavelength giving minimum SSR). The wavelengths selected were 570, 465 and 485 nm for 1-pentanol, 1-octanol and MIBC, respectively. Table 3.2 summarizes the absorbance errors (95% CI) for samples and standards.



Table 3.2 - Relative absorbance errors for the analysis of samples and standards of various frothers at a low and a high concentration (5 replicates)

Frother	Mode	Concentration (ppm)	Absorbance		Relative error 95 % CI
			Average	St. Dev.	
F150	Sample	5	1.602	0.015	1.2
	Stock	5	1.602	0.033	2.6
1-pentanol	Sample	2	0.786	0.022	3.4
		7	2.222	0.023	1.3
	Stock	2	0.775	0.025	4.1
		7	2.193	0.027	1.5
1-octanol	Sample	2	0.686	0.016	2.8
		8	2.853	0.024	1.0
	Stock	2	0.698	0.046	8.3
		8	2.741	0.135	6.1
MIBC	Sample	1	0.505	0.004	0.9
		4	1.853	0.012	0.8
	Stock	1	0.485	0.011	2.8
		4	1.871	0.033	2.2

These results demonstrate, as expected, there is larger error in analysis of samples which includes preparation of stock solution (Figure 3.18), and for low- rather than high-concentration solutions (Figure 3.19). The errors are more significant for alcohols, as a consequence of their low solubility, and larger for 1-octanol than 1-pentanol. Although the solubility of these two alcohols is well above the concentration of the stock solution used for preparation of the standards (also the samples in this exercise), ensuring complete dissolution requires longer times and thorough homogenization every time an aliquot is taken. As most commercial frothers are blends with an unknown composition, exercises to quantify reproducibility are routinely performed given the diverse conditions found in the field. When standard deviations have been high (over 4%) at the plant, attempts were made to identify the source of additional error, which generally were a combination of sample dilution errors, water quality issues, or frother properties that made necessary special precautions for storing samples.

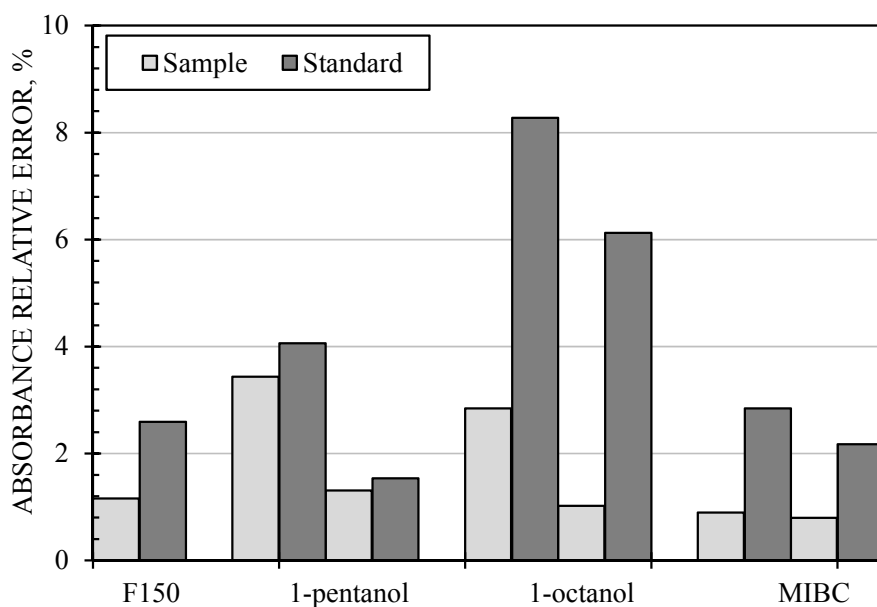


Figure 3.18 - Relative error in absorbance in the analysis of samples and standards of different frothers

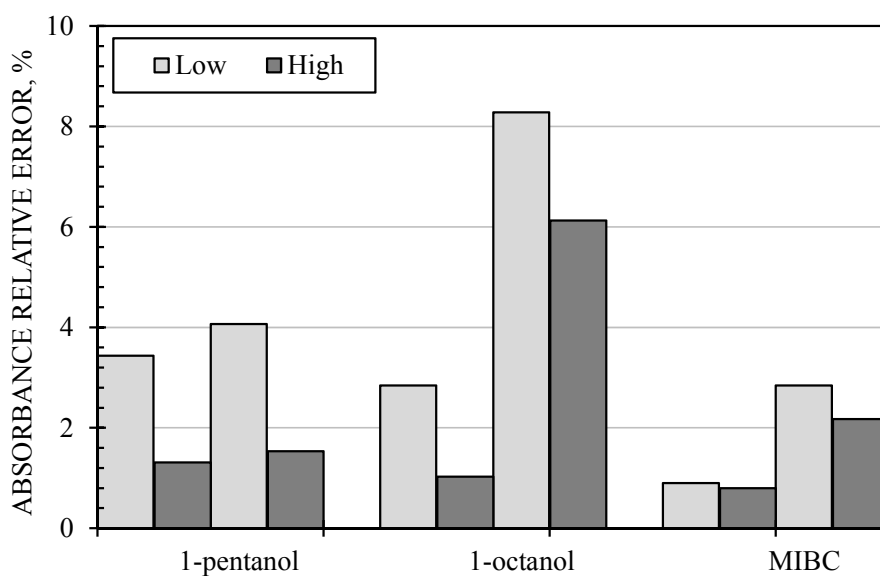


Figure 3.19 - Relative errors in absorbance in the analysis of low- and high-concentration solutions of different frothers

### 3.7 DETECTION LIMIT

An attempt was made to establish the minimum concentration that can be detected and analyzed. Dilute samples of 1-octanol in two concentration ranges, below 1 ppm (0.1, 0.2, 0.3, 0.4, and 0.5) and below 0.1 ppm (0.01, 0.03, 0.05, and 0.08) were prepared and analyzed. The calibration spectra for 1-octanol were obtained and used to construct the calibration curve, at 486 nm (minimum SSR), displayed in Figure 3.20.

The results demonstrated that the calibration curve gives accurate concentrations of solutions as low as 0.2 ppm, as illustrated in Figure 3.21. Below 0.1 ppm, the technique is still able to detect the presence of the frother, but the error in the determination of the concentration is too high for practical purposes.

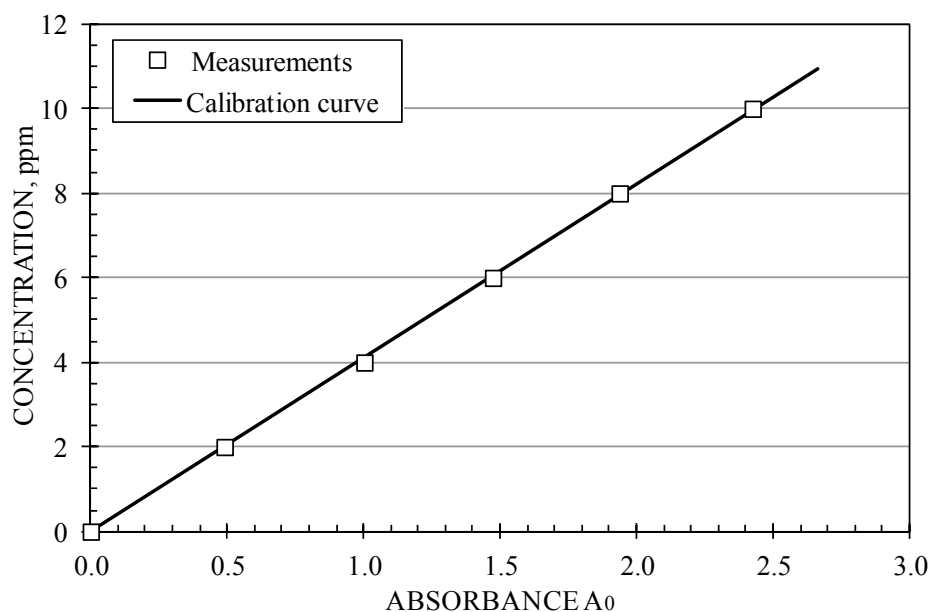


Figure 3.20 - Calibration curve constructed for 1-octanol at 486 nm (minimum SSR)

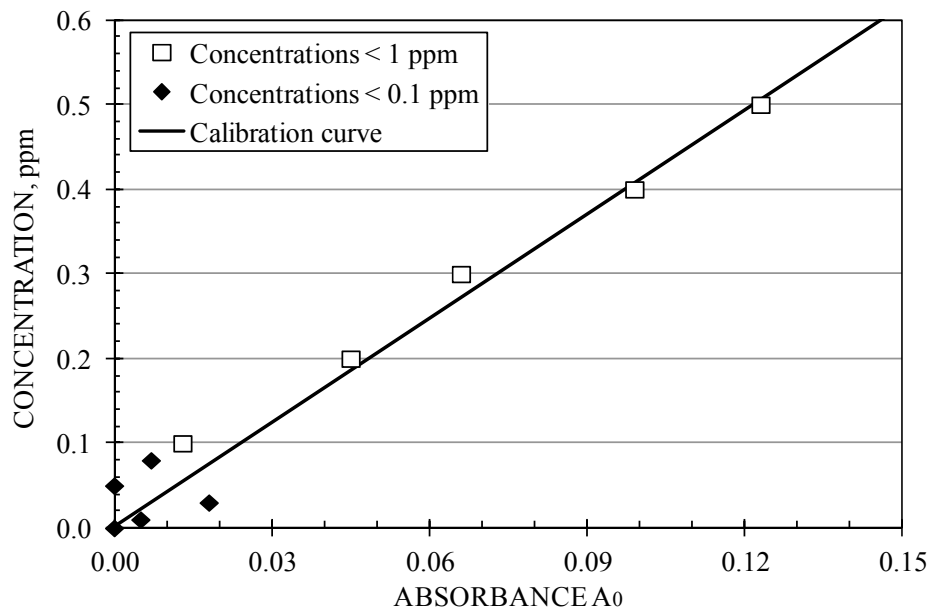


Figure 3.21 - Calibration curve predictions for low-concentration solutions of 1-octanol

### 3.8 CONCLUDING REMARKS

The literature review indicated that there have been limited techniques used in the analysis of frothers; from those used, the colorimetric technique seemed the most appropriate for analysis of industrial pulp samples in concentrator installations. Its use, however, required to extend the technique to a wider range of frothers and to speed up analysis while retaining reliability.

As the work progressed, it became clear that scrutinizing every aspect of the procedure had the potential to increase accuracy (validity) and precision (reliability). Reagent specifications were demonstrated to be of great importance: only ethanol-stabilized chloroform should be used, and calibration curves should be prepared close in time to the analyses because chloroform shelf life may have an effect. It was demonstrated that there is a significant effect of the amount of indicator added on the color intensity of the final solution, and consequently on the absorbance spectrum. The procedure calls for the addition of a small amount of indicator (0.1 mL), therefore, the selection of a device for injecting the exact indicator dosage was necessary (in our case a chromatography syringe).

The analysis includes boiling a frother/sulfuric acid mixture to form a colored solution; the UV-VIS absorbance of this solution depends on the boiling time. Errors are minimized if the selected time is in a range where differences of one to two minutes result in minor absorbance changes. In general, longer boiling times are more convenient, but a long one may compromise the daily analysis rate. However, selection of longer times is convenient if the frother chemical structure is unknown, the water quality to prepare standards is suspect, no ice is available to stop the reaction quickly, or the analytical laboratory is located at high altitude.

The method requires the construction of calibration curves with standards prepared using water free of organic compounds. Spectra of standards prepared with plant process waters were in some cases very different from those obtained when tap water was used. Tests run to establish possible effects of high concentrations of the most common ions (Na, K, Ca and Mg) showed that there was no effect when frother was not present and some minor effects for MIBC solutions; the largest being that of the  $Mg^{++}$  ions.

Two criteria were established for construction of calibration curves: the selection of the standard concentrations and the selection of the wavelength. Statistical considerations indicate that errors associated with the use of a calibration curve are larger at the extremes and minimum at the average concentration of the standards. Thus, the selection of standard concentrations is such that their average concentration corresponds with the approximate value expected in the plant samples. When dilution of plant samples is necessary the resultant concentrations should aim for the center of the calibration curve concentration range. At the same time, a different criterion to select wavelength was developed based on minimizing the sum of squared residuals (SSR); a residual is the difference between measured and estimated (using the calibration curve) standard concentrations.

The analysis procedure was modified by using a blank (concentrated sulfuric acid with the Komarowsky indicator) as reference solution in the collection of spectra to eliminate contributions from factors not related to frother. This made it possible to collect a 0-ppm

standard spectrum which was subtracted from the other standards for the construction of the calibration curve; a linear curve going through the origin was fitted to the calibration data. Also, a full spectrum was collected by increasing the wavelength range from 300 to 700 nm.

The reproducibility of the technique was determined from standard deviation measurements of samples prepared from the same stock solution, and for samples which included preparation of a stock solution; the results, about 1% and 2.5%, respectively, were both considered acceptable given the many steps involved in the analytical procedure. Measurements of the detection limit by consecutive dilutions demonstrated that the calibration curve gives accurate concentrations of solutions as low as 0.2 ppm. Below 0.1 ppm, the technique is still able to detect the presence of the frother, but the error in the determination of the concentration is too high for analytical purposes.

## CHAPTER 4 - FROTHER ANALYSIS DATABASE

The frother analysis technique is based on the formation of a colored solution with absorbance proportional to frother concentration over a certain range. The calculation of concentration requires the comparison of the sample absorbance at some selected wavelength (see Chapter 3) with a calibration curve (frother concentration vs. absorbance) constructed with values collected from solutions of known concentration (standards) at the selected wavelength. Maximum concentration is defined by instrument limitations: in the present case, the maximum detectable absorbance (minimum transmittance sensed by the detector) for the UV spectrophotometer in use, in plant and lab applications, was 3.

Analysis accuracy and precision depends on the calibration curve. The initial decision in constructing the calibration curve is to select standard concentrations covering the maximum possible range while keeping absorbance below the maximum detectable. Statistical considerations indicate that errors are minimized at the center of the calibration range when the standard concentrations are equally spaced throughout the range. Knowledge of the maximum concentration corresponding to an absorbance of 3 makes it possible to select standards and construct a calibration curve with the widest application range. In this case, the calibration will neither cover too narrow an absorbance range (Figure 4.1a), the case of PPG425, nor have concentrations out of range (Figure 4.1b), as in the the case of 1-hexanol.

In general, the calibration curves for the research work and plant campaigns, covered concentration ranges which were not the widest nor the most convenient, as the maximum possible concentration was unknown. Compiling calibration curves into a database documents the experiences that can be used to select the most convenient standard concentrations, as experience has indicated that the calibration curves tend to linear for the whole range of absorbances. This is illustrated in Figure 4.2 for PPG425, which shows a calibration curve that equally fits a narrow concentration range (data in Figure 4.1a) and a wide concentration range of standards.

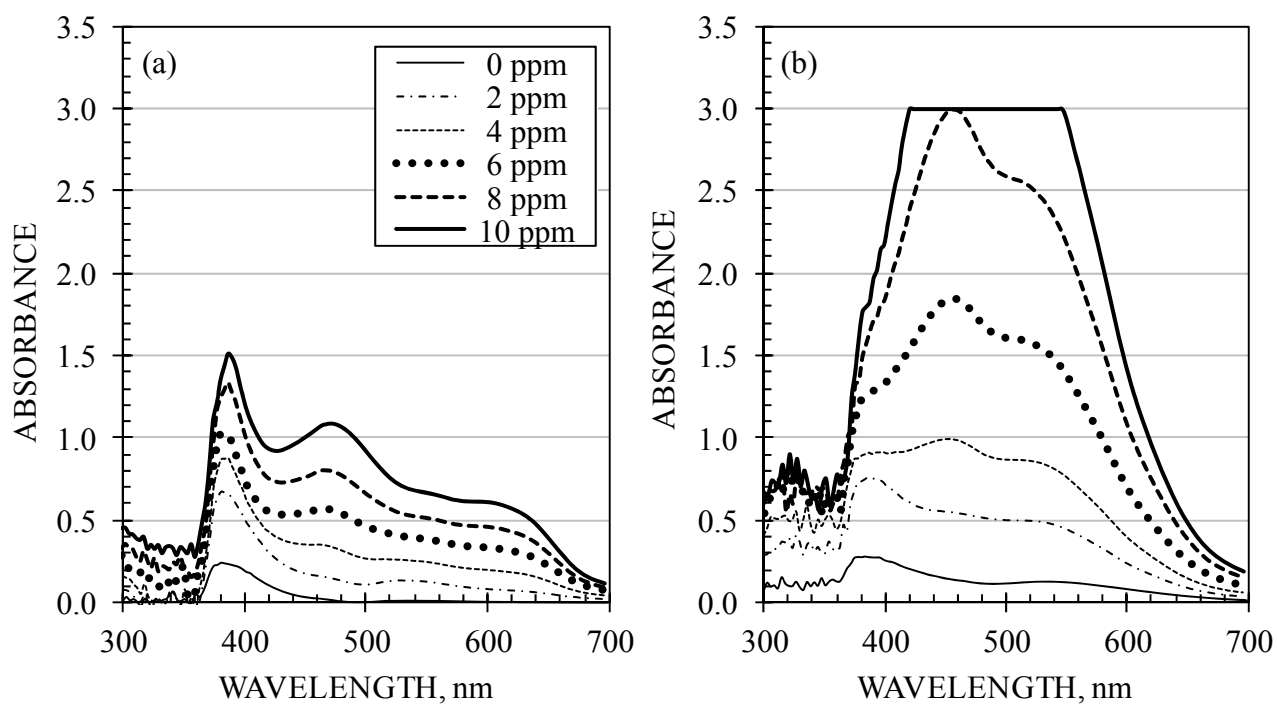


Figure 4.1 - Calibration spectra: (a) covering a too narrow absorbance range, and (b) with one standard out of range (absorbance > 3 over wavelength~ 420-550 nm)

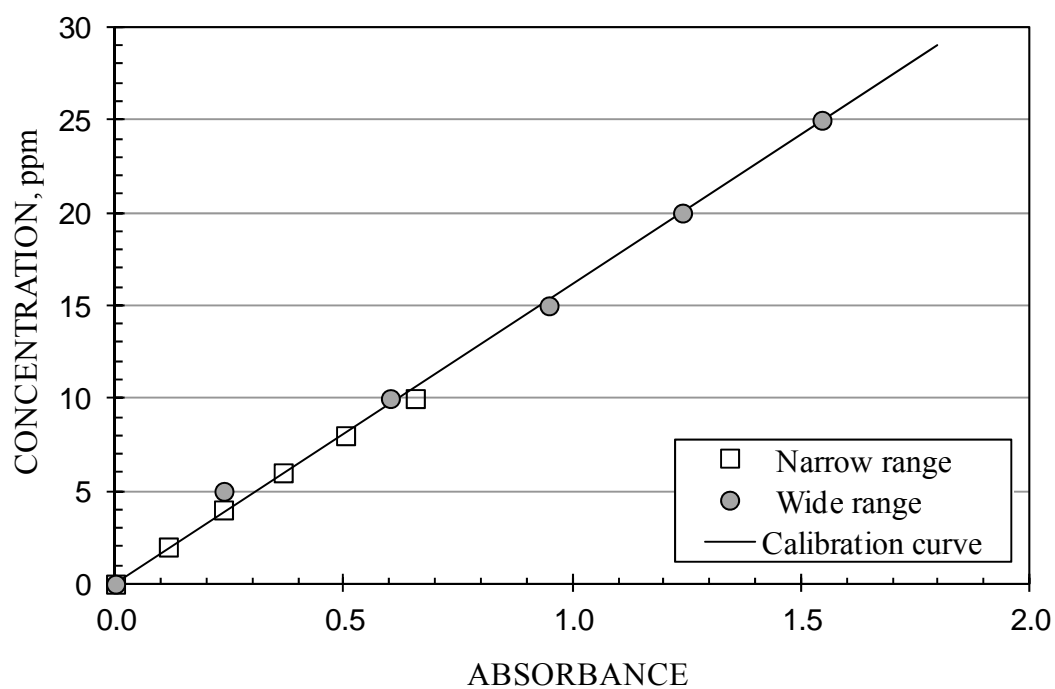


Figure 4.2 - Calibration curve obtained with standards covering narrow and wide concentration ranges (wavelength 552 nm)



The procedure to estimate the maximum standard concentration from the calibration data is based on extrapolating the calibration equation to an absorbance  $A_0$  (absorbance minus absorbance of the 0-ppm standard) equal to 3. This may result in a standard concentration with an absorbance larger than 3. However, as the absorbance of 0-ppm standards is low for the whole range of wavelengths, the value estimated with this procedure is close to the value giving the maximum absorbance 3; therefore, the value reported in the database should be taken as a close indication of the maximum concentration but on the high side. While the concentration range of standards is important it is necessary to keep in mind that there are some uncontrollable factors such as water quality and reagent specifications that also play a role, which may affect the spectra and change the reported optimum wavelength for calibration curve construction or the maximum concentration for an absorbance 3.

The database integrates results used in the construction of calibration curves of chemical reagents involved in research work at McGill (8 samples), commercial frothers (in use at plants) collected in surveys or sent by sponsors (23 samples), and natural oils of interest to us and other research institutions (8 samples). The spectra for every entry are included in Appendix 1. A list of the frothers included in the database is presented in Table 4.1; details of the respective linear calibration curves and the estimated maximum standard concentrations are included in Table 4.2.

A summary of selected data for every frother was condensed to a single page for quick reference (Appendix 1). The calibration curves were constructed following the procedure described in Section 3.5. The information includes for every frother: supplier, molecular weight, dilution water for preparation of standards, date of the analysis, the calibration spectra, the calibration curve, the calibration equation, and the maximum concentration estimated by extrapolation of the calibration curve. Examples of database entries are given for pentanol (Figure 4.3), PPG 425 (Figure 4.4), MIBC (Figure 4.5), F150 (Figure 4.6) and a natural eucalyptus oil (Figure 4.7).

Table 4.1 - Frothers analyzed

Sample	Frother			Analysis date
	Name	Supplier	Type	
1	F150	Flottec	Commercial	April 11, 2010
2	F140	Flottec	Commercial	April 12, 2010
3	MIBC	0	Commercial	April 14, 2010
4	DF250	Dow	Commercial	April 16, 2010
5	Pentanol	Sigma Aldrich	Chemical reagent	April 17, 2010
6	Butanol	Sigma Aldrich	Chemical reagent	April 17, 2010
7	Hexanol	Sigma Aldrich	Chemical reagent	April 18, 2010
8	Octanol	Sigma Aldrich	Chemical reagent	April 18, 2010
9	TX10713	Nalco	Commercial product	April 21, 2010
10	TX13072	Nalco	Commercial product	April 22, 2010
11	DVS4U021	Nalco	Commercial product	April 24, 2010
12	U250C	Nalco	Commercial product	April 25, 2010
13	Senfroth7	Senmin	Commercial product	April 25, 2010
14	Senfroth400	Senmin	Commercial product	April 26, 2010
15	Senfrothxp200	Senmin	Commercial product	April 28, 2010
16	Senfroth6000	Senmin	Commercial product	May 3, 2010
17	Senfroth516	Senmin	Commercial product	May 04, 2010
18	Senfroth250	Senmin	Commercial product	May 04, 2010
19	PolyfrothW31	Huntsman	Commercial product	May 05, 2010
20	OreprepF501oz	Cytec	Commercial product	May 06, 2010
21	PolyfrothW34	Huntsman	Commercial product	May 07, 2010
22	DSF004	Orica Chemicals	Commercial product	May 07, 2010
23	F160-10	Flottec	Commercial product	May 09, 2010
24	PolyfrothH20	Huntsman	Commercial product	May 10, 2010
25	E. Citriodora	JKMRC	Natural product	May 11, 2010
26	E. Globulus	JKMRC	Natural product	May 21, 2010
27	E. Polybractea	JKMRC	Natural product	May 22, 2010
28	E. Smithii	JKMRC	Natural product	May 23, 2010
29	E. Radiata	JKMRC	Natural product	May 24, 2010
30	E. Eucaliptol	JKMRC	Natural product	May 25, 2010
31	E.17483	JKMRC	Natural product	May 25, 2010
32	E.17340	JKMRC	Natural product	May 26, 2010
33	E.17084	JKMRC	Natural product	May 26, 2010
34	MIBC2	-	Commercial product	June 09, 2010
35	MIBC	Sigma Aldrich	Commercial product	May 01, 2011
36	PPG425	Sigma Aldrich	Commercial product	May 01, 2011
37	PPG425	Sigma Aldrich	Commercial product	July 07, 2011
38	Octanol	Sigma Aldrich	Commercial product	May 01, 2011

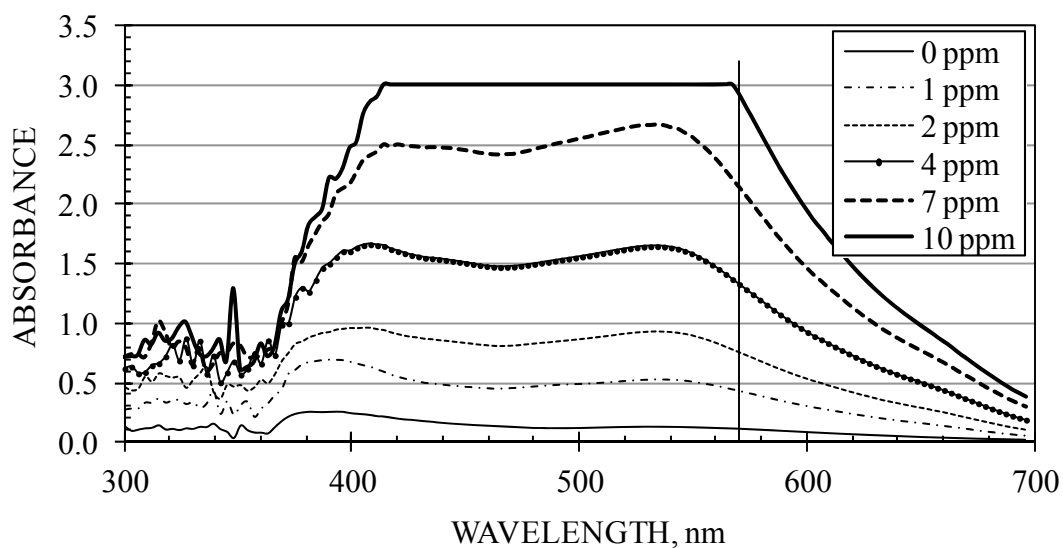
Table 4.2 - Calibration results and maximum standard concentration

Sample	Frother name	Calibration curve			Maximum standard concentration (ppm)
		Wavelength (nm)	Slope (ppm)	R <sup>2</sup>	
1	F150	531	14.9	0.992	45
2	F140	510	11.1	0.999	33
3	MIBC	558	3.3	0.980	10
4	DF250	534	17.3	0.997	52
5	Pentanol	570	3.5	0.997	10
6	Butanol	507	24.5	0.998	74
7	Hexanol	549	3.4	0.996	10
8	Octanol	486	3.5	0.999	10
9	TX10713	489	8.2	0.999	25
10	TX13072	522	14.5	0.991	44
11	DVS4U021	555	3.6	0.995	11
12	U250C	420	16.1	0.999	48
13	Senfroth7	465	4.1	0.999	12
14	Senfroth400	471	10.3	1.000	31
15	Senfrothxp200	438	21.9	0.998	66
16	Senfroth6000	-	-	-	-
17	Senfroth516	447	18.1	0.999	54
18	Senfroth250	456	14.7	0.996	44
19	PolyfrothW31	447	11.2	0.997	34
20	OreprepF50102	513	6.4	1.000	19
21	PolyfrothW34	435	22.2	0.995	66
22	DSF004	540	8.1	1.000	24
23	F160-10	513	13.7	1.000	41
24	PolyfrothH20	474	3.7	0.999	11
25	E. Citriodora	462	9.6	0.993	29
26	E. Globulus	486	12.5	0.989	37
27	E. Polybractea	414	16.7	0.996	50
28	E. Smithii	414	20.5	0.996	62
29	E. Radiata	459	14.0	0.993	42
30	E. Eucaliptol	408	17.2	0.984	52
31	E.17483	465	15.2	0.993	46
32	E.17340	480	8.3	0.924	25
33	E.17084	471	13.4	0.436	40
34	MIBC2	573	4.4	0.991	13
35	MIBC	432	2.5	0.999	8
36	PPG425	543	15.5	0.997	46
37	PPG425	552	16.2	0.996	49
38	Octanol	486	4.1	1.000	12

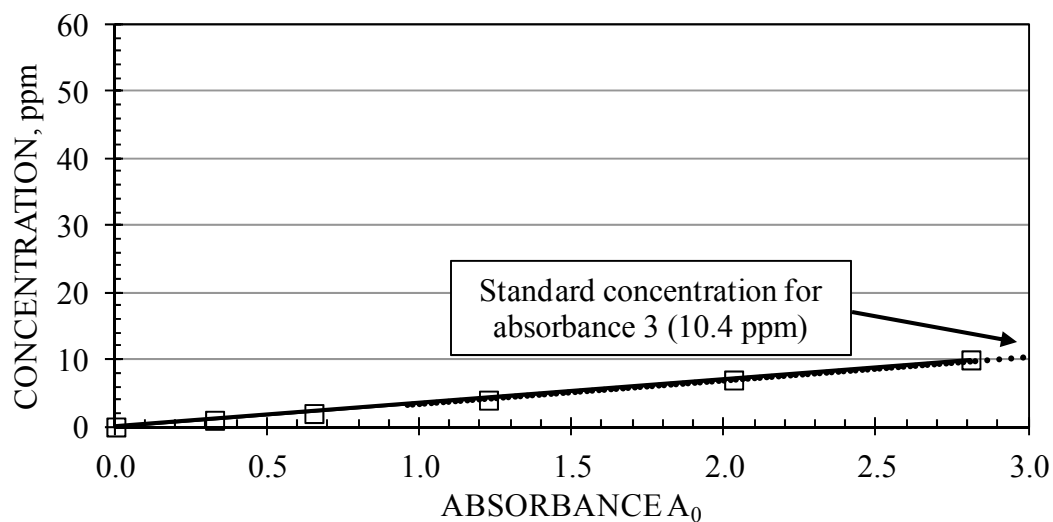
FROTHER: Pentanol  
 SUPPLIER: Sigma Aldrich  
 MOLECULAR WEIGHT: 88  
 DILUTION WATER: McGill tap  
 DATE: 17/04/2010

SAMPLE 5

CALIBRATION SPECTRA:



CALIBRATION CURVE:



EQUATION:

$$C \text{ (ppm)} = 3.481 A_0 \quad C \leq 10 \text{ ppm}$$

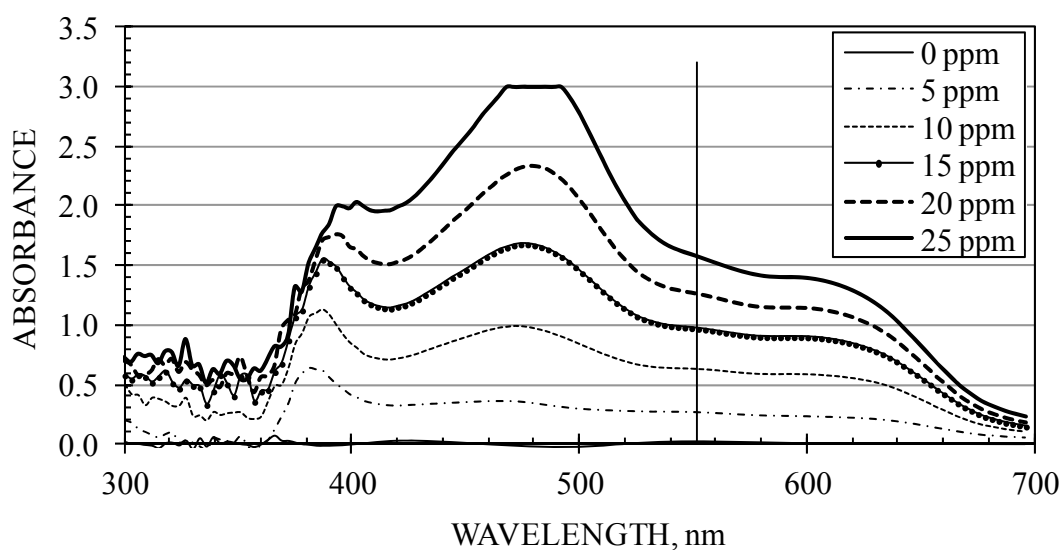
where  $A_0$  is the measured absorbance minus that of the 0 ppm standard (both at 570 nm)

Figure 4.2 - Database entry for pentanol

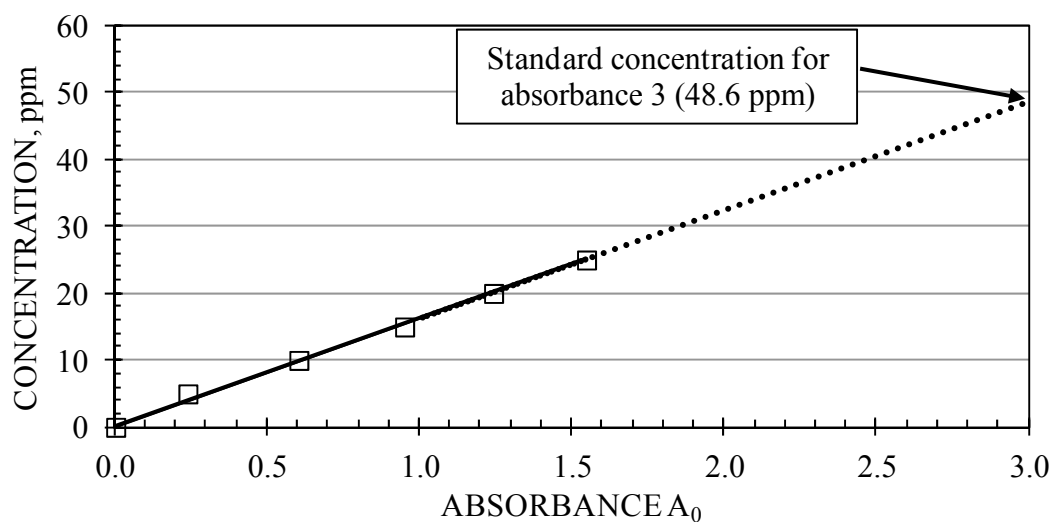
FROTHER: PPG425  
 SUPPLIER: Sigma Aldrich  
 MOLECULAR WEIGHT: 425  
 DILUTION WATER: McGill tap  
 DATE: 07/07/2011

SAMPLE 37

CALIBRATION SPECTRA:



CALIBRATION CURVE:



EQUATION:

$$C \text{ (ppm)} = 16.189 A_0 \quad C \leq 25 \text{ ppm}$$

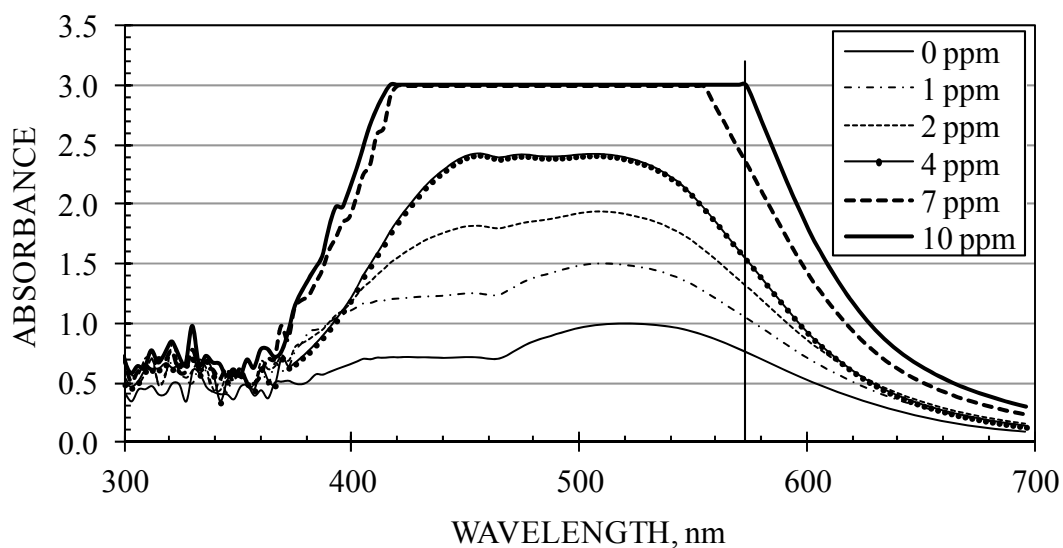
where  $A_0$  is the measured absorbance minus that of the 0 ppm standard (both at 552 nm)

Figure 4.3 - Database entry for PPG425

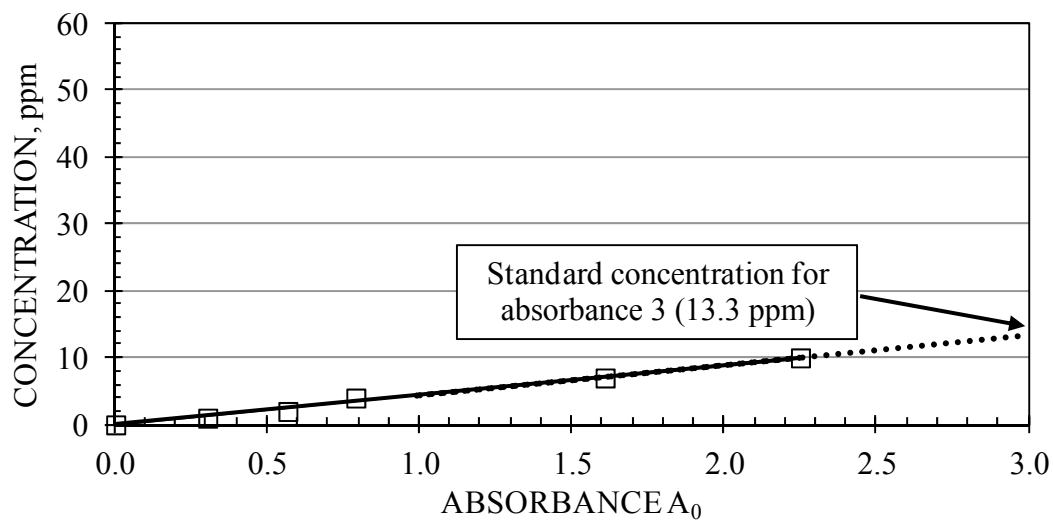
FROTHER: MIBC2  
 SUPPLIER: Sigma Aldrich  
 MOLECULAR WEIGHT: 102.18  
 DILUTION WATER: McGill tap  
 DATE: 09/06/2010

SAMPLE 34

CALIBRATION SPECTRA:



CALIBRATION CURVE:



EQUATION:

$$C \text{ (ppm)} = 4.422 A_0 \quad C \leq 10 \text{ ppm}$$

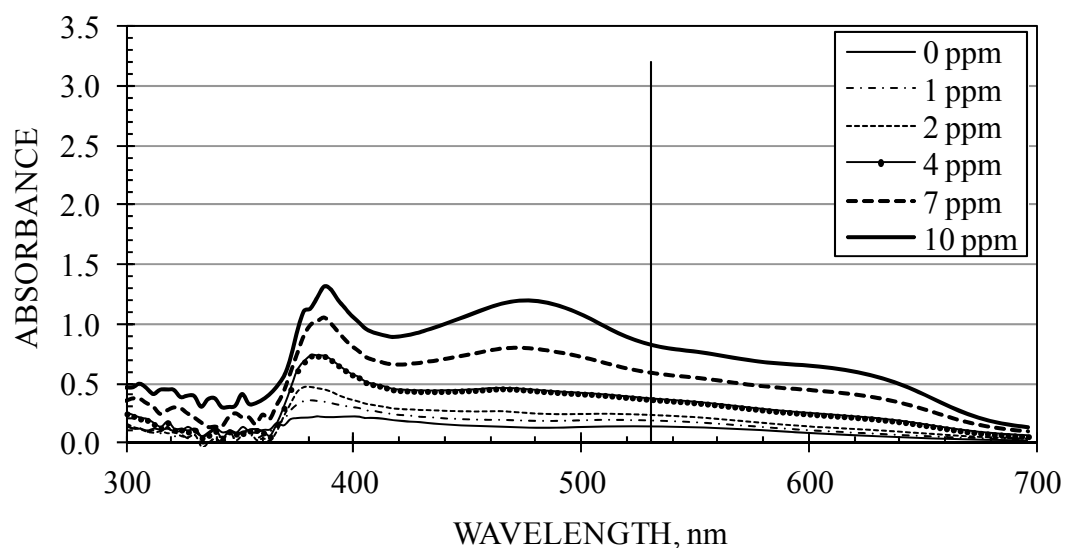
where  $A_0$  is the measured absorbance minus that of the 0 ppm standard (both at 573 nm)

Figure 4.4 - Database entry for a MIBC

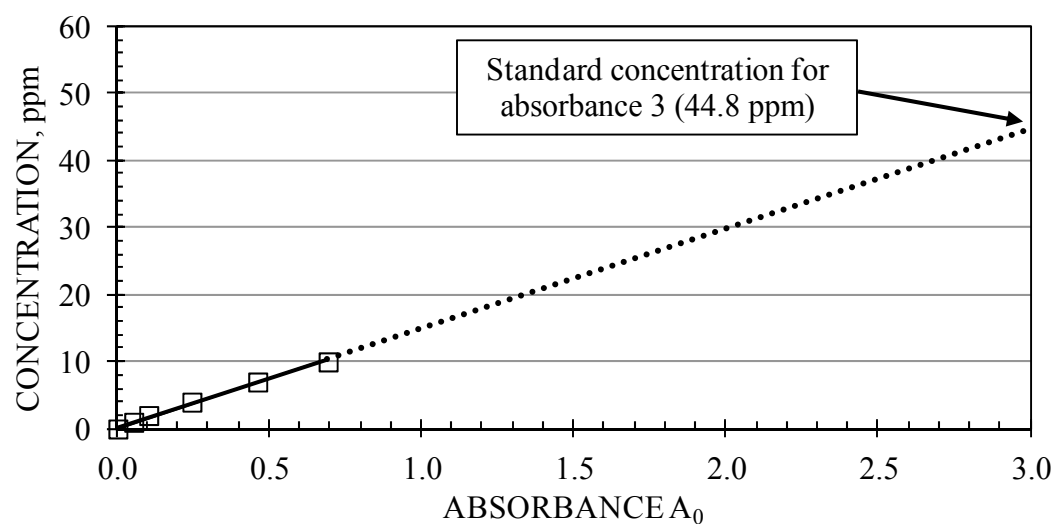
FROTHER: F150  
 SUPPLIER: Flottec  
 MOLECULAR WEIGHT: na  
 DILUTION WATER: McGill tap  
 DATE: 11/04/2010

SAMPLE 1

CALIBRATION SPECTRA:



CALIBRATION CURVE:



EQUATION:

$$C \text{ (ppm)} = 14.945 A_0 \quad C \leq 10 \text{ ppm}$$

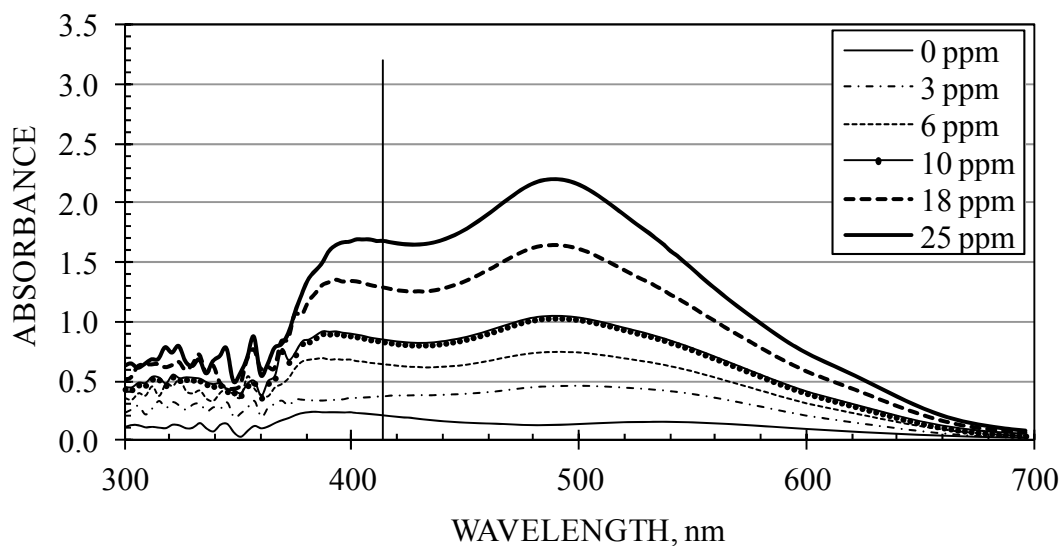
where  $A_0$  is the measured absorbance minus that of the 0 ppm standard (both at 531 nm)

Figure 4.5 - Database entry for F150

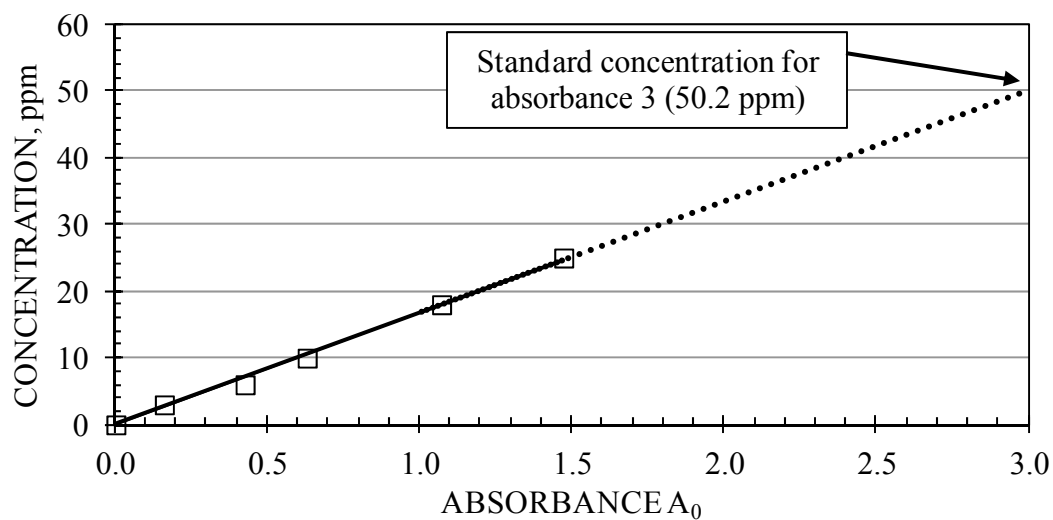
FROTHER: E.Polybractea  
 SUPPLIER: JKMRC  
 MOLECULAR WEIGHT: NA  
 DILUTION WATER: McGill tap  
 DATE: 22/05/2010

SAMPLE 27

CALIBRATION SPECTRA:



CALIBRATION CURVE:



EQUATION:

$$C \text{ (ppm)} = 16.728 A_0 \quad C \leq 25 \text{ ppm}$$

where  $A_0$  is the measured absorbance minus that of the 0 ppm standard (both at 414 nm)

Figures 4.6 - Database entry for a eucalyptus oil sample



## **CHAPTER 5 – FROTHER ANALYSIS: APPLICATIONS IN FUNDAMENTAL RESEARCH**

### **5.1 INTRODUCTION**

The refinement of the colorimetric technique for frother analysis resulted in highly reproducible concentration measurements with relative standard deviation of about 2.5% (including preparation of the stock solution). This makes it possible to mass balance frother around flotation units which was exploited in two applications: determination of the effect of operating conditions on frother partitioning (ratio of overflow to underflow concentrations) and direct measurement of frother coverage on bubbles. In the case of partitioning, procedures were proposed and tested to demonstrate that the sometimes large differences in concentration between the overflow to underflow streams could occur. In the case of frother coverage, development of novel equipment and procedures was required.

### **5.2 FROTHER PARTITIONING**

#### **5.2.1 Establishing techniques**

##### Measurements in bubble column

The laboratory column (0.1 m diameter and 3 m high) was equipped with sensors and electronics to collect signals on-line (Figure 5.1). A mass flow meter/controller was used to measure and control the gas flow rate. Water temperature was measured using a probe installed through the column wall. Pressure transmitters were used to collect differential pressure close to the top of the column in order to estimate gas holdup and to correct gas flow rates and bubble sizes to conditions at the top of the column. The location of the two pressure taps defined the test section for gas dispersion parameters to be determined. The feed solution (frother in water), prepared in a 60 L tank, was introduced using a peristaltic pump above the top pressure tap to limit disturbances in the test section. Level was controlled by manipulation of the valve in the underflow line. Air was dispersed through a porous SS cylindrical sparger, which can be exchanged to vary bubble size range. All instruments were interfaced to a computer and signals were monitored and

stored for subsequent off-line inspection and analysis. Bubble size was measured in some tests using the McGill bubble size analyzer (bubble viewer).

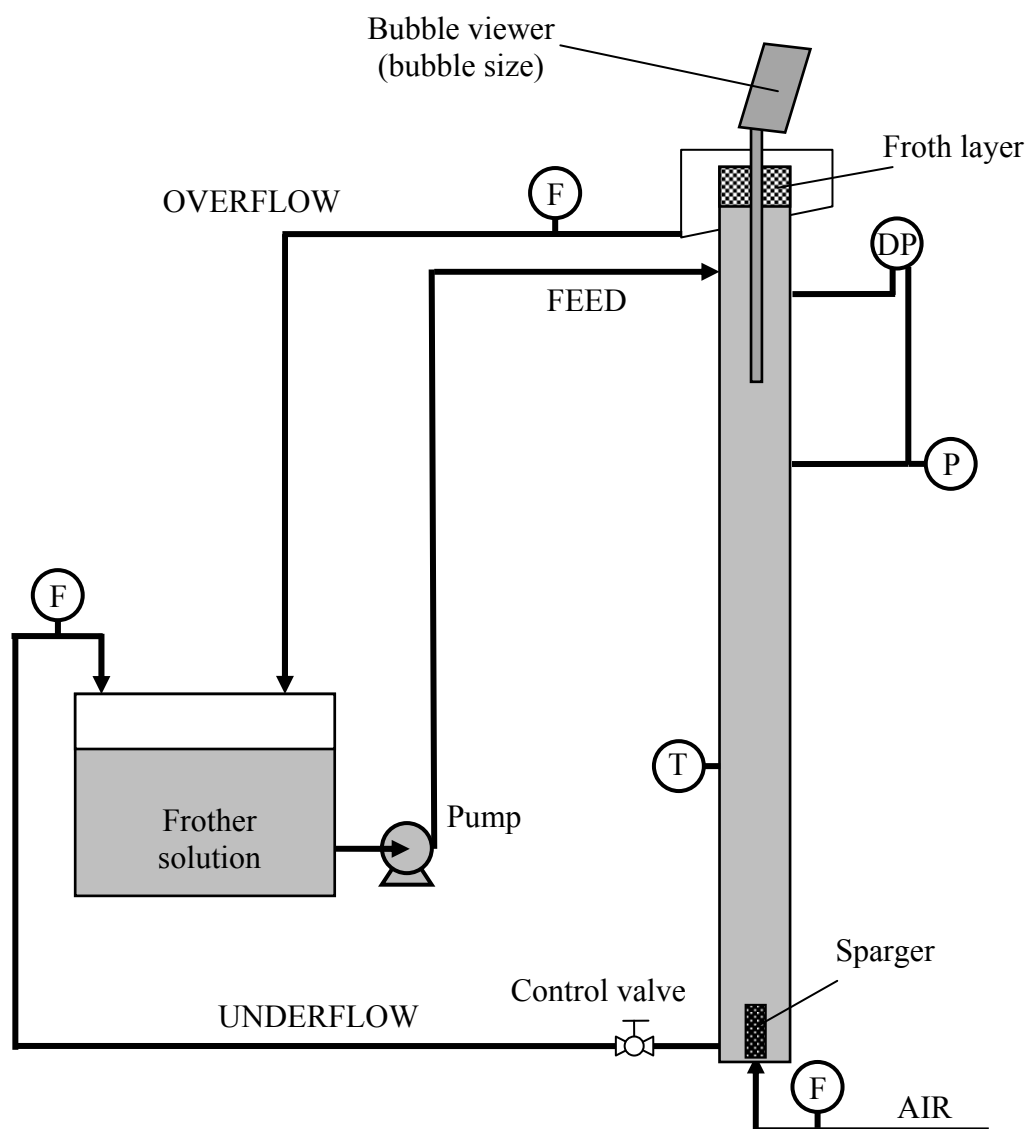


Figure 5.1 - Details of laboratory bubble column installation

The column was run in closed loop with the over- and underflow streams returned to the feed tank. The feed solution was prepared by adding the required amount of frother to 50 L of water. Feed flow rate was about 5 L/min with a constant 5-cm froth layer, which was manually controlled with the valve on the underflow line. The feed flow rate was

considered as the summation of the over- and overflow streams, both measured by weighing timed samples. Once steady signals were obtained, samples of the overflow and underflow streams were collected for frother analysis. After bubble size was measured, the column and the feed tank were drained and washed in preparation for the next experiment.

The variables expected to affect partitioning, when froth depth is fixed, are frother concentration and gas flow rate. The effect of frother concentration was explored by analyzing the samples from the under- and overflow streams in two series of tests (Sets 1 and 2), run at increasing frother (DF250) concentration, at the same gas velocity ( $J_g = 2$  cm/s). These sets were not replicates, as they were run with spargers of different porosity. The overflow concentrations were, as expected, consistently higher than those in the underflow (Figure 5.2), and overflow to underflow concentration ratios decreased as the underflow concentration increased (Figure 5.3). The results demonstrate that the analysis technique is suitable for studying the effects of operating variables on partitioning.

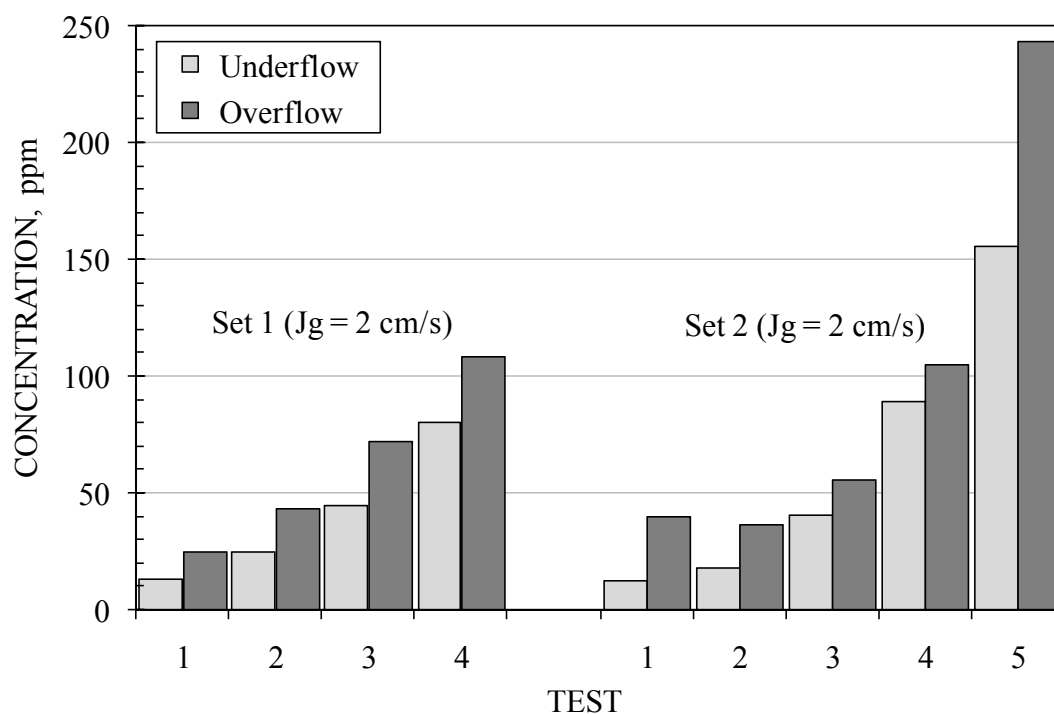


Figure 5.2 - Stream concentrations as a function of frother (DF250) concentration

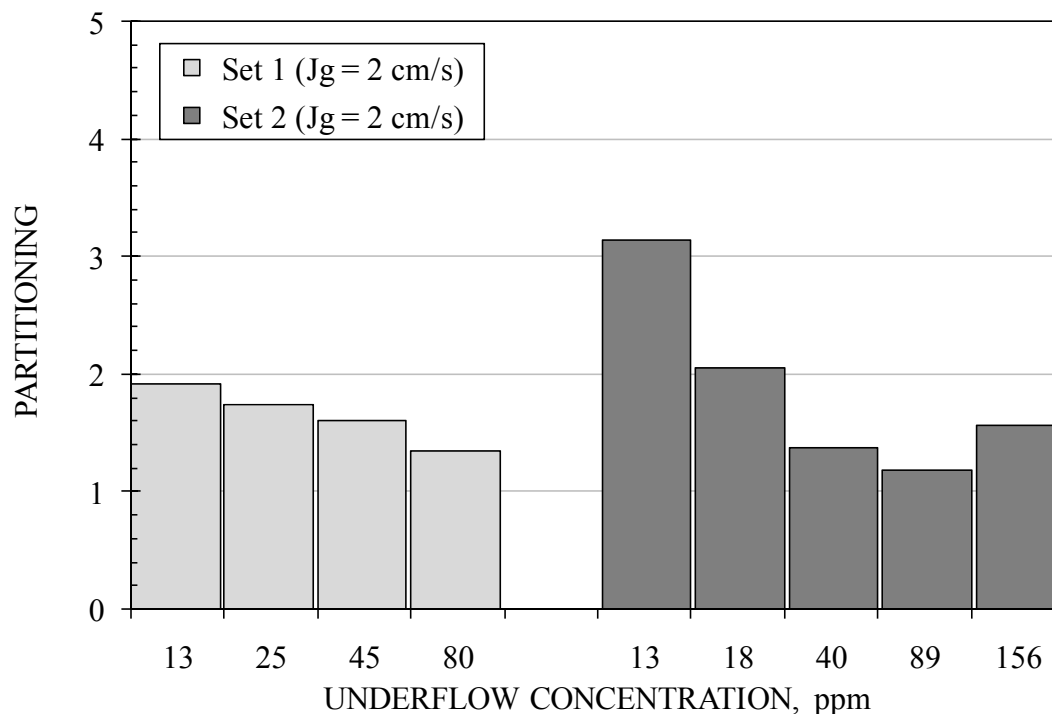


Figure 5.3 - Partitioning as a function of underflow concentration (DF250) in bubble column tests

The effect of gas flow rate on partitioning was investigated in two series of tests: one run with PPG425 at low concentration (around 2 ppm), and a second with the commercial version of the same frother (F150) at a high concentration (around 50 ppm). The results again showed higher overflow frother concentration in every case (Figure 5.4), but here partitioning decreased as the gas flow rate increased at low concentrations but remained constant for the high concentration test series (Figure 5.5). The higher overflow concentration is a consequence of adsorbed frother on the bubble surface being released after the bubbles burst in the overflow stream. The resulting concentration depends on the amount of frother released and the water overflow rate. The higher partitioning in the low concentration series (PPG425), and its decrease with gas flow rate, indicated that the increase in water overflow rate with increasing gas flow rate was more important than the increase in frother derived from the bubbles. In the case of the high concentration series (F150), the constant partitioning indicated that both sources of frother, from adsorption on the bubble and in the overflow solution, are close to being in balance as gas flow rate is increased.

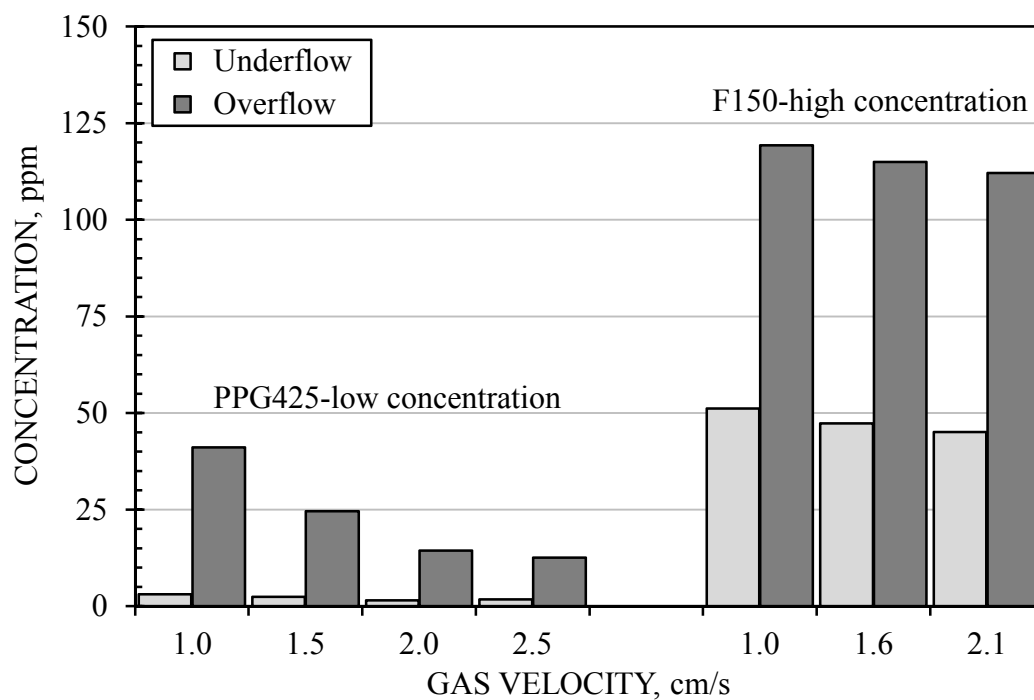


Figure 5.4 - Stream concentrations measured in tests run at several gas velocities in bubble column

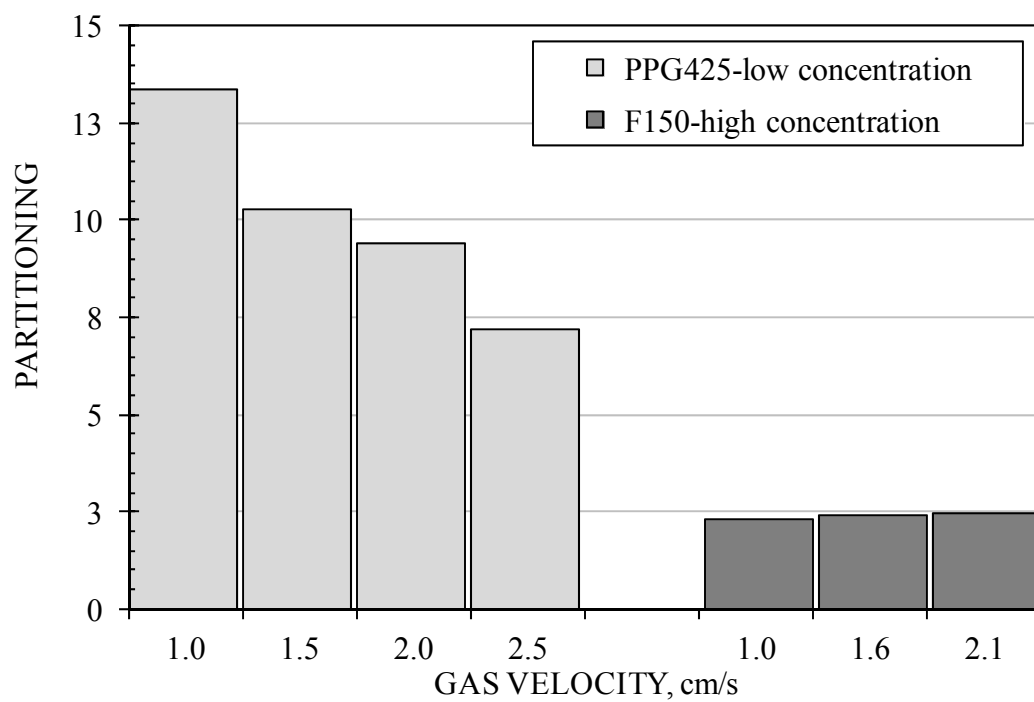


Figure 5.5 - Partitioning as a function of gas velocity for two frother/concentration conditions in bubble column

### Measurements in Jameson cell

A laboratory Jameson cell was assembled by combining an L-150 downcomer, supplied by Xstrata, with a 15-cm diameter separation chamber. The unit was instrumented to continuously monitor and register air/water flow rates and delivery pressures, as well as gas holdup, froth depth and bubble size using the McGill bubble size analyzer (Figure 5.6).

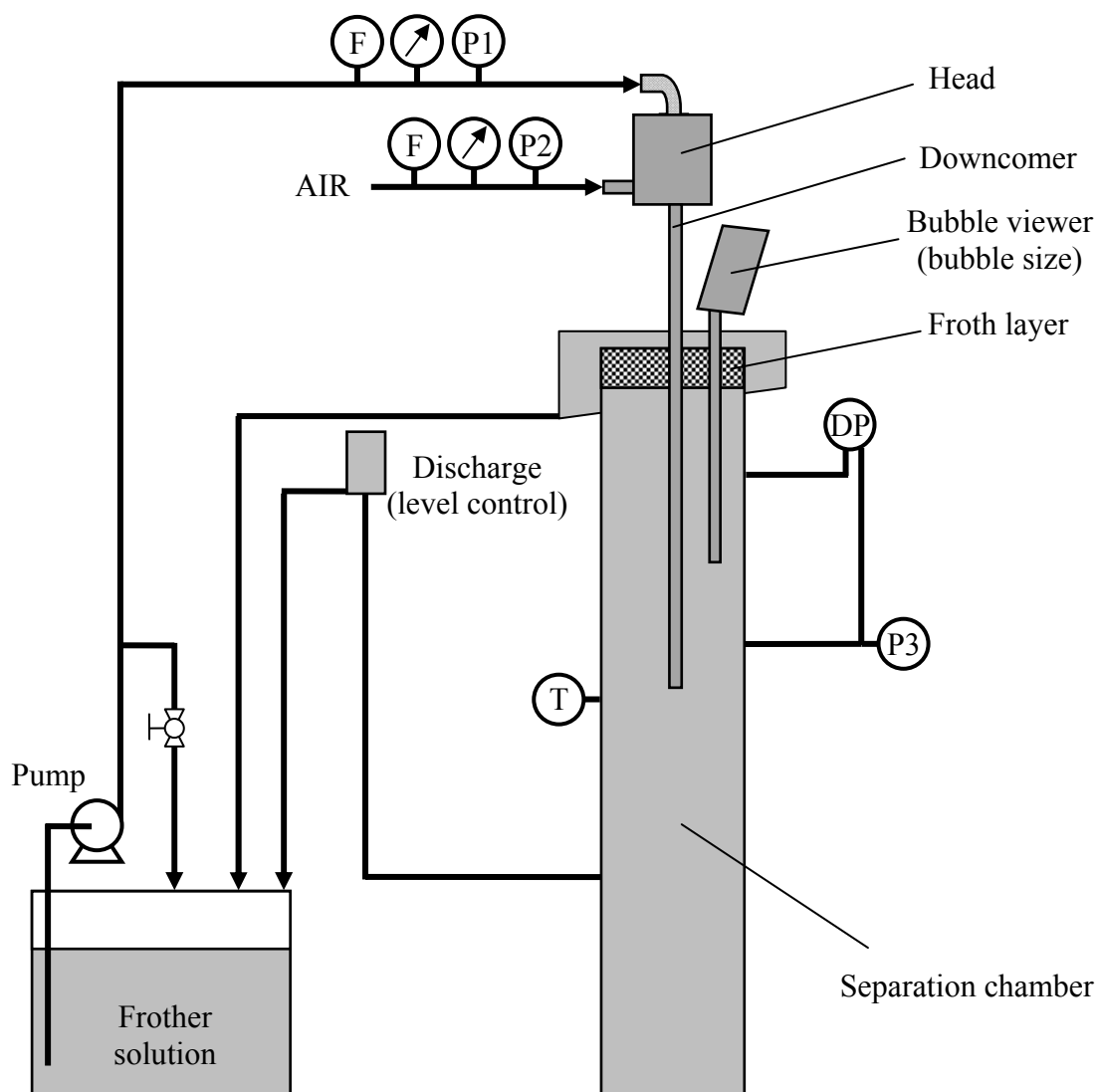


Figure 5.6 - Details of downcomer installation

The frother solution (DF250) was delivered to the head of the downcomer using a centrifugal pump at a flow rate of 17 L/min. The flow was measured using a magnetic flow meter and manually controlled using a by-pass loop. Delivery pressure (P1) was monitored using a pressure transmitter in the feed line. Air was delivered from a compressed air line and monitored and controlled using a mass flow meter/controller. The vacuum induced by the water jet (P2) was monitored using both a pressure transmitter and a vacuum gauge.

The downcomer was installed vertically in the separation chamber. The water jet, created with a 5-mm orifice, was aligned to enter the centre of the downcomer. A section of the separation chamber above the downcomer outlet was selected to measure gas dispersion parameters defined by the pressure taps used for measuring differential pressure ( $\Delta P$ ). The water temperature was measured using an integrated circuit probe. Bubble size was measured using the McGill bubble size analyzer. Bubble images were collected with a Cannon GL50 digital camera (resolution 1233x1045 pixels). The unit was operated over a range of air-to-liquid (pulp) ratios (APR) at a froth depth of 5 cm controlled by adjusting the height of the separation chamber discharge.

The effect of frother concentration on partitioning was determined by collecting samples of the under- and overflow streams, once steady instrument signals were obtained. The results showed, as in the column study, higher overflow than underflow concentrations for every test (Figure 5.7). Partitioning, which as before decreased as the underflow concentration increased (Figure 5.8), was consistent with that measured in the column.

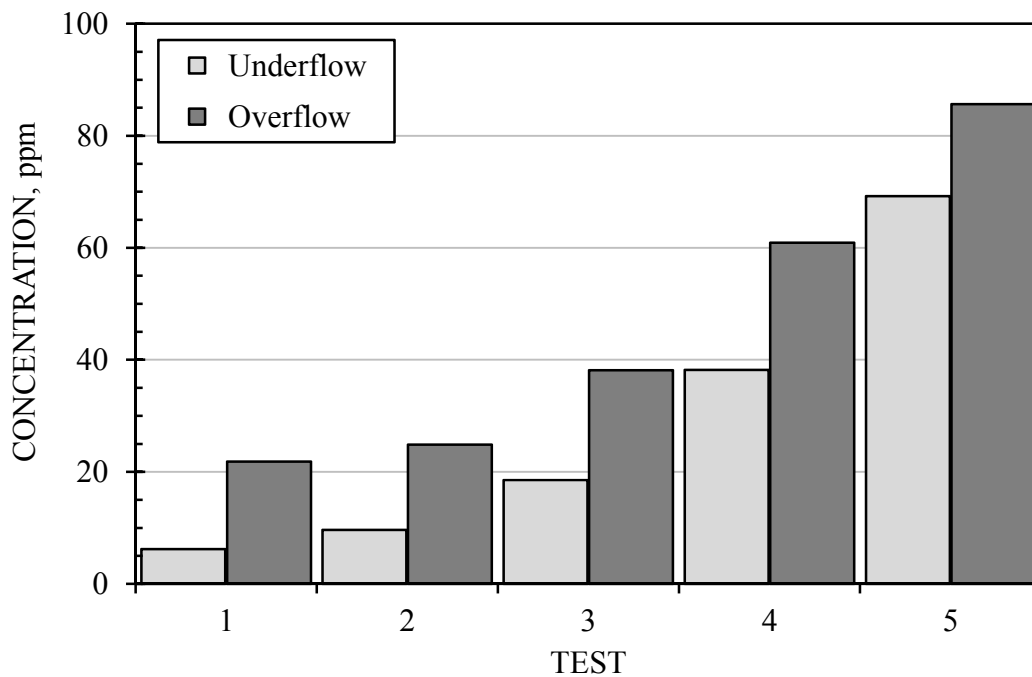


Figure 5.7 - Stream concentrations measured in tests run at several frother (DF250) concentrations in Jameson cell

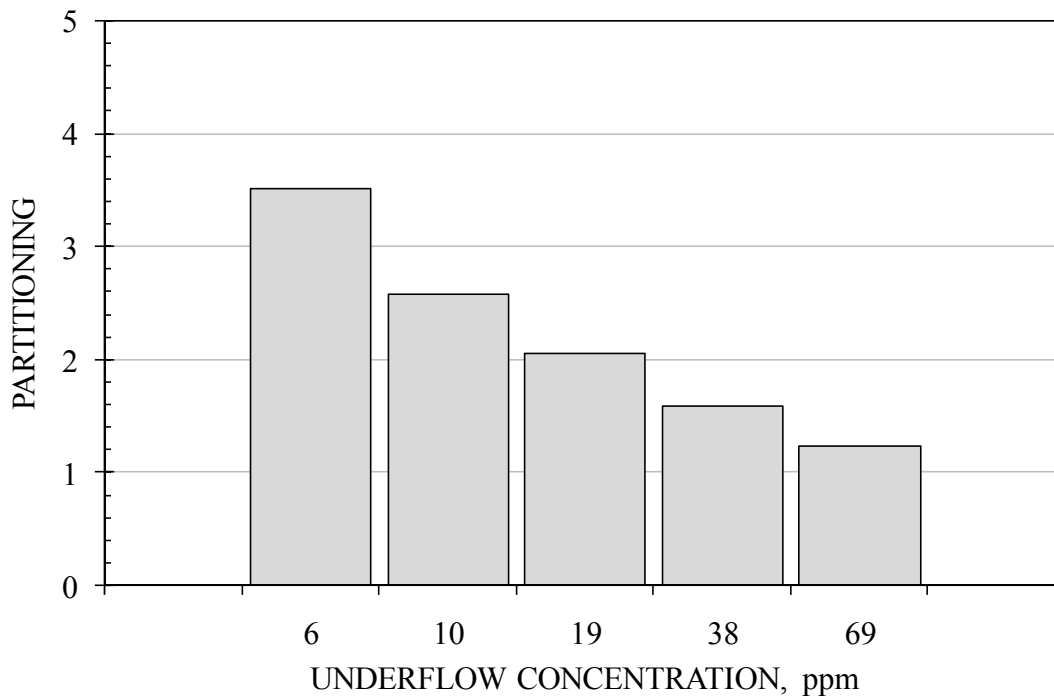


Figure 5.8 - Partitioning as a function of underflow frother (DF250) concentration in Jameson cell tests



## **5.3 FROTHER COVERAGE**

### **5.3.1 Introduction**

The frother functions in flotation result from interaction with the air/water interface (bubble surface). The interaction involves exchange of frother molecules between the bubble surface and surrounding solution. Equilibrium is reached when the rate of these two processes is the same. Measurement of coverage (surface concentration or adsorption density) is given by either mass of frother or number of molecules per unit of bubble surface area.

Knowledge of coverage will help not only to understand and characterize the adsorption process, but also has practical implications, for example in establishing frother consumption and dosage rates, and in selecting number and location of addition points. Measurement of frother coverage under conditions similar to those in flotation machines (swarms of bubbles with average size below 3 mm) can be simulated in a laboratory column. To calculate coverage, the total bubble surface area flux leaving the column is required, which can be determined from measurements of gas flow rate and bubble size distribution, provided that coalescence and bursting are eliminated.

Ideally the approach requires that adsorption equilibrium is achieved, and that the adsorbed frother is only released once the bubbles leave with the overflow stream. The former is assumed here given the height of the column and residence time of the bubbles. The latter is accomplished by operating with no froth layer and installing a 'bubble-guiding' head on the top of the column to direct bubbles to burst outside the unit.

### **5.3.2 Theoretical Considerations**

The approach proposed for estimation of frother coverage requires measurement of two quantities: the amount of frother leaving the column in the overflow stream, and the total bubble surface area flux at the top of the column. The amount of frother leaving the column in the overflow stream is the summation of that in the water and that adsorbed on the surface of the bubbles. The bubble surface area flux is determined from the

measurement of the gas flow rate and the Sauter mean bubble diameter calculated from the bubble size distribution, both at the ambient pressure and temperature of the test.

The frother mass balance applied to the column is:

$$Q_F \rho_F C_F = Q_O \rho_O C_O + Q_U \rho_U C_U \quad (5.1)$$

where  $Q$  is a stream volumetric flow rate in L/min,  $\rho$  is density in kg/L,  $C$  is concentration in mg/kg (ppm), and the subscripts F, O, and U correspond to the feed, overflow and underflow streams, respectively. The feed, overflow and underflow stream densities are taken as corresponding to water. The frother adsorbed on the surface of bubbles leaving the column is calculated from a mass balance (relative to the feed concentration) for the overflow stream:

$$W_O = Q_O \rho_O (C_O - C_F) \quad (5.2)$$

where  $W$  is frother mass flow rate in mg/min. Comparison with the frother removed from the solution by the bubbles, determined from a mass balance (relative to the feed) for the underflow stream, is used to provide redundant data to establish the accuracy of the balance:

$$W_U = Q_U \rho_U (C_F - C_U) \quad (5.3)$$

The bubble surface area flux  $S_b$  (1/s) leaving the column is calculated from the gas flow rate  $Q_g$  (L/min) at the top of the column, the cross sectional area of the column  $A_C$  (cm<sup>2</sup>), and the Sauter mean bubble diameter  $D_{32}$  (mm), using the following equation:

$$S_b = \frac{1000 Q_g}{A_C D_{32}} \quad (5.4)$$

The gas flow rate at the top of the column is calculated from that delivered to the column ( $Q_{st}$ ) reported at standard conditions (1 atm and 0 °C), using

$$Q_g = Q_{st} \frac{(273 + T)}{273} \quad (5.5)$$

No correction for pressure is necessary as the laboratory is practically at sea level.

The frother coverage (in nmol/cm<sup>2</sup>) on the surface of bubbles overflowing the column is calculated from the frother adsorbed,  $W_o$ , divided by the interfacial area generated per unit time:

$$\text{Coverage} = \frac{1,000,000 W_o}{60 M_w S_b A_c} \quad (5.6)$$

where  $M_w$  is the frother molecular weight. Coverage can be used to calculate the area occupied by one molecule ( $A_{\text{molecule}}$ ) in nm<sup>2</sup>, by using Avogadro's number  $N$  ( $6.023 \times 10^{23}$  molecules/mol) and factors to transform nmol into mol, and cm<sup>2</sup> into nm<sup>2</sup>:

$$A_{\text{molecule}} = \frac{10^{23}}{N \text{ Coverage}} \quad (5.7)$$

Coverage can also be estimated from the Gibbs adsorption isotherm equation. In our application, the adsorption of frother, i.e., non-ionic surfactant, the appropriate isotherm is:

$$\Gamma_i = -\frac{1}{RT} \left( \frac{\partial \gamma}{\partial \ln C_i} \right)_{T,P} \quad (5.8)$$

where  $\Gamma_i$  is the surface excess of the frother (molg/m<sup>2</sup>),  $\gamma$  is surface tension (N/m),  $C_i$  is the frother concentration (molg/L),  $R$  is the universal gas constant (8.314 J/molg K) and  $T$  is the absolute temperature (K). Average surface excess is calculated from the slope of surface tension against log of the concentration.

$$\Gamma_i = -\frac{\text{Slope}}{RT} \quad (5.9)$$

The average area occupied by one molecule can be calculated from the surface excess in an analogous manner to Equation 5.7:

$$A_{\text{molecule}} = \frac{10^{18}}{N \Gamma_i} \quad (5.10)$$

### 5.3.3 Experimental Aspects

The bubble column (0.1 m diameter and 3 m high) was instrumented to collect the required information on-line (Figure 5.9) and furnished with a cylindrical stainless steel sparger to disperse the air.

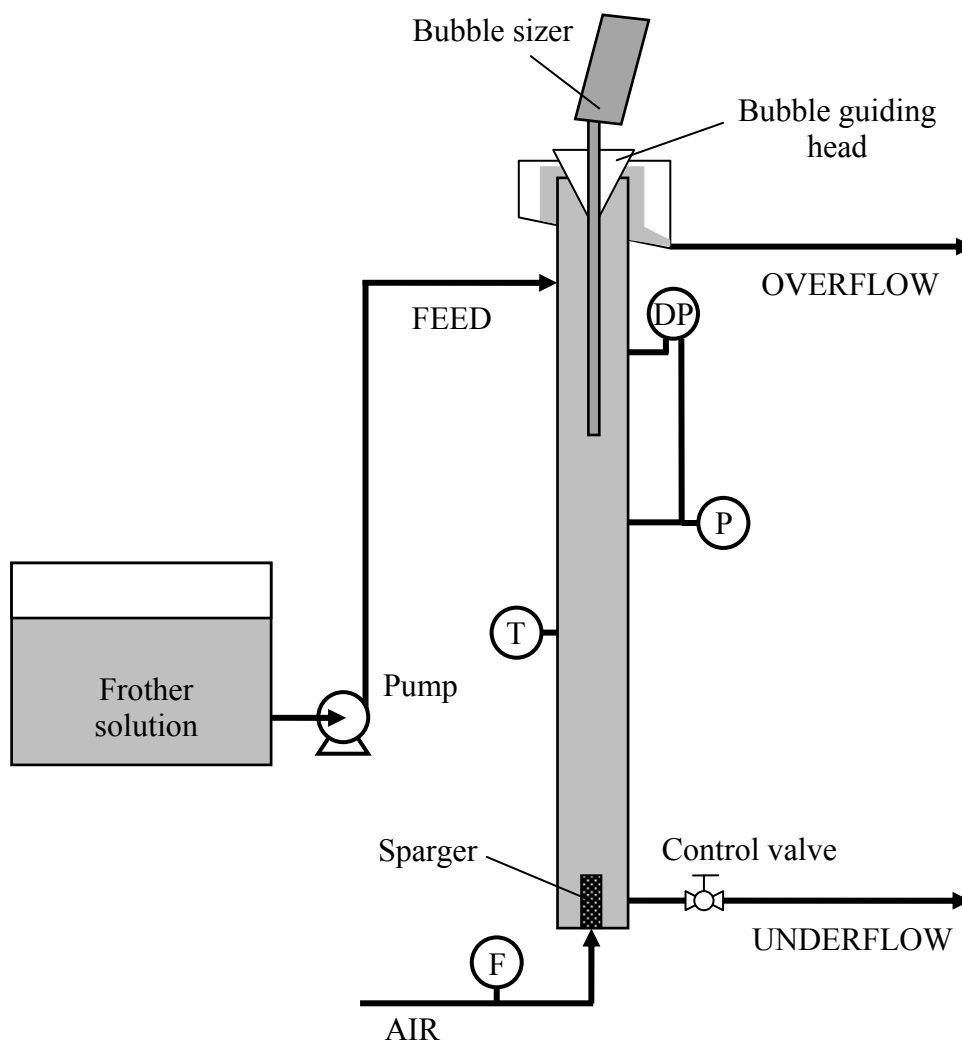


Figure 5.9 - Details of laboratory bubble column setup

A mass flow meter/controller was used to measure and control the gas flow rate. Water temperature was measured using a probe installed in the column wall. Pressure transmitters were used to collect differential pressure close to the top to estimate gas holdup, and hydrostatic pressure near the bottom to correct gas flow rates and bubble sizes to conditions at the top of the column. The feed solution was introduced about 0.4

m from the top and delivered using a peristaltic pump from a 300 L tank sufficient in capacity to provide about 60 minutes of continuous, open-loop operation. The underflow rate was controlled using a manual valve installed in the line. All instruments were interfaced to a computer and readings were collected and stored once every second for subsequent off-line analysis.

An important component was the PVC “bubble guiding” head designed to avoid bubble bursting within the column by directing bubbles out of the column without exposure to the open air until they joined the overflow stream. The column was run in open loop (overflow and underflow streams were discarded) to make sure that the feed frother concentration was constant. The feed solution was prepared by addition of the selected amount of frother to the feed tank. A continuous overflow rate (no froth layer) was maintained by controlling the underflow rate using the valve in the underflow line. The feed flow rate set point was 5 L/min, and the overflow rate was about 0.5 L/min. The operational feed flow rate was calculated as the sum of the under- and overflow streams, both measured by weighing timed samples. Once steady traces for the signals were obtained, samples of the feed, overflow, and underflow streams were collected for frother analysis. Bubble size was then measured and the column and feed tank were drained and thoroughly washed in preparation for the next experiment.

#### **5.3.4 Results**

The test frothers were polypropylene glycol molecular weight 425 (PPG-425), 1-octanol and methyl isobutyl carbinol (MIBC). Because of measurement errors (sampling and analytical) it is important to have redundant data to reconcile the data to have consistent mass balances. The redundant data are the mass balance on the underflow measuring the frother ‘lost’ along with the mass balance on the overflow measuring the frother ‘gained’. The reconciliation was done by the conventional Lagrangian multiplier approach (Wills and Napier-Munn, 2007). For every test, the under- and overflow rates and frother analysis results are included in Table 5.1 along with the reconciled concentrations. The differences between measured and reconciled concentrations are in most cases around 1% for the feed and underflow streams, and around 0.1% for the overflow stream, which

demonstrates that column operation was stable and frother analysis was accurate. This is further illustrated in Figure 5.10, which shows almost no differences between the mass balance obtained from measured and reconciled data. However, stream mass balances relative to the feed concentration (Equations 5.2 and 5.3), were more sensitive to measurement errors (Figure 5.11) as the mass flow of frother adsorbed on bubbles is much smaller than that in the stream.

Table 5.1 - Stream flow rates and measured and reconciled concentrations

Frother	Conc. (ppm)	Flow rate (L/min)		Measured concentration (ppm)			Reconciled concentration (ppm)		
		U/F	O/F	Feed	U/F	O/F	Feed	U/F	O/F
PPG425	5	3.80	0.50	4.68	4.18	9.29	4.73	4.14	9.28
PPG425	10	3.80	0.49	9.80	8.62	17.29	9.69	8.72	17.30
PPG425	20	3.78	0.49	21.63	20.48	30.58	21.64	20.47	30.58
PPG425	30	3.77	0.52	29.95	30.97	43.21	31.35	29.74	43.04
PPG425	40	3.77	0.51	43.46	41.43	59.03	43.50	41.40	59.03
PPG425	60	3.75	0.52	59.24	58.21	71.65	59.57	57.92	71.61
1-octanol	2	3.94	0.51	2.55	2.36	3.57	2.52	2.38	3.58
1-octanol	5	3.91	0.52	6.44	5.98	8.23	6.33	6.08	8.24
1-octanol	10	3.91	0.52	13.30	12.91	16.76	13.33	12.88	16.76
1-octanol	20	3.93	0.51	25.32	24.15	37.35	25.51	23.99	37.33
1-octanol	30	3.85	0.51	37.24	35.71	61.08	38.03	35.00	60.98
1-octanol	40	3.84	0.49	49.49	47.89	66.47	49.77	47.64	66.44
1-octanol	60	3.93	0.51	70.79	68.05	95.44	71.03	67.84	95.41
MIBC	2	3.90	0.49	2.94	2.52	2.78	2.72	2.71	2.80
MIBC	5	3.77	0.50	5.63	5.59	6.11	5.64	5.58	6.11
MIBC	10	3.83	0.50	11.23	11.19	12.22	11.28	11.16	12.22
MIBC	20	3.84	0.52	21.78	21.91	23.27	21.95	21.77	23.25
MIBC	30	3.84	0.50	33.35	33.56	35.24	33.58	33.36	35.21
MIBC	40	3.77	0.51	46.48	47.31	48.44	47.02	46.84	48.37
MIBC	60	3.70	0.51	67.62	67.62	68.51	67.68	67.57	68.50

The coverage results for the three frothers as a function of the feed (reconciled) concentration are displayed in Figure 5.12. Gas dispersion measurements and parameters for calculation of coverage are included in Table 5.2. Two of the frothers (PPG425 and MIBC) reached a coverage which was independent of the frother concentration, even for concentrations as low as 2 ppm. This suggests not only that adsorption-desorption equilibrium is attained in the time the bubbles remain in the column, but more significantly, that packing of frother molecules on the bubble surface is independent of the concentration in the bulk. The results for 1-octanol are different, as the amount of frother on the surface of bubbles increases steadily with concentration up to about 40 ppm, suggesting a denser surface packing which requires higher bulk concentrations to reach the adsorption-desorption equilibrium and full coverage.

The calculation of the surface area occupied by one molecule from the Gibbs equation is illustrated in Figure 5.13. The surface tension data were taken from measurements by Zhang, W. (2012). The surface excess corresponds to the slope of the line, and is the value used to calculate the average area occupied by one molecule (Equation 5.9), with values 7.65, 1.85 and 0.89 nm<sup>2</sup> for MIBC, PPG425 and 1-octanol, respectively. These average values are compared with the areas measured at the different concentrations in the column (Figure 5.14); the results are of the same order of magnitude.

In the case of 1-octanol the surface tension vs. concentration data do not fit a straight line as well as in the other two cases (Figure 5.13c). By taking the ‘slope’ between consecutive points surface excess as a function of frother concentration can be determined. A comparison between surface excess vs. concentration results obtained in the column and from the surface tension data (plotted at the average concentration of the pair of selected points) for 1-octanol is presented in Figure 5.15. The results show a close correspondence supporting that 1-octanol differs from the other two in that surface coverage increases with concentration.

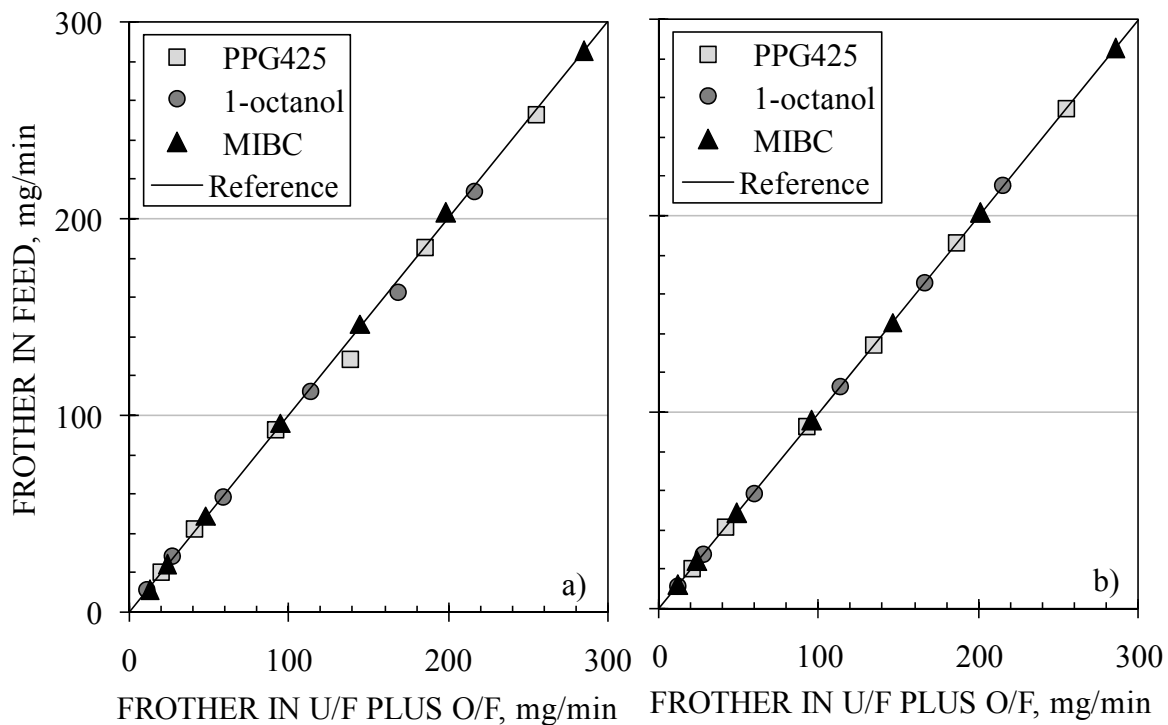


Figure 5.10 - Total mass balances obtained from a) measured, and b), reconciled data

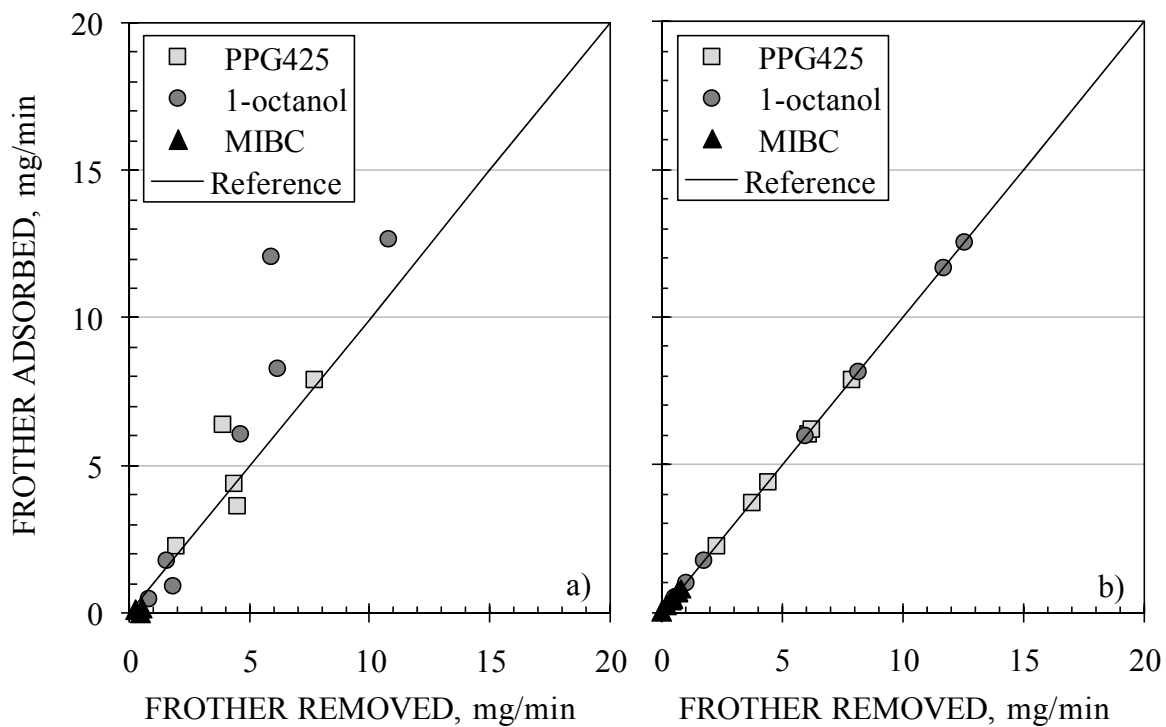


Figure 5.11 - Stream mass balances obtained from a) measured, and b), reconciled data



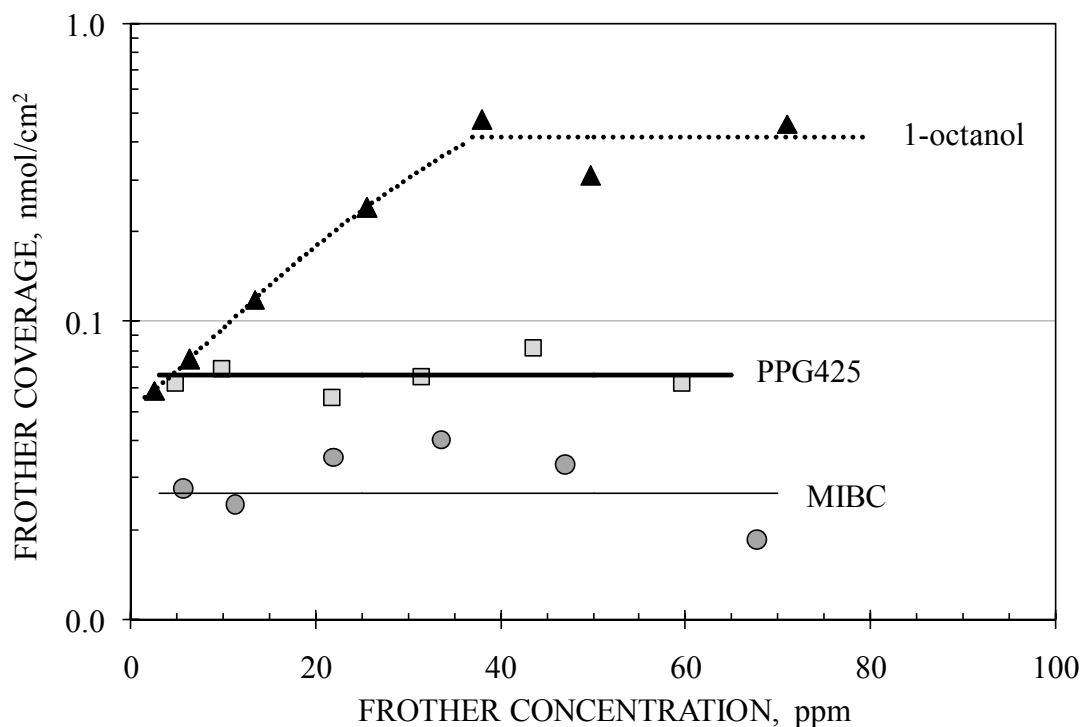


Figure 5.12 - Frother coverage results as a function of feed frother concentration

The accuracy of the coverage measurement does depend on the operating conditions selected; conditions that favour adsorption on the bubbles and hence maximize the difference between the overflow and feed concentrations are required. Careful selection of gas flow rates, feed frother concentration, and overflow/underflow split ratios that lead to larger differences between overflow and feed concentrations will result in better defined coverage results. The choice of surfactant is also a factor; more active surfactants, i.e., give higher coverage, will enhance the accuracy of the coverage measurement. This is evident in the case of 1-octanol which gives a more pronounced change in coverage and surface tension with concentration permitting coverage as a function of concentration to be determined.

The results demonstrate that direct measurement of surface coverage based on mass balancing frother is successful, which for the purpose of this thesis, further demonstrates

that the refined frother analysis technique is robust and can be effectively used in the analysis of frother systems.

Table 5.2 - Gas dispersion measurements and coverage results

Frother	Conc. (ppm)	$J_g$ (cm/s)	$D_b$ (mm)	$S_b$ (1/s)	$W_o$ (mg/min)	Coverage (nmol/cm <sup>2</sup> )	Molecular area (nm <sup>2</sup> )
PPG425	5	0.50	2.30	13.0	1.45	0.054	3.08
PPG425	10	0.50	1.79	16.8	2.27	0.065	2.54
PPG425	20	0.50	1.27	23.6	4.82	0.099	1.68
PPG425	30	0.50	0.87	34.5	6.29	0.088	1.88
PPG425	40	0.50	0.70	43.0	3.79	0.043	3.89
PPG425	60	0.50	0.66	45.4	4.34	0.046	3.59
1-octanol	2	0.50	2.07	14.5	0.54	0.059	2.82
1-octanol	5	0.50	1.43	20.9	0.99	0.075	2.22
1-octanol	10	0.50	1.28	23.4	1.76	0.119	1.39
1-octanol	20	0.50	0.77	38.8	5.97	0.243	0.68
1-octanol	30	0.50	0.78	38.4	11.66	0.480	0.35
1-octanol	40	0.50	0.72	41.7	8.17	0.310	0.54
1-octanol	60	0.50	0.70	42.7	12.55	0.464	0.36
MIBC	2	0.50	2.59	11.6	0.04	0.007	24.6
MIBC	5	0.50	1.76	17.0	0.23	0.028	6.03
MIBC	10	0.50	0.77	39.0	0.47	0.024	6.83
MIBC	20	0.50	0.77	39.0	0.68	0.035	4.74
MIBC	30	0.50	0.73	40.9	0.82	0.040	4.13
MIBC	40	0.50	0.71	42.3	0.70	0.033	5.01
MIBC	60	0.50	0.66	45.2	0.42	0.019	8.91

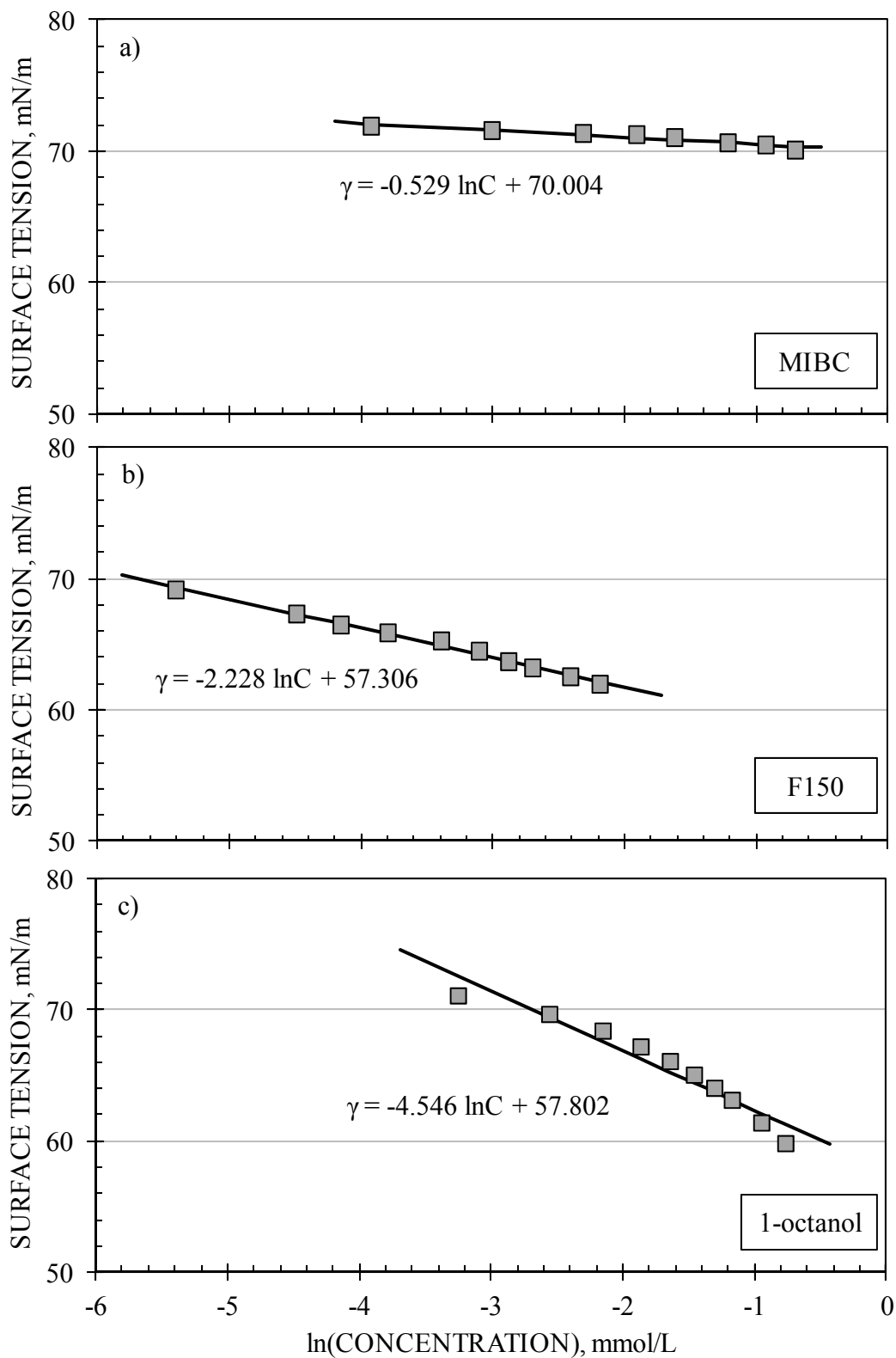


Figure 5.13 - Determination of surface excess from surface tension data for frothers MIBC, F150 and 1-octanol

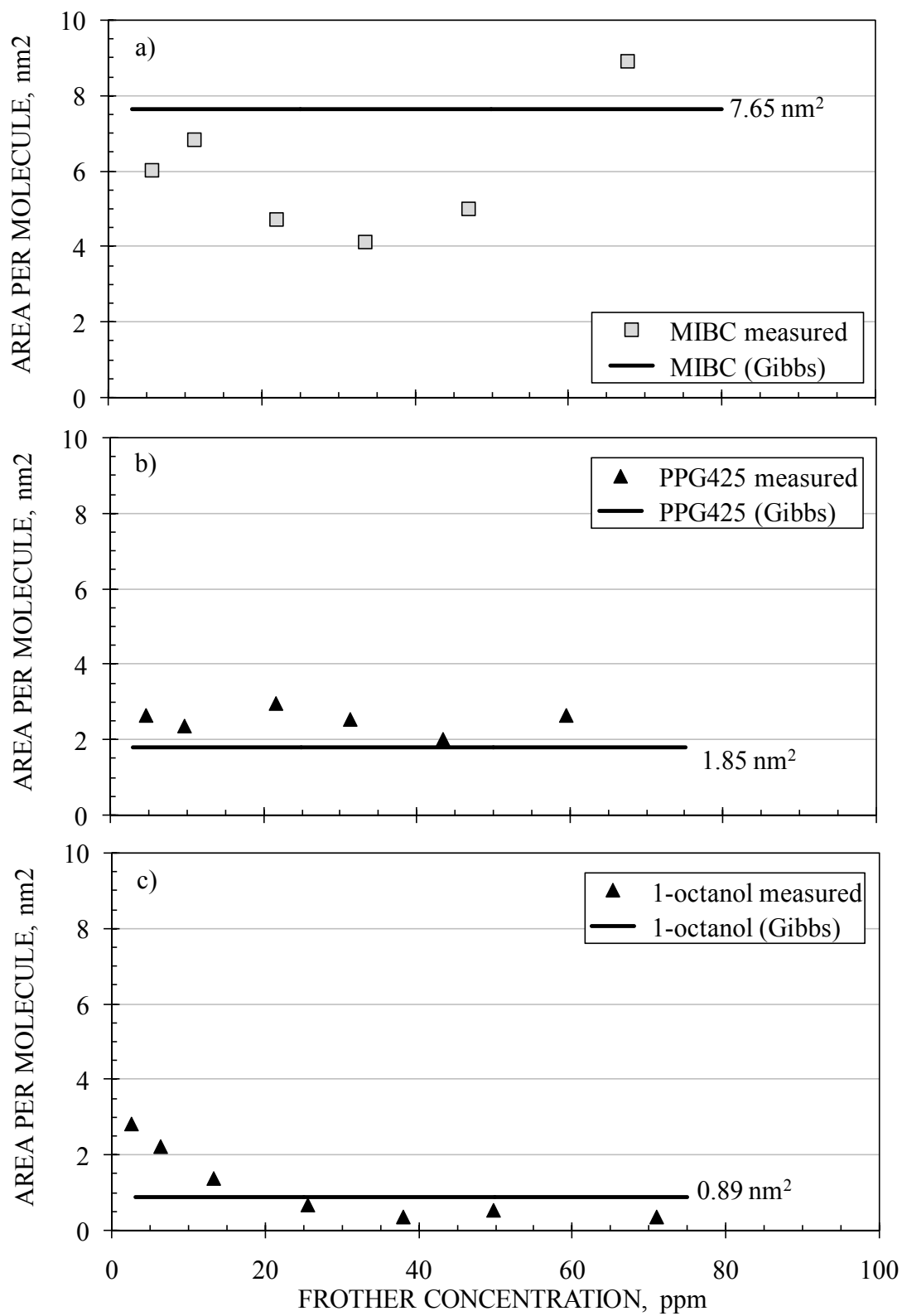


Figure 5.14 - Measured and predicted average areas of adsorbed molecules on the surface of bubbles: a) MIBC, b) PPG425, and c), 1-octanol

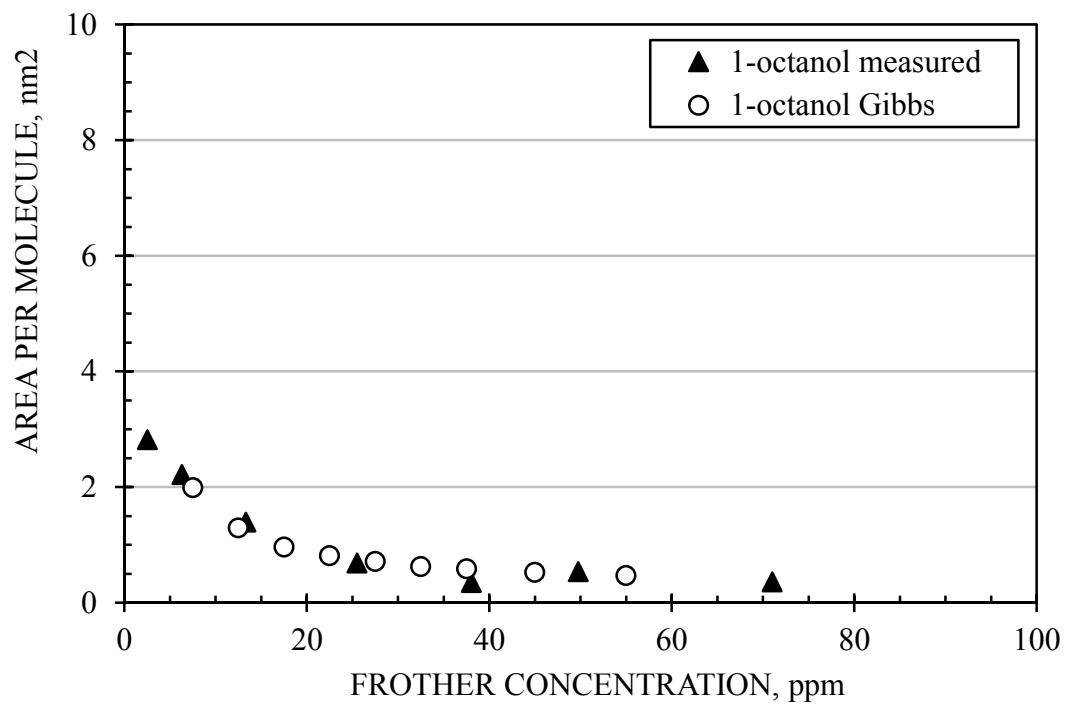


Figure 5.15 - Measured and predicted areas of adsorbed molecules on the surface of bubbles for 1-octanol

## CHAPTER 6 – INDUSTRIAL APPLICATIONS OF FROTHER ANALYSIS

### 6.1 INTRODUCTION

After the work to refine the technique was completed and the analyses were proven to be reliable, the method was to be integrated with gas dispersion measurements in plant, which was the original driving force for the development of the technique. The transferring of this technique to operations makes it possible to address operational concerns regarding frother delivery and distribution; this technology transfer is the subject of this chapter.

The gas dispersion variables bubble size and gas holdup are affected by frother concentration. Frother is added to maintain the desired bubble size and froth characteristics by maintaining a target concentration in the water around the bubble formation region. The target concentration is today conveniently expressed in terms of the critical coalescence concentration, CCC (Cho and Laskowski, 2002 a, b). Most plants dose frother based on feed tonnage, a variable difficult to control, which means solution concentration can vary as tonnage changes. If the frother level is about or below the CCC, then variable concentration results in inconsistent bubble size and gas holdup. Maintaining frother concentration near but above CCC is becoming an operational target (Cappuccitti and Nasset, 2009).

The integration of frother analysis and gas dispersion measurements should make it possible to identify if variable frother concentration is the reason for variable flotation performance. Variations in frother dosage can occur because of unstable frother delivery, incomplete dissolution, dilution by addition of launder and wash water, uneven distribution into cell lines, and frother partitioning into the concentrate stream. Concentration differences between circuit stages, variations in one cell over time, and concentration decreases down a line of cells, have been demonstrated. The presence of residual frother in recycle waters and the introduction of contaminants with frother-like

properties with other reagents used in flotation (e.g., some xanthate collectors which have alcohol diluents) are other causes of variation in frother concentration.

The variation in frother concentration around a circuit can be established through sampling and analysis. A comprehensive determination of concentration in time and location around a circuit offers a way for operations to identify issues associated with frother delivery and distribution: this procedure is referred to as 'frother distribution mapping'.

To illustrate the technology transfer, this chapter documents experiences in four on-site campaigns, namely: two campaigns at Codelco's Chuquicamata concentrator in northern Chile, one campaign at Codelco-Salvador Division (Chile), one campaign at CMDI Collahuasi (Chile), a campaign at Vale's Voisey's Bay concentrator in eastern Canada, and one at Newcrest's Telfer Gold Mines in Western Australia. Frothers in use at the time of the campaigns were Nalcofroth and Nalflote (Nalco), F160-10 (Flottec), and DSF004 (Dow Chemical), respectively.

## **6.2 REQUIREMENTS FOR IN-PLANT FROTHER ANALYSES**

Frother analysis at plant sites presents challenges not directly related to the analytical procedure. Three in particular are discussed: 1) selection of spectrum collection rate, 2) measurement of analysis standard deviation, and 3) determination of the effect of sample storage time.

1. The UV-VIS spectrometer allows collection of spectra at different speeds (slow, medium and fast) and, by using the maximum speed, significant time can be saved in plant campaigns. It is necessary to establish whether the spectrum collection speed affects the reproducibility of the analysis. Spectra were collected for the same sample at the three speeds, in the wavelength range between 400 and 700 nm, with wavelength intervals of 5 nm, which is suitable for most frothers. The results for a rougher line feed sample at Chuquicamata showed differences in the wavelength

ranges 400 to 450 nm and 550 to 570 nm (Figure 6.1), but practically identical spectra in most of the green region (490-570 nm). Selecting a wavelength from the green region to construct the calibration curve gave consistent results between the three speeds (Figure 6.2).

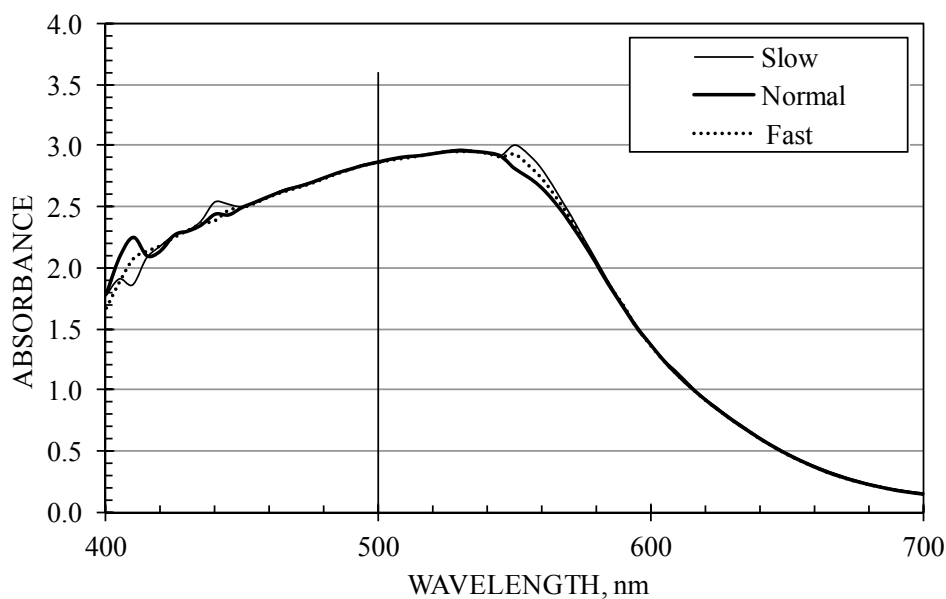


Figure 6.1 - UV-VIS spectra obtained at the three speeds

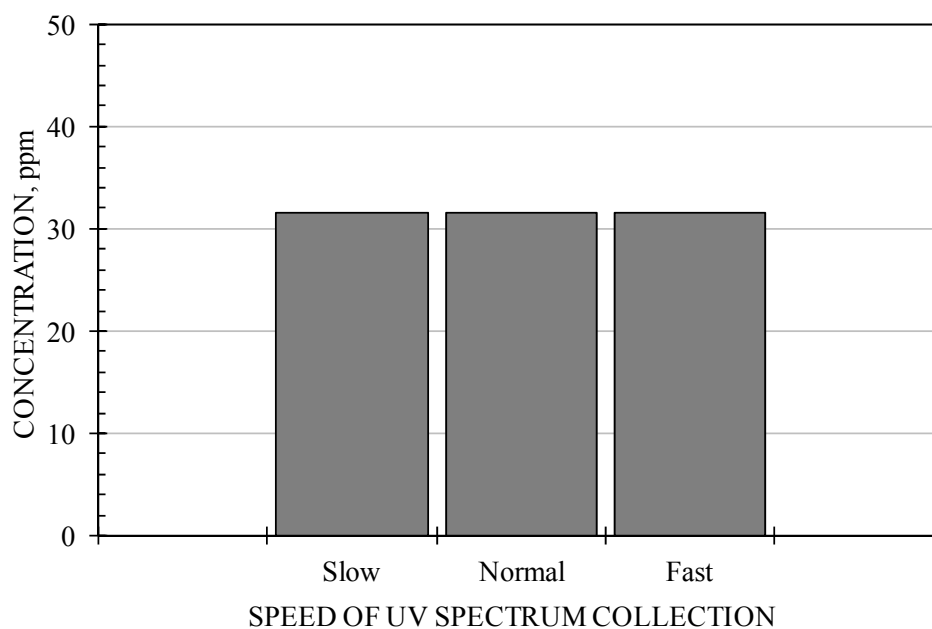


Figure 6.2 - Concentrations (at 500 nm) with spectrum collection rates



2. It is also important to establish the analysis error (standard deviation), relevant to the plant site, more than once when process water is used for construction of the calibration curve. The sources of error depend on factors sometimes unique to an operation, but primarily because of variability of water quality and reagent specifications. Experience has demonstrated that errors are about 50% higher than those obtained in the laboratory, as illustrated in the following examples (Figure 6.3):
- Results of four analyses of a 12 ppm standard solution prepared with process water at Chuquicamata: Average concentration was 10.63 ppm with a standard deviation of 0.18 ppm, which means an error of  $\pm 0.59$  ppm at 95% confidence interval (C.I.);
  - Results of five analysis of the feed to a rougher line at Telfer: Average concentration was 5.12 ppm with a standard deviation of 0.23 ppm, which means error of  $\pm 0.65$  ppm at 95% C.I.; and
  - Results of five analysis of the feed to a rougher line at Telfer, same as the previous example but on a different day: Average concentration was 9.89 ppm with a standard deviation of 0.45 ppm, which means an error of  $\pm 1.24$  ppm at 95% C.I.

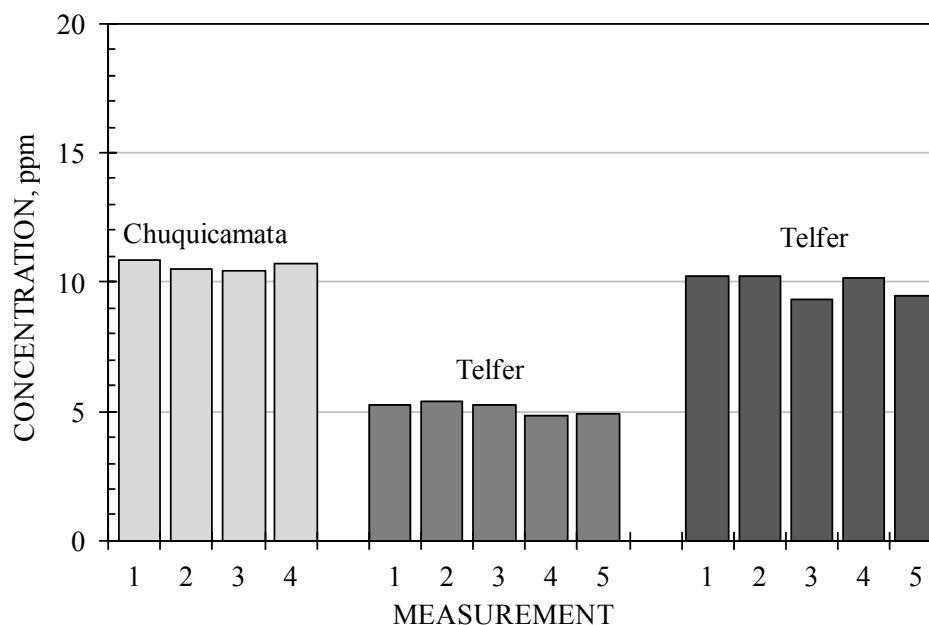


Figure 6.3 - Measurement of analysis standard deviation in plant sites

These errors are similar to those measured at McGill for frother solutions in the same concentration range (Section 3.6).

- Another aspect is the analysis rate, currently at about 20 samples per day. Campaigns often result in the collection of more than 20 in a day; therefore, a fraction will be processed more than 24 hours after being collected. It is important to establish if there is an effect of storage time on determination of sample concentration, especially as most plants do not have low temperature storage facilities.

The effect of sample storage time was assessed by collecting a large volume of a single sample maintained at the counter top for several days. The analysis of aliquots processed on successive days demonstrated that it was affected by storage time (Figure 6.4). The results showed, in the case of a rougher feed sample at Chuquicamata, up and down concentration changes of about 5 to 10% between days, which were larger than the error in the analysis. In the Telfer case, the concentration in the rougher feed decreased steadily for the first four days, but unexpectedly started to increase after that. These results indicate that precautions must be taken when samples cannot be analyzed on the same day of collection; guidelines for sample storage need to be established.

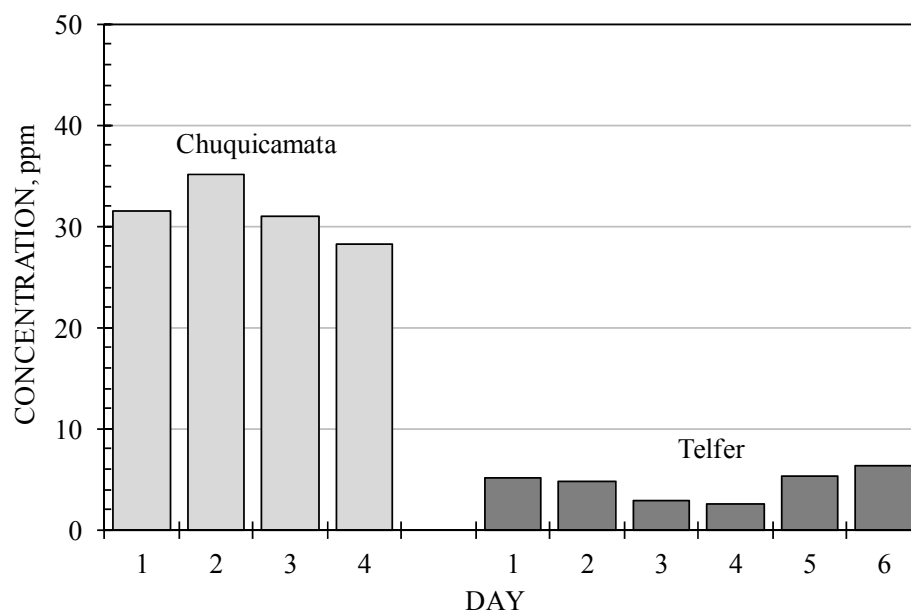


Figure 6.4 - Determination of effect of storage time on analysis results

### **6.3 FROTHER CONTENT IN PROCESS AND RECYCLE WATERS**

Analysis of plant samples presents a challenge in deciding what water to use in the preparation of standards. The analysis is expected to be unaffected by most inorganic contaminants, as demonstrated in Section 3.4, with the possible exception of high magnesium concentration. In plants there are normally two sources of water: tap (potable) and process waters. Process water seems the preferable option as it will have the same level of inorganic constituents in the standards as in the samples, but if this water contains remnant frother then its use will require deduction of the remnant frother presence. Therefore process waters have to be tested for residual frother, itself useful information for operations.

Commonly the frother residual concentration is measured by constructing a calibration curve with standards prepared with tap water. When the absorbance of the test sample is the same as that for the tap water, then the process water is free of frother, and a calibration curve established with the process water can be used. When the absorbance for the process water sample is larger than that for tap water, then the analysis is run using the tap water calibration curve. The presence of remnant frother in process water has been the case in every concentrator, illustrated from the first campaign at Chuquicamata. The unit, a single 300 m<sup>3</sup> cell, was run using a feed prepared by diluting cyclone O/F with a process water of unknown source. The analysis of this water detected a residual frother concentration between 14 and 15 ppm (Figure 6.5).

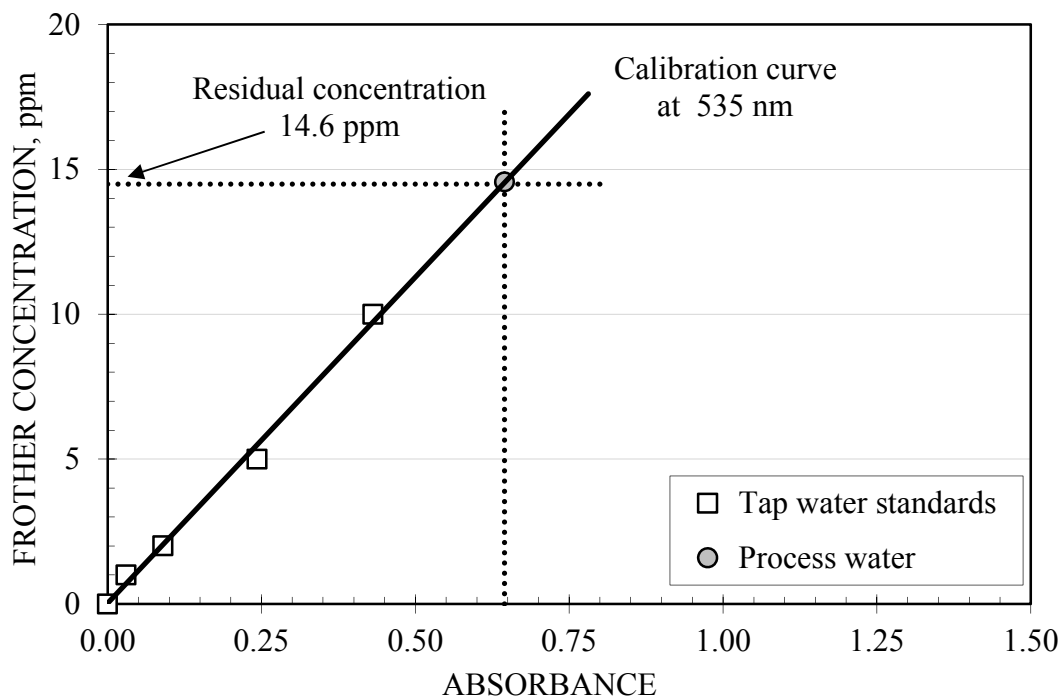


Figure 6.5 - Determination of remnant frother concentration

In the second campaign at Chuquicamata, which involved measurement of frother concentration in every cell in the circuit, the selection of water for construction of the calibration curve became complicated. Chuquicamata is an old concentrator which has gone through a series of modifications and expansions over its life. The flowsheet includes three rougher circuits (A0, A1 and A2) with a common cleaner/scavenger (Section 6.7). The process (recycle) water used in the three circuits was different as the waters came from different sources. A calibration curve was prepared with tap water at 505 nm. Samples of the process water from each bank and a composite sample collected from the thickeners supplying recycle waters showed different frother concentrations (Figure 6.6).

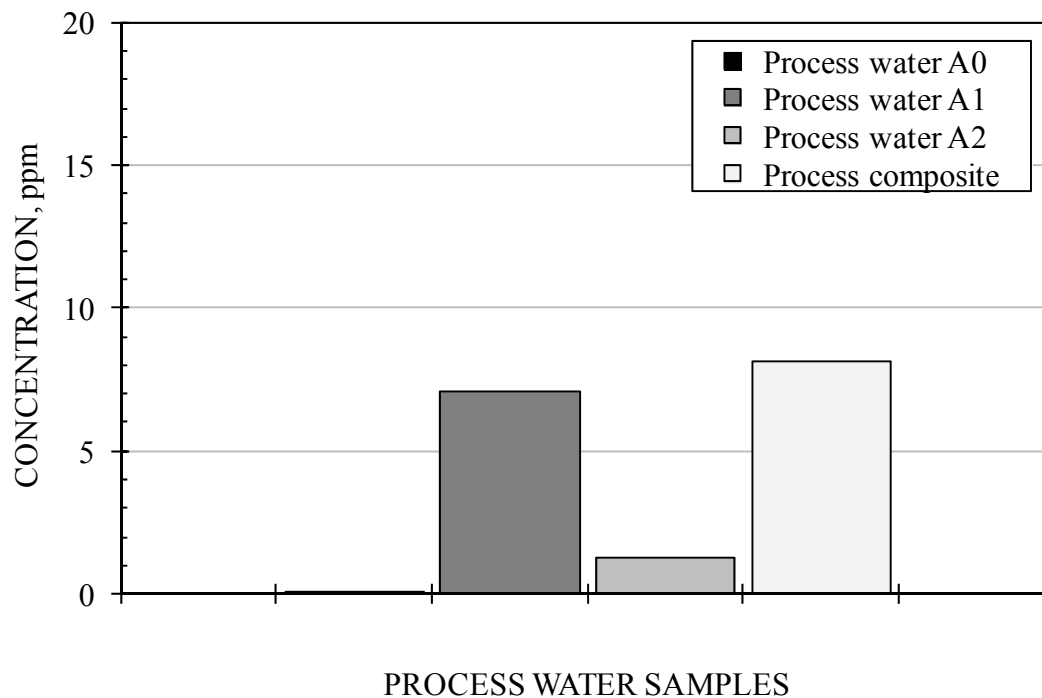


Figure 6.6 - Remnant frother in samples of process waters

The low concentration measured in the sample from circuit A0 (0.3 ppm) makes this water a good candidate for use in the construction of the calibration curve. However, it was decided to run the analysis using the tap water calibration curve, as there was no guarantee that contaminant levels were the same in the three circuits, and advantages (higher accuracy) of using A0 process water may not apply to the analysis of samples from banks A1 and A2.

#### 6.4 INTERFERING SPECIES

Any OH-containing organic is likely to interfere in the analysis. One example derives from collectors which are sometimes diluted with organic solvents, usually low molecular-weight alcohols, to reduce viscosity and facilitate delivery. As these solvents, for the purpose of the analysis, have a response similar to frothers, analysis of a collector sample is required to establish how significant the contaminant contribution may be.

A 10-ppm collector standard was routinely analyzed in site visits to assess interference. When the absorbance of this standard was above 0.1, a calibration curve was constructed. In these cases, the frother concentration will be overestimated by a factor that depends on the collector addition rate and the slope of the calibration curve. Frother concentration corrections are difficult to establish because the fraction of the collector that affects the absorbance is unknown.

Experience, however, has indicated that the effect of collector on absorbance is smaller than that of residual frother. A calculation based on the worst-case scenario, considering that all the collector components that affect absorbance are present in the sample, gives the following: at Chuquicamata (Figure 6.7), overestimation is about 1.9 ppm, in Codelco-Salvador Division in Chile (Figure 6.8) ca. 3.9 and 3.1 ppm for frothers 1 and 2, respectively, and at Telfer (Figure 6.9) ca. 1 ppm. At high frother concentration (> 15 ppm) these errors may not be significant when determining the frother distribution map.

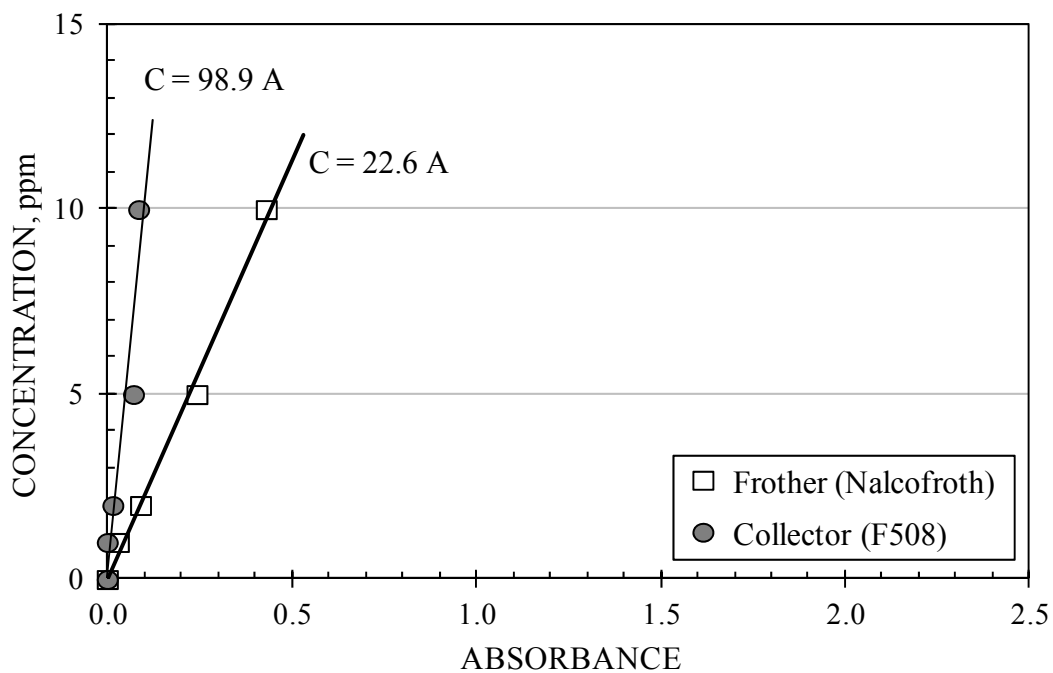


Figure 6.7 - Calibration curves in tap water for the combination frother/collector in use at Chuquicamata

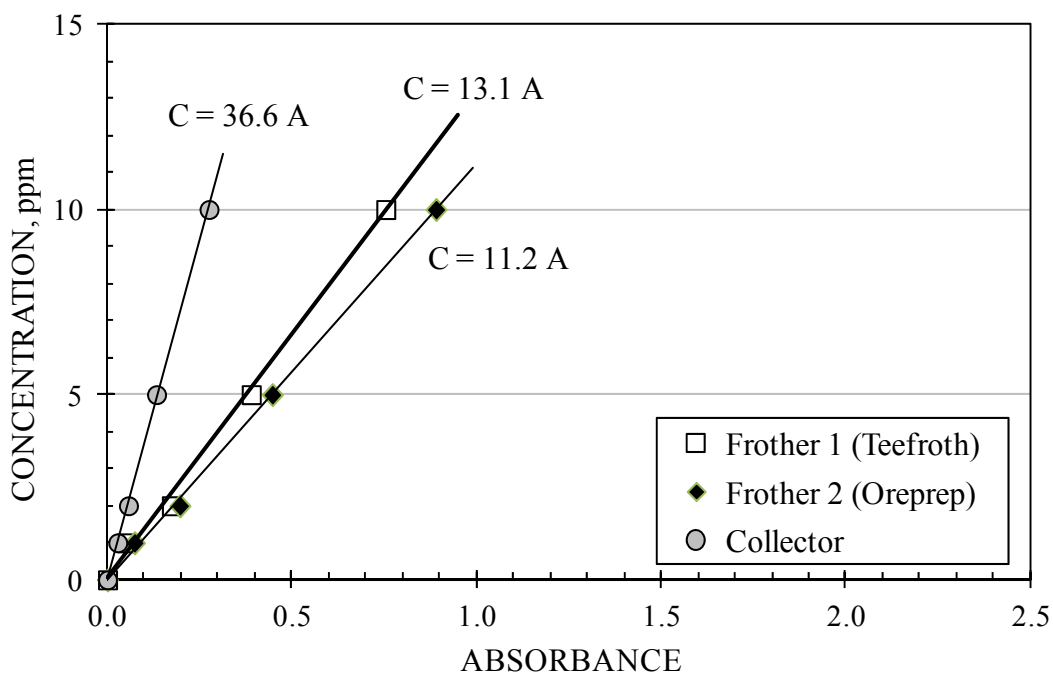


Figure 6.8 - Calibration curves in tap water for the combination frothers/collector in use at Codelco-Salvador Division (Chile)

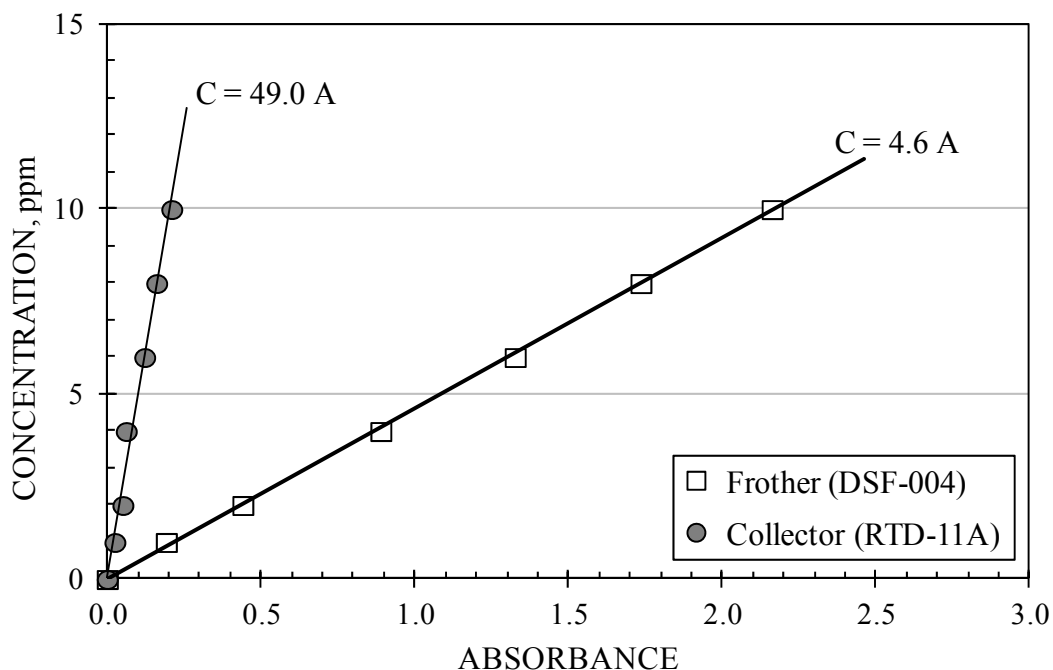


Figure 6.9 - Calibration curves in tap water for the combination frothers/collector in use at Telfer

## 6.5 STABILITY OF FROTHER DELIVERY

A common request is to establish the stability of frother delivery. Testing consistency in delivery is done by collecting pulp samples from one cell over time with frother dosage held steady according to the control room. The results of the exercise at Chuquicamata, with samples collected about every half an hour from 11:45 to 14:15, and from 19:00 to 19:55 after the tonnage was reduced to one half the original (at 17:00) are shown in Figure 6.10. The figure shows frother concentration (Nalcofroth) varying from 13 to about 15 ppm. As frother is dosed based on solids tonnage (i.e., g/tonne) and not with the purpose of achieving a certain liquid phase concentration in the cell, variations such as those shown in Figure 6.10 may be common. Whether these variations impact metallurgical performance, as a consequence of changes in bubble size (concentrations in this case are close to the usual CCC range for frothers) and/or froth characteristics, may determine the level of effort warranted to correct it. The frother delivery system did



handle the 50% tonnage reduction well, keeping the solution concentration close to the same range.

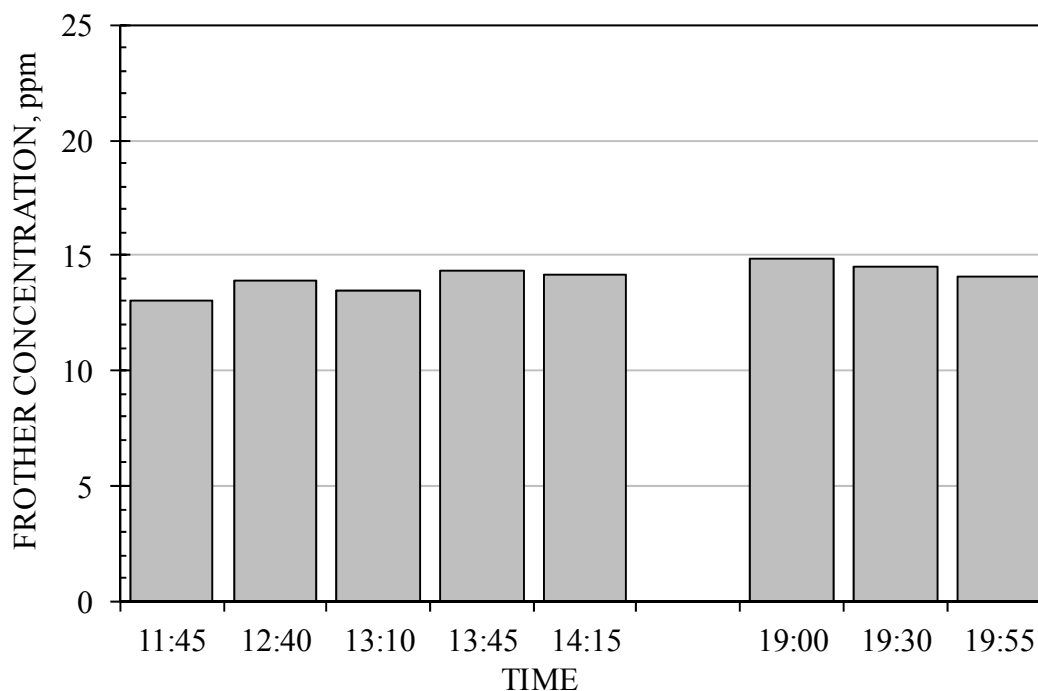


Figure 6.10 - Frother concentration measured in a cell over time at Chuquicamata

Measurement of frother concentration down a bank is another way to assess frother delivery. In this case samples down the bank are collected as simultaneously as possible to have a spatial concentration profile at a given time. The exercise at Salvador in a nine-cell rougher bank (Figure 6.11) showed a frother (Oreprep) concentration profile with a pattern, decreasing from about 32 ppm at the head of the bank down to ca. 20 ppm at mid-bank then rising again, that may reflect a cyclical variation in the feed frother concentration associated with the delivery system. The results reveal frother concentrations which seem to be higher than the CCC, i.e., more than enough to control bubble size, a consequence, in this case, of high frother content in the recycle water. The concentration in the feed to the bank is higher than that measured in any cell and may reflect partitioning of frother to the froth, another factor that can now be explored with the analytical technique.

The frother concentration variations measured in and between cells in a bank, prompted determination of the standard deviation, to establish whether the differences were statistically significant.

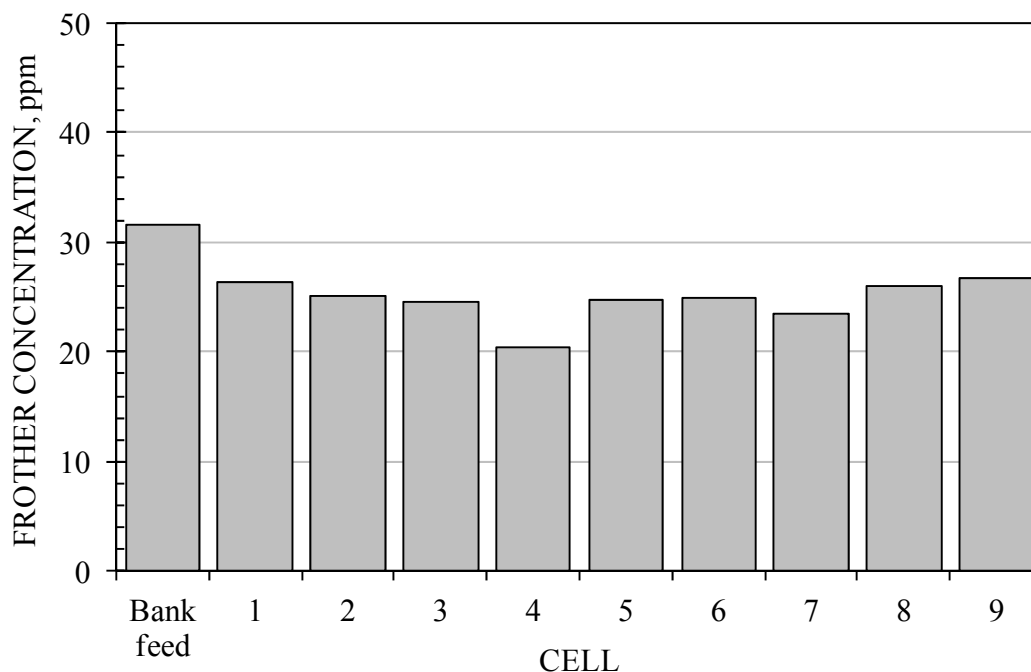


Figure 6.11 - Frother concentration profile measured in a nine-cell bank at Codelco-Salvador Division (Chile)

## 6.6 DETERMINATION OF FROTHER PARTITIONING

Frother transfers (partitions) from the pulp to the froth and into the cell overflow (concentrate) stream by adsorption on the surface of rising bubbles that release the adsorbed frother when they burst outside the cell. This partitioning increases frother concentration in the concentrate water. The phenomenon has been verified in the laboratory (Zhang et al., 2009) and the plant (Gelinas and Finch, 2007), and has been exploited to measure frother coverage on the bubble (Zangoi et al., 2012).

Partitioning has potential practical consequences, among them: increasing bubble size in the pulp (by reducing frother concentration in the pulp water); altering froth properties (excess frother in the froth can cause excessive froth stability); influencing subsequent

cell and downstream circuit behaviour. Frother partitioning correlates with bubble survival rate in the froth layer, a parameter related to froth recovery.

Frother partitioning has been measured in several plants. For example, the results obtained at Telfer (Figure 6.12) showed partitioning occurring in every cell of a rougher bank (Outotec 150 m<sup>3</sup>). Concentrations in the concentrate stream were as high as 36 ppm for concentrations in the pulp of about 4 ppm, and varied widely from cell to cell.

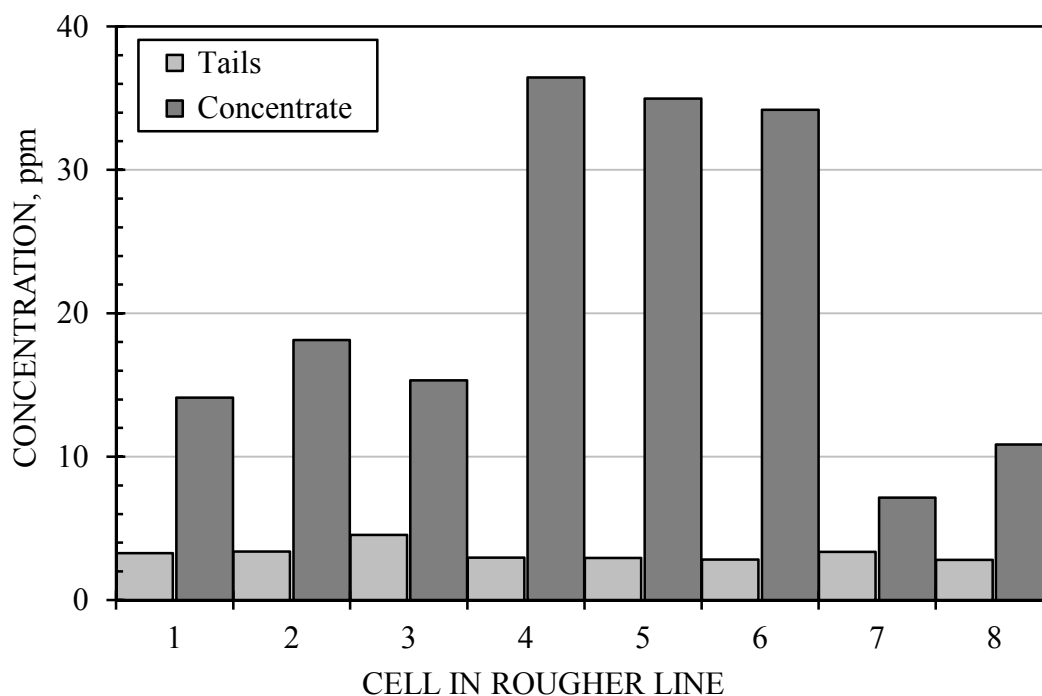


Figure 6.12 - Frother partitioning measured in rougher cells at Telfer

Measurements at Voisey's Bay (Figure 6.13) showed a steady decrease in concentrate frother concentration down the bank (cells were Dorr Oliver 38 m<sup>3</sup>). The results obtained at the three Chuquicamata rougher circuits (A0, A1 and A2) showed diverse responses (Figure 6.14): at A0 (Wemco 56 m<sup>3</sup>), concentrations in the concentrate varied broadly, while in A1 (Outotec 150 m<sup>3</sup>), there was no partitioning in the first two cells and then a steady decrease in concentrate frother concentration down the bank. In circuit A2 (Outotec 150 m<sup>3</sup>), there was a general increase in concentrate frother concentration over the first six cells. In each circuit the pulp frother concentration varied in a manner

apparently independent of the concentrate frother concentration but in all cases pulp frother concentrations were above the CCC.

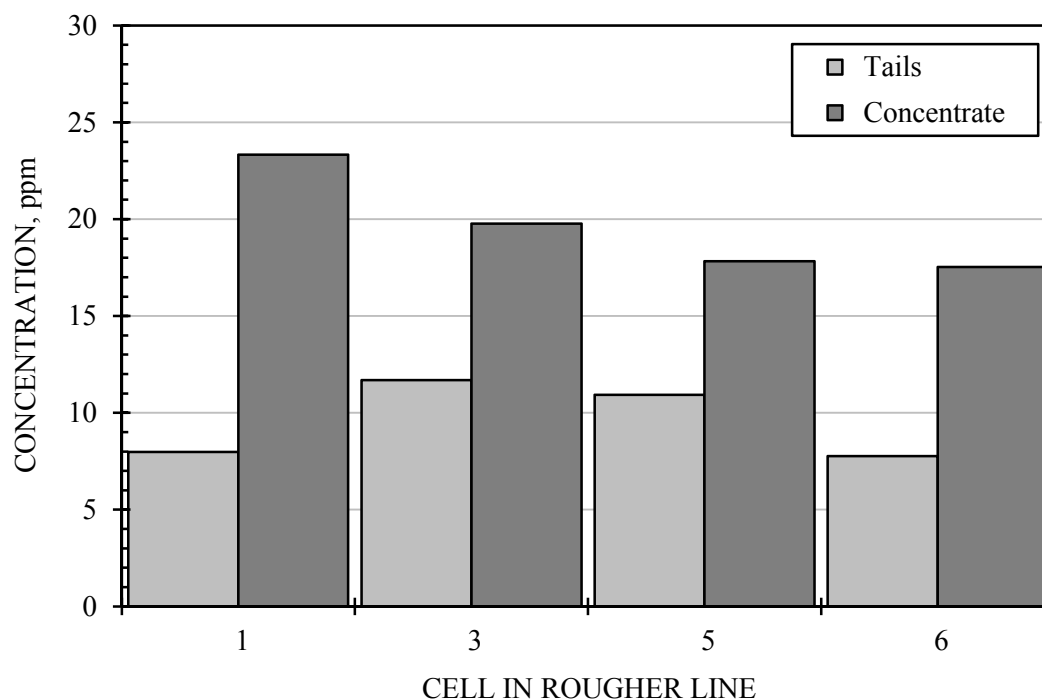


Figure 6.13 - Frother partitioning measured in rougher cells at Voisey's Bay

These results demonstrate that partitioning is common, regardless of frother and cell types. The magnitude of the differences between the pulp and concentrate streams can vary widely even for the same cell types and in the same line. The origin of these variations is not known but must reflect the relative amount of bubble surface and entrained water being carried into the froth and into the overflow.

Measuring frother partitioning in plant would help identify the effect of operating variables on the phenomenon. Finding ways of controlling partitioning may give operators a new tool for optimizing metallurgical performance. Whether partitioning can be manipulated by control of operating variables remains to be seen. Frother partitioning appears to be a promising research area.

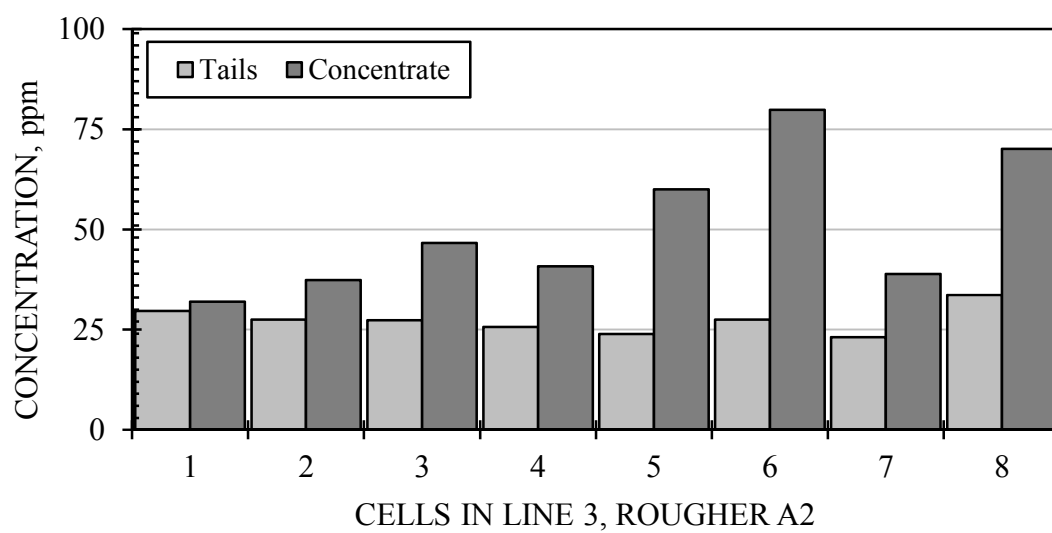
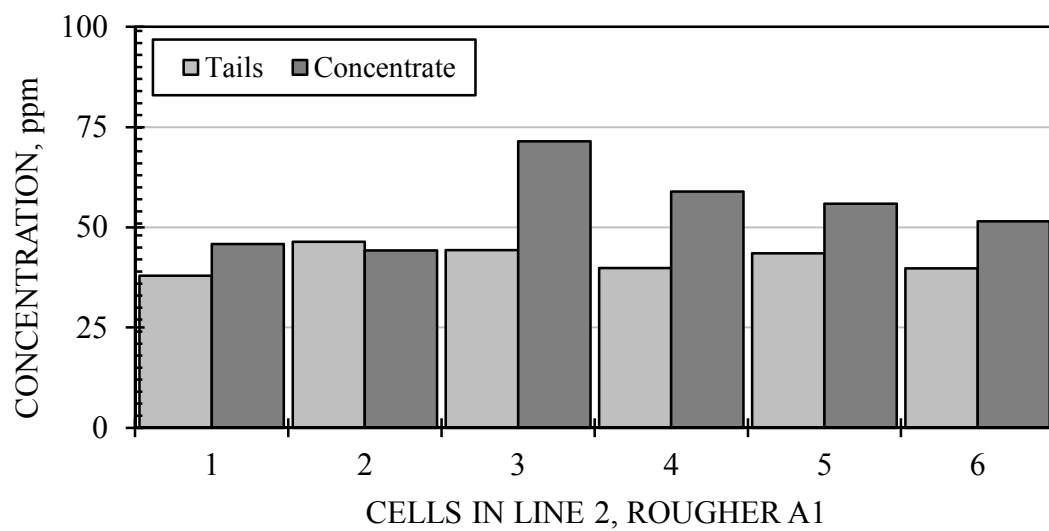
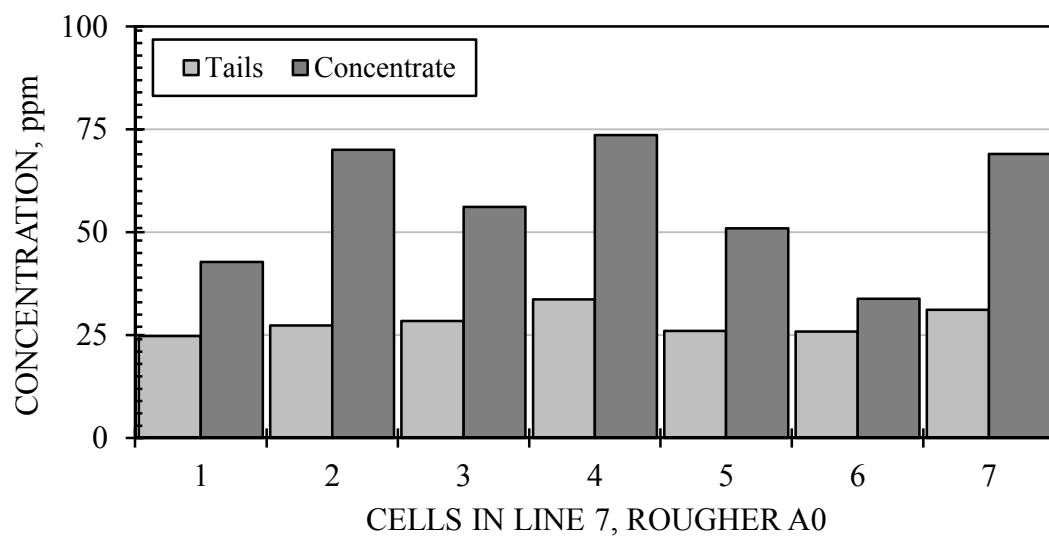


Figure 6.14 - Frother partitioning measured in rougher circuits at Chuquicamata

## 6.7 CONSTRUCTION OF FROTHER DISTRIBUTION MAPS

A frother distribution map is an exercise to establish, by the collection and analysis of appropriate samples, the distribution of frother throughout a concentrator. Proper operation of flotation cells requires delivering frother in a manner that every cell in the circuit runs with the target concentration, usually a value above the CCC. This is not always the case for a number of reasons:

- 1) Inadequate addition rate or number and location of frother addition points;
- 2) Delivery from distribution boxes whose content is not homogeneous as a consequence of inconsistent input stream blending;
- 3) Incomplete dissolution at the addition point, particularly in the case of low solubility frothers, which may result in the formation of droplets (possibly captured by bubbles and carried into the concentrate) and making conditioning necessary.
- 4) Variable concentration of remnant frother in recycle waters; and
- 5) Varying degrees of frother partitioning in cells.

Problems like these can be detected by constructing a frother distribution map for the flotation circuit.

To illustrate the exercise, the construction of a frother (Nalflote from Nalco) map for the flotation circuit of Codelco's Chuquicamata concentrator in Chile is described. The concentrator has a rougher section made up of three circuits (A0, A1, and A2) comprising lines with different cell types and sizes, each circuit associated with its own grinding circuit, and with all lines feeding a common cleaner-scavenger section (Figure 6.15). Rougher A0 has twelve lines of Wemco-56-m<sup>3</sup> cells: six of 7 cells arranged in three banks (2x2x3), and six lines of 8 cells arranged in four banks (2x2x2x2). Rougher A1 includes two lines of 6 Outotec-160-m<sup>3</sup> cells in a 2x2x2 arrangement, while Rougher A2 includes three lines of 8 Outotec-160-m<sup>3</sup> cells in a 2x2x2x2 arrangement.

A major component of the work is the selection of sampling points. The selected samples must be collected simultaneously (or over the shortest possible time) and should not

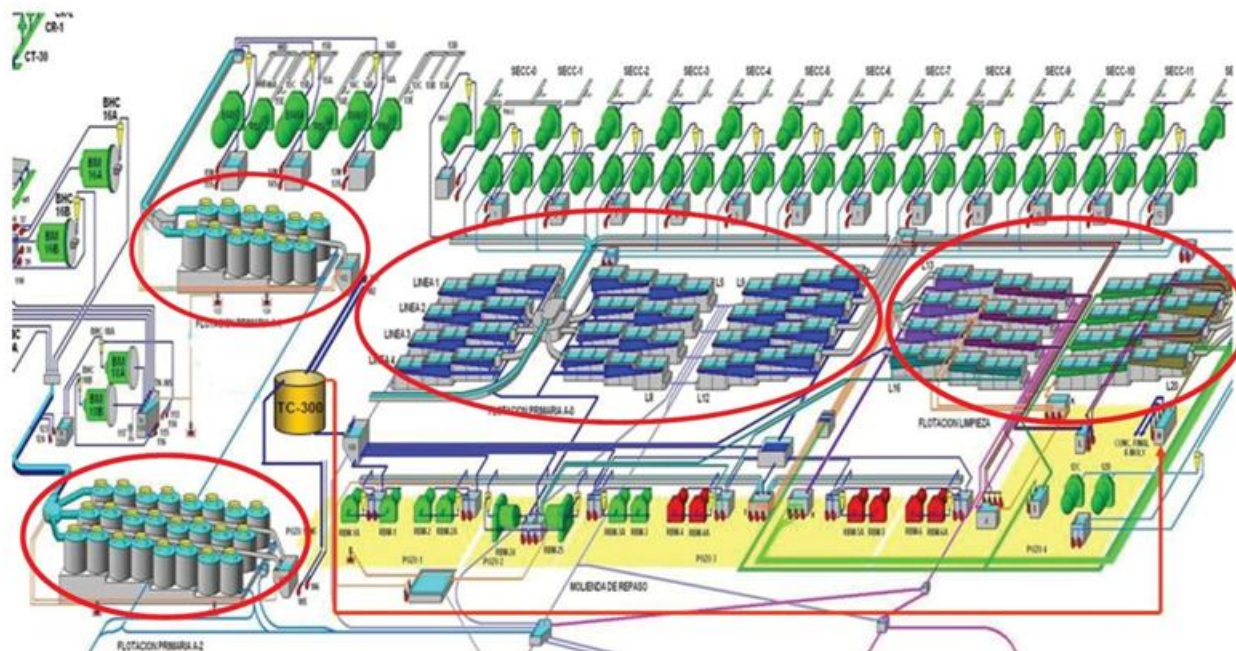


Figure 6.15 - Chuquicamata flotation circuit

exceed the analysis daily rate (20 samples), unless it is demonstrated that the analysis results are not affected by sample storage. Experience has demonstrated that the detection of frother distribution problems requires the collection of the following set of samples:

- 1) Feed lines to establish whether distribution boxes effectively mix incoming streams;
- 2) Streams in and out of a line of cells (feed, tails and concentrate), to ensure frother levels are adequate (i.e., within the target level of CCC) in every cell and to estimate an average value for frother partitioning (which can be determined provided no launder water is used);
- 3) Streams in and out of a circuit (combined feed, tails and concentrate), to run frother mass balances;
- 4) Streams around a frother addition point to find out whether frother dissolves readily; and
- 5) Water samples to detect the presence of remnant frother in recycle or other process waters.

### **6.7.1 Sampling Program and Analysis**

According to the circuit characteristics and restrictions imposed by accessibility to stream sampling points, a program to take 48 pulp samples was designed (Table 6.2).

With the exception of the water streams, given the size of the concentrator and sampling personnel gathered, all pulp samples were taken in 35 minutes. At the time of testing, two rougher lines of the A0 rougher circuit (Lines 4 and 11), and two of the cleaner-scavenger section (Lines 17 and 20), were not in operation.

A total of 75 analyses were performed:

- 1) Forty eight pulp samples including 44 plant samples, 1 replicate of a sample to determine the effect of the UV-VIS spectrum collection speed, and 3 repetitions of one sample on consecutive days to establish stability.
- 2) Twenty-two standards for the construction of three calibration curves including six concentrations each: in tap water (McGill), in tap water (Chuquicamata Characterization Laboratory Metallurgical-Microscopy Research), and in process water (thickeners), and four repeats to establish the standard deviation of the analysis; and
- 3) Five water samples.

As only a maximum of 20 analyses could be performed daily some of the samples were processed on the second day but all within 32 hours after collection.

### **6.7.2 Results and discussion**

Examination of the frother concentration in the line feeds helped establish whether frother delivery and addition points provided enough frother for cell concentrations above the CCC. The results showed, for all the circuit, that the feed concentration to most lines was around or above 20 ppm (Figure 6.16), a value considered high enough to ensure that the concentration in the last cell of the line is larger than the expected CCC (estimated as 15 ppm for the frother in use). There were a few exceptions: the cases of Line 3 in A0, Line 1 in A1, and Lines 18 and 19 in the scavengers, with concentrations of 16 ppm and



less. These low concentrations at the head of the line may result in cells with concentrations below the 15 ppm CCC target.

Table 6.2 - Samples collected for construction of frother distribution map

<b>CIRCUIT</b>	<b>SAMPLING POINTS</b>	<b>SAMPLES</b>
Rougher A0	Line feeds (12)	17
	Combined concentrates: Lines 1 to 4, 5 to 8 and 9 to 12 (3)	
	Combined tailings: Lines 1 to 4 and 5 to 12 (2)	
Rougher A1	Rougher circuit feed (1)	6
	Line feeds (2)	
	Combined concentrate: Lines 1 and 2 (1)	
	Line tailings (2)	
Rougher A2	Rougher circuit feed (1)	12
	Line feeds (3)	
	Line concentrates (3)	
	Line tailings (3)	
	Combined concentrate: Lines 1 to 3 (1)	
	Combined tailings: Lines 1 to 3 (1)	
Cleaner/Scavenger	Line feeds (4)	7
	Combined concentrates (2)	
	Line tailings (1)	
Recleaner/Scavenger	Four line feeds (4)	6
	Combined concentrate (1)	
	Combined tailings (1)	
Water	Water in roughers A0, A1 and A2 (3)	5
	Process (thickener) water (1)	
	Laboratory tap water (1)	

In the case of Rougher A0, the results showed concentration differences which in some cases were significant. There were two distribution boxes: one feeding the first eight lines, and the other feeding the last four. Major feed concentration differences were detected in the lines supplied from the first box (Figure 6.16a), with lower values for the first three lines (the lowest concentration was measured in Line 3) compared to those in the last four (differences as large as 10 ppm between concentrations in Lines 1 and 2 compared to those obtained in Lines 5 to 8), and in those of the four lines supplied by the second box. As the first box is receiving pulp from two different grinding circuits, these results demonstrate poor homogenization. In the case of Roughers A1 and A2 (Figure 6.16b), the results showed a more even distribution probably as a consequence of the lower number of lines fed from a single distribution box, but the frother addition rate in the feed to Rougher A1 should be increased to have concentrations over 20 ppm. The concentration in the Cleaner-Scavenger lines is also low (Figure 6.16c) and an additional frother dosage point seems to be necessary.

Determining the concentration in the feed, concentrate and tailings streams of a line of cells makes it possible to establish whether every cell in the line operates with adequate frother level, and to estimate an average value for frother partitioning, if no launder water is in use. The concentration in the tailings stream is expected to be the same or smaller than that in the feed as a consequence of frother partitioning, which was the case for the lines in Roughers A1 and A2 (Figure 6.17). The concentration in each cell is expected to be between the feed and the tailings stream concentrations. The results indicated that Rougher A1 and A2 cells were operating with frother concentrations above CCC (i.e., above 15 ppm). Access limitations prevented the collection of line tailings samples in Rougher A0.

As argued previously, frother partitioning may give an indication of froth zone performance. A comparison between concentrations in the tailings and concentrate line streams, when no launder water is used, gives an average value of frother partitioning in the line cells. The results obtained in Rougher A2, the only circuit which physically allowed sample collection of line concentrate streams, showed as expected higher

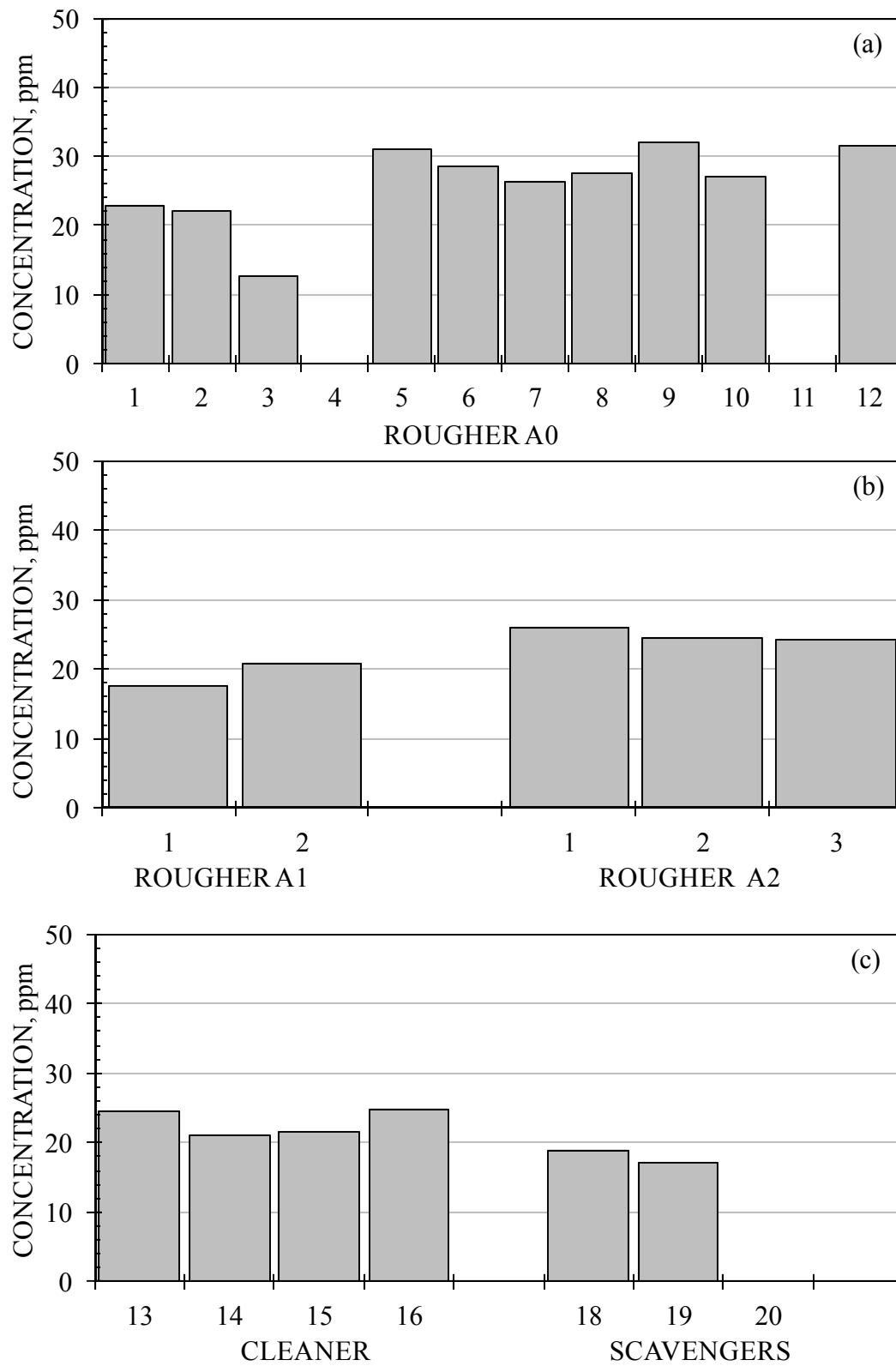


Figure 6.16 - Concentration of frother in line feeds to different circuits

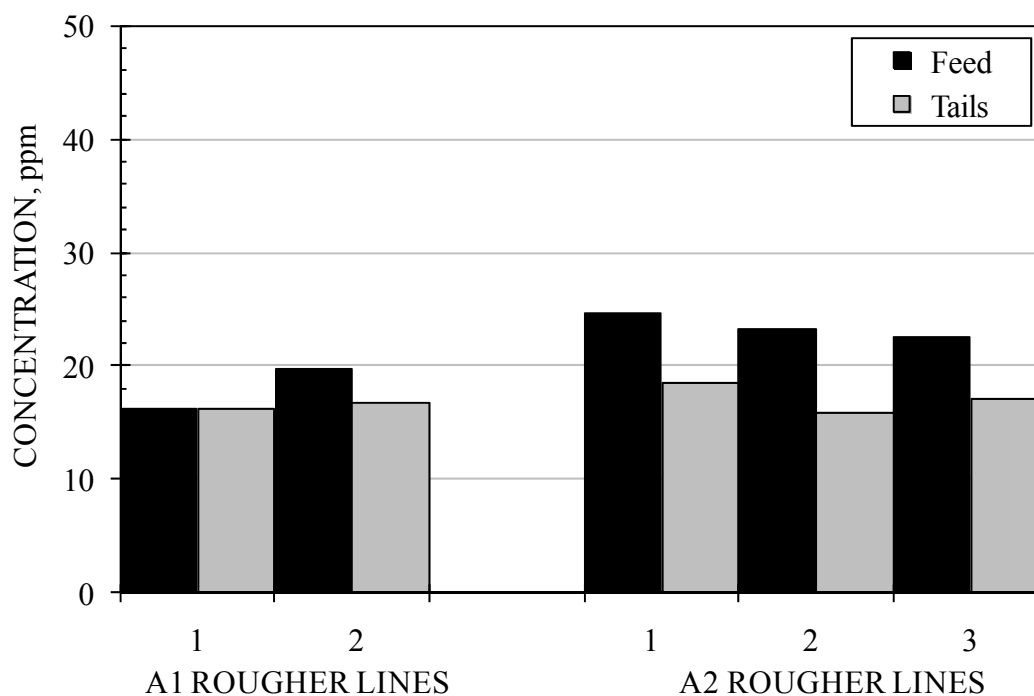


Figure 6.17 - Measured concentration in feed and tailings streams (Roughers A1 and A2)

concentrations in the concentrate than in the tailings streams (Figure 6.18). These results confirm those in a separate gas dispersion measurement campaign in which tailings and concentrate samples were also collected simultaneously in every cell in the line (Figure 6.19). Note in the figure the wide range of partitioning values in the different cells, and the higher frother addition rate suggested by the tails results.

In the case of Rougher A0, only samples of combined concentrates (lines 1 to 4, lines 5 to 8, and lines 9 to 12) and combined tails (lines 1 to 4, and lines 5 to 12) could be collected. The results showed frother concentrations in the composite tail streams over 20 ppm (Figure 6.20), which were, as expected, similar or slightly lower than those in the line feeds, indicating that all cells were operating with frother levels above the CCC. The concentration in the concentrate streams was lower than in the feeds but this was a consequence of dilution by launder water in this part of the circuit. Frother mass balances could not be done because stream flow rates were not available.

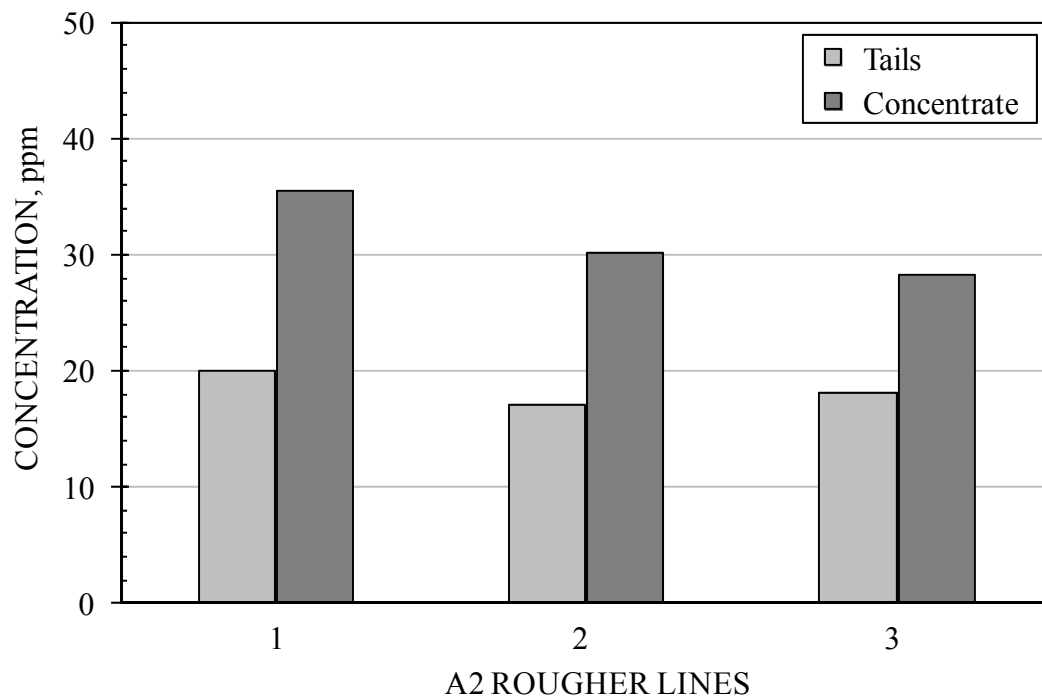


Figure 6.18 - Measured concentrations in tailings and concentrate streams (Rougher A2)

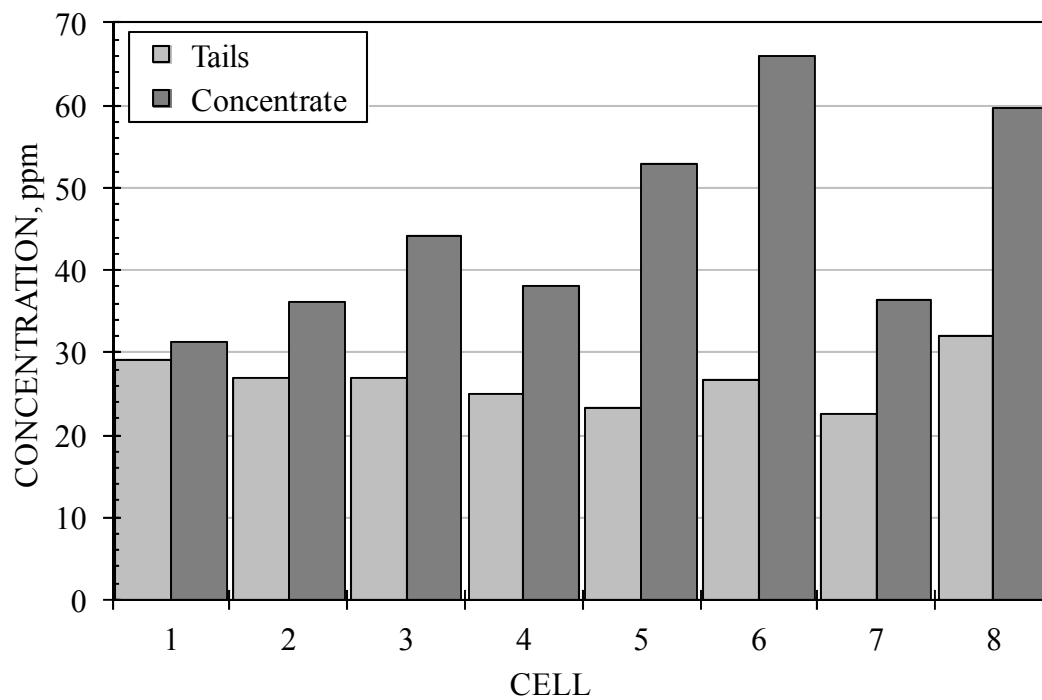


Figure 6.19 - Measured concentrations in tailings and concentrate streams (Rougher A2)

Frother concentrations obtained around the addition point of Roughers A1 and A2 showed similar values (Figure 6.21) in the feed streams coming from the grinding section (around 11 and 9 ppm in Roughers A1 and A2, respectively). Frother addition in both cases aimed to increase concentrations to about 20 to 25 ppm but the results showed lower and different values in the feed lines of Rougher A1. These results indicate if the addition rate was properly estimated, that the dissolution of frother was not complete and the contents of the distribution box were not homogeneous. In the case of Rougher A2, the frother concentration in the feed to the different lines was even and at the target value.

Analysis of the water samples (Figure 6.22) showed that the process water contained 8 ppm of remnant frother, and as it is used in the grinding circuit, it is believed to be the source of the frother in the rougher feed streams. The water circulation in the concentrator is complex and the water available for dilution and launder use was not the same in the different circuits, as demonstrated by the analysis results, which showed no frother in the case of Rougher A0, about 1 ppm in that of Rougher A2, and 7 ppm in that of Rougher A1.

### **6.7.3 Conclusions**

In summary, the results demonstrated that most cells are operating with concentrations above the CCC, estimated as 15 ppm. However, there are lines with feed concentrations below 20 ppm which may go below the CCC depending on operating conditions. Concentrations in line feeds below 20 ppm should be avoided to ensure stable gas dispersion characteristics.

There are indications that the content of distribution boxes is not homogeneous with regard to frother, which leads to different frother concentrations in the feed to the lines. This may be a consequence of short dissolution times for the frother, but poor stream mixing may also play a role. The frother addition rate to Rougher A1 should be revised. Analysis of frother concentration in water samples showed that there is remnant frother in the process water and in the water available in some of the circuits.

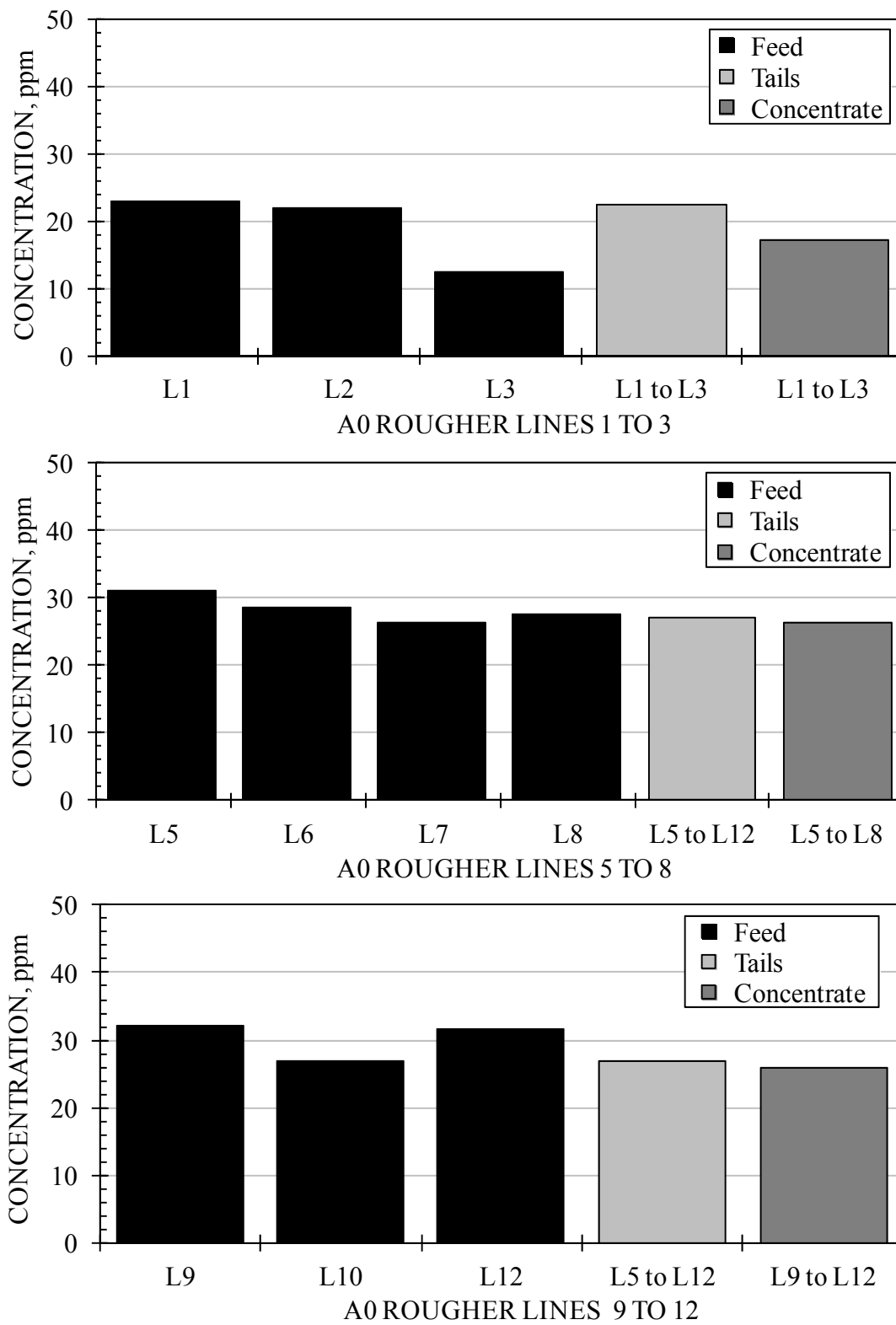


Figure 6.20 - Measured concentrations in Rougher A0 streams

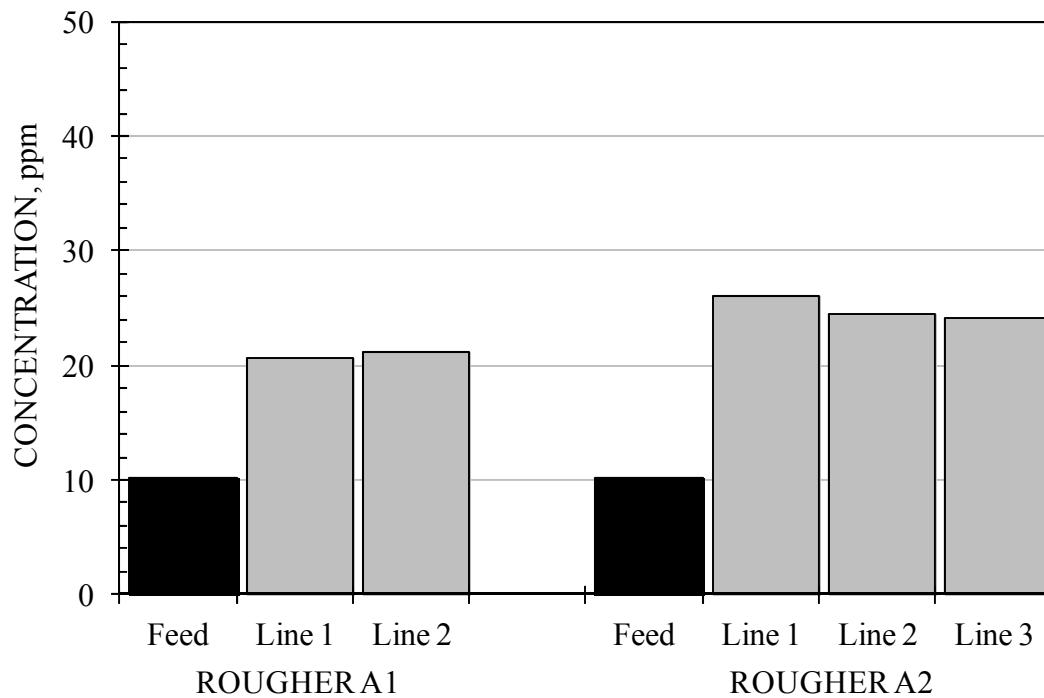


Figure 6.21 - Measured concentrations in streams of Rougher circuits A1 and A2

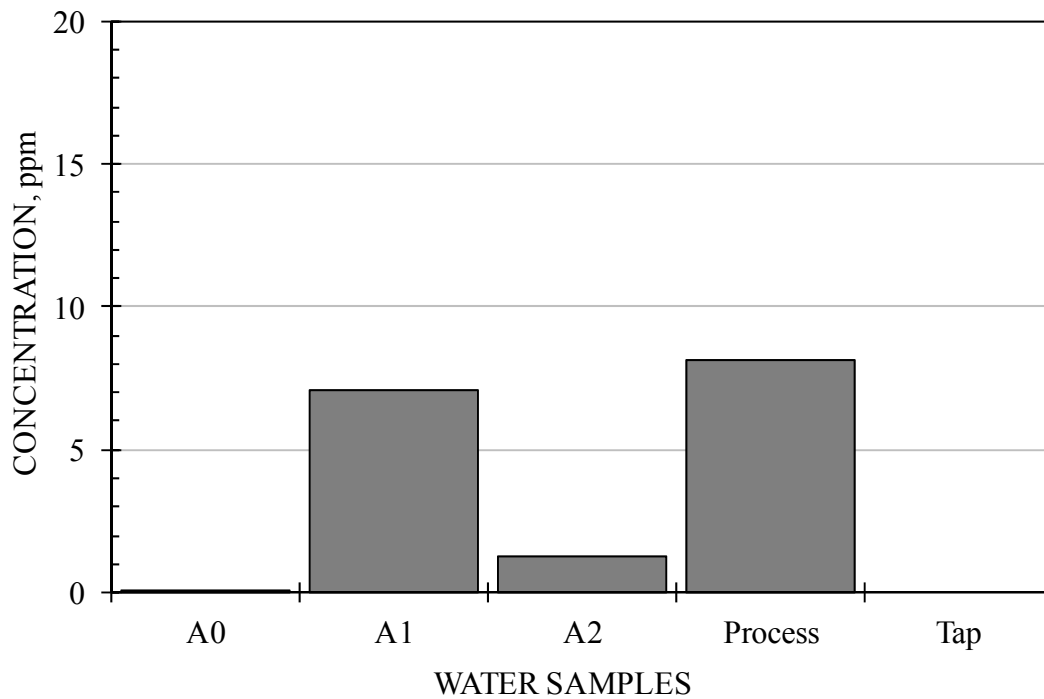


Figure 6.22 - Frother concentrations in streams water samples



## CHAPTER 7 – CONCLUSIONS AND CONTRIBUTIONS TO ORIGINAL RESEARCH AND KNOWLEDGE

### 7.1 CONCLUSIONS

#### 7.1.1 Refinement of colorimetric analysis technique

The prime objective, to devise a frother analysis technique for reliable measurement of concentration in industrial flotation circuits, was met.

Specific conclusions in reaching that objective are as follows:

- 1) Of the analysis methods in the literature the colorimetric technique was selected as the most promising for on-site work;
- 2) The method was refined to increase reproducibility in the following ways:
  - a. Replacing volumetric preparation of frother solutions by weighing of components;
  - b. Reduction in concentration to facilitate preparation in the case of low solubility frothers;
  - c. Use of a chromatographic syringe to measure and add Komarowsky indicator (0.1 mL);
  - d. Collection of UV-VIS spectra for the full operational wavelength range (300-700 nm);
  - e. Use of a blank (concentrated sulfuric acid with the Komarowsky indicator) as a reference for UV-VIS spectra collection;
  - f. Inclusion of a sample with no frother, as a 0-ppm standard, in the data to construct calibration curves;
  - g. Selection of wavelength for construction of calibration curves as the value resulting in the minimum sum of squared residuals; and
  - h. Processing of samples in batches, which increased the daily analysis rate to 20 samples.

- 3) Reproducibility showed relative errors at the 95% confidence interval of about 1% for samples prepared from the same stock solution (the case of industrial samples) and 2.5% for samples which included preparation of stock solution; and
- 4) Detection limit was about 0.2 ppm; below 0.1 ppm, the technique is still able to detect the presence of the frother, but the error in the concentration is too high for analytical purposes;

### 7.1.2 Applications of technique

In industrial trials, analysis and plant-related issues were identified:

- 1) Analysis was affected by sample storage time; samples needed to be processed the same day they are collected;
- 2) Recycle and process waters often contained remnant frother;
- 3) Variations in concentration indicated unstable frother delivery;
- 4) Cells and lines were found operating below the critical coalescence concentration which may indicate too low dosage rates or poorly located addition points;
- 5) Distributions boxes could show non-homogeneity leading to different frother concentration in the feed to the lines; and
- 6) Cases of insufficient time to fully dissolve some frothers suggesting the need for a conditioning tank.

In fundamental work, the technique was used to study frother partitioning and bubble coverage:

- 1) Frother partitioning was measured in laboratory bubble columns and Jameson cells, and in industrial mechanical cells. Partitioning, defined as ratio of overflow to underflow concentration, decreased as the feed concentration increased and decreased as the gas flow rate increased at low concentrations, but remained constant for high concentrations. The higher concentration in the overflow compared to the underflow is a consequence of adsorbed frother on the bubble surface being released after bubble bursting, consequently these trends indicate that both the amount of frother adsorbed and the water overflow rate were affected by gas rate; and

- 2) Direct measurement of the bubble area covered by one frother molecule based on mass balancing the frother delivered to and leaving a bubble column gave results within the same order of magnitude as values calculated from the Gibbs adsorption isotherm.

## **7.2 CLAIMS TO ORIGINAL RESEARCH**

- 1) The refinement of the colorimetric frother analysis technique, specifically:

In spectra collection, the use of a blank solution (sulfuric acid with the Komarowsky indicator) as a reference, and the inclusion of a 0-ppm standard (a sample with no frother going through the whole analytical procedure) to subtract color contributions from sources other than the frother, resulted in linear curves that go through the origin. In spectra processing, minimizing the sum of squared residuals to select the wavelength increased reliability;

- 2) Refinement of the technique made possible the following contributions to fundamental studies and to the diagnosis of industrial circuits:
  - a. A technique for the direct measurement of bubble frother coverage based on mass balancing the frother delivered and leaving a bubble column. The approach required development of a specially designed head to prevent bubble bursting until outside the column, and an operating procedure to run with no froth and a steady overflow stream;
  - b. A procedure for measuring frother partitioning in industrial cells and circuits; and
  - c. A procedure for construction of frother distribution maps for flotation plants. Measurements demonstrated significant concentration variations in time and place.

### 7.3 CONTRIBUTIONS TO KNOWLEDGE

The principal contribution of this thesis is a refined analytical technique for frothers which will be of use in the optimization of flotation circuits. Other contributions include:

- 1) The development of a frother analysis database by compiling calibration curves constructed in this work. Knowledge of the maximum concentration corresponding to an absorbance of 3 makes it possible to select standards and construct calibration curves with the widest application range;
- 2) The demonstration that reagent specifications and freshness may have a major impact on the reproducibility of the analysis. Only ethanol-stabilized chloroform should be utilized and calibration curves should be prepared close in time to their use;
- 3) The demonstration that during the chloroform extraction step equilibrium is reached before all frother is extracted. This indicates that the agitation procedure and separation time must be consistent with those used in the construction of the calibration curve;
- 4) The realization that the color of the final solution for UV-VIS spectra collection depends on boiling time. Boiling times less than 40 minutes may be selected only when analysis rate dictates a faster pace;
- 5) The convenience of having concentration vs. absorbance calibration curves going through the origin achieved by including a 0-ppm standard to subtract contributions from factors not related to frother;
- 6) The demonstration that certain collectors can interfere in the frother analysis when construction of a calibration curve for the collector is necessary.

## 7.4 RECOMMENDATIONS

- 1) The development of a training program for technology transfer to operations;
- 2) As many commercial frothers are blends (e.g. alcohols and glycols), it is important to determine the concentration of individual components when industrial samples are analyzed. The development of procedures to separate component contributions in the colorimetric technique is necessary;
- 3) Characterization of frother distribution during chloroform extraction is important. The distribution coefficient for frothers may further improve analysis reliability; for example, frothers with low distribution coefficient may require more than two extraction stages for acceptable reproducibility;
- 4) Establishment of relationship between frother partitioning and cell operating conditions; and
- 5) Further bubble frother coverage experiments selecting surfactants and operating conditions to minimize effect of measurement errors.

## REFERENCES

1. Addison, C.C. (1945). "The properties of freshly formed surfaces. Part IV: The influence of chain length and structure on the static and dynamic surface tensions of aqueous-alcoholic solutions", *Journal of Chemical Society*, 98–106.
2. Ahmed, N. and Jameson, G.J. (1985). "The effect of bubble size on the rate of flotation of fine particles", *International Journal of Mineral Processing*, Vol. 14 (3), 195–215.
3. Amelunxen, P. and Rothman, P. (2009). "The online determination of bubble surface area flux using the CiDRA GH-100 sonar gas holdup meter", *Workshop on Automation in Mining, Mineral, and Metal Industry (IFACMMM 2009)*, Viña del Mar, Chile, October 14–16.
4. Aston, J.R., Lane, J.E. and Healy, T.W. (1989). "Frothing in Flotation", Chapter 10, "The Solution and Interfacial Chemistry on Nonionic Surfactants used in Coal Flotation", Gordon and Breach Science Publishers, 229–256.
5. Ata, S. (2008). "Coalescence of bubbles covered by particles", *Langmuir*, Vol. 24, 6085–6091.
6. Azgomi, F., Gomez, C.O. and Finch, J.A. (2007). "Correspondence of gas holdup and bubble size in presence of different frothers", *International Journal of Mineral Processing*, Vol. 83 (1–2), 1–11.
7. Azgomi, F., Gomez, C.O. and Finch, J.A. (2009). "Frother persistence: A measure using gas holdup", *Minerals Engineering*, Vol. 22 (9–10), 874–878.
8. Bikerman, J.J. (1973). "Foams", Springer-Verlag, New York.
9. Booth, R.B. (1973). "Foams: Theory and Industrial Applications", Chapter on "Froth Flotation", Reinhold Publishing Corp, 243–281.
10. Bormett, G.A., Bartels M.J. and Markham, D.A. (1995). "Determination of 2-butoxyethanol and butoxyacetic acid in rat and human blood by gas chromatography-mass spectrometry", *Journal of Chromatography B*, Vol. 665, 315–325.
11. Cappuccitti, F. and Nasset, J.E. (2009). "Frother and collector effects on flotation cell hydrodynamics and their implication on circuit performance", *Proceeding of 48<sup>th</sup> annual Conference of Metallurgists of CIM Sudbury, Ontario, Canada*. C.O. Gomez, J.E. Nasset and R. Rao, Eds., 169–180.
12. Cappuccitti, F. and Finch, J.A. (2008). "Development of new frothers through hydrodynamic characterization", *Minerals Engineering*, Vol. 21 (12–14), 944–948.

13. Chang, C.H. and Franses, E.I. (1995). "Adsorption dynamics of surfactants at air/water interface: a critical review of mathematical models, data and mechanisms", *Colloids and Surfaces A: Physicochemical and Engineering Aspects*, Vol. 100, 1–45.
14. Cho, Y.S. and Laskowski, J.S. (2002b). "Bubble coalescence and its effect on dynamic foam stability", *Canadian Journal of Chemical Engineering*, Vol. 80, 299–305.
15. Cho, Y.S. and Laskowski, J.S. (2002a). "Effect of flotation frothers on bubble size and foam stability", *International Journal of Mineral Processing*, Vol. 64 (2–3), 69–80.
16. Coles, H.W. and Tournay, W.E. (1942). "The Komarowsky color reaction for aliphatic alcohols", *Industrial and Engineering Chemistry*, Vol. 14 (1), 20–22.
17. Comley, B.A., Harris, P.J., Bradshaw, D.J. and Harris, M.C. (2002). "Frother characterization using dynamic surface tension measurements", *International Journal of Mineral Processing*, Vol. 64, 81–100.
18. Comley, B.A., Vera, M. and Franzidis, J.P. (2007). "Interpretation of the effect of frother type and concentration on flotation performance in an OK3 cell", *Minerals and Metallurgical Processing Journal*, Vol. 24 (4), 243–252.
19. Crabtree, J.R. and Bridgwater, J. (1971). "Bubble coalescence in viscous liquids", *Chemical Engineering Science*, Vol. 26, 839–851.
20. Crozier, R.D. and Klimpel, R.R. (1989). "Frothing in Flotation", Chapter 11, "Frothers: Plant Practice", Gordon and Breach Science Publishers, 257–280.
21. Cytec Mining Chemicals Handbook (2002). "Flotation of Sulfide Ores", Chapter 6, Cytec Industries Inc., 118.
22. Dahlke, R., Gomez, C.O. and Finch, J.A. (2005). "Operating range of a flotation cell determined from gas holdup vs. gas rate", *Minerals Engineering*, Vol. 18 (9), 977–980.
23. Dai, Z., Fornasiero, D. and Ralston, J. (2000). "Particle-bubble collision models – a review", *Advances in Colloid and Interface Science*, Vol. 85 (2-3), 231–256.
24. Davies, J.T. and Rideal, E.K. (1961). "Interfacial phenomena", Academic Press New York, 371.
25. Davies, J.T. (1957). "Proceeding of 2<sup>nd</sup> International Congress of Surface Activity", Vol. 1, London, 426.
26. Dobby, G.S. and Finch, J.A. (1986). "Particle collection in columns-gas rate and bubble size effects". *Canadian Metallurgical Quarterly*, Vol. 25 (1), 9–13.

27. Dukhin, S.S., Kretzschmar, G. and Miller, R. (1995). "Studies in Interface Science", Chapter 4, Dynamics of Adsorption at Liquid Interfaces, D. Mobius and R. Miller, Eds., Elsevier.
28. Ekkert, L. (1928). "Beitrag zu den farbenreaktionen einiger alkohole", Pharmazeutische Zentralhalle für Deutschland, Vol. 69, 289–296.
29. Fainerman, V.B. (1992). "Adsorption kinetics from concentrated micellar solutions of ionic surfactants at the water-air interface", Colloids and Surfaces, Vol. 62, 333–347.
30. Fellenberg, Th. (1910). "Ueber Farbenreaktionen aromatischer aldehyde und ihre anwendbarkeit bei der analyse von spirituosen", Mitteilungen aus Lebensmitteluntersuchung und Hygiene, Vol. 1, 311–350.
31. Finch, J.A., Nasset, J.E. and Acuna, C. (2008). "Role of frother on bubble production behaviour in flotation", Minerals Engineering, Vol. 21, 949–957.
32. Finch, J.A., Gelinas, S. and Moyo, P. (2006). "Frother-related research at McGill University", Minerals Engineering, Vol. 19, 726–733.
33. Finch, J.A. and Dobby, G.S. (1990). "Column Flotation". Pergamon Press, New York.
34. Frumkin, A. and Levich, V.G. (1947). "On surfactants and interfacial motion", Zhurnal Fizicheskoi Khimii, Vol. 21, 1183–1204.
35. Fuerstenau, D.W. (1999). "Advances in flotation technology". Proceedings of Symposium of Advances in Flotation Technology. SME Annual Meeting. Edited by Parekh B.K. and Miller J.D. Society for Mining, Metallurgy and Exploration, Littleton, Colorado.
36. Garibay, R.P., Gallegos, P.M., Uribe, A. and Nava, F. (2002). "Effect of collection zone height and operating variables on recovery of overload flotation columns", Minerals Engineering, Vol. 15 (5), 325–331
37. Gelinas, S. and Finch, J.A. (2007). "Frother analysis: Some plant experiences", Minerals Engineering, Vol. 20 (14), 1303–1308.
38. Gelinas, S. and Finch, J.A., (2005). "Colorimetric determination of common industrial frothers", Minerals Engineering, Vol. 18 (2), 263–266.
39. Giachetti, C., Zanolò, G., Verga, G.R., Perovanni, F. and Assandri, A. (1996). "Gas chromatographic determination of some glycol ethers and glycol ether acetates by FID, 0-FID, and MS detection. Preliminary applications in simultaneous monitoring of these chemicals in biological matrices", Journal of High Resolution Chromatography, Vol. 19, 383–391.



40. Godbole, S.P., Schumpe, A., Shah, Y.T. and Carr, N.L. (1984). "Hydrodynamics and mass transfer in non-Newtonian solutions in a bubble column", American Institute of Chemical Engineers, Vol. 30, 213–220.
41. Gomez, C.O. and Finch, J.A. (2011). "Effect of frothers on cell characterization and circuit performance", P90 AMIRA project internal report.
42. Gomez, C.O. and Finch, J.A. and Muñoz-Cartes, D. (2011). "An Approach to characterize frother roles in flotation", 8<sup>th</sup> International Mineral Processing Seminar Procemin, W. Kracht, R. Kuyvenhoven, S. Lynch-Watson and G. Montes-Atenas, Eds., Gecamin Ltda, Santiago, Chile, 223–231.
43. Gomez, C.O., Maldonado, M., Finch, J.A. and Araya, R. (2010). "Viscosity Effects on Bubble Shape and Terminal Velocity", Proceedings of the 49<sup>th</sup> Conference of Metallurgists, 57–74.
44. Gomez, C.O. and Finch, J.A. (2007). "Gas dispersion measurements in flotation cells", International Journal of Mineral Processing, Vol. 84, 51–58.
45. Gomez, C.O. and Finch, J.A. (2002). "Gas dispersion measurements in flotation machines", CIM Bulletin, Vol. 95 (1066), 73–38.
46. Gorain, B.K., Franzidis, J.P. and Mainlapig, E.V. (1999). "The empirical prediction of bubble surface area flux in mechanical flotation cells from cell design and operating data", Minerals Engineering, Vol. 12 (3), 309–322.
47. Gorain, B.K., Franzidis, J.P. and Mainlapig, E.V. (1998). "The effect of froth residence time on the kinetics of flotation", Minerals Engineering, Vol. 11 (7), 627–638.
48. Gorain, B.K., Franzidis, J.P. and Mainlapig, E.V. (1997). "Studies on impeller type, impeller speed and air flow rate in an industrial scale flotation cell-Part 4: Effect of bubble surface area flux on flotation performance", Minerals Engineering, Vol. 10 (4), 367–379.
49. Gorain, B.K., Franzidis, J.P. and Mainlapig, E.V. (1995). "Studies on impeller type, impeller speed and air flow rate in an industrial scale flotation cell-Part 1: Effect on bubble size distribution", Minerals Engineering, Vol. 8 (6), 615–635.
50. Grau, R. and Heiskanen, K. (2005). "Bubble size distribution in laboratory scale flotation cells", Minerals Engineering, Vol. 18, 1164–1172.
51. Gredelj, S., Zanin, M. and Grano, S.R. (2009). "Selective flotation of carbon in the Pb-Zn carbonaceous sulphide ores of Century Mine, Zinifex", Minerals Engineering, Vol. 22 (3), 279–288.
52. Griffin, W.C. (1954). "Calculation of HLB values of non-ionic surfactants", Journal of the Society of Cosmetic Chemists, Vol. 5, 249–256.

53. Griffin, W.C. (1949). "Classification of surface-active agents by HLB", *Journal of the Society of Cosmetic Chemists*, Vol. 1, 311–326.
54. Hadler, K., Aktas, Z. and Cilliers, J.J. (2005). "The effects of frother and collector distribution on flotation performance", *Minerals Engineering*, Vol. 18 (2), 171–177.
55. Harris, C.C., (1976). "Flotation machines", Fuerstenau, M.C. (E.d), A.M. Gaudin, Memorial Volume, Vol. 2, SME of AIME, 753–815.
56. Harris, P.J. (1982). "Frothing Phenomena and Frothers", *Principles of Frothers*, Chapter 13, R.P. King, Ed., 237–250.
57. Hernandez, H., Gomez, C.O. and Finch, J.A. (2003). "Gas dispersion and de-inking in a flotation column", *Minerals Engineering*, Vol. 16 (6), 739–744.
58. Huang C.T., Su Y.Y. and Hsieh Y.Z. (2002). "Optimization of the headspace solid-phase microextraction for determination of glycol ethers by orthogonal array design", *Journal of Chromatography A*, Vol. 977 (1), 9–16.
59. Hunter, T.N., Pugh, R.J., Franks, G.V. and Jameson, G.J. (2008). "The role of particles in stabilising foams and emulsions", *Advances in Colloids and Interface Science*, Vol. 137, 57–81.
60. Jachminska, B., Warszynski, P. and Malysa, K. (2001). "Influence of adsorption kinetics and bubble motion on stability of the foam films formed at n-octanol, n-hexanol and n-butanol solution surface", *Colloids and Surfaces A: Physicochemical and Engineering Aspects*, Vol. 192, 177–193.
61. Jachminska, B., Warszynski, P. and Malysa, K. (1998). "Effect of motion on lifetime of bubbles at n-butanol solution surface", *Colloids and Surfaces A: Physicochemical and Engineering Aspects*, Vol. 143, 429–440.
62. Jachminska, B., Lukenheimer, K. and Malysa, K. (1995). "Effect of position of the functional group on the equilibrium and dynamic surface properties of butyl alcohols", *Journal of Colloid and Interface Science*, Vol. 176, 31–38.
63. Johansson, G. and Pugh, R.J. (1992). "The influence of particle size and hydrophobicity on the stability of mineralised froths", *International Journal of Mineral Processing*, Vol. 34, 1–21.
64. Kitchener, J. (1992). "Chapter 1 - Minerals and Surfaces", *Colloid Chemistry in Mineral Processing*, Elsevier Science Publishers B.V., 1–35.
65. Klassen, V.I. and Mokrousov, V.A. (1963). "An Introduction to the Theory of Flotation", English translation by J. Leja and G. W. Poling, Butterworths, London.

66. Klimpel, R. and Isherwood, S. (1991). "Some industrial implications of changing frother chemical structure", *International Journal of Mineral Processing*, Vol. 33, 369–381.
67. Klimpel, R.R. and Hansen, R.D. (1988). "Reagents in mineral technology", *Surfactant Science Series*, Vol. 27, 385–409.
68. Klimpel, R.R. (1984). "Use of chemical reagents in flotation", *Chemical Engineering*, Vol. 91, 75–79.
69. Kracht, W. and Finch, J.A. (2009b). "Bubble break-up and the role of frother and salt", *International Journal of Mineral Processing*, Vol. 92 (3–4), 153–161.
70. Kracht, W. and Finch, J.A. (2009a). "Using sound to study bubble coalescence". *Journal of Colloid and Interface Science*, Vol. 332 (1), 237–245.
71. Krzan, M., Zawala, J. and Matysa, K. (2007). "Development of steady state adsorption distribution over interface of a bubble rising in solutions of n-alkanols (C5, C8) and n-alkyltrimethylammonium bromides (C8, C12, C16)", *Colloids and Surfaces A: Physicochemical and Engineering Aspects*, Vol. 298, 42–51.
72. Laskowski, J.S., Cho, Y. S. and Ding, K. (2003a). "Effect of frothers on bubble size and foam stability in potash ore flotation systems", *The Canadian Journal of Chemical Engineering*, Vol. 81, 63–69.
73. Laskowski, J.S., Tlhone, T., Williams, P. and Ding, K. (2003b). "Fundamental properties of the polyoxypropylene alkyl ether flotation frothers", *International Journal of Mineral Processing*, Vol. 72, 289–299.
74. Laskowski, J.S. (2003). "Fundamental properties of flotation frothers", *Proceedings of the 22<sup>nd</sup> International Mineral Processing Congress (IMPC)*, Cape Town, South Africa, 788–797.
75. Laskowski, J.S. and Woodburn, E.T. (1998). "Frothers in flotation", *Frothing in Flotation II*, Chapter 1, J.S. Laskowski and E.T. Woodburn, Eds., Gordon and Breach Science Publishers, 1–50.
76. Leja, J. and Schulman, J.H., (1954). "Flotation theory: Molecular interactions between frothers and collectors at solid liquid air interfaces", *Transaction of the American Institution of Mining and Metallurgy Engineering (AIME)*, Vol. 199 (22), 1–228.
77. Li, H. and Prakash, A. (1997). "Heat transfer and hydrodynamics in a three-phase slurry bubble column", *Industrial and Engineering Chemistry Research*, Vol. 36, 4688–94.
78. Lovell, V.M. (1982). "Industrial flotation reagents", *Principles in Flotation*, R.P. King, Ed., South African Institute of Mining and Metallurgy, Vol. 3, 73–91.

79. Mackay, R.A. (1987). "Solubilization", "Nonionic Surfactants", Physical Chemistry, Chapter 6, M.J. Schick, Ed., Marcel Dekker, Inc – New York, 297–547.
80. Malysa, E., Malysa, K. and Czarnecki, J. (1987). "A method of comparison of frothing and collecting properties of frothers", Colloids and Surfaces, Vol. 23, 29–39.
81. Malysa, K., Lukenheimer, K., Miller, R. and Hempt, C. (1985). "Surface elasticity and dynamic stability of wet foams", Colloids and Surfaces, Vol. 16, 9–20.
82. Malysa, K. (1981). "Surface elasticity and frothability of n-octanol and n-octanoic acid solutions", Colloids and Surfaces, Vol. 3, 329–338.
83. McBain, J.W. and Swain, R.C. (1936). "Proceedings of the Royal Society A: Mathematical, Physical and Engineering Sciences", Vol. 154, 608–623.
84. Metso Minerals CBT (Computer Based Training), (2002). "Mill Operator Training Package: Flotation Module", Formerly Brenda Process Technology CBT (Computer Based Training) (1996).
85. Moyo, P., Gomez, C.O. and Finch, J.A. (2007). "Characterizing frothers using water carrying rate", Canadian Metallurgical Quarterly, Vol. 46 (3), 215–220.
86. Neme, F., Coppola, L. and Böhm, U. (1997). "Gas holdup and mass transfer in solid suspended bubble columns in presence of structured packings", Chemical Engineering Technology, Vol. 20, 297–303.
87. Nasset, J.E., Zhang, W. and Finch J.A. (2012). "A benchmarking tool for assessing flotation cell performance", Proceedings 44<sup>th</sup> Annual Meeting of the Canadian Mineral Processors (CIM), 183–209.
88. Nasset, J.E., Finch, J.A. and Gomez, C.O. (2007). "Operating variables affecting the bubble size in forced-air mechanical flotation machines", 9<sup>th</sup> Mill Operators' Conference. Fremantle, Western Australia.
89. Nilsson, G. (1957). "Adsorption of tritiated sodium dodecyl sulfate at the solution surface measured with a windowless, high humidity gas flow proportional counter", Journal of Physical Chemistry, Vol. 61, 1135–1142.
90. Nguyen, A.V. and Schulze, H.J. (2004). "Colloidal Science of Flotation", A.V. Nguyen and H.J. Schulze, Eds., Surfactant Science Series, Marcel Dekker, Inc.
91. Nguyen, A.V., Harvey, P.A. and Jameson, G.J. (2003). "Influence of gas flow and frothers on water recovery in a froth column", Minerals Engineering, Vol. 16 (11), 1143–1147.

92. Parkhomovski, V.L., Petrunyak, D.G. and Paas, L. (1976). "Determination of methylisobutylcarbinol in waste waters of concentration plants", *Obogashchenie Rud*, Vol. 21 (2), 44–5.
93. Pugh, R.J. (2007). "The Physics and Chemistry of Frothers", *Froth Flotation: A Century of Innovation*, M.C. Fuerstenau, G. Jameson and R.H.Yoon, Eds., SME Publications, 259–281.
94. Quinn, J.J., Maldonado, M., Gomez, C.O. and Finch, J.A. (2013). "Experimental study on the shape–velocity relationship of an ellipsoidal bubble in inorganic salt solutions", *Minerals Engineering*, Vol. 55, 5–10.
95. Rafiei, A.A. and Finch, J.A. (2009). "A comparison of bubble rise velocity profile of two surfactants to explain gas hold up data", *Proceeding of 48<sup>th</sup> annual Conference of Metallurgists of CIM Sudbury, Ontario, Canada*. C.O. Gomez, J.E. Nessel and R. Rao, Eds., Sudbury, Ontario, 183–192.
96. Rafiei, A.A., Robbertze, M. and Finch, J.A. (2011). "Gas holdup and single bubble velocity profile", *International Journal of Mineral Processing*, Vol. 98 (1–2), 89–93.
97. Rao, S.R. and Leja, J. (2004). "Surface Chemistry of Froth Flotation", 2<sup>nd</sup> Edition, Kluwer Academic Publication, New York, 644–648.
98. Rosen, M.J. (1989). "Surfactants and Interfacial Phenomena", Wiley, New York.
99. Ross, V.E. and van Deventer, J.S.J. (1988). "Mass transport in flotation column froths", *Proceedings of an International Symposium on Column Flotation*, A.I.M.E, KV.S. Sastry, Ed., 129–139.
100. Ross, S. and Morrison, I.D. (1987). "A simple graphical method to evaluate surface elasticities and surface concentrations from rectilinear isothermal plots", *Langmuir*, Vol. 4, 485–486.
101. Sam, A., Gomez, C.O. and Finch, J.A. (1996). "Axial velocity profiles of single bubbles in water/frother solutions", *International Journal of Mineral Processing*, Vol. 47, 177–196.
102. Shah, Y.T., Godbole, S.P. and Deckwer, W.D. (1982). "Design parameters estimations for bubble column reactors", *American Institute of Chemical Engineers*, Vol. 28 (3), 353–79.
103. Smith, C.D., Hadler, K. and Cilliers, J.J. (2009). "The total air addition and air profile for flotation bank", 48<sup>th</sup> annual conference of metallurgists of CIM Sudbury, Ontario, Canada.
104. Subrahmanyam, T.V. and Forssberg, E. (1988). "Froth stability, particle entrainment and drainage in flotation - A review", *International Journal of Mineral Processing*, Vol. 23, 33–53.

105. Sweet, C., van Hoogstraten, J., Harris, M.C. and Laskowski, J.S. (1997). "The effect of frothers on bubble size and frothability of aqueous solutions", Processing of Complex Ores, Mineral Processing and the Environment. J.A. Finch, S.R. Rao and I. Holubec, Eds. CIMM & P Montreal Quebec, 235–245.
106. Tan, S.N., Fornasiero, D., Sedev, R. and Ralston, J. (2006). "The interfacial conformation of polypropylene glycols and their foam properties", Minerals Engineering, Vol. 19, 703–712.
107. Tan, S.N. (2005). "The marangoni effect and transient foam stability of low molecular weight polypropylene glycols". Ph.D. Thesis, University of South Australia.
108. Tan, S.N., Fornasiero, D., Sedev, R. and Ralston, J. (2005). "Marangoni effect in aqueous polypropylene glycol foams", Journal of Colloid and Interface Science, Vol. 286, 719–729.
109. Tanaka, K. and Igarashi, A. (2005). "Determination of Nonionic Surfactants", Chapter 3 in Handbook of Detergents Part C: Analysis, H. Waldhoff and R. Spilker, Eds., 149–214.
110. Tao, D., Luttrell, G.H. and Yoon, R.H. (2000). "A parametric study of froth stability and its effect on column flotation of fine particles", International Journal of Mineral Processing, Vol. 59, 25–43.
111. Tsatouhas, G., Grano, S.R. and Vera, M. (2006). "Case studies on the performance and characterization of the froth phase in industrial flotation circuits", Minerals Engineering, Vol. 19 (6–8), 774–783.
112. Velulemans, H., Groeseneken, D., Masschelein, R. and Van Vlem, E. (1987). "Survey of glycol ether exposures in Belgian industries and workshops", American Industrial Hygiene Association Journal, Vol. 48 (8), 671–676.
113. Wang, L. and Yoon, R. (2007). "Effects of surface forces and film elasticity on foam stability", International Journal of Mineral Processing, Vol. 85, 101–110.
114. Wills, B.A. and Napier-Munn, T. (2006). "Wills' Mineral Processing Technology", 7<sup>th</sup> ed, 1–29.
115. Wilson, A., Epstein, M.B. and Ross, J. (1957). "The adsorption of sodium lauryl sulfate and lauryl alcohol at the air-liquid interface", Journal of Colloid Science, Vol. 12 (4), 345–355.
116. Wrobel, S.A. (1951). Bulletin and Proceedings of the Australasian Institute of Mining and Metallurgy, Vol.61, 505.

117. Xu, M., Finch, J.A. and Uribe-Salas, A. (1991). "Maximum gas and bubble surface rates in flotation columns", *International Journal of Mineral Processing*, Vol. 32 (3–4), 233–250.
118. Yasunishi, A., Fukuma, M. and Muroyama, K. (1986). "Measurement of behavior of gas bubbles and gas holdup in a slurry bubble column by a dual electroresistivity probe method", *Journal of Chemical Engineering of Japan*, Vol. 19, 444–449.
119. Yianatos, J., Contreras, F., Morales, P., Coddou, F., Elgueta, H. and Ortiz, J. (2010). "A novel scale-up approach for mechanical flotation cells", *Minerals Engineering*, Vol. 23 (11–13), 877–884.
120. Yoon, R.H. and Luttrell, G.H. (1986). "The effect of bubble size on fine coal flotation", *Coal Preparation*, Vol. 2, 179–192.
121. Zanin, M., Wightman, E., Grano, S.R. and Franzidis, J.P. (2009). "Quantifying contributions to froth stability in porphyry copper plants", *International Journal of Mineral Processing*, Vol. 91, (1–2), 19–27.
122. Zangooi, A., Gomez, C.O. and Finch, J.A. (2012). "A technique for the direct measurement of bubble frother coverage", *Proceedings of 25<sup>th</sup> International Mineral Processing Congress (IMPC)*.
123. Zangooi, A., Gomez, C.O. and Finch, J.A. (2010). "Frother analysis in industrial flotation cells", *Canadian Metallurgy Quarterly*, Vol. 49 (4), 389–396.
124. Zhang, W., Zhu, S. and Finch, J.A. (2013). "Frother partitioning in dual-frother systems: Development of analytical technique", *International Journal of Mineral Processing*, Vol. 119, 75–82.
125. Zhang, W., Nasset, J.E., Rao, R. and Finch, J.A. (2012). "Characterizing frothers through Critical Coalescence Concentration (CCC)95-Hydrophile-Lipophile Balance (HLB) relationship", *Minerals*, Vol. 2, 208–227.
126. Zhang, W. (2012). "Frothers and frother blends: A structure-function study", *McGill PhD thesis*.
127. Zhang, W., Nasset, J.E. and Finch, J.A. (2010). "Water recovery and bubble surface area flux in flotation", *Canadian Metallurgy Quarterly*, Vol. 49 (4), 353–362.
128. Zhang, Y. and Finch, J.A. (2001). "A note on single bubble motion in surfactant solutions", *Journal of Fluid Mechanics*, Vol. 429, 63–66.
129. Zhang, Z., Yang, M.J. and Pawliszyn, J. (1994). "Solid-phase microextraction", *Analytical Chemistry*, Vol. 66 (17), 844–853.

130. Zhang, Z. and Pawliszyn, J. (1993). "Headspace solid-phase microextraction", *Analytical Chemistry*, Vol. 65, 1843–1852.
131. Zhou, Z.A., Egiebor, N.O. and Plitt, L.R. (1993). "Frother effects on bubble motion in a swarm", *Canadian Metallurgical Quarterly*, Vol. 32 (2), 89–96.
132. Zieminski, S.A., Caron, M.M. and Blackmore, R.B. (1967). "Behavior of air bubbles in dilute aqueous solutions", *Industrial and Engineering Chemistry Fundamentals*, Vol. 6 (2), 233–242.

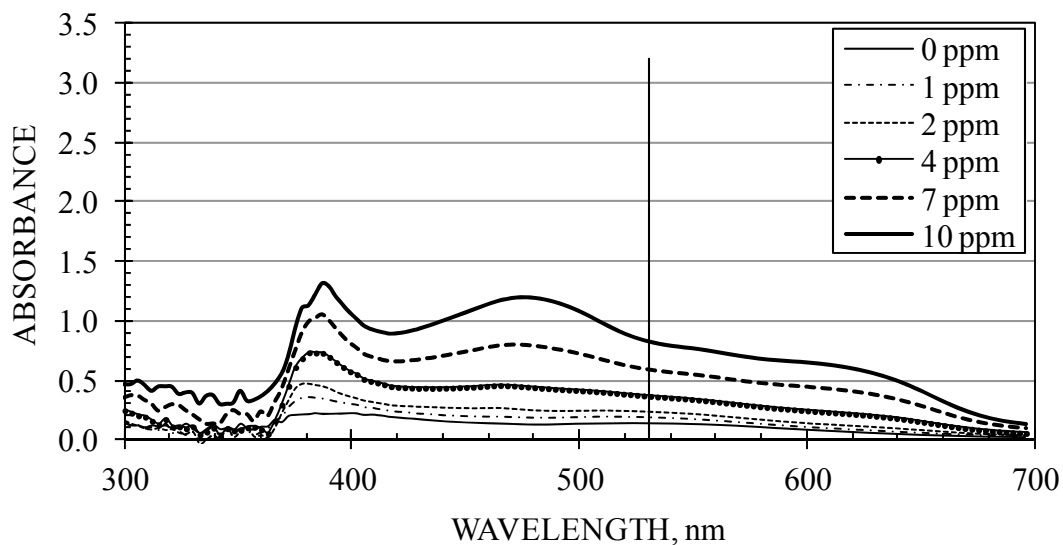


**APPENDIX 1**

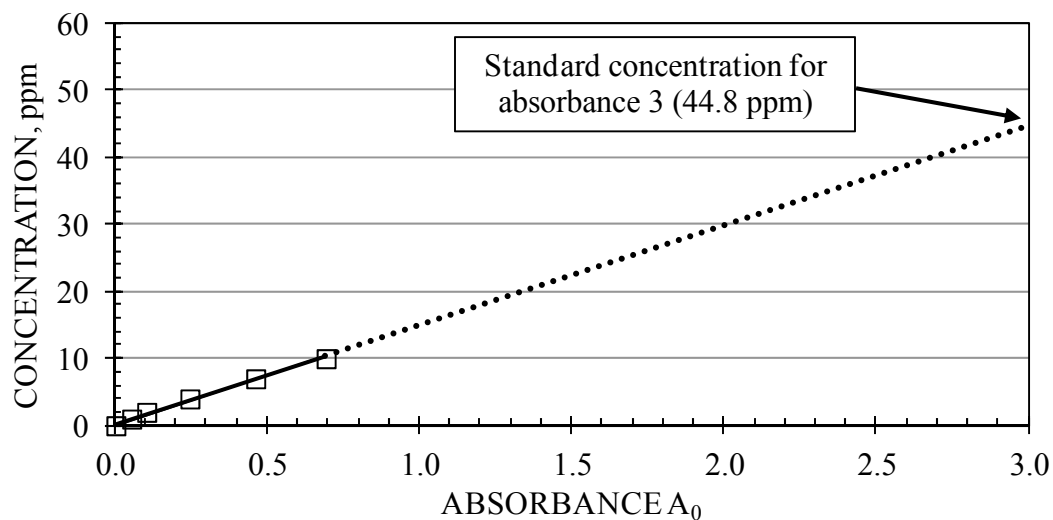
FROTHER: F150  
 SUPPLIER: Flottec  
 MOLECULAR WEIGHT: na  
 DILUTION WATER: McGill tap  
 DATE: 11/04/2010

SAMPLE 1

CALIBRATION SPECTRA:



CALIBRATION CURVE:



EQUATION:

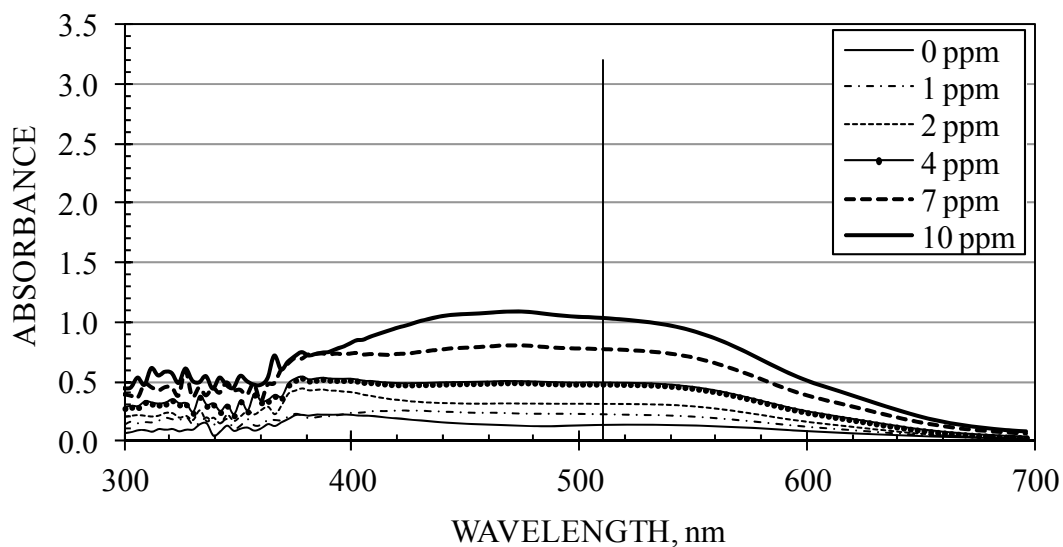
$$C \text{ (ppm)} = 14.945 A_0 \quad C \leq 10 \text{ ppm}$$

where  $A_0$  is the measured absorbance minus that of the 0 ppm standard (both at 531 nm)

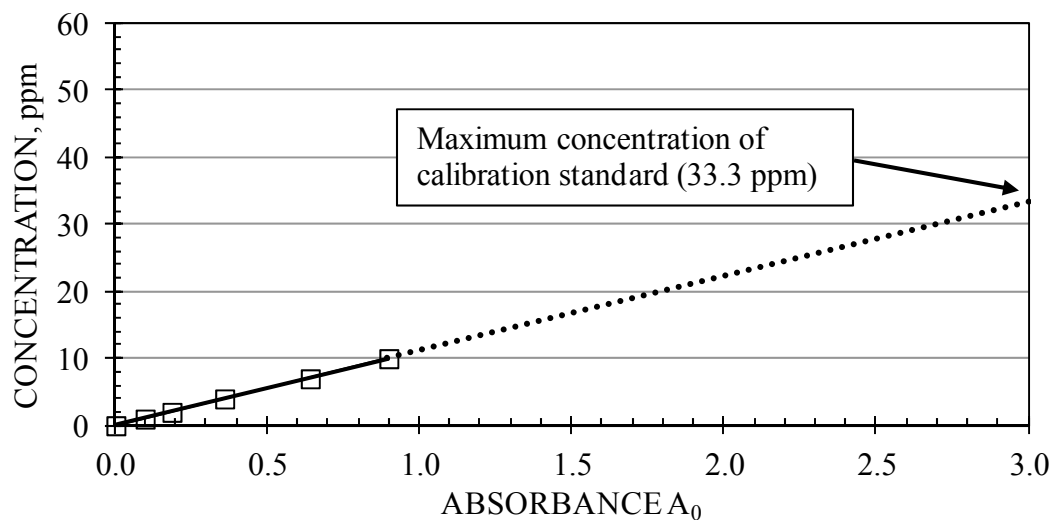
FROTHER: F140  
 SUPPLIER: Flottec  
 MOLECULAR WEIGHT: 225  
 DILUTION WATER: McGill tap  
 DATE: 12/04/2010

SAMPLE 2

CALIBRATION SPECTRA:



CALIBRATION CURVE:



EQUATION:

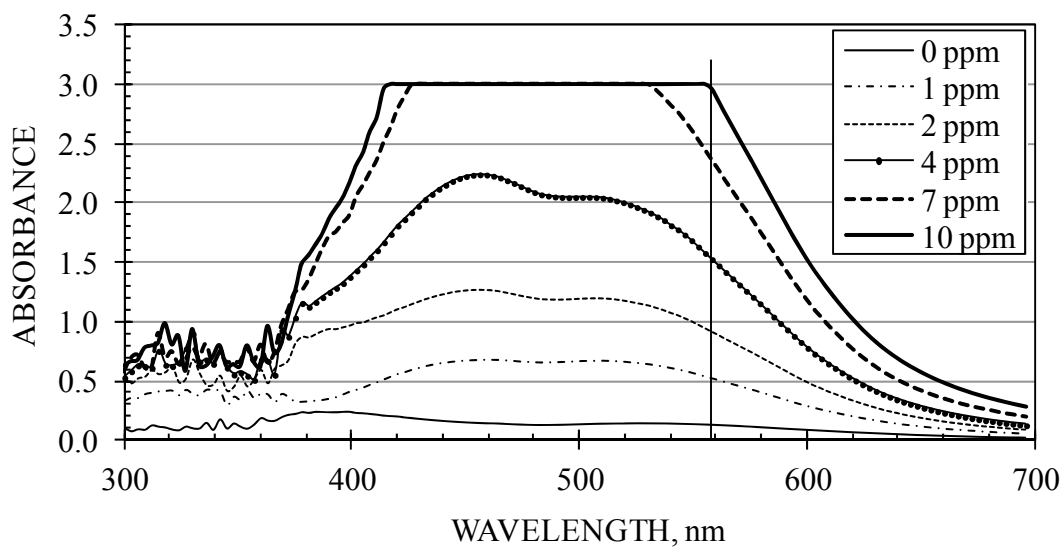
$$C \text{ (ppm)} = 11.097 A_0 \quad C \leq 10 \text{ ppm}$$

where  $A_0$  is the measured absorbance minus that of the 0 ppm standard (both at 510 nm)

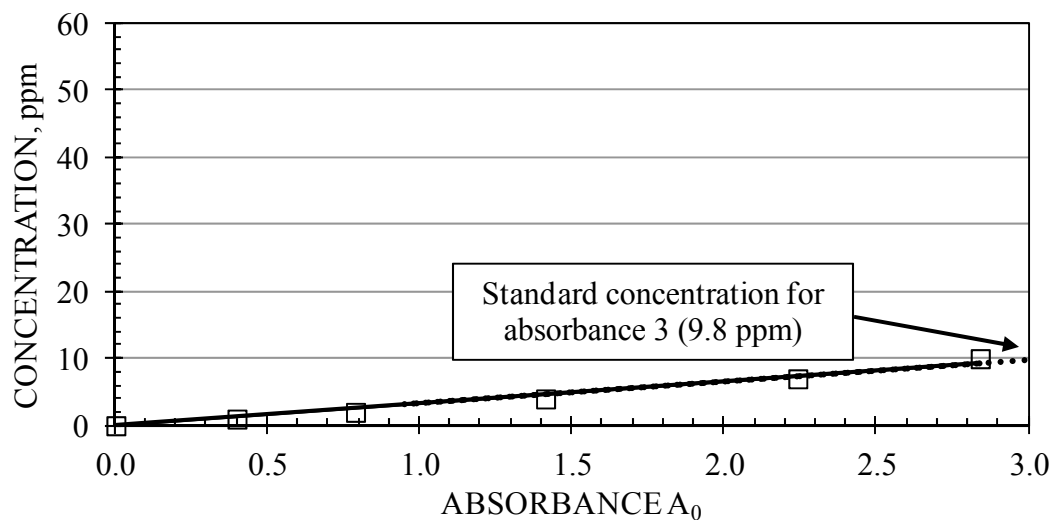
FROTHER: MIBC  
 SUPPLIER: Flottec  
 MOLECULAR WEIGHT: na  
 DILUTION WATER: McGill tap  
 DATE: 14/04/2010

SAMPLE 3

CALIBRATION SPECTRA:



CALIBRATION CURVE:



EQUATION:

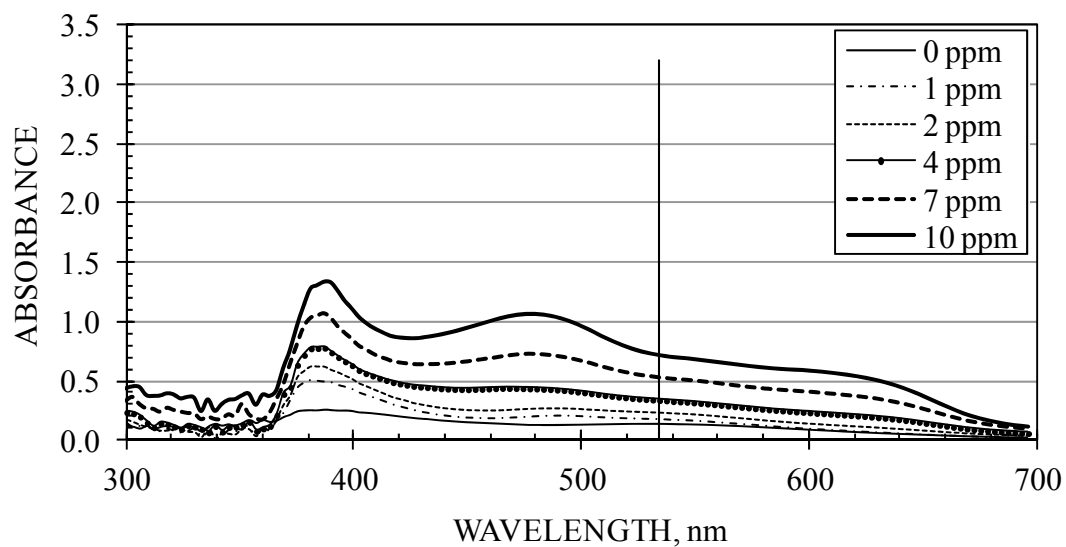
$$C \text{ (ppm)} = 3.264 A_0 \quad C \leq 10 \text{ ppm}$$

where  $A_0$  is the measured absorbance minus that of the 0 ppm standard (both at 558 nm)

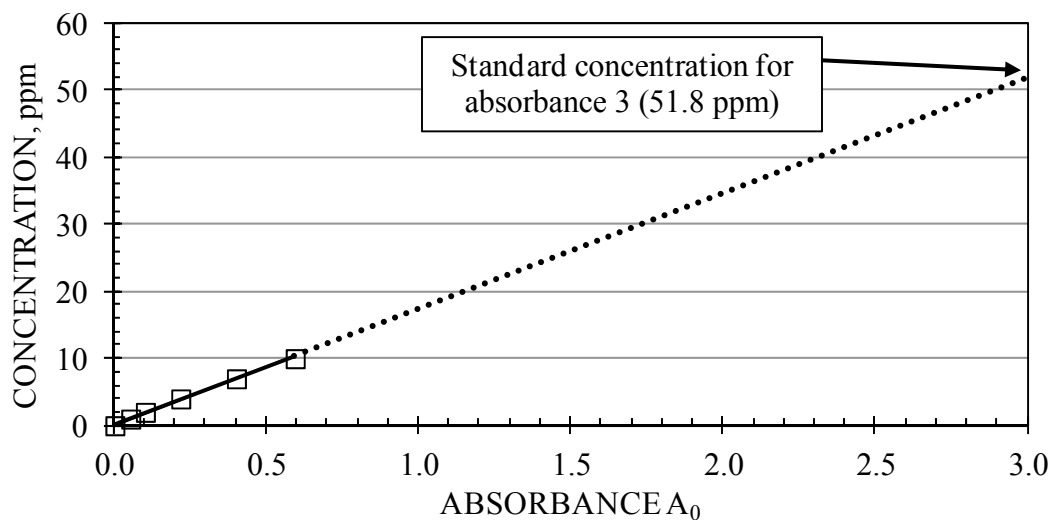
FROTHER: DF250  
 SUPPLIER: Dow  
 MOLECULAR WEIGHT: 264.35  
 DILUTION WATER: McGill tap  
 DATE: 16/04/2010

SAMPLE 4

CALIBRATION SPECTRA:



CALIBRATION CURVE:



EQUATION:

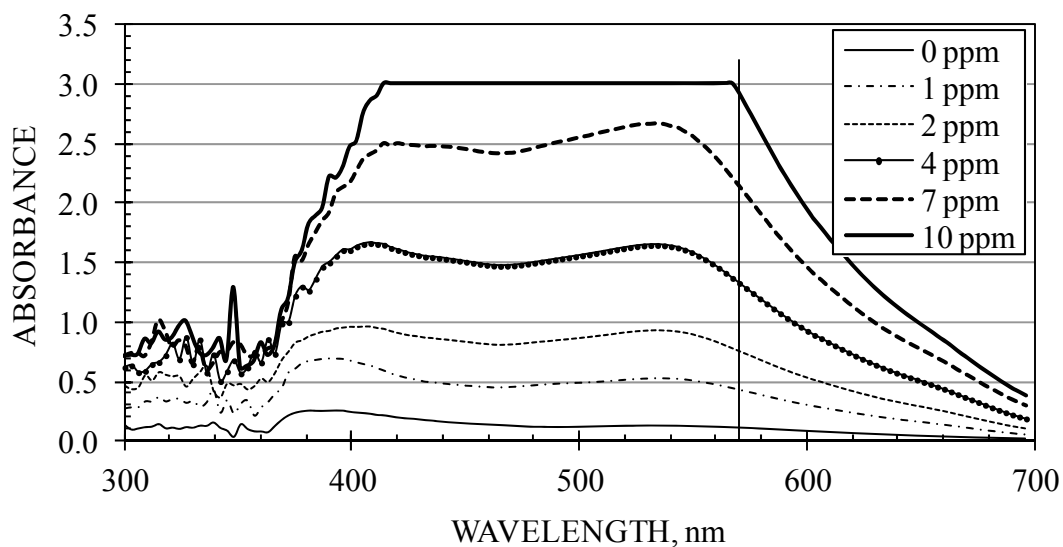
$$C \text{ (ppm)} = 17.273 A_0 \quad C \leq 10 \text{ ppm}$$

where  $A_0$  is the measured absorbance minus that of the 0 ppm standard (both at 534 nm)

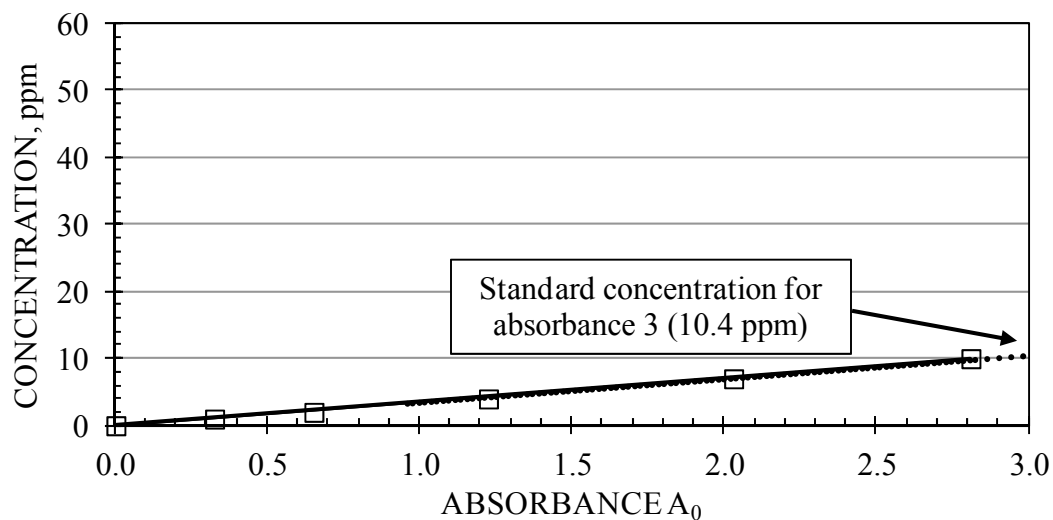
FROTHER: Pentanol  
 SUPPLIER: Sigma Aldrich  
 MOLECULAR WEIGHT: 88  
 DILUTION WATER: McGill tap  
 DATE: 17/04/2010

SAMPLE 5

CALIBRATION SPECTRA:



CALIBRATION CURVE:



EQUATION:

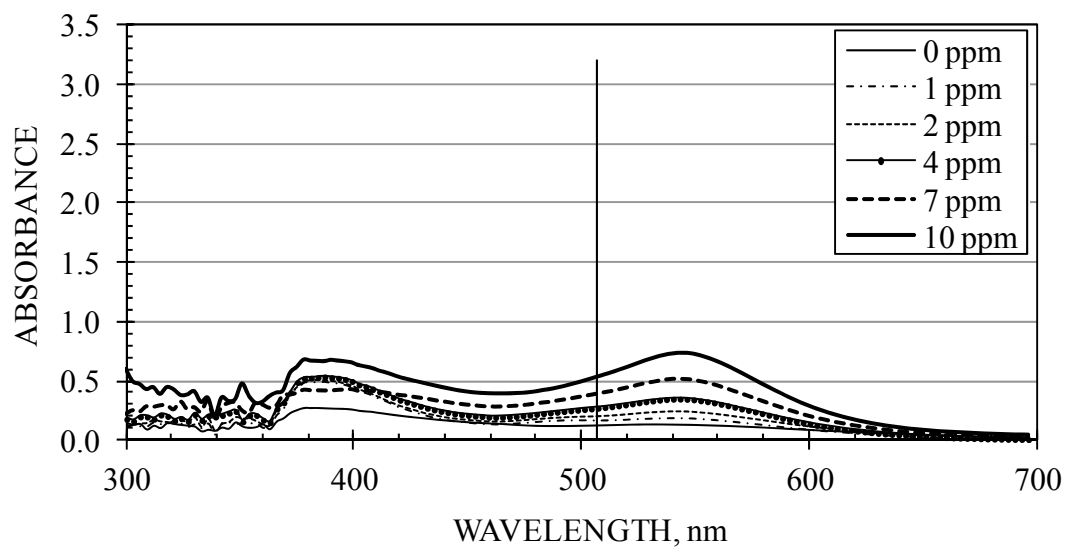
$$C \text{ (ppm)} = 3.481 A_0 \quad C \leq 10 \text{ ppm}$$

where  $A_0$  is the measured absorbance minus that of the 0 ppm standard (both at 570 nm)

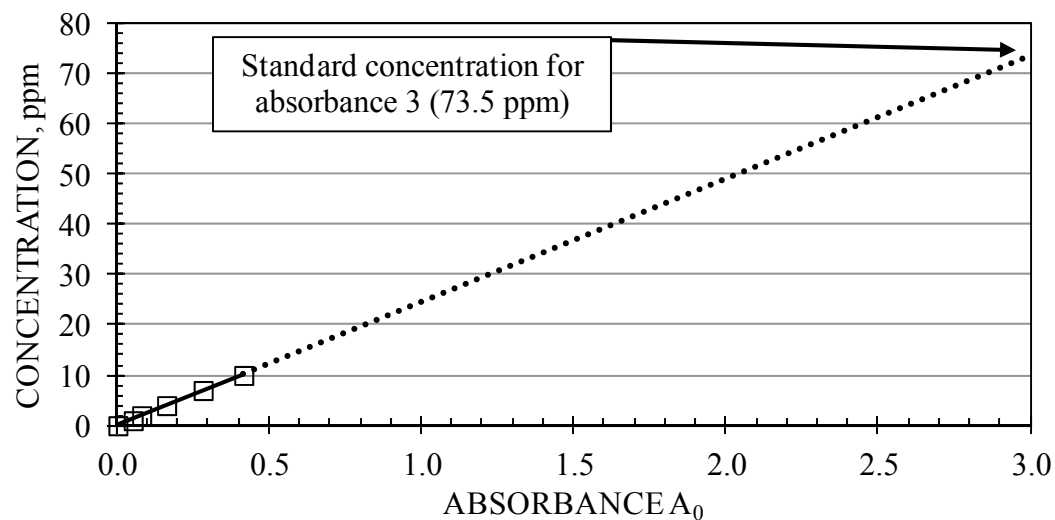
FROTHER: Butanol  
 SUPPLIER: Sigma Aldrich  
 MOLECULAR WEIGHT: 74  
 DILUTION WATER: McGill tap  
 DATE: 17/04/2010

SAMPLE 6

CALIBRATION SPECTRA:



CALIBRATION CURVE:



EQUATION:

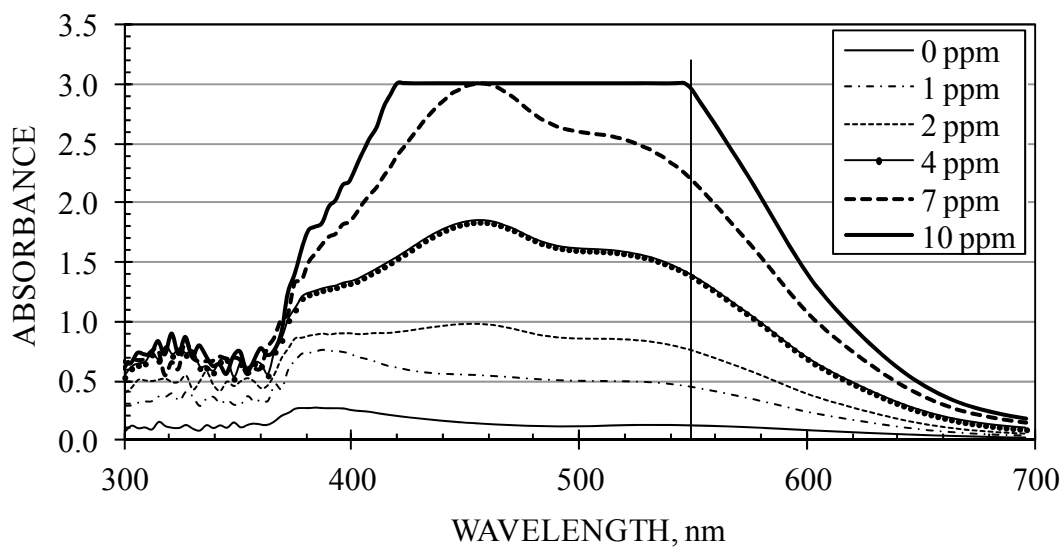
$$C \text{ (ppm)} = 24.496 A_0 \quad C \leq 10 \text{ ppm}$$

where  $A_0$  is the measured absorbance minus that of the 0 ppm standard (both at 507 nm)

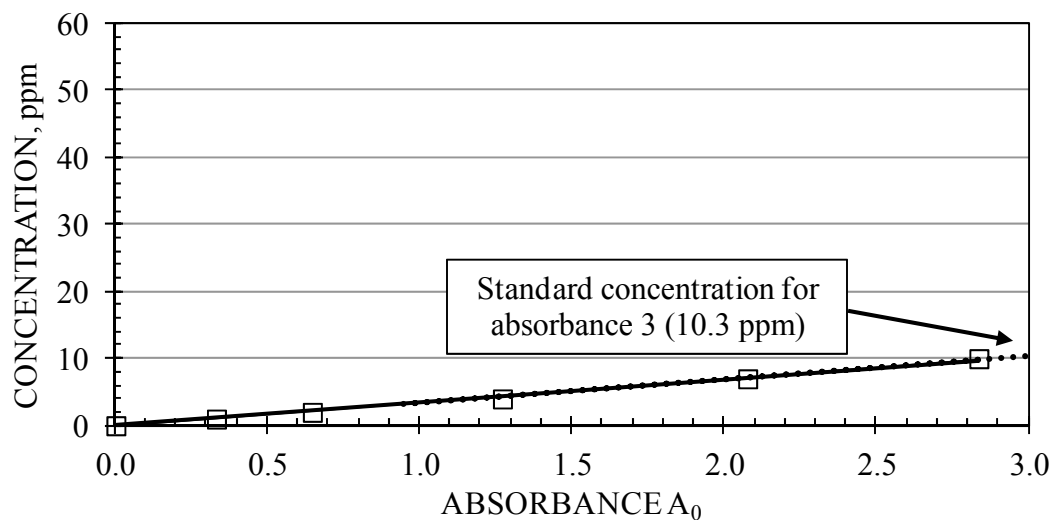
FROTHER: Hexanol  
 SUPPLIER: Sigma Aldrich  
 MOLECULAR WEIGHT: 102  
 DILUTION WATER: McGill tap  
 DATE: 18/04/2010

SAMPLE 7

CALIBRATION SPECTRA:



CALIBRATION CURVE:



EQUATION:

$$C \text{ (ppm)} = 3.426 A_0 \quad C \leq 10 \text{ ppm}$$

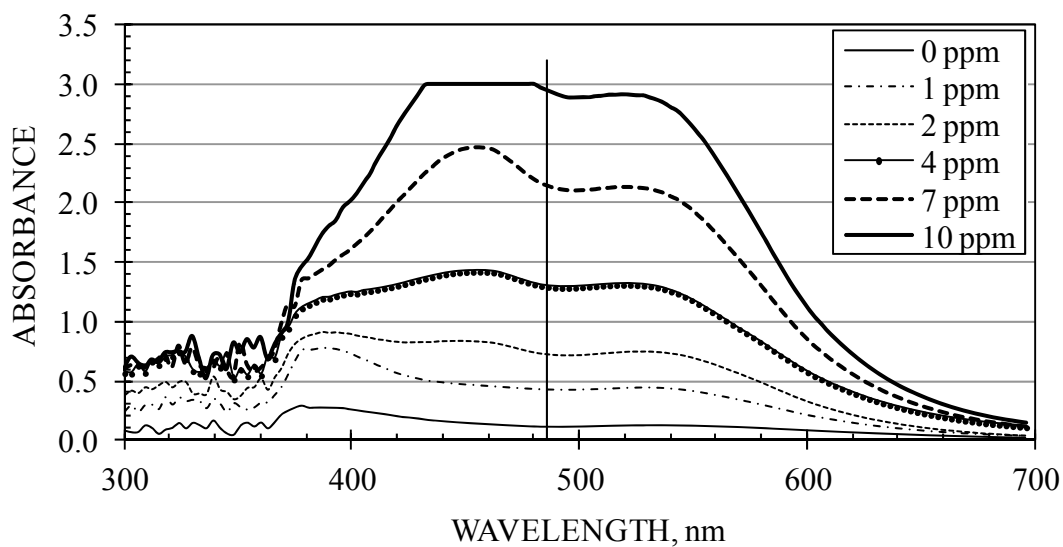
where  $A_0$  is the measured absorbance minus that of the 0 ppm standard (both at 549 nm)



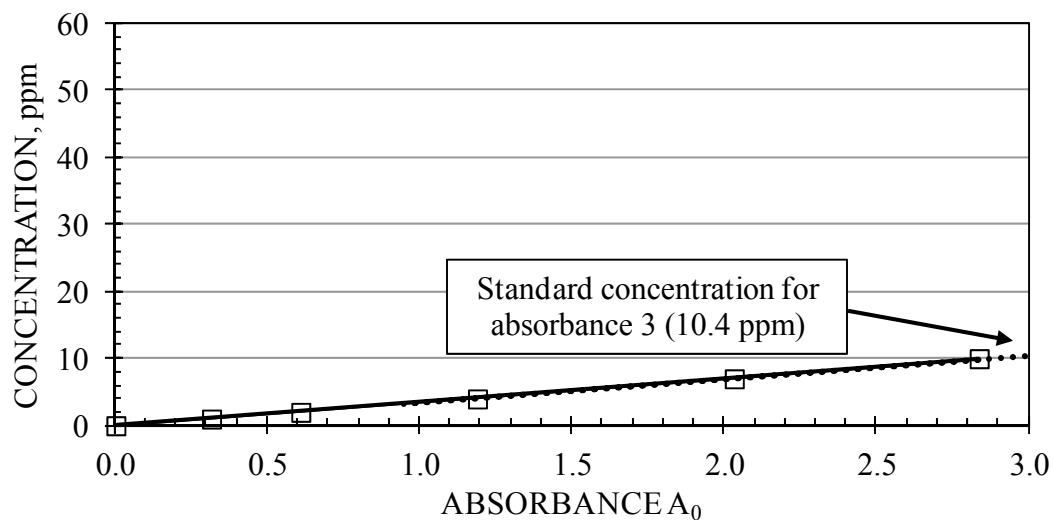
FROTHER: Octanol  
 SUPPLIER: Sigma Aldrich  
 MOLECULAR WEIGHT: 130  
 DILUTION WATER: McGill tap  
 DATE: 18/04/2010

SAMPLE 8

CALIBRATION SPECTRA:



CALIBRATION CURVE:



EQUATION:

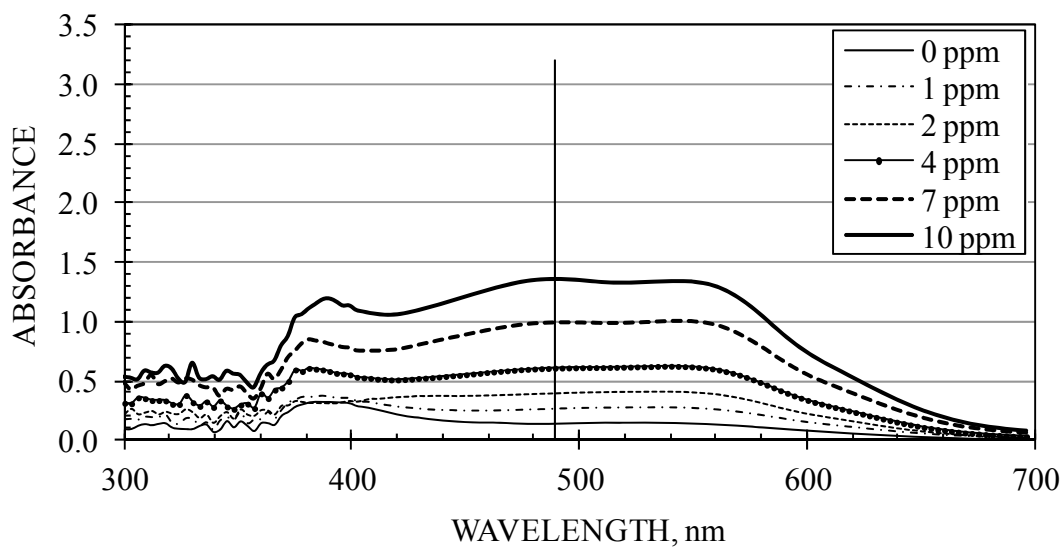
$$C \text{ (ppm)} = 3.480 A_0 \quad C \leq 10 \text{ ppm}$$

where  $A_0$  is the measured absorbance minus that of the 0 ppm standard (both at 486 nm)

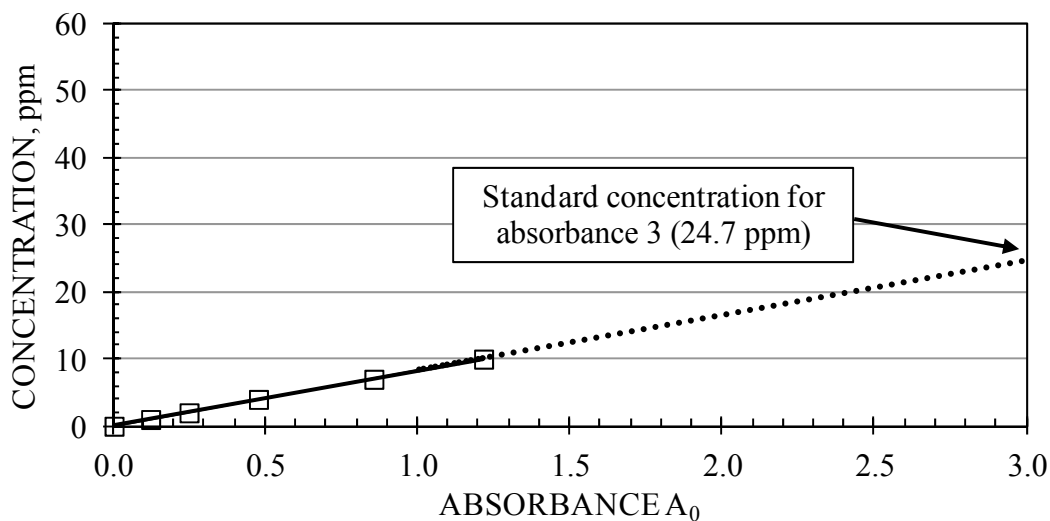
FROTHER: TX10713  
 SUPPLIER: Nalco  
 MOLECULAR WEIGHT: na  
 DILUTION WATER: McGill tap  
 DATE: 21/04/2010

SAMPLE 9

CALIBRATION SPECTRA:



CALIBRATION CURVE:



EQUATION:

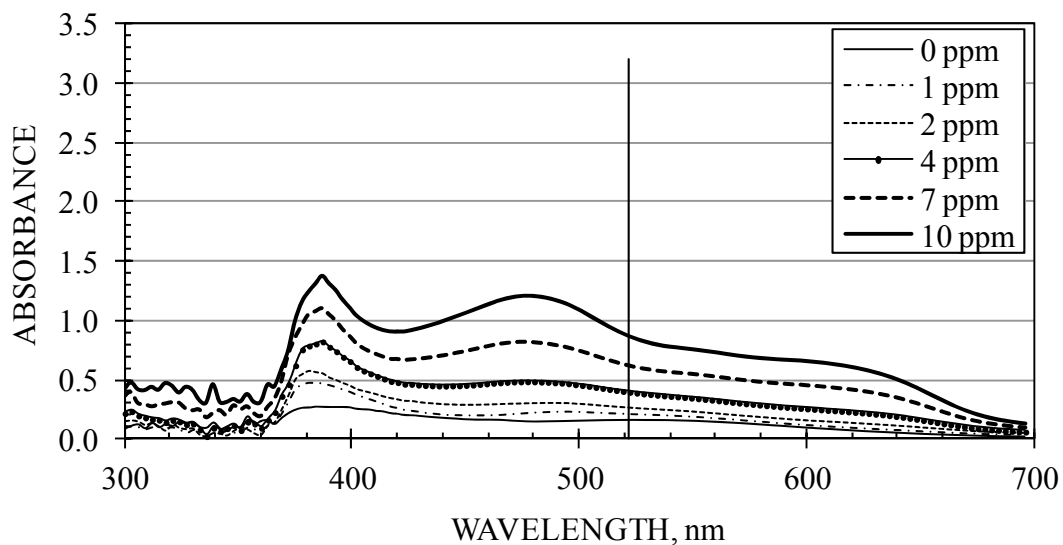
$$C \text{ (ppm)} = 8.248 A_0 \quad C \leq 10 \text{ ppm}$$

where  $A_0$  is the measured absorbance minus that of the 0 ppm standard (both at 489 nm)

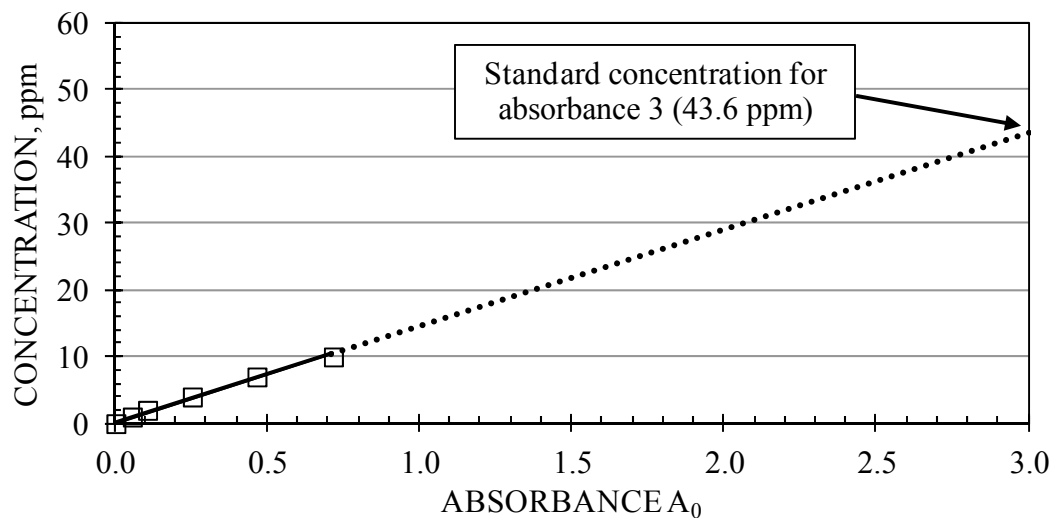
FROTHER: TX13072  
 SUPPLIER: Nalco  
 MOLECULAR WEIGHT: na  
 DILUTION WATER: McGill tap  
 DATE: 22/04/2010

SAMPLE 10

CALIBRATION SPECTRA:



CALIBRATION CURVE:



EQUATION:

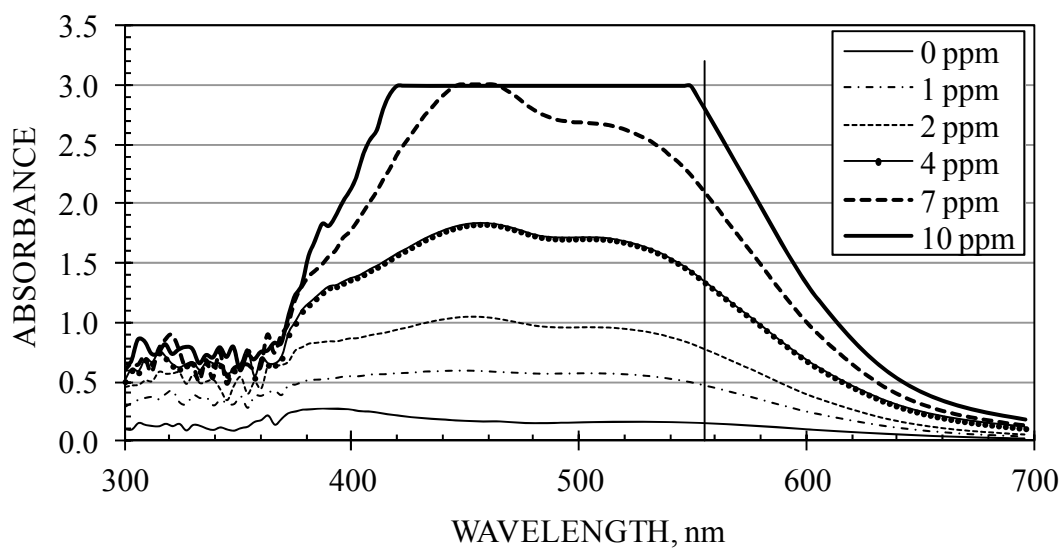
$$C \text{ (ppm)} = 14.542 A_0 \quad C \leq 10 \text{ ppm}$$

where  $A_0$  is the measured absorbance minus that of the 0 ppm standard (both at 522 nm)

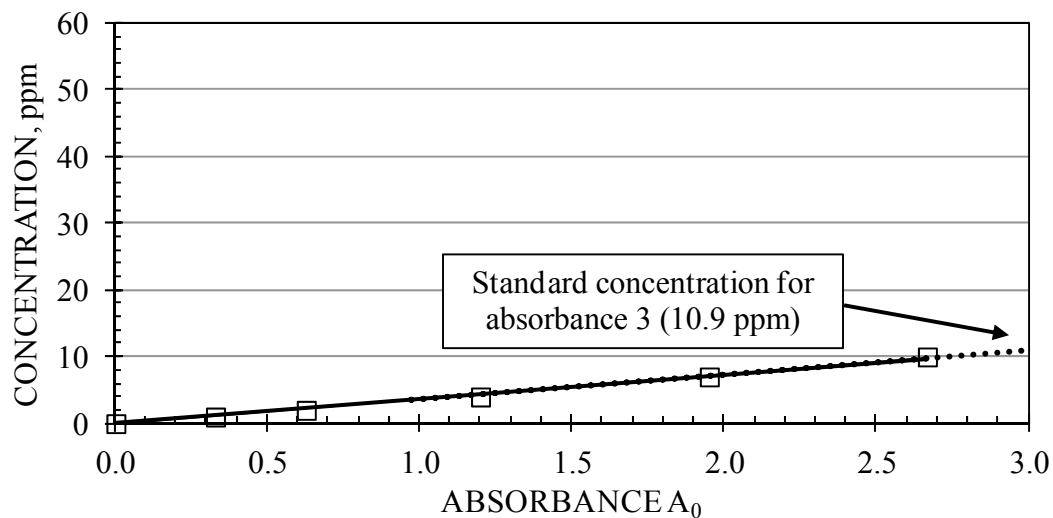
FROTHER: DVS4U021  
 SUPPLIER: Nalco  
 MOLECULAR WEIGHT: na  
 DILUTION WATER: McGill tap  
 DATE: 24/04/2010

SAMPLE 11

CALIBRATION SPECTRA:



CALIBRATION CURVE:



EQUATION:

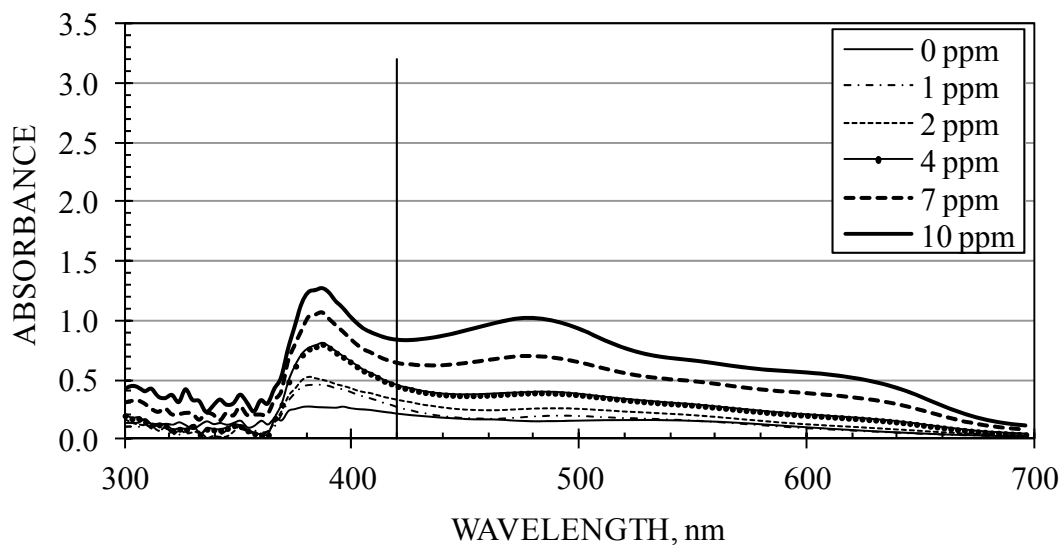
$$C \text{ (ppm)} = 3.638 A_0 \quad C \leq 10 \text{ ppm}$$

where  $A_0$  is the measured absorbance minus that of the 0 ppm standard (both at 555 nm)

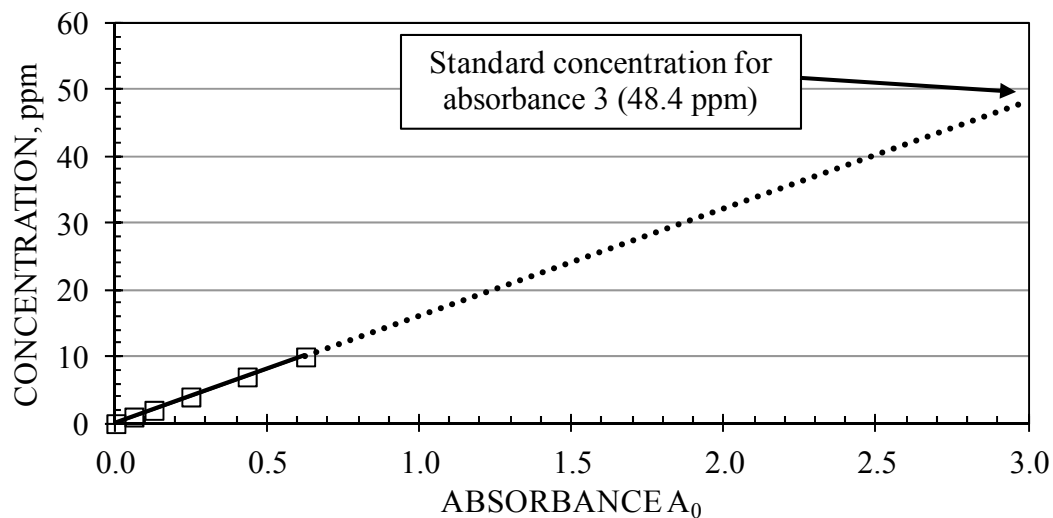
FROTHER: U250C  
 SUPPLIER: Nalco  
 MOLECULAR WEIGHT: na  
 DILUTION WATER: McGill tap  
 DATE: 25/04/2010

SAMPLE 12

CALIBRATION SPECTRA:



CALIBRATION CURVE:



EQUATION:

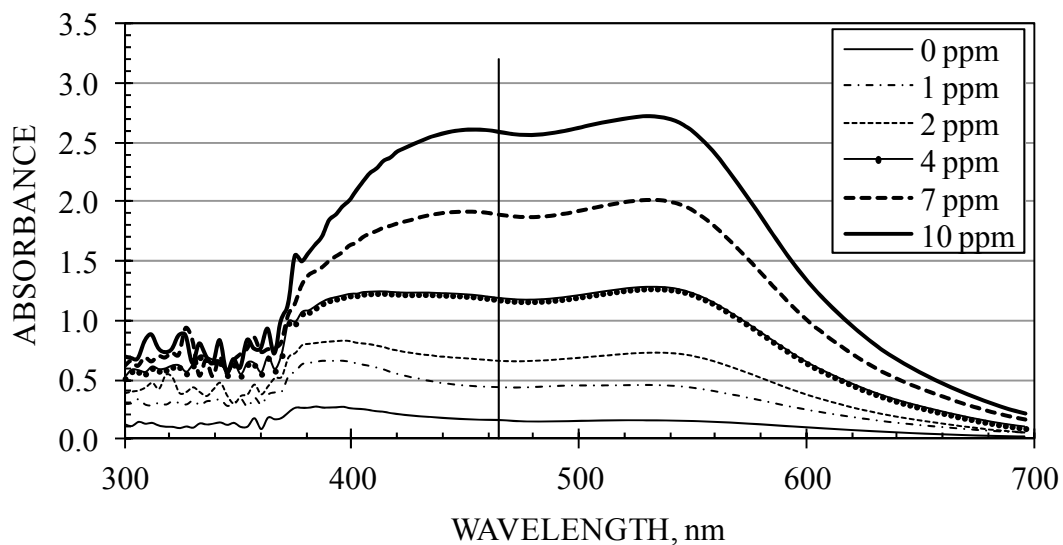
$$C \text{ (ppm)} = 16.128 A_0 \quad C \leq 10 \text{ ppm}$$

where  $A_0$  is the measured absorbance minus that of the 0 ppm standard (both at 420 nm)

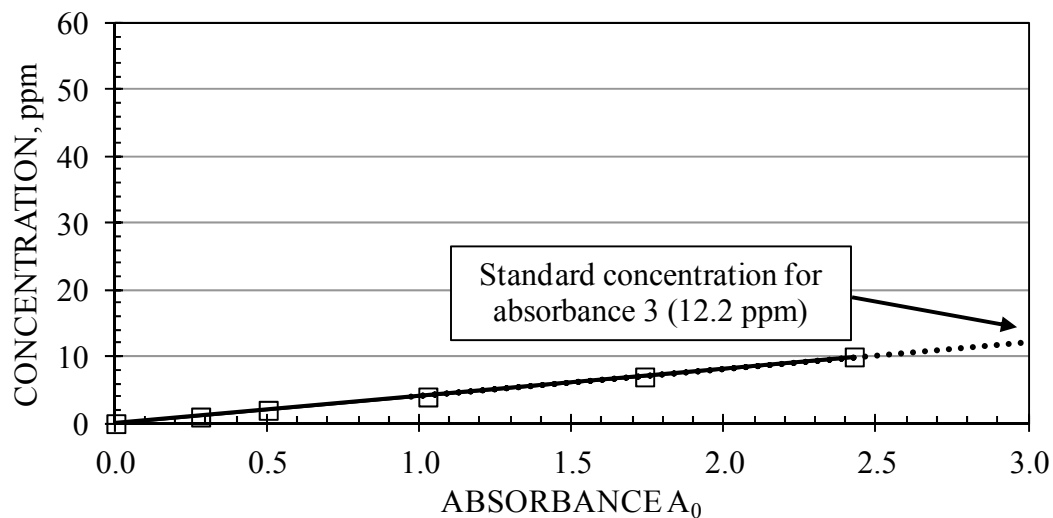
FROTHER: Senfroth7  
 SUPPLIER: Senmin  
 MOLECULAR WEIGHT: na  
 DILUTION WATER: McGill tap  
 DATE: 25/04/2010

SAMPLE 13

CALIBRATION SPECTRA:



CALIBRATION CURVE:



EQUATION:

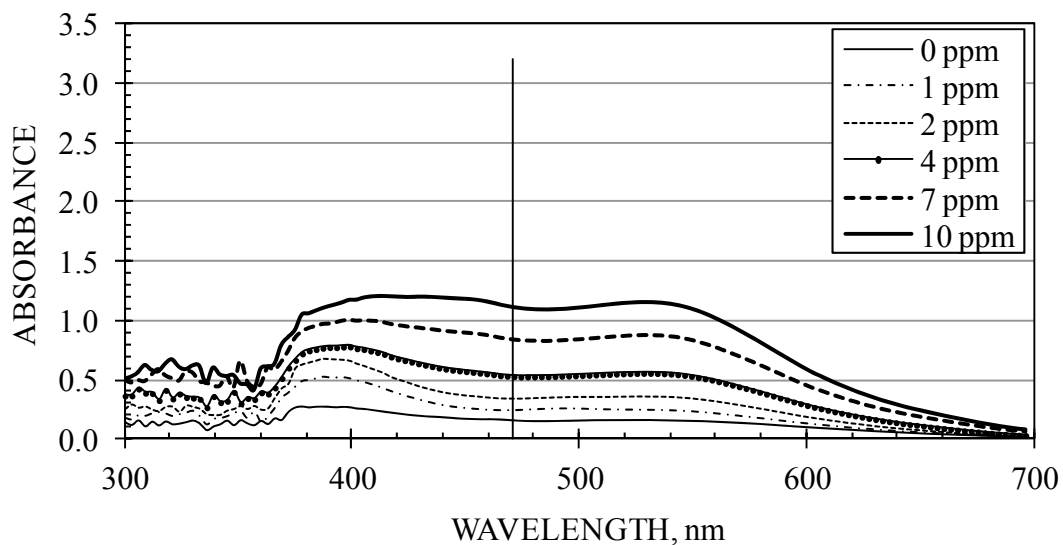
$$C \text{ (ppm)} = 4.069 A_0 \quad C \leq 10 \text{ ppm}$$

where  $A_0$  is the measured absorbance minus that of the 0 ppm standard (both at 465 nm)

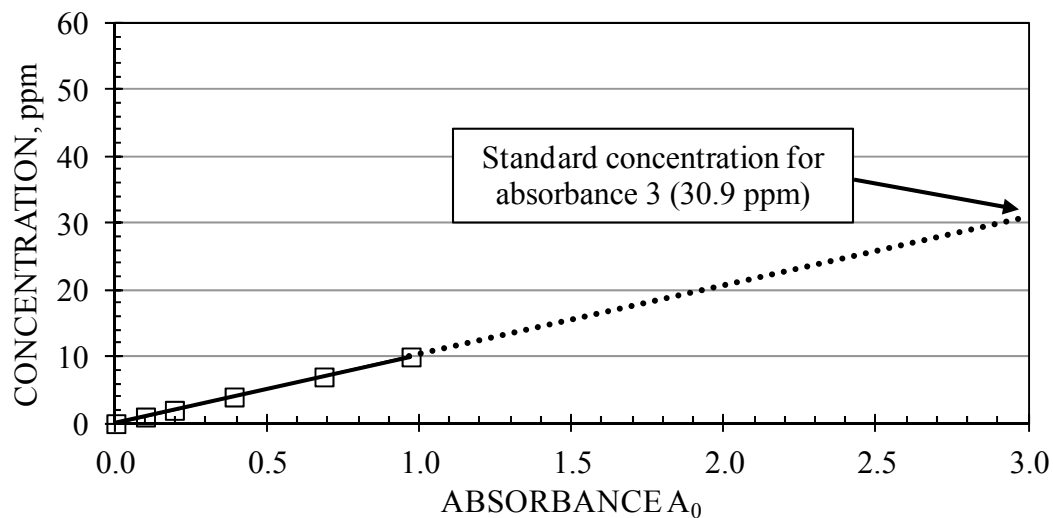
FROTHER: Senfroth400  
 SUPPLIER: Senmin  
 MOLECULAR WEIGHT: na  
 DILUTION WATER: McGill tap  
 DATE: 26/04/2010

SAMPLE 14

CALIBRATION SPECTRA:



CALIBRATION CURVE:



EQUATION:

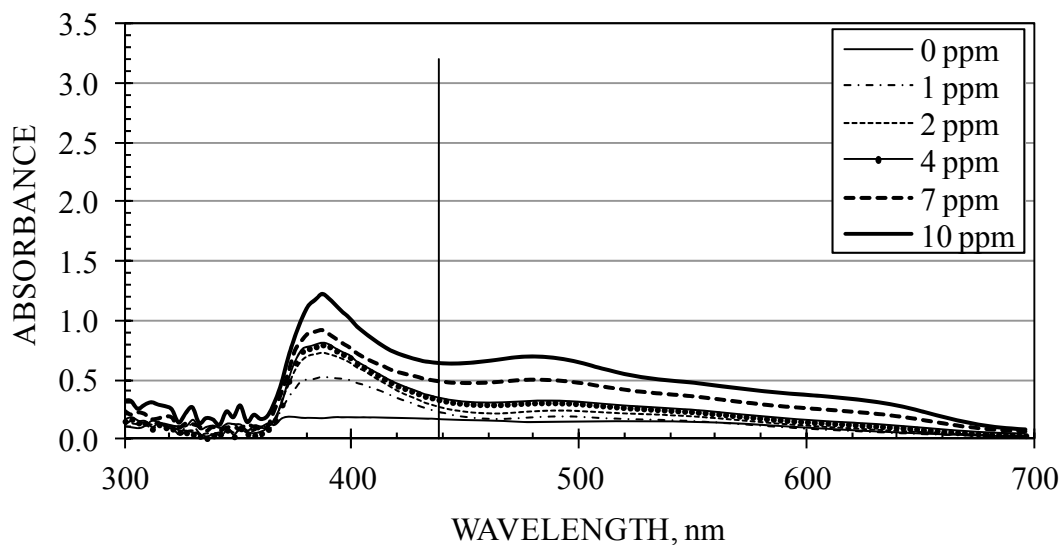
$$C \text{ (ppm)} = 10.300 A_0 \quad C \leq 10 \text{ ppm}$$

where  $A_0$  is the measured absorbance minus that of the 0 ppm standard (both at 471 nm)

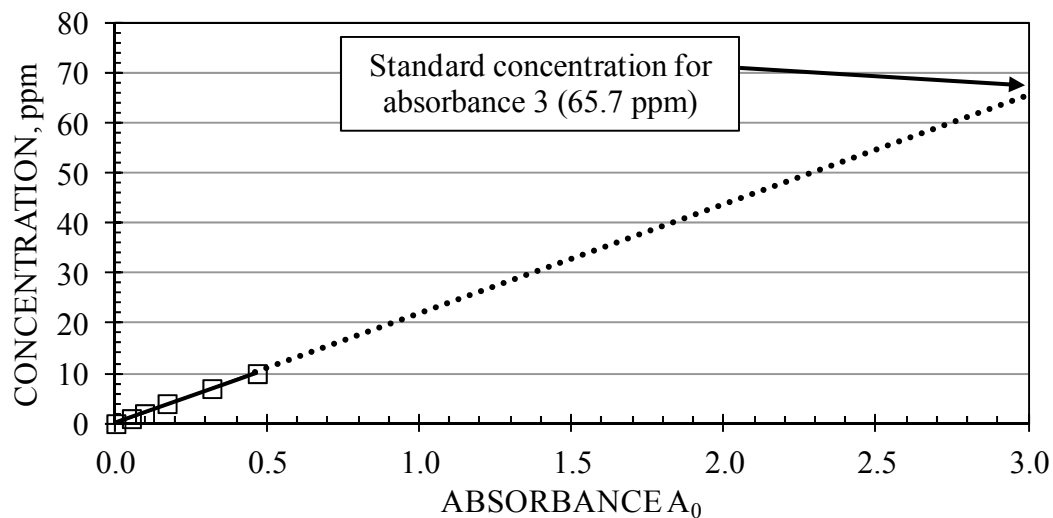
FROTHER: Senfrothxp200  
 SUPPLIER: Senmin  
 MOLECULAR WEIGHT: na  
 DILUTION WATER: McGill tap  
 DATE: 28/04/2010

SAMPLE 15

CALIBRATION SPECTRA:



CALIBRATION CURVE:



EQUATION:

$$C \text{ (ppm)} = 21.898 A_0 \quad C \leq 10 \text{ ppm}$$

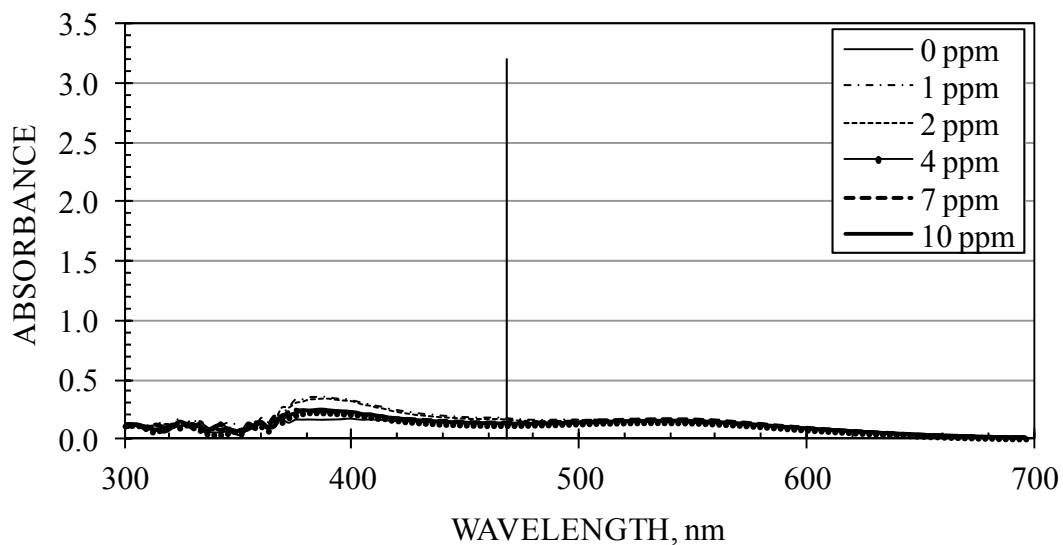
where  $A_0$  is the measured absorbance minus that of the 0 ppm standard (both at 438 nm)



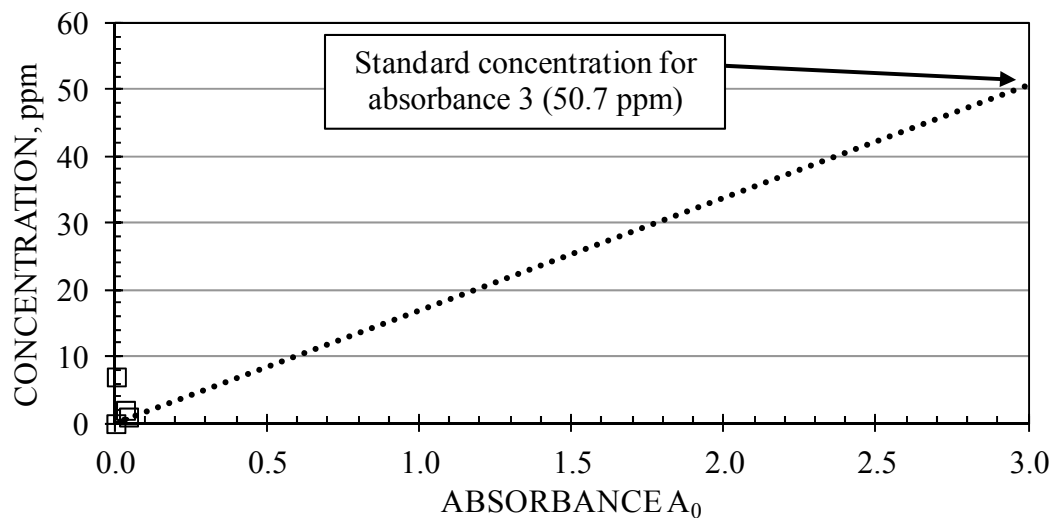
FROTHER: Senfroth6000  
 SUPPLIER: Senmin  
 MOLECULAR WEIGHT: na  
 DILUTION WATER: McGill tap  
 DATE: 03/05/2010

SAMPLE 16

CALIBRATION SPECTRA:



CALIBRATION CURVE:



EQUATION:

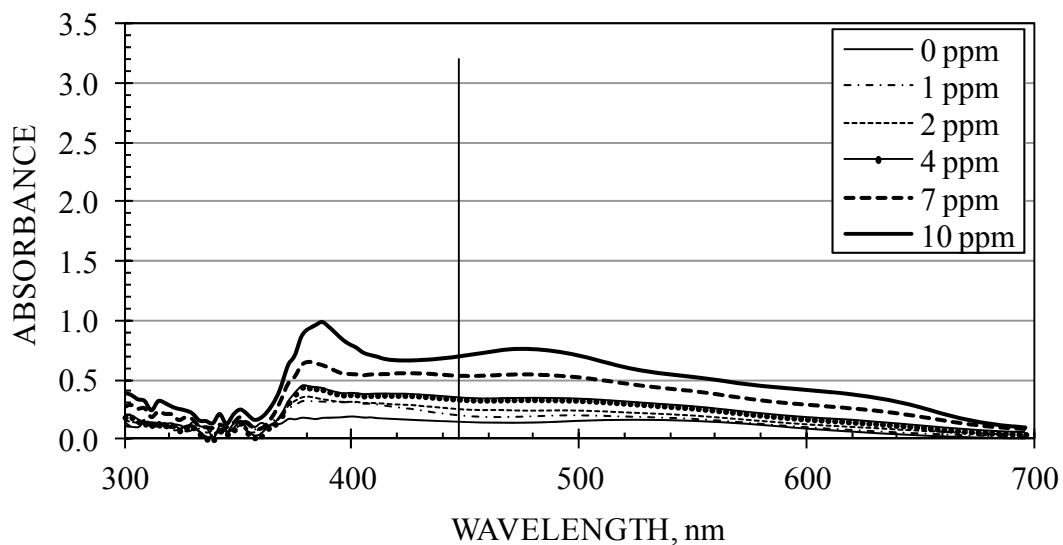
$$C \text{ (ppm)} = 16.896 A_0 \quad C \leq 10 \text{ ppm}$$

where  $A_0$  is the measured absorbance minus that of the 0 ppm standard (both at 468 nm)

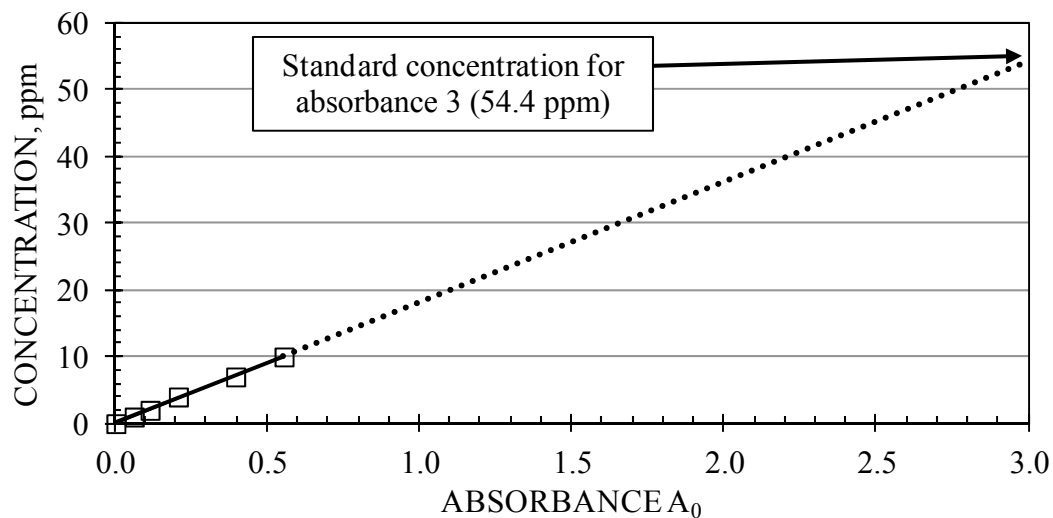
FROTHER: Senfroth516  
 SUPPLIER: Senmin  
 MOLECULAR WEIGHT: na  
 DILUTION WATER: McGill tap  
 DATE: 04/05/2010

SAMPLE 17

CALIBRATION SPECTRA:



CALIBRATION CURVE:



EQUATION:

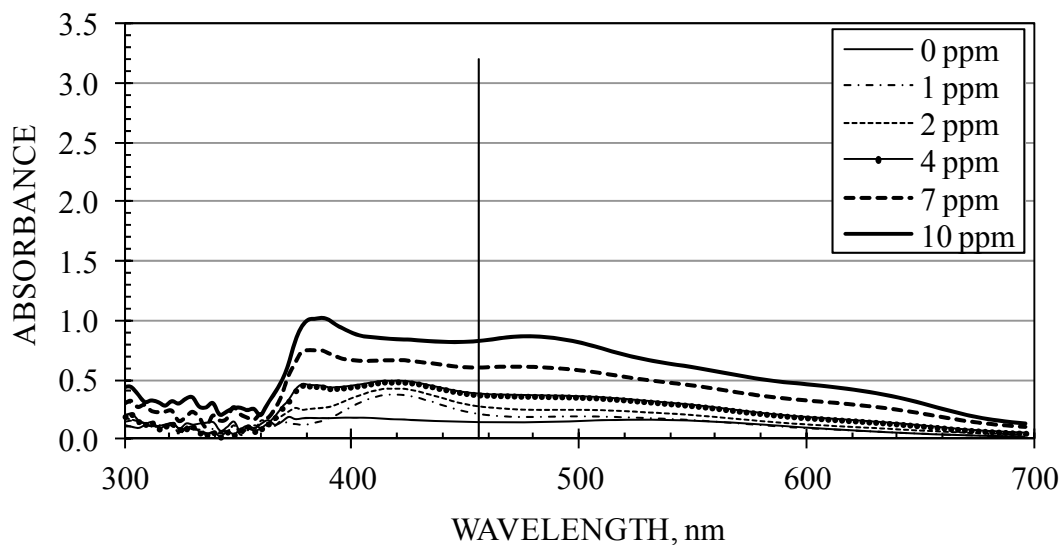
$$C \text{ (ppm)} = 18.122 A_0 \quad C \leq 10 \text{ ppm}$$

where  $A_0$  is the measured absorbance minus that of the 0 ppm standard (both at 447 nm)

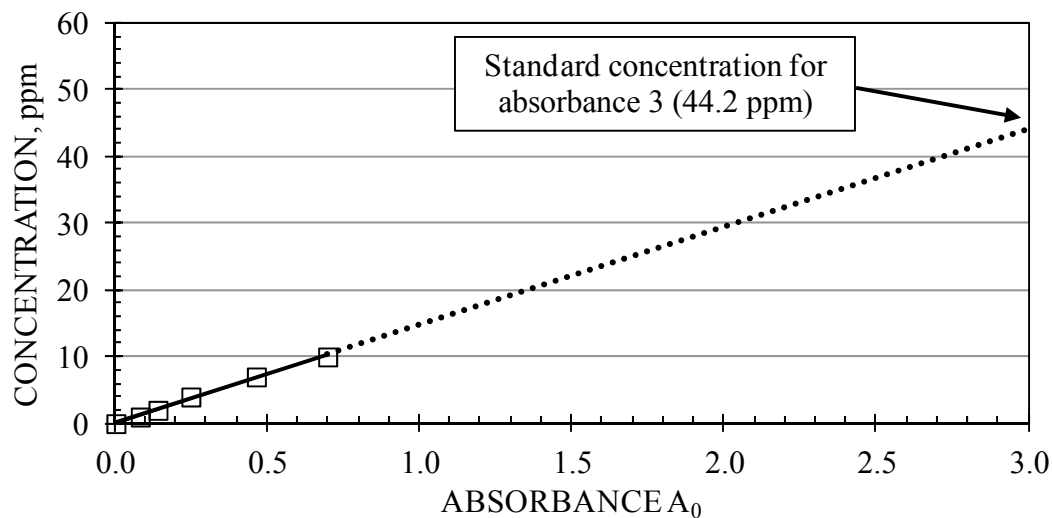
FROTHER: Senfroth250  
 SUPPLIER: Senmin  
 MOLECULAR WEIGHT: na  
 DILUTION WATER: McGill tap  
 DATE: 04/05/2010

SAMPLE 18

CALIBRATION SPECTRA:



CALIBRATION CURVE:



EQUATION:

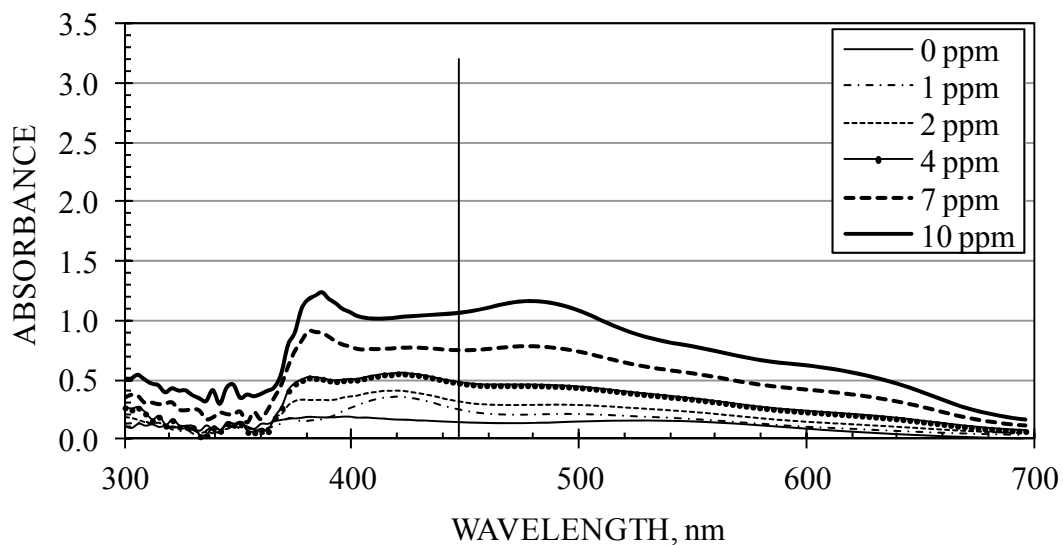
$$C \text{ (ppm)} = 14.737 A_0 \quad C \leq 10 \text{ ppm}$$

where  $A_0$  is the measured absorbance minus that of the 0 ppm standard (both at 456 nm)

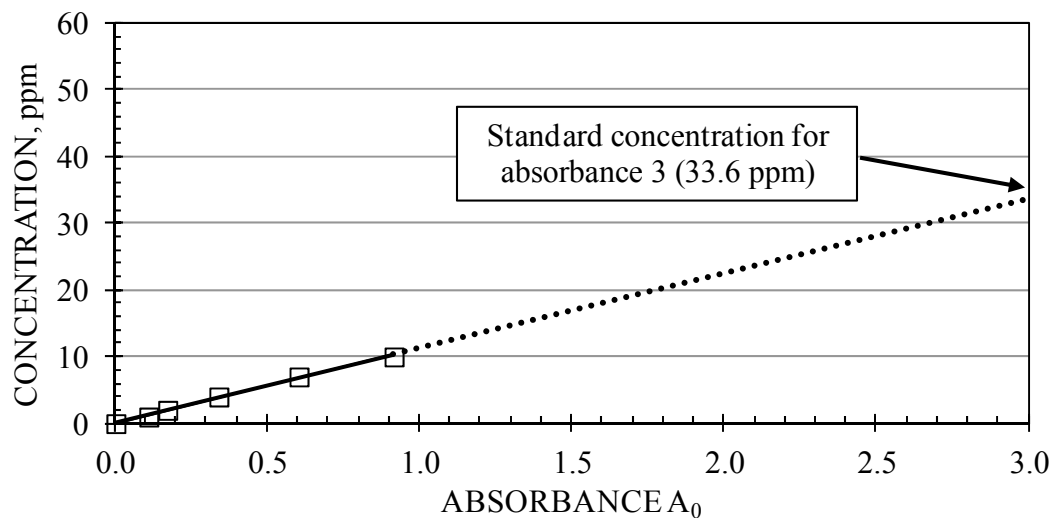
FROTHER: PolyfrothW31  
 SUPPLIER: Huntsman  
 MOLECULAR WEIGHT: na  
 DILUTION WATER: McGill tap  
 DATE: 05/05/2010

SAMPLE 19

CALIBRATION SPECTRA:



CALIBRATION CURVE:



EQUATION:

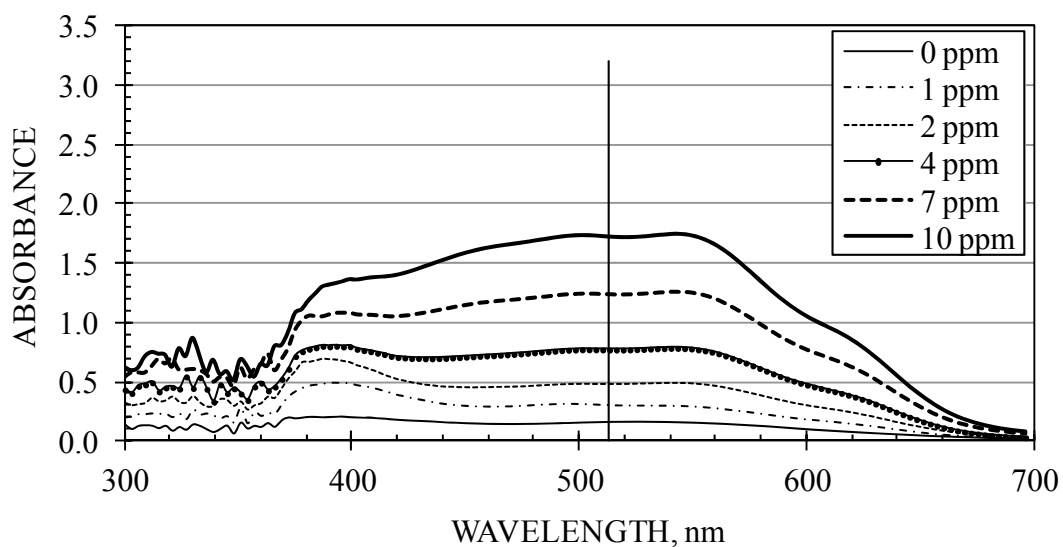
$$C \text{ (ppm)} = 11.216 A_0 \quad C \leq 10 \text{ ppm}$$

where  $A_0$  is the measured absorbance minus that of the 0 ppm standard (both at 447 nm)

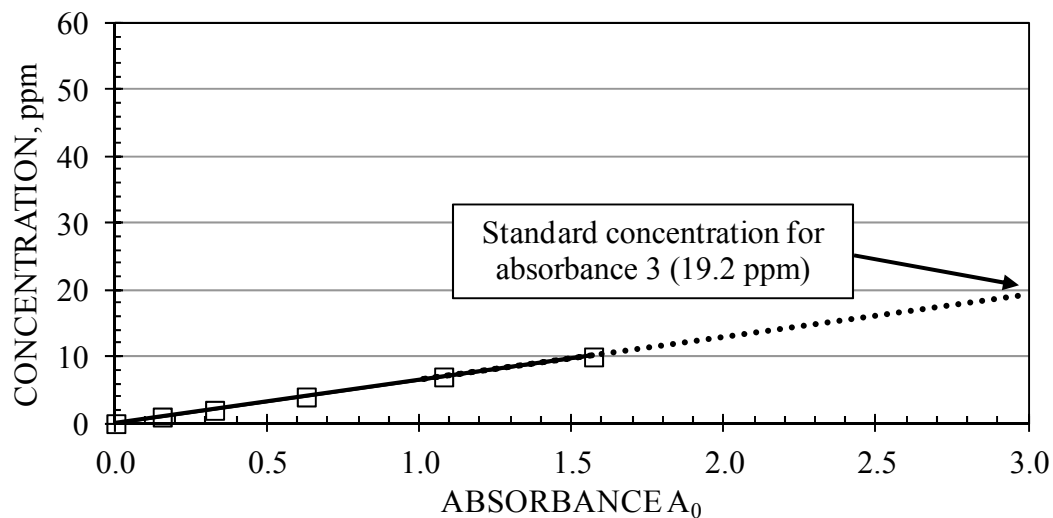
FROTHER: OreprepF50102  
 SUPPLIER: JKMRC  
 MOLECULAR WEIGHT: na  
 DILUTION WATER: McGill tap  
 DATE: 06/05/2010

SAMPLE 20

CALIBRATION SPECTRA:



CALIBRATION CURVE:



EQUATION:

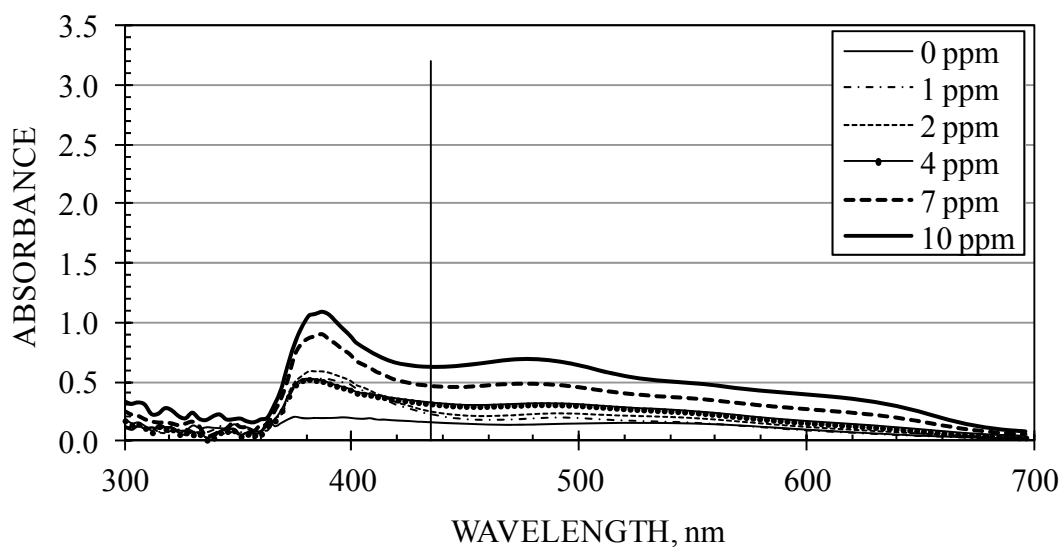
$$C \text{ (ppm)} = 6.411 A_0 \quad C \leq 10 \text{ ppm}$$

where  $A_0$  is the measured absorbance minus that of the 0 ppm standard (both at 513 nm)

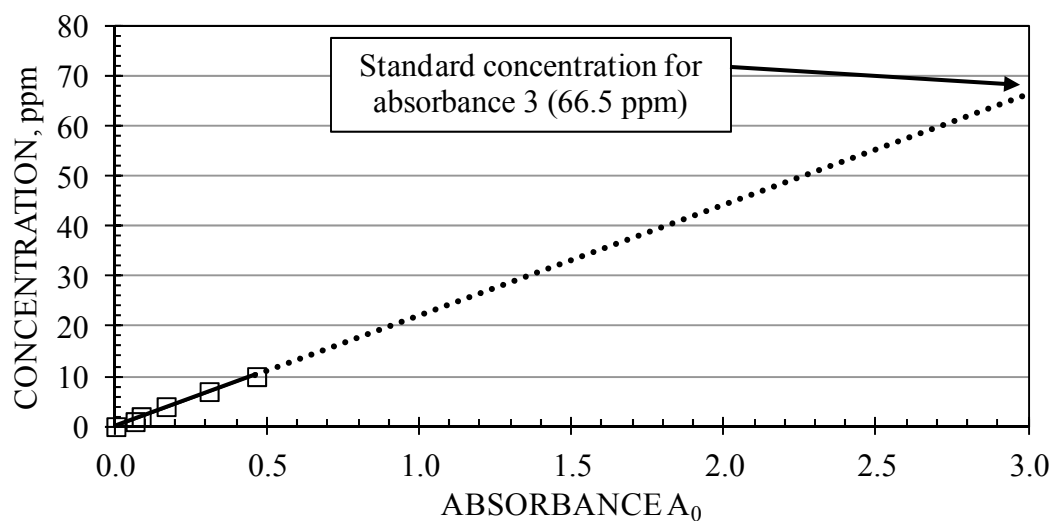
FROTHER: PolyfrothW34  
 SUPPLIER: Huntsman  
 MOLECULAR WEIGHT: na  
 DILUTION WATER: McGill tap  
 DATE: 07/05/2010

SAMPLE 21

CALIBRATION SPECTRA:



CALIBRATION CURVE:



EQUATION:

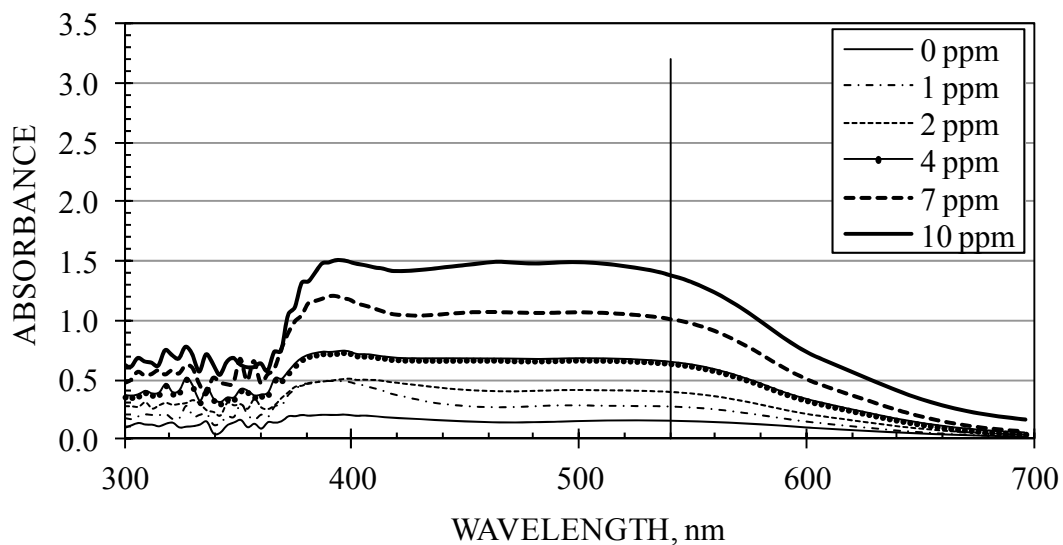
$$C \text{ (ppm)} = 22.166 A_0 \quad C \leq 10 \text{ ppm}$$

where  $A_0$  is the measured absorbance minus that of the 0 ppm standard (both at 435 nm)

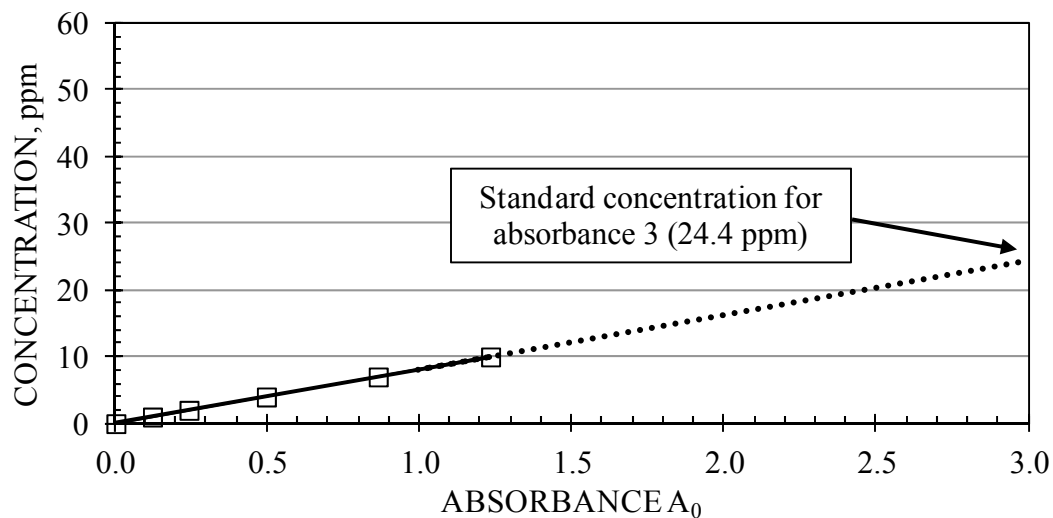
FROTHER: DSF004  
 SUPPLIER: Telfer  
 MOLECULAR WEIGHT: na  
 DILUTION WATER: McGill tap  
 DATE: 07/05/2010

SAMPLE 22

CALIBRATION SPECTRA:



CALIBRATION CURVE:



EQUATION:

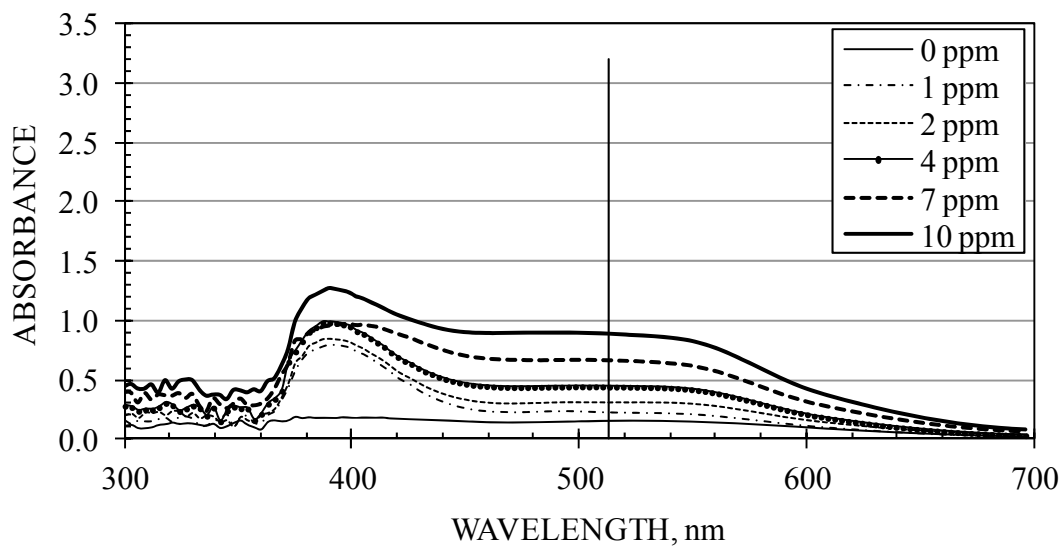
$$C \text{ (ppm)} = 8.133 A_0 \quad C \leq 10 \text{ ppm}$$

where  $A_0$  is the measured absorbance minus that of the 0 ppm standard (both at 540 nm)

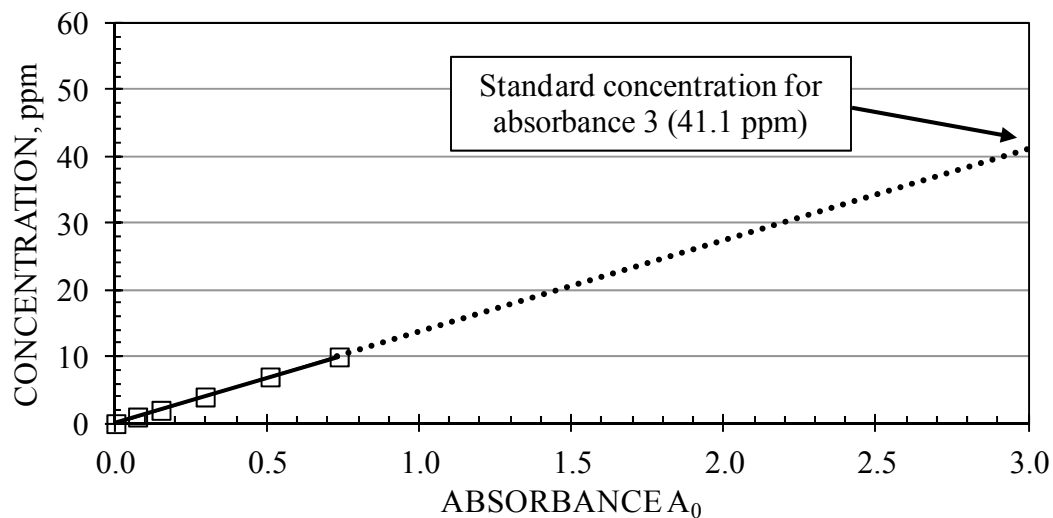
FROTHER: F160-10  
 SUPPLIER: Flottec  
 MOLECULAR WEIGHT: 264  
 DILUTION WATER: McGill tap  
 DATE: 09/05/2010

SAMPLE 23

CALIBRATION SPECTRA:



CALIBRATION CURVE:



EQUATION:

$$C \text{ (ppm)} = 13.697 A_0 \quad C \leq 10 \text{ ppm}$$

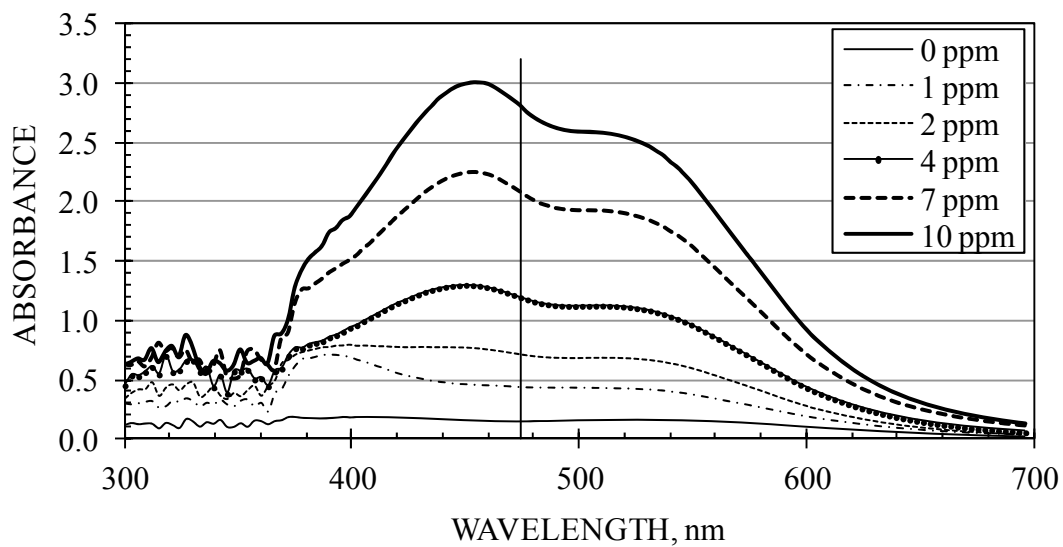
where  $A_0$  is the measured absorbance minus that of the 0 ppm standard (both at 513 nm)



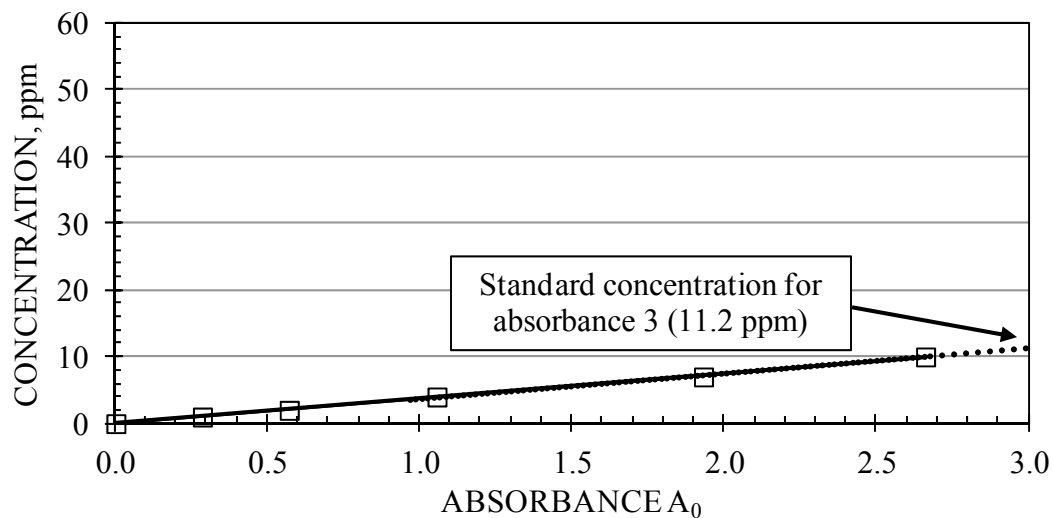
FROTHER: PolyfrothH20  
 SUPPLIER: Huntsman  
 MOLECULAR WEIGHT: na  
 DILUTION WATER: McGill tap  
 DATE: 10/05/2010

SAMPLE 24

CALIBRATION SPECTRA:



CALIBRATION CURVE:



EQUATION:

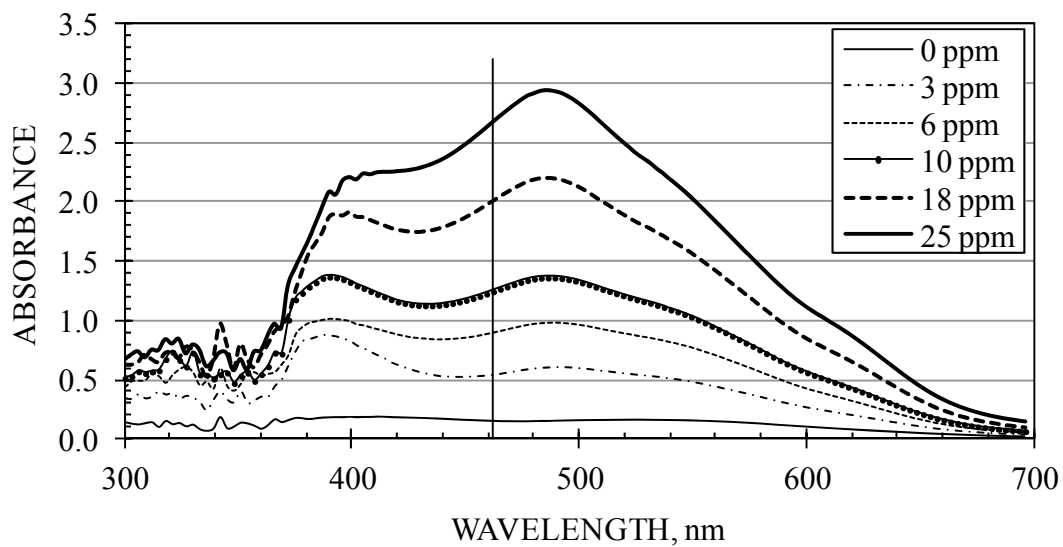
$$C \text{ (ppm)} = 3.717 A_0 \quad C \leq 10 \text{ ppm}$$

where  $A_0$  is the measured absorbance minus that of the 0 ppm standard (both at 474 nm)

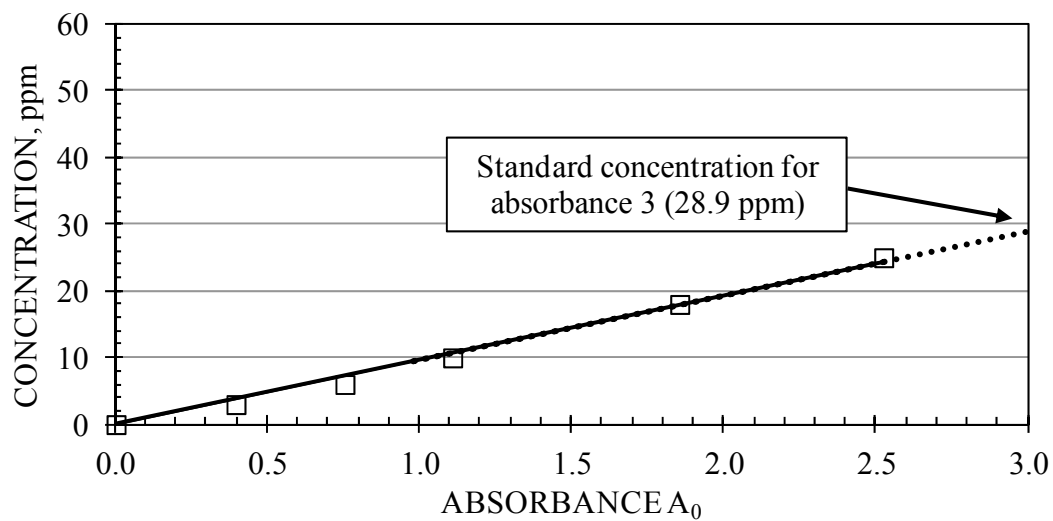
FROTHER: E.Citriodora  
 SUPPLIER: JKMRC  
 MOLECULAR WEIGHT: na  
 DILUTION WATER: McGill tap  
 DATE: 11/05/2010

SAMPLE 25

CALIBRATION SPECTRA:



CALIBRATION CURVE:



EQUATION:

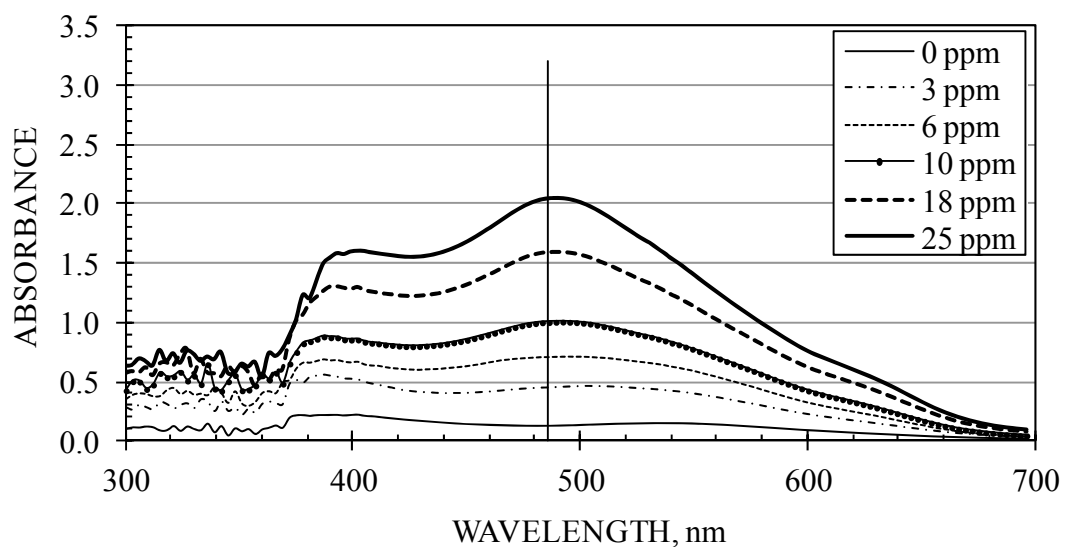
$$C \text{ (ppm)} = 9.642 A_0 \quad C \leq 25 \text{ ppm}$$

where  $A_0$  is the measured absorbance minus that of the 0 ppm standard (both at 462 nm)

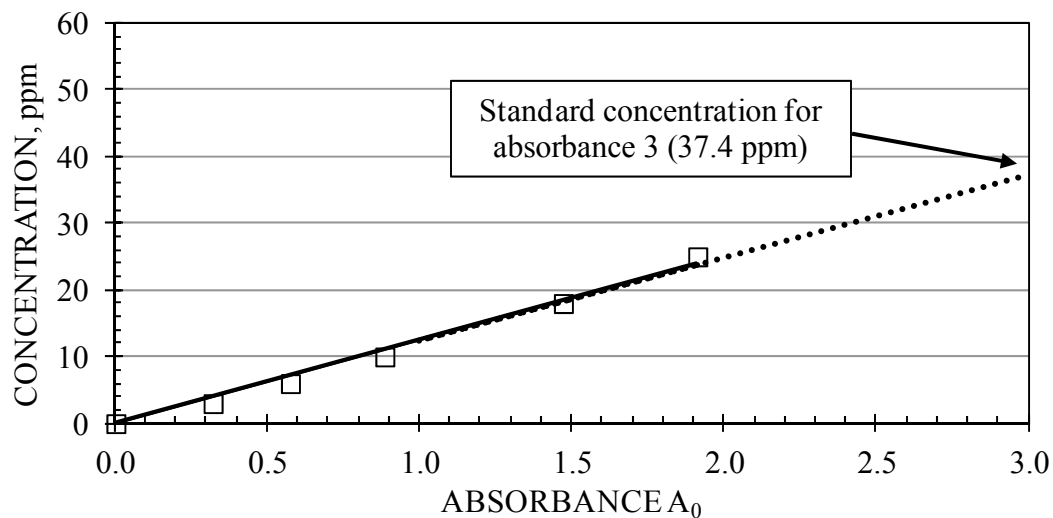
FROTHER: E.Globulus  
 SUPPLIER: JKMRC  
 MOLECULAR WEIGHT: na  
 DILUTION WATER: McGill tap  
 DATE: 21/05/2010

SAMPLE 26

CALIBRATION SPECTRA:



CALIBRATION CURVE:



EQUATION:

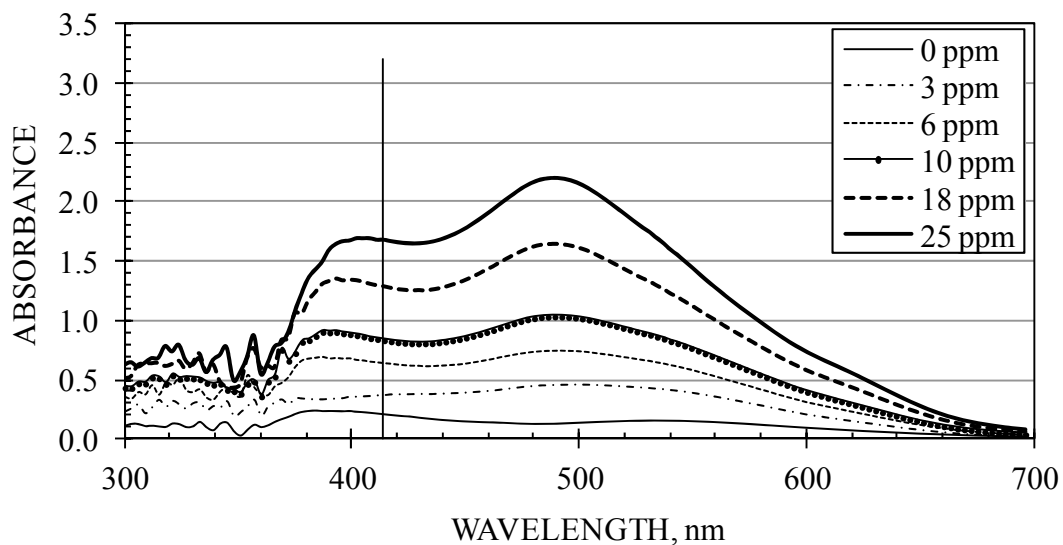
$$C \text{ (ppm)} = 12.460 A_0 \quad C \leq 25 \text{ ppm}$$

where  $A_0$  is the measured absorbance minus that of the 0 ppm standard (both at 486 nm)

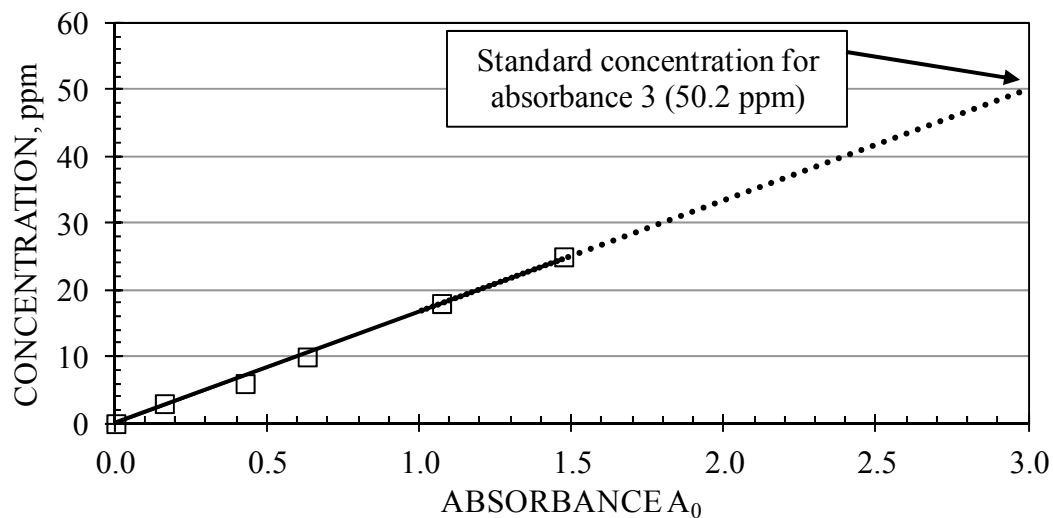
FROTHER: E.Polybractea  
 SUPPLIER: JKMRC  
 MOLECULAR WEIGHT: NA  
 DILUTION WATER: McGill tap  
 DATE: 22/05/2010

SAMPLE 27

CALIBRATION SPECTRA:



CALIBRATION CURVE:



EQUATION:

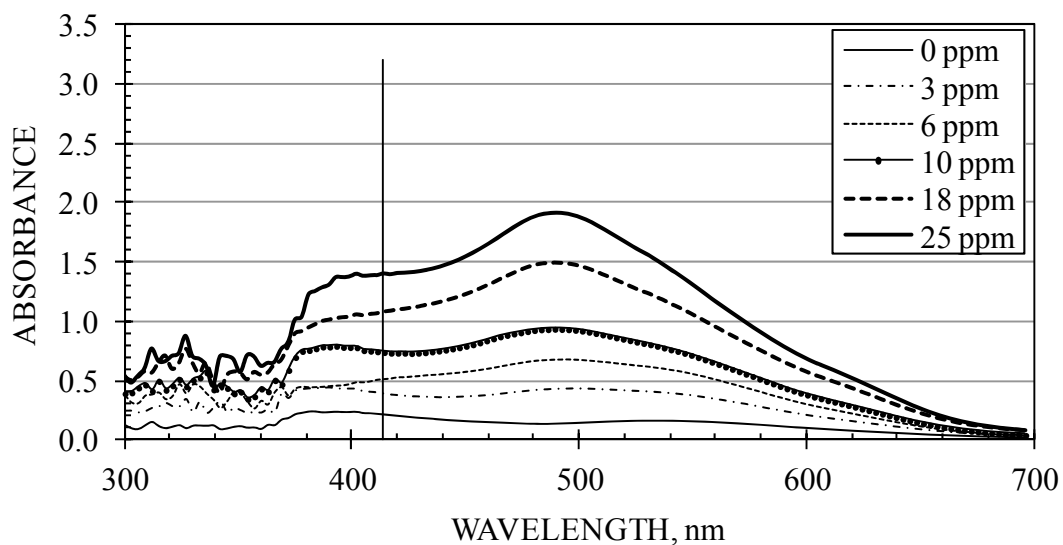
$$C \text{ (ppm)} = 16.728 A_0 \quad C \leq 25 \text{ ppm}$$

where  $A_0$  is the measured absorbance minus that of the 0 ppm standard (both at 414 nm)

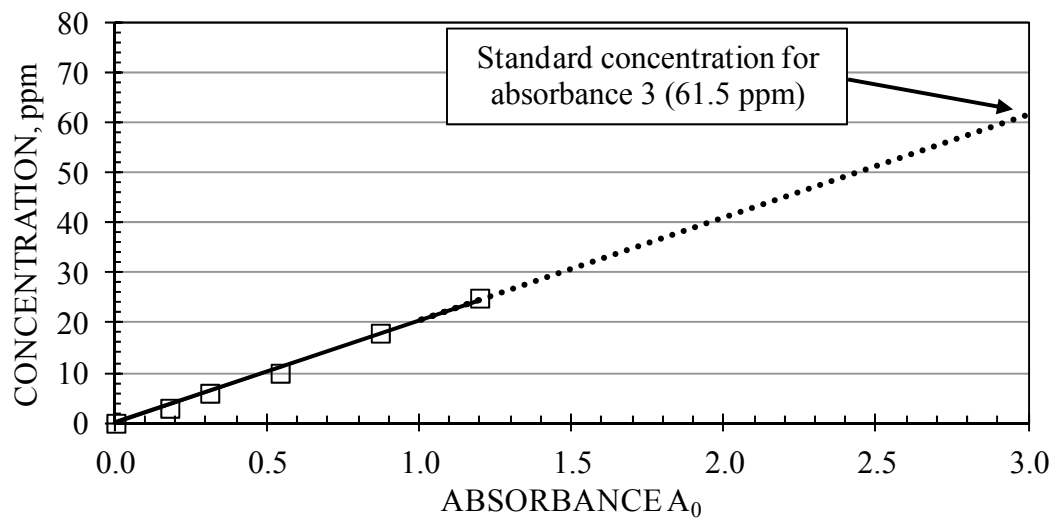
FROTHER: E.Smithii  
 SUPPLIER: JKMRC  
 MOLECULAR WEIGHT: na  
 DILUTION WATER: McGill tap  
 DATE: 23/05/2010

SAMPLE 28

CALIBRATION SPECTRA:



CALIBRATION CURVE:



EQUATION:

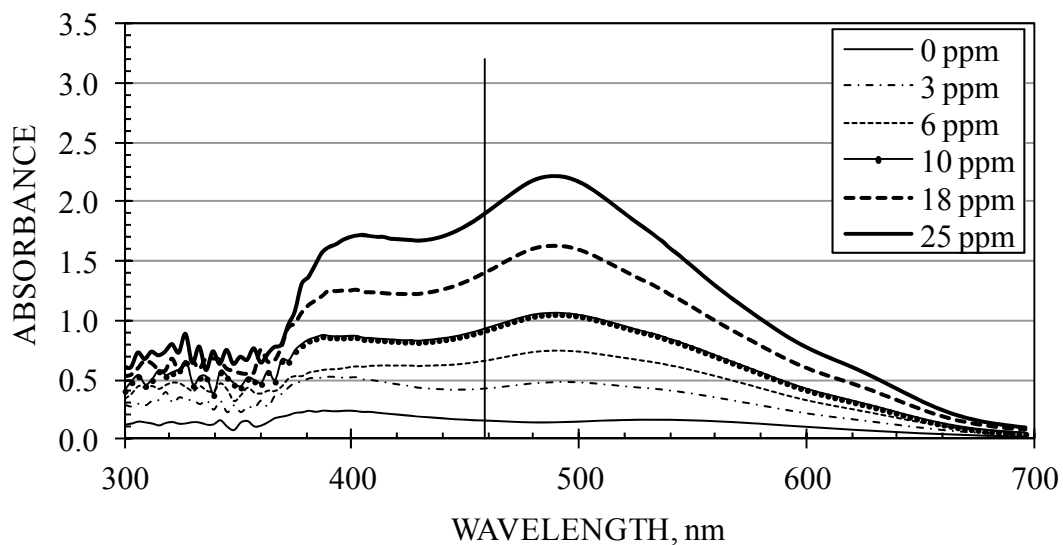
$$C \text{ (ppm)} = 20.511 A_0 \quad C \leq 25 \text{ ppm}$$

where  $A_0$  is the measured absorbance minus that of the 0 ppm standard (both at 414 nm)

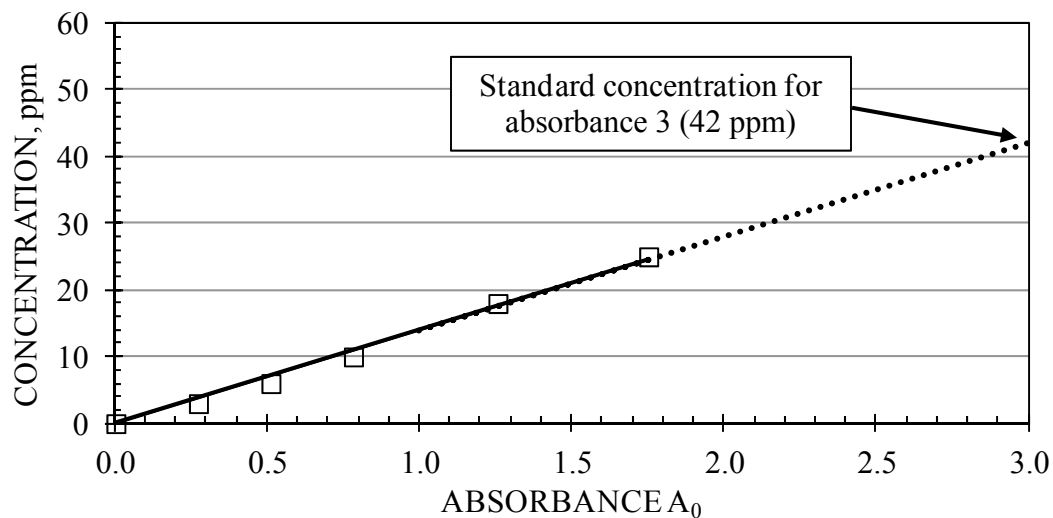
FROTHER: E.Radiata  
 SUPPLIER: JKMRC  
 MOLECULAR WEIGHT: na  
 DILUTION WATER: McGill tap  
 DATE: 24/05/2010

SAMPLE 29

CALIBRATION SPECTRA:



CALIBRATION CURVE:



EQUATION:

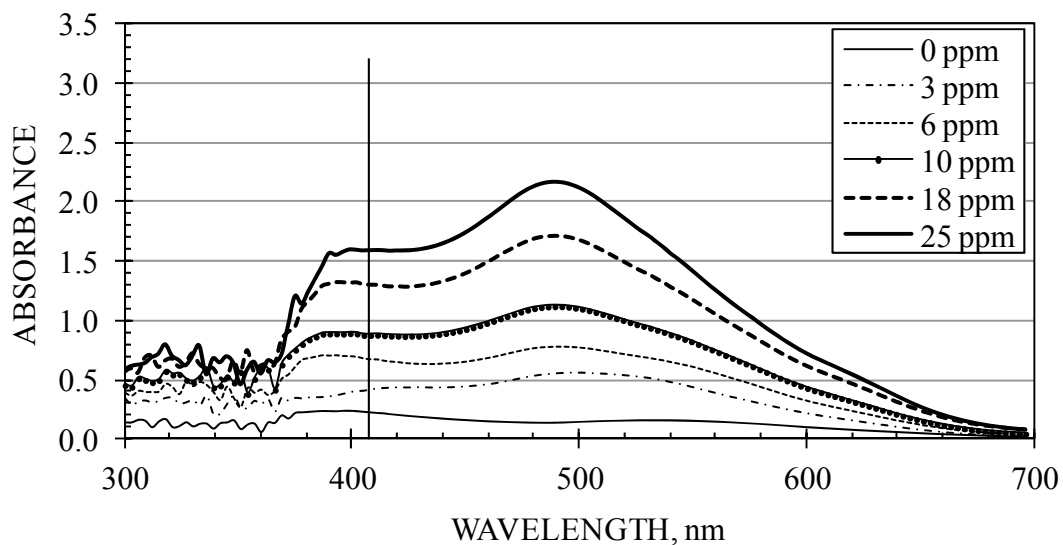
$$C \text{ (ppm)} = 13.991 A_0 \quad C \leq 25 \text{ ppm}$$

where  $A_0$  is the measured absorbance minus that of the 0 ppm standard (both at 459 nm)

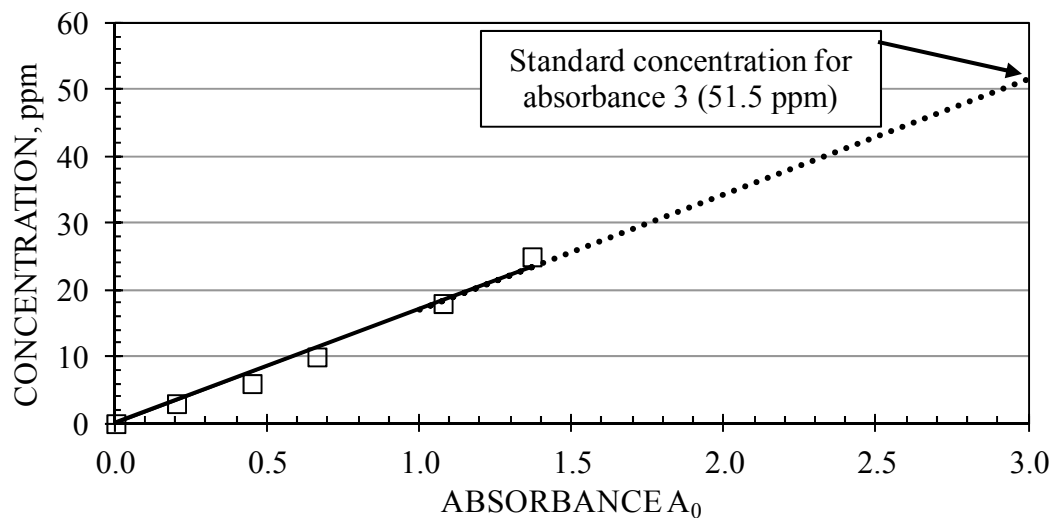
FROTHER: E.Eucaliptol  
 SUPPLIER: JKMRC  
 MOLECULAR WEIGHT: na  
 DILUTION WATER: McGill tap  
 DATE: 25/05/2010

SAMPLE 30

CALIBRATION SPECTRA:



CALIBRATION CURVE:



EQUATION:

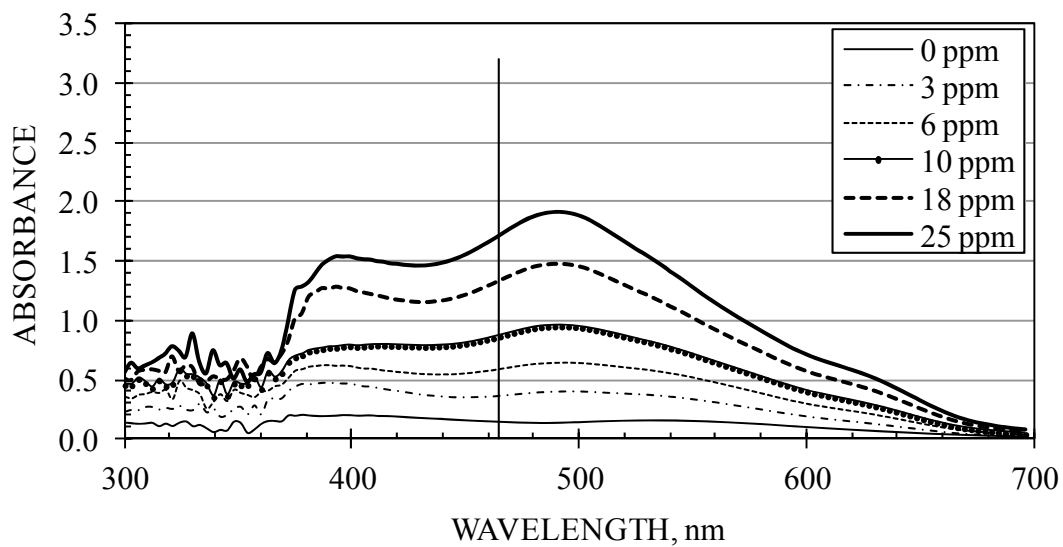
$$C \text{ (ppm)} = 17.150 A_0 \quad C \leq 25 \text{ ppm}$$

where  $A_0$  is the measured absorbance minus that of the 0 ppm standard (both at 408 nm)

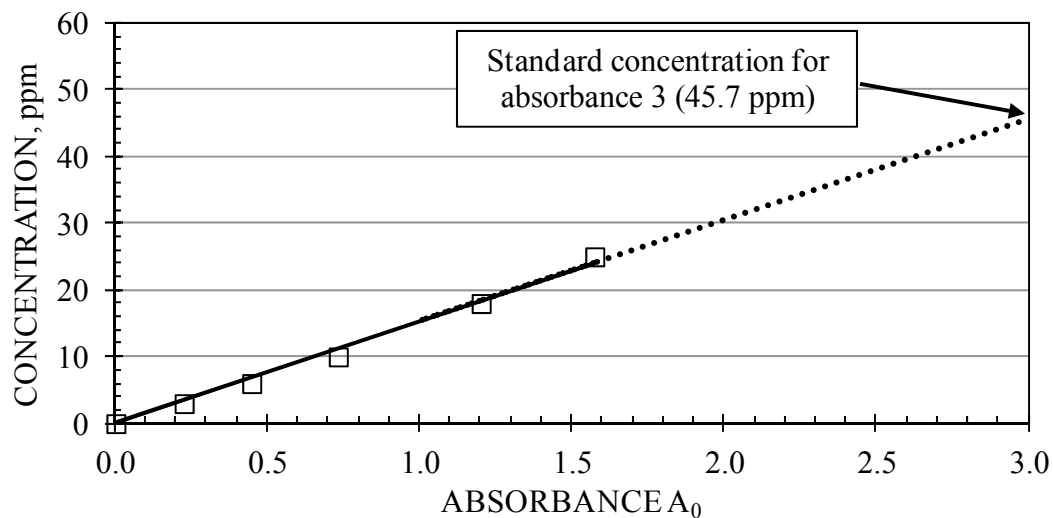
FROTHER: E.17483  
 SUPPLIER: JKMRC  
 MOLECULAR WEIGHT: na  
 DILUTION WATER: McGill tap  
 DATE: 25/05/2010

SAMPLE 31

CALIBRATION SPECTRA:



CALIBRATION CURVE:



EQUATION:

$$C \text{ (ppm)} = 15.249 A_0 \quad C \leq 25 \text{ ppm}$$

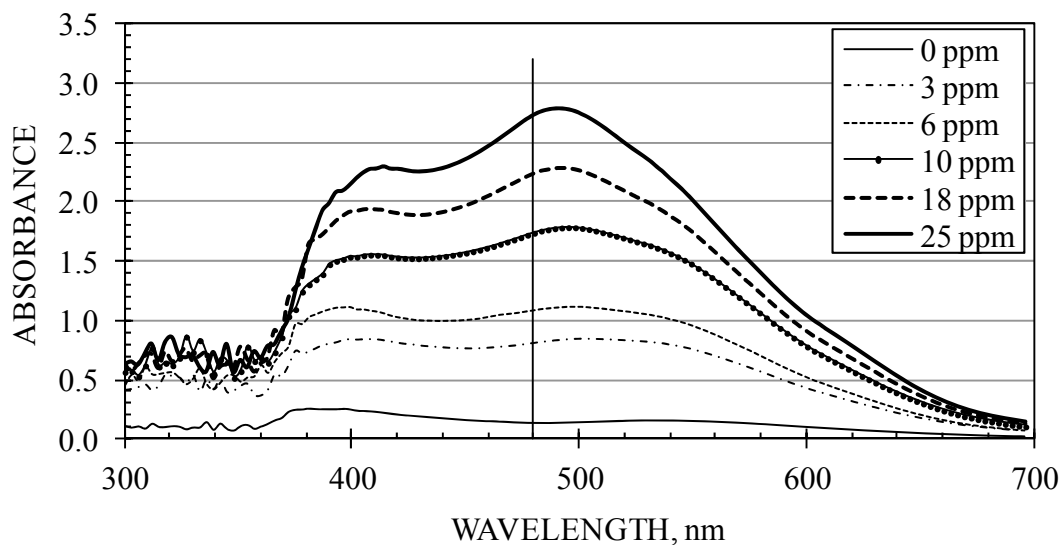
where  $A_0$  is the measured absorbance minus that of the 0 ppm standard (both at 465 nm)



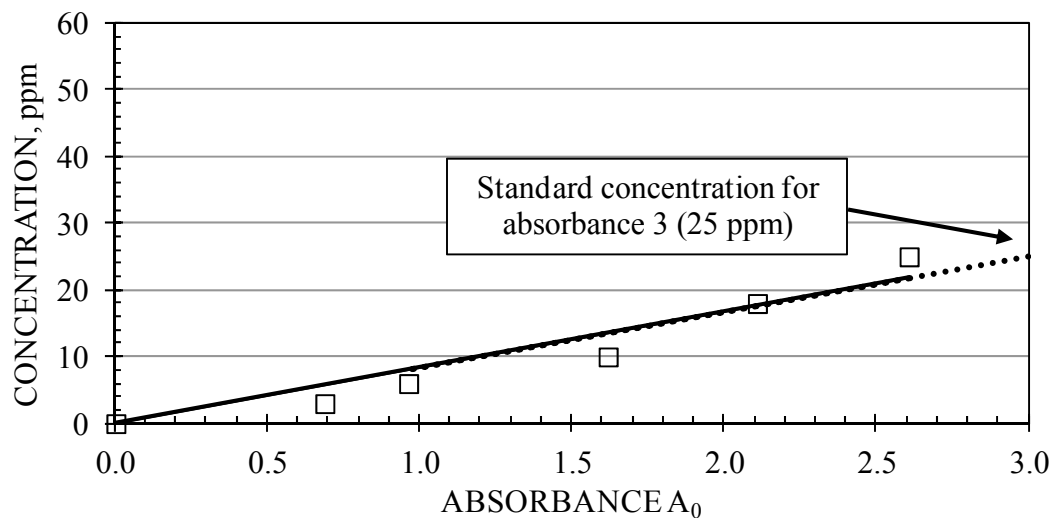
FROTHER: E.17340  
 SUPPLIER: JKMRC  
 MOLECULAR WEIGHT: na  
 DILUTION WATER: McGill tap  
 DATE: 26/05/2010

SAMPLE 32

CALIBRATION SPECTRA:



CALIBRATION CURVE:



EQUATION:

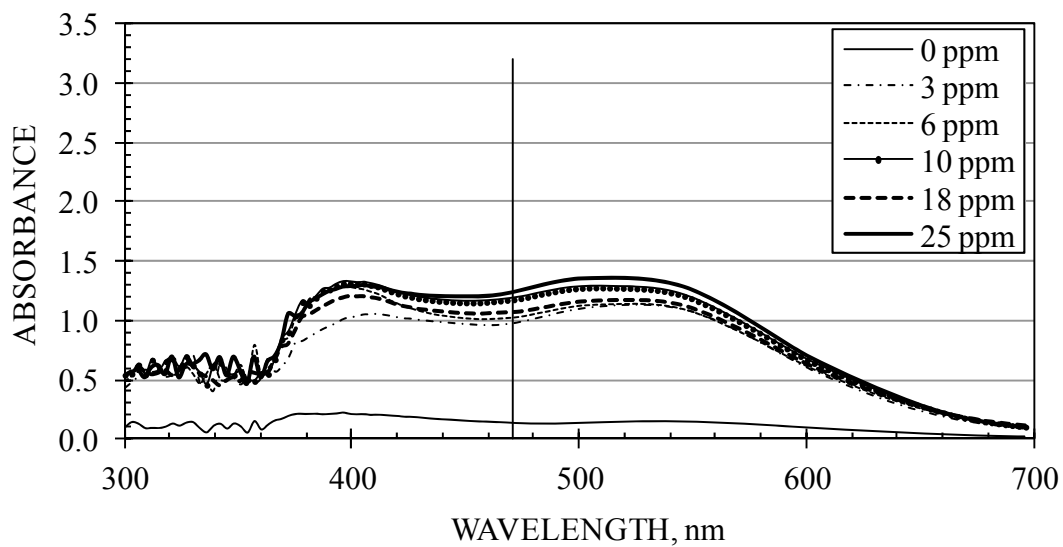
$$C \text{ (ppm)} = 8.343 A_0 \quad C \leq 25 \text{ ppm}$$

where  $A_0$  is the measured absorbance minus that of the 0 ppm standard (both at 480 nm)

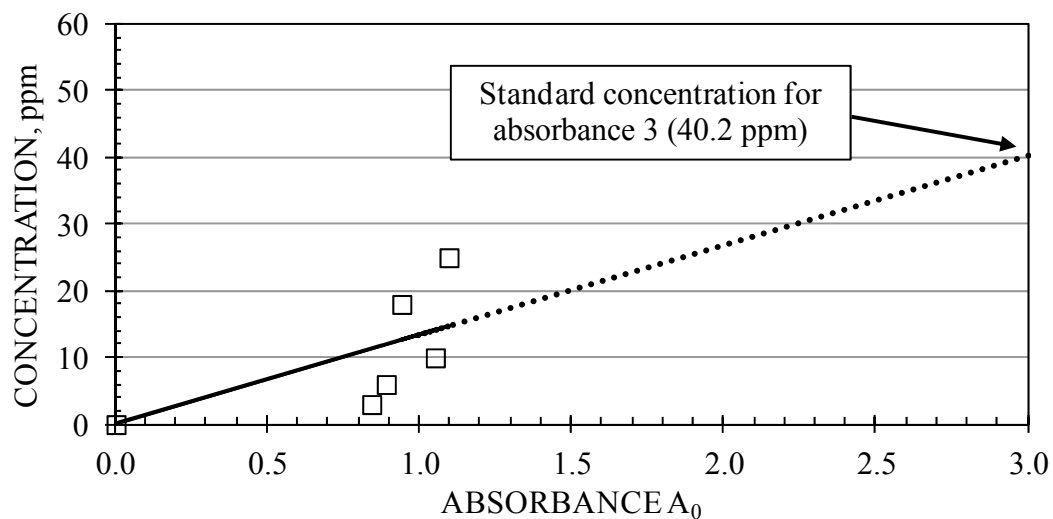
FROTHER: E.17084  
 SUPPLIER: JKMRC  
 MOLECULAR WEIGHT: na  
 DILUTION WATER: McGill tap  
 DATE: 26/05/2010

SAMPLE 33

CALIBRATION SPECTRA:



CALIBRATION CURVE:



EQUATION:

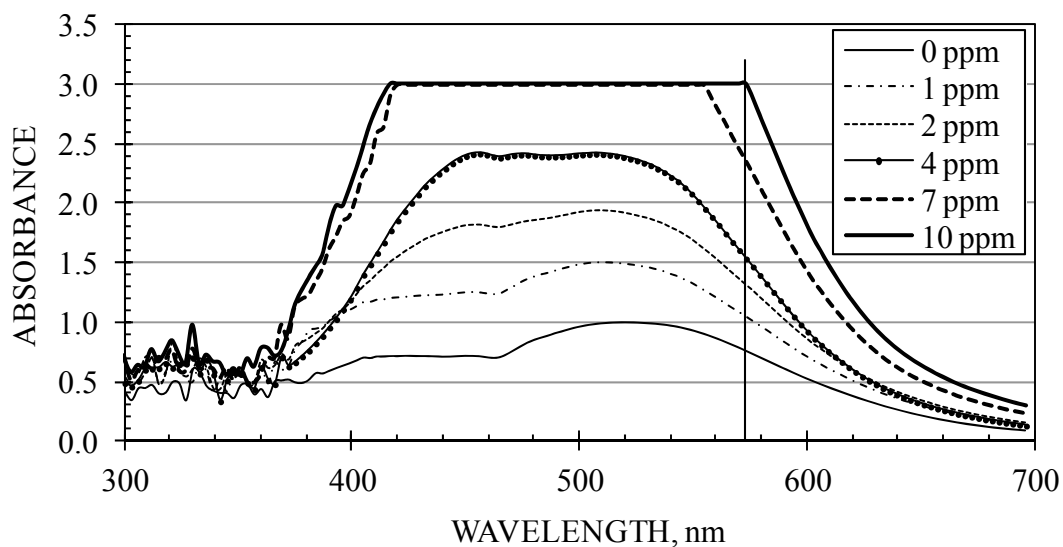
$$C \text{ (ppm)} = 13.394 A_0 \quad C \leq 25 \text{ ppm}$$

where  $A_0$  is the measured absorbance minus that of the 0 ppm standard (both at 471 nm)

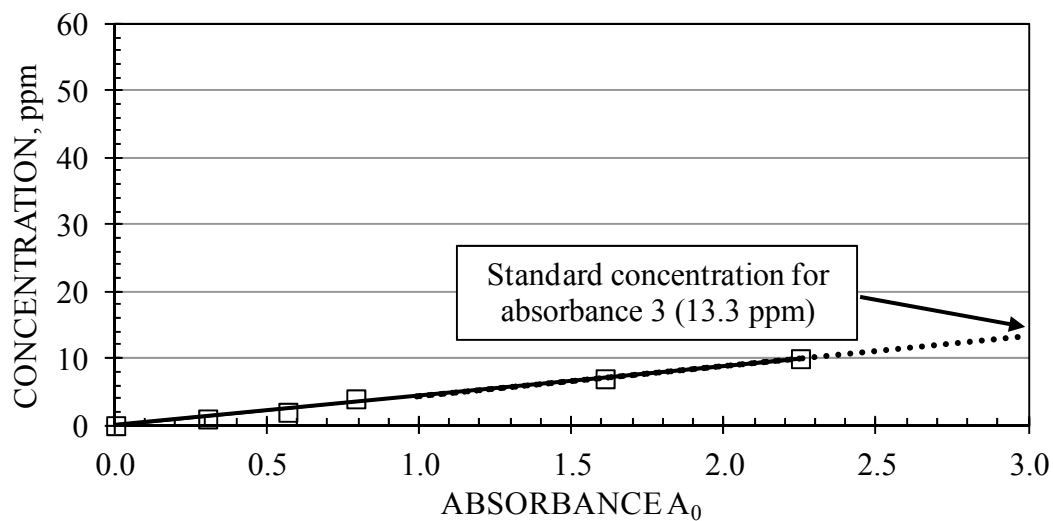
FROTHER: MIBC2  
 SUPPLIER: Sigma Aldrich  
 MOLECULAR WEIGHT: 102.18  
 DILUTION WATER: McGill tap  
 DATE: 09/06/2010

SAMPLE 34

CALIBRATION SPECTRA:



CALIBRATION CURVE:



EQUATION:

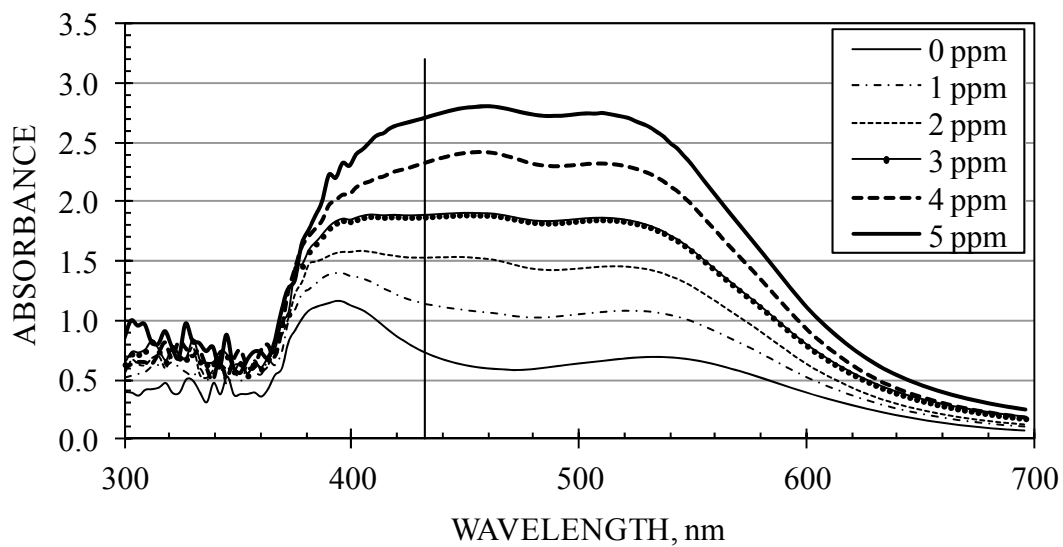
$$C \text{ (ppm)} = 4.422 A_0 \quad C \leq 10 \text{ ppm}$$

where  $A_0$  is the measured absorbance minus that of the 0 ppm standard (both at 573 nm)

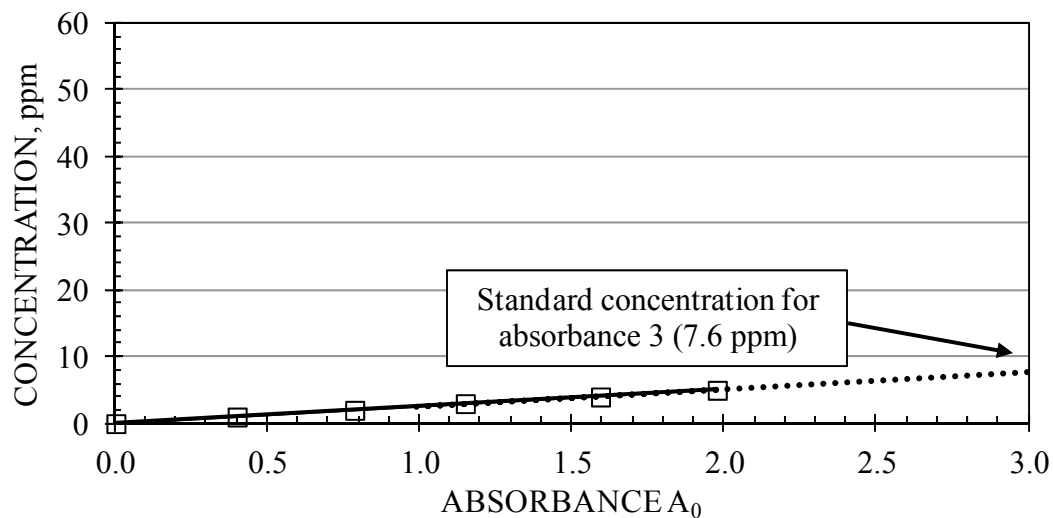
FROTHER: MIBC  
 SUPPLIER: Sigma Aldrich  
 MOLECULAR WEIGHT: 102.18  
 DILUTION WATER: McGill tap  
 DATE: 01/05/2011

SAMPLE 35

CALIBRATION SPECTRA:



CALIBRATION CURVE:



EQUATION:

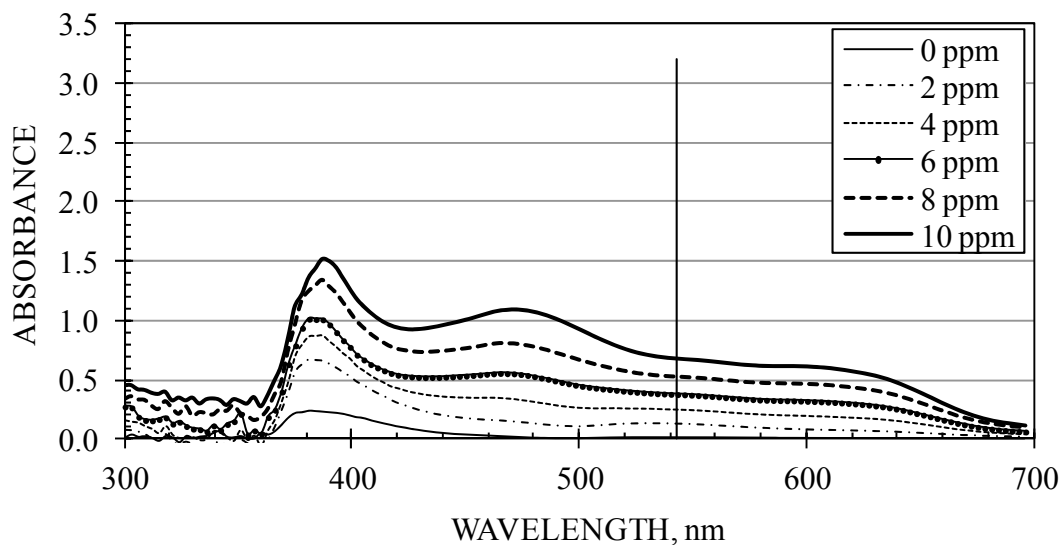
$$C \text{ (ppm)} = 2.541 A_0 \quad C \leq 5 \text{ ppm}$$

where  $A_0$  is the measured absorbance minus that of the 0 ppm standard (both at 432 nm)

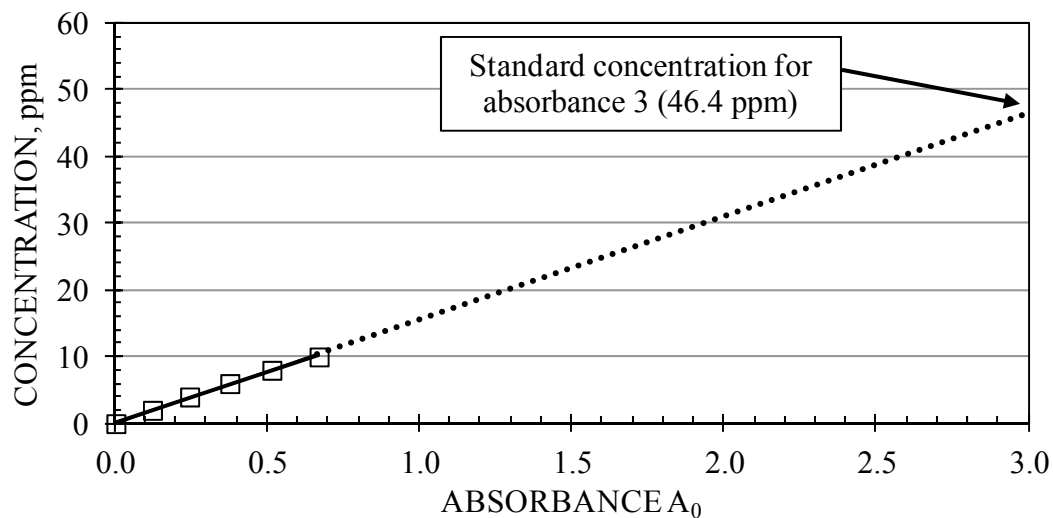
FROTHER: PPG425  
 SUPPLIER: Sigma Aldrich  
 MOLECULAR WEIGHT: 425  
 DILUTION WATER: McGill tap  
 DATE: 01/05/2011

SAMPLE 36

CALIBRATION SPECTRA:



CALIBRATION CURVE:



EQUATION:

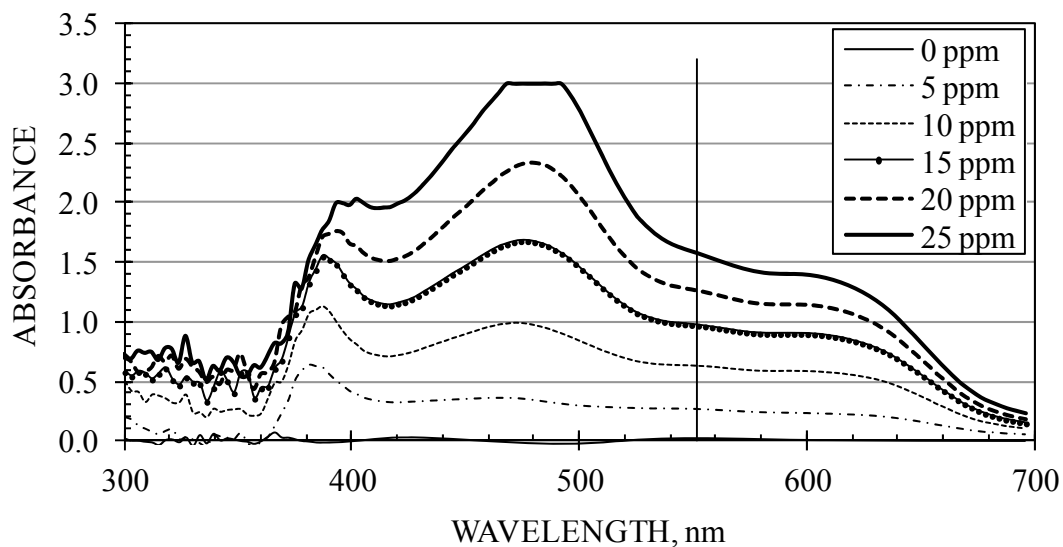
$$C \text{ (ppm)} = 15.456 A_0 \quad C \leq 10 \text{ ppm}$$

where  $A_0$  is the measured absorbance minus that of the 0 ppm standard (both at 543 nm)

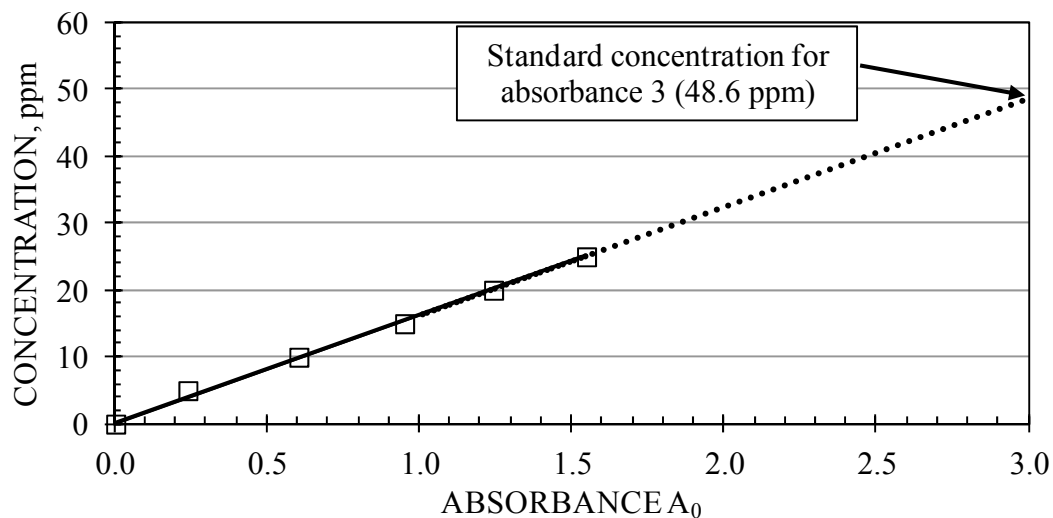
FROTHER: PPG425  
 SUPPLIER: Sigma Aldrich  
 MOLECULAR WEIGHT: 425  
 DILUTION WATER: McGill tap  
 DATE: 07/07/2011

SAMPLE 37

CALIBRATION SPECTRA:



CALIBRATION CURVE:



EQUATION:

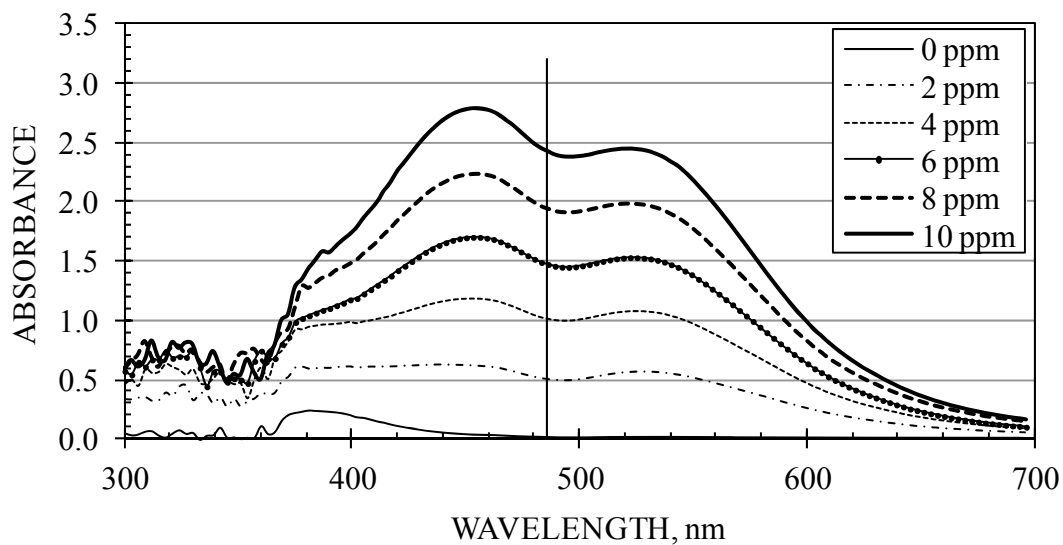
$$C \text{ (ppm)} = 16.189 A_0 \quad C \leq 25 \text{ ppm}$$

where  $A_0$  is the measured absorbance minus that of the 0 ppm standard (both at 552 nm)

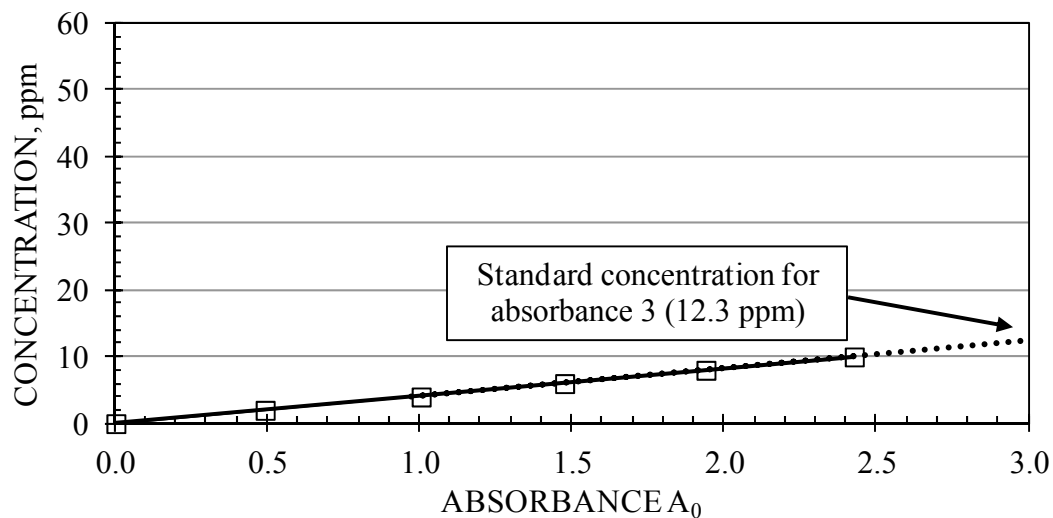
FROTHER: Octanol  
 SUPPLIER: Sigma Aldrich  
 MOLECULAR WEIGHT: 130.22  
 DILUTION WATER: McGill tap  
 DATE: 01/05/2011

SAMPLE 38

CALIBRATION SPECTRA:



CALIBRATION CURVE:



EQUATION:

$$C \text{ (ppm)} = 4.107 A_0 \quad C \leq 10 \text{ ppm}$$

where  $A_0$  is the measured absorbance minus that of the 0 ppm standard (both at 486 nm)